UNIVERSITY OF Southampton

University of Southampton Research Repository

Copyright © and Moral Rights for this thesis and, where applicable, any accompanying data are retained by the author and/or other copyright owners. A copy can be downloaded for personal non-commercial research or study, without prior permission or charge. This thesis and the accompanying data cannot be reproduced or quoted extensively from without first obtaining permission in writing from the copyright holder/s. The content of the thesis and accompanying research data (where applicable) must not be changed in any way or sold commercially in any format or medium without the formal permission of the copyright holder/s.

When referring to this thesis and any accompanying data, full bibliographic details must be given, e.g.

Thesis: Author (Year of Submission) "Full thesis title", University of Southampton, name of the University Faculty or School or Department, PhD Thesis, pagination.

Data: Author (Year) Title. URI [dataset]

UNIVERSITY OF Southampton

Faculty of Medicine

Human Development and Health

Cartilage Tissue Engineering Using Human Embryonic Stem Cells

by

Lauren Asha Griffith

ORCID ID: https://orcid.org/0000-0001-7746-6755

Thesis for the degree of Doctor of Philosophy

March 2020

University of Southampton

Abstract

Faculty of Medicine
Human Disease and Health
Thesis for the degree of Doctor of Philosophy
Cartilage Tissue Engineering Using Human Embryonic Stem Cells
by
Lauren Asha Griffith

Osteoarthritis (OA) is the most prevalent joint disease and is a leading cause of disability, particularly amongst the elderly. OA is caused by articular cartilage degradation. Hyaline articular cartilage covers the ends of bones and enables the smooth articulation of joints by reducing friction and functioning as a shock absorber. Articular cartilage is susceptible to damage and due to its avascular phenotype, self-repair is limited. Current early intervention strategies, including autologous chondrocyte implantation, typically produce fibrous rather than hyaline cartilage and frequently fail to provide a long-term solution. Most patients ultimately require total joint replacement surgery, a late stage treatment option that carries appreciable risks. An alternative early intervention treatment that focusses on replacing damaged tissue with hyaline cartilage is required; tissue engineering provides a platform to move from cell- to tissue-based treatments and facilitates the *in vitro* generation of hyaline tissue for cartilage repair.

Human embryonic stem cells (hESCs) are pluripotent and therefore have the potential to differentiate into cells from all three germ layers. They can also proliferate indefinitely *in vitro* without showing signs of cellular senescence. hESCs therefore overcome many of the limitations associated with primary chondrocytes and adult stem cells.

This study demonstrates the generation of a successful and highly reproducible protocol for the generation of hESC-derived cartilage. hESC-derived chondrocytes formed mechanically-stable hyaline-like cartilage in pellet culture that was able to repair a partial-thickness defect in *ex-vivo* organotypic culture. Furthermore, co-culture of hESC-derived cartilage pellets with native cartilage enabled the generation of previously unattainable volumes of healthy hyaline-like cartilage, exceeding 6mm in diameter.

In conclusion, this thesis demonstrates the scaffold-free generation of healthy, hyaline tissue engineered cartilage on a scale that has not previously been demonstrated. Use of hESC-derived chondrocytes has overcome limitations of scale-up and has enabled the development of bioengineered cartilage of clinically relevant proportions. This work provides compelling evidence for the use of hESC-derived cartilage in the development of new treatments for cartilage damage.

Table of Contents

Table of Contents ..... **i**

Table of Tables ..... **vii**

Table of Figures ..... **ix**

Research Thesis: Declaration of Authorship ..... **xv**

Acknowledgements ..... **xvii**

Definitions and Abbreviations ..... **xix**

Chapter 1 Introduction **1**

1.1 Socioeconomic burden of musculoskeletal disease 1

1.2 Osteoarthritis: Current treatment interventions and their limitations 1

1.2.1 Physiology and structure of Articular Cartilage 1

1.2.1.1 Developmental chondrogenesis and cartilage maintenance 4

1.2.2 Osteoarthritis (OA) 8

1.2.3 OA treatments 10

1.2.3.1 Immune privileged status of cartilage 13

1.3 A tissue engineering approach to cartilage repair 14

1.3.1 Scaffold-based cartilage tissue engineering 14

1.3.2 Scaffold-free cartilage tissue engineering 16

1.3.3 Mechanical testing of tissue engineered cartilage constructs 17

1.4 Choosing the right cells for tissue engineering 18

1.4.1 Pluripotent stem cells (PSCs) 20

1.4.1.1 Regulation of pluripotency 22

1.4.1.2 Human Embryonic Stem Cells (hESCs) 22

1.4.1.3 Human Induced Pluripotent Stem Cells (hiPSCs) 23

1.4.2 Advantages of using hESCs over hiPSCs for regenerative medicine 25

1.5 Harnessing the potential of hESCs for cartilage tissue engineering 27

1.5.1 Differentiation of hESCs into chondrocytes 27

1.5.1.1 Differentiation via Embryoid Bodies (EBs) 27

1.5.1.2 Differentiation via co-culture 28
1.5.1.3 Differentiation via MSC-intermediates 29
1.5.1.4 Directed differentiation 30
1.5.2 Cartilage tissue engineering using PSC-derived chondrocytes 31
1.5.3 Effective differentiation into chondrocytes and cartilage generation 32
1.5.3.1 Importance of mechanical stimulation in tissue engineering 32
1.6 Summary 35
1.7 Hypothesis 37
1.8 Project aims and objectives 37

Chapter 2 Materials and Methods 39

2.1 Human Embryonic Stem Cell (hESC) culture 39
2.1.1 Derivation of Mouse Embryonic Fibroblasts (MEFs) 39
2.1.2 Culturing and irradiating MEFs 39
2.1.3 Culture of HUES7 hESCs on feeder layers 40
2.1.4 Feeder free culture of HUES7 hESCs 40
2.2 Directed differentiation of HUES7 hESCs into chondrocytes 41
2.3 Human Articular Chondrocyte (HAC) cell culture 45
2.3.1 Isolation of HACs 45
2.3.2 HAC maintenance and culture 45
2.4 Gene expression analysis 46
2.4.1 Isolation of total RNA 46
2.4.2 cDNA synthesis 47
2.4.3 PCR to confirm lack of genomic DNA contamination 48
2.4.4 Taqman® quantitative real time-PCR (RT-qPCR) 49
2.4.4.1 RT-qPCR set up and amplification 49
2.4.4.2 $2^{-\Delta\Delta CT}$ method 50
2.5 Histology 50
2.5.1 Fixation, processing and embedding of fixed tissue 50
2.5.2 Sectioning 51
2.5.3 Safranin O staining 51

2.5.4 Immunostaining 52

2.6 Image analysis 55

2.6.1.1 Quantitative image analysis of Safranin O and immunohistochemical staining 55

Chapter 3 Differentiation of hESCs into Chondrocytes 58

3.1 Introduction 58

3.2 Aims and objectives 59

3.3 Methods 60

3.3.1 Immunocytochemistry 60

3.3.2 Directed differentiation of hESCs to chondrocytes and stage-specific gene expression analysis 61

3.3.3 Western Blotting 63

3.3.3.1 Protein isolation 63

3.3.3.2 Protein quantification 63

3.3.3.3 SDS polyacrylamide gel electrophoresis (SDS-PAGE) 64

3.3.3.4 Gel transfer and detection of proteins 65

3.3.3.5 Densitometry 67

3.3.4 Statistics 68

3.3.4.1 RT-qPCR analysis 68

3.3.4.2 Western Blot analysis 68

3.4 Results 69

3.4.1 Characterisation of HUES7 hESCs 69

3.4.2 Directed differentiation of hESCs towards chondrocytes 80

3.4.2.1 Cells exhibit morphological changes throughout the DDP 80

3.4.2.2 Hypoxic differentiation is beneficial for generation of hESC-derived chondrocytes 86

3.4.2.3 Developmental stage-specific changes in gene expression during differentiation 91

3.4.2.4 Western blot analysis of pluripotency and chondrogenic marker expression in hESC-derived chondrocytes 96

3.4.2.5 Expression of SOX9 and type II collagen in hESC-derived chondrocytes maintained under different conditions 98

3.5 Discussion 104

Chapter 4 Cartilage generation using an Acoustofluidic Bioreactor 110

4.1 Introduction 110

4.2 Aims and objectives 112

4.3 Methods 112

4.3.1 Fabrication of bioreactor devices 112

4.3.2 Culture of cells in an acoustofluidic bioreactor 116

4.3.3 Whole mount staining hESC-derived chondrocyte bioreactor constructs using Safranin O 118

4.4 Results 119

4.4.1 Conductance testing 119

4.4.2 HACs form hyaline-like cartilage following 21-day bioreactor culture 121

4.4.3 hESC-derived chondrocytes do not generate hyaline-like cartilage following bioreactor culture. 138

4.5 Discussion 139

Chapter 5 Pellet Culture 142

5.1 Introduction 142

5.3 Aims and objectives 144

5.4 Methods 144

5.4.1 HAC pellet culture 144

5.4.2 hESC-derived cartilage pellet culture 144

5.4.3 Alkaline Phosphatase staining 144

5.4.4 Isolation of RNA from pellet cultures 145

5.4.5 Mechanical testing 147

5.4.5.1 Native cartilage 148

5.4.5.2 Cartilage pellets 150

5.4.6 Statistical analysis 153

5.4.6.1 Image analysis and mechanical testing 153

5.4.6.2 RT-qPCR analysis....153
5.6 Results....154
5.6.1 HAC pellet culture....154
5.6.1.1 HACs form hyaline cartilage in pellet culture....154
5.6.1.2 Cartilage formation is not enhanced by extended culture....156
5.6.2 hESC-derived cartilage pellet culture....161
5.6.2.1 hESC-derived chondrocytes form cartilage with a type II collagen rich matrix....161
5.6.2.3 Optimum culture period for hESC-derived chondrocytes is 4 weeks....173
5.6.2.4 hESC-derived cartilage pellet gene expression analysis....176
5.6.2.5 Pellets generated from HACs and hESC-derived chondrocytes are not undergoing hypertrophy....178
5.6.2.6 Extended culture enhances cartilage generation in hESC-derived cartilage pellets....180
5.6.2.7 hESC-derived cartilage pellets are mechanically similar to native cartilage....202
5.7 Discussion....205
Chapter 6 *Ex-vivo* organotypic culture....211
6.1 Introduction....211
6.2 Aims and objectives....213
6.3 Methods....214
6.3.1 *Ex-vivo* organotypic partial thickness chondral defect culture....214
6.3.2 *Ex-vivo* organotypic co-culture....215
6.3.3 Transmission Electron Microscopy (TEM)....215
6.3.3.1 Sample preparation....215
6.3.3.2 Sectioning....216
6.3.3.3 Imaging....216
6.4 Results....217
6.4.1 hESC-derived cartilage pellet, organotypic defect culture....217

6.4.1.1 Culture of hESC-derived cartilage pellet in a partial thickness defect results in defect repair 217
6.4.1.2 hESC-derived chondrocyte generated defect repair tissue expresses chondrogenic markers 222
6.4.1.3 Evidence of matrix remodelling in immature fibrous repair tissue but not mature neocartilage 225
6.4.2 hESC-derived cartilage pellet co-culture with native cartilage 227
6.4.2.1 hESC-derived chondrocyte co-culture with native cartilage results in large proteoglycan rich hyaline neocartilage constructs..... 227
6.4.2.2 hESC-derived chondrocyte neocartilage expresses key chondrogenic markers 232
6.4.2.3 Evidence of matrix remodelling in neocartilage co-cultures..... 237
6.4.3 Ultrastructure of bioengineered cartilage generated using co-culture 243
6.5 Discussion..... 247

Chapter 7 Final discussion 254

7.1 Clinical relevance 258
7.2 Future work..... 260

Appendix A 261

7.3 Mathematica code for generating E from full thickness native cartilage 261
7.4 Mathematica code for generating E from cartilage pellets..... 264

Appendix B Review article 268

List of References 289

Table of Tables

Table 1.1 **Overview of epidemiology and treatment options for musculoskeletal diseases.** 12

Table 2.1 **Growth factor concentrations for the directed differentiation of hESCs into chondrocytes.** 43

Table 2.2 **List of Taqman probes used for RT-qPCR** 50

Table 2.3 **List of antibodies used for immunostaining.** 53

Table 2.4 **AEC Stock recipe.** 54

Table 2.5 **AEC working solution recipe.** 54

Table 3.1 **List of antibodies used for immunocytochemistry** 61

Table 3.2 **Chondrogenic media preparation** 62

Table 3.3 **Preparation of bis-acrylamide gels used for electrophoresis.** 64

Table 3.4 **Preparation of buffers for Western Blotting.** 65

Table 3.5 **Antibodies used for Western Blotting.** 67

Table 3.6 **DDPs performed under hypoxia were more successful than those performed at 20% O_2.** 91

Table 5.1 **Activation buffer recipe.** 145

Table 5.2 **AS-B1/Fast Violet recipe.** 145

Table 5.3 **Summary of mechanical testing data from articular cartilage and pellets.** 204

Table of Figures

Figure 1.1 **Diagram depicting the principle structure and components of hyaline articular cartilage.** 3

Figure 1.2 **Regulatory control of chondrocyte gene expression via SMAD signalling.** 7

Figure 1.1.3 **Schematic diagram depicting stages of Osteoarthritis (OA) in the knee.** 9

Figure 1.4 **Cell potency and lineage restriction** 19

Figure 1.5 **Derivation and differentiation of pluripotent stem cells and differentiation.** 21

Figure 1.6 **Benefits and drawbacks of using adult stem cells and pluripotent stem cells for clinical applications.** 26

Figure 2.1 **Schematic representation of DDP.** 41

Figure 2.2 **Representative image of a PCR gel imaged under UV light.** 49

Figure 2.3 **Area of interest (AOI) selection for image analysis.** 55

Figure 3.1 **Representative BSA standard curve used to calculate sample protein concentrations.** 63

Figure 3.2 **HUES7 hESCs cultured at 20% or 5% O_2 form tightly packed colonies.** 69

Figure 3.3 **HUES7 hESCs cultured at 20% oxygen tension express key intracellular pluripotency markers.** 71

Figure 3.4 **Localisation of HUES7 hESCs cultured at 20% oxygen tension express key intracellular pluripotency markers.** 72

Figure 3.5 **HUES7 hESCs cultured at 5% oxygen tension express key intracellular pluripotency markers.** 73

Figure 3.6 **Localisation of HUES7 hESCs cultured at 5% oxygen tension express key intracellular pluripotency markers.** 74

Figure 3.7 **HUES7 hESCs cultured at 20% oxygen tension express the cell surface marker TRA-1-60 but not SSEA1.** 76

Figure 3.8 **Localisation of HUES7 hESCs cultured at 20% oxygen tension express the cell surface marker TRA-1-60 but not SSEA1.** 77

Table of Figures

Figure 3.9 **HUES7 hESCs cultured at 5% oxygen tension express the cell surface marker TRA-1-60 but not SSEA1.** 78

Figure 3.10 **Localisation of HUES7 hESCs cultured at 5% oxygen tension express the cell surface marker TRA-1-60 but not SSEA1.** 79

Figure 3.11 **A directed differentiation protocol to generate chondrocytes from hESCs.** 80

Figure 3.12 **hESCs cultured at 5% O_2 and differentiated at 20% O_2 (5-20% O_2) exhibit morphological changes over the course of the DDP.** 83

Figure 3.13 **hESCs cultured and differentiated at 5% O_2 (5-5% O_2) exhibit morphological changes over the course of the DDP.** 85

Figure 3.14 **Stage 3 cells differentiated at 5% O_2 express the chondrogenic marker *COL2A1* at a higher level than cells differentiated at 20% O_2.** 86

Figure 3.15 **hESC-derived chondrocytes differentiated at both 20% and 5% O_2 express the chondrogenic marker SOX9.** 88

Figure 3.16 **hESC-derived chondrocytes differentiated at both 20% and 5% O_2 deposit the extracellular matrix protein type II collagen** 89

Figure 3.17 **OCT4 is no longer detectable by immunocytochemistry in hESC-derived chondrocytes.** 90

Figure 3.18 **Stage-specific changes in gene expression of cells differentiated at 5% O_2 (5-5% O_2).** 93

Figure 3.19 **Line graphs depicting temporal expression patterns of stage-specific genes in cells differentiated at 5% O_2 (5-5% O_2).** 95

Figure 3.20 **hESC-derived chondrocytes differentiated at 5% O_2 exhibit negligible pluripotency marker expression and robust expression of chondrogenic markers.** 97

Figure 3.21 **Differential expression of SOX9 in hESC-derived chondrocytes differentiated at 5% O_2 and maintained at 5% O_2 for 7 days in different media.** 99

Figure 3.22 **hESC-derived chondrocytes differentiated at 5% O_2 and cultured at 5% O_2 for 7 days in different culture media maintained type II collagen expression.** .. 101

Figure 3.23 **No significant difference in expression of SOX9 and type II collagen in hESC-derived chondrocytes differentiated at 5% O_2 and cultured at 5% O_2 in different media for 7 days.** 103

Figure 4.1 **Ultrasonic standing wave trap formation (USWT) results in cell aggregation at pressure nodes** 111

Figure 4.2 **Acoustofluidic bioreactor fabrication**. 114

Figure 4.3 **Components of assembled acoustofluidic bioreactor.** 115

Figure 4.4 **Schematic depiction of the peak-to-peak voltage (Vpp) of a sinusoidal wave**. 116

Figure 4.5 **Schematic representation of frequency sweeping.** 117

Figure 4.6 **Set up of the acoustofluidic bioreactor for cell culture.** 118

Figure 4.7 **Resonant frequencies and conductance plots of each resonator on an acoustofluidic bioreactor.** 120

Figure 4.8 **Patient 1 generated hyaline-like cartilage following 21-days culture in an acoustofluidic bioreactor (construct 2).** 123

Figure 4.9 **Patient 1 generated hyaline-like cartilage following 21-days culture in an acoustofluidic bioreactor (construct 2).** 126

Figure 4.10 **Patient 1 generated hyaline-like cartilage following 21-days culture in an acoustofluidic bioreactor (construct 3).** 129

Figure 4.11 **Patient 2 generated hyaline-like cartilage following 21-days culture in an acoustofluidic bioreactor (construct 1).** 132

Figure 4.12 **Patient 2 generated hyaline-like cartilage following 21-days culture in an acoustofluidic bioreactor (construct 2)** 135

Figure 4.13 **Image analysis of Safranin O staining performed on HACs cultured in an acoustofluidic bioreactor for 21-days.** 137

Figure 4.14 **Whole mount Safranin O staining of hESC-derived chondrocytes cultured in an acoustofluidic bioreactor for 21-days.** 138

Table of Figures

Figure 5.1 **Mechanical testing rig used for compression of native cartilage and cartilage pellets.** 147

Figure 5.2 **Representative curve mapping graph generated by Mathematica code for mechanical testing of full thickness cartilage.** 149

Figure 5.3 **Representative curve mapping graph generated by Mathematica code for mechanical testing of pellets.** 152

Figure 5.4 **HAC pellet culture.** 155

Figure 5.5 **Extended culture did not increase pellet area.** 157

Figure 5.6 **Extended culture did not increase Safranin O staining intensity.** 158

Figure 5.7 **Extended culture did not increase type II collagen staining intensity.** 160

Figure 5.8 **Photographs of hESC-derived cartilage pellets cultured for 3, 4 or 5 weeks.** 161

Figure 5.9 **hESC-derived cartilage pellets cultured for 3, 4 or 5 weeks, experiment 1.** 163

Figure 5.10 **hESC-derived cartilage pellets cultured for 3, 4 or 5 weeks, experiment 2.** 166

Figure 5.11 **hESC-derived cartilage pellets cultured for 3, 4 or 5 weeks, experiment 3.** 169

Figure 5.12 **hESC-derived cartilage pellets cultured for 3, 4 or 5 weeks, experiment 4.** 172

Figure 5.13 **Type II collagen staining of HAC pellets and hESC-derived cartilage pellets used for image analysis.** 174

Figure 5.14 **Image analysis of type II collagen staining performed on HAC and hESC-derived cartilage pellets.** 175

Figure 5.15 **Gene expression analysis of pluripotency genes in hESCs and hESC-derived cartilage pellets.** 176

Figure 5.16 **Gene expression analysis of pluripotency and chondrogenic genes expressed in HAC and hESC-derived cartilage pellets.** 177

Figure 5.17 **ALP staining of hESC-derived chondrocyte and HAC pellets.** 179

Figure 5.18 **Limited expression of proteoglycans in a hESC-derived** cartilage **pellet cultured for 13 weeks.** 180

Figure 5.19 **hESC-derived cartilage pellet cultured for 13 weeks expresses chondrogenic markers.**.....183

Figure 5.20 **Remodelling of hESC-derived cartilage pellets cultured for 13 weeks.** 186

Figure 5.21 **Limited expression of proteoglycans in a hESC-derived cartilage pellet cultured for 16 weeks.**.....187

Figure 5.22 **hESC-derived cartilage pellet cultured for 16 weeks expresses chondrogenic markers.**.....190

Figure 5.23 **Remodelling of hESC-derived cartilage pellets cultured for 16 weeks.** 193

Figure 5.24 **Robust expression of proteoglycans in a hESC-derived cartilage pellet cultured for 16 weeks**.....195

Figure 5.25 **hESC-derived cartilage pellet cultured for 19 weeks expresses chondrogenic markers.**.....198

Figure 5.26 **Remodelling of hESC-derived cartilage pellets cultured for 19 weeks.** 201

Figure 5.27 **Comparison of Young's elastic modulus between native cartilage and pellet cultures.**.....203

Figure 6.1 **Schematic depiction of *ex vivo* organotypic partial thickness chondral defect set up.**.....214

Figure 6.2 **Schematic depiction of *ex vivo* organotypic co-culture set up.**.....215

Figure 6.3 **Repair of a partial thickness defect in native cartilage by a hESC-derived cartilage pellet.** 218

Figure 6.4 **hESC-derived cartilage pellet generates hyaline-like repair tissue in partial thickness defect.** 221

Figure 6.5 **hESC-derived cartilage pellet repair tissue expresses chondrogenic markers.**224

Figure 6.6 **Expression of remodelling markers in neocartilage generated from hESC-derived chondrocytes pellet defect repair tissue.** 226

Figure 6.7 **Neocartilage generation from hESC-derived chondrocytes following 16-weeks co-culture with native cartilage (experiment 1).** 230

Table of Figures

Figure 6.8 **Neocartilage generation from hESC-derived chondrocytes following 16-weeks co-culture with native cartilage (experiment 2).** 232

Figure 6.9 **Neocartilage generated via organotypic co-culture expresses chondrogenic markers (experiment 1).** 234

Figure 6.10 **Neocartilage generated via organotypic co-culture expresses chondrogenic markers (experiment 2).** 236

Figure 6.11 **Evidence of matrix remodelling in neocartilage generated via organotypic co-culture (experiment 1).** 239

Figure 6.12 **Evidence of matrix remodelling in neocartilage generated via organotypic co-culture (experiment 2).** 242

Figure 6.13 **Evidence of hESC-derived chondrocytes producing collagen in organotypic co-culture.** 244

Figure 6.14 **TEM of chondrocytes in hESC-derived cartilage.** 246

Figure 7.1 **Schematic representation of cartilage generation from hESCs** 256

Research Thesis: Declaration of Authorship

Print name: Lauren Asha Griffith

Title of thesis: Cartilage Tissue Engineering Using Human Embryonic Stem Cells

I declare that this thesis and the work presented in it are my own and has been generated by me as the result of my own original research.

I confirm that:

1. This work was done wholly or mainly while in candidature for a research degree at this University;
2. Where any part of this thesis has previously been submitted for a degree or any other qualification at this University or any other institution, this has been clearly stated;
3. Where I have consulted the published work of others, this is always clearly attributed;
4. Where I have quoted from the work of others, the source is always given. With the exception of such quotations, this thesis is entirely my own work;
5. I have acknowledged all main sources of help;
6. Where the thesis is based on work done by myself jointly with others, I have made clear exactly what was done by others and what I have contributed myself;
7. Parts of this work have been published as:

Jevons, L.A., Houghton, F.D., and Tare, R.S. (2018). Augmentation of musculoskeletal regeneration: role for pluripotent stem cells. Regen Med 13, 189-206.

Signature: Date:

Acknowledgements

Firstly, I would like to thank the Rosetrees Trust, the Institute for Life Sciences and the University of Southampton for funding this research. I would like to thank my supervisors Dr Franchesca Houghton and Dr Rahul Tare for all the support and guidance they have offered me during my PhD. I am grateful for your door always being open, and for your continued encouragement. I would also like to thank my supervisors Dr Peter Glynne-Jones and Martyn Hill, whose engineering expertise has been invaluable. I would also like to extend this thanks to Dr Umesh Jonnalagadda who dedicated a great deal of time to helping me with the engineering aspects of this research. I would also like to thank Katherine Arnold, a project student, who developed the codes used to analyse the mechanical testing data.

I have been fortunate to be both a part of the Houghton lab and the Bone and Joint research group during my PhD and I am very grateful for the friendship and support I have received from members of both groups.

Finally, I would like to thank my wonderful family and husband whose constant love and support has been my anchor during the difficult times.

Definitions and Abbreviations

ACI	Autologous chondrocyte implantation
AEC	3-Amino-9-ethylcarbazole
AKT	Protein kinase B
ALK	Anaplastic lymphoma tyrosine-kinase (receptor)
ALP	Alkaline phosphatase
BMD	Bone mineral density
BMMSC	Bone marrow-derived mesenchymal stem cell
BMP4	Bone morphogenic protein 4
BSA	Bovine serum albumin
CDH1	Gene encoding E-cadherin
cDNA	Complementary DNA
COL2A1	Gene encoding Type II Collagen
COL10A1	Gene encoding Type X Collagen
CO_2	Carbon dioxide
COMP	Cartilage oligomeric matrix protein
CXCR4	Gene encoding chemokine receptor type 4
DALYs	Disability-adjusted life year
DAPI	4',6-Diamidino-2-Phenylindole, Dihydrochloride
DDP	Directed differentiation protocol
DDP-BM	Directed differentiation protocol-basal medium
DEPC	Diethyl pyrocarbonate
dH_2O	distilled water
DMD	Duchenne muscular dystrophy
DMEM	Dulbecco's modified Eagle's medium
DMEM-F12	Dulbecco's modified Eagle's medium-Ham's F12 medium
DMSO	Dimethyl sulfoxide
dNTPs	Deoxynucleotides
DPX	Distyrene Plasticizer Xylene
EB	Embryoid body
EDTA	Ethylenediaminetetraacetic acid
ESC	Embryonic stem cell
EtOH	Ethanol
FasL	Fas ligand
FBS	Fetal bovine serum

FCS	Fetal Calf serum
FGF2	Fibroblast growth factor 2
FITC	Fluorescein isothiocyanate
FOXO	Forkhead box O transcription factor
GAG	Glycosaminoglycans
GDF5	Growth/differentiation factor 5
gDNA	Genomic DNA
GSC2	Gene encoding Goosecoid 2
HAC	Human articular chondrocyte
hESC	Human embryonic stem cell
hiPSC	Human induced pluripotent stem cell
HIF	Hypoxia inducible factor
HUVECs	Human umbilical vein-derived endothelial cells
IGF-1	Insulin-like growth factor-1
IgG	Immunoglobulin G
IgM	Immunogloblin M
IHH	Indian hedgehog
iMEF	Irradiated mouse embryonic fibrobast
iPSC	Induced pluripotent stem cell
ITS	Insulin-Transferrin-Selenium
KDR	Gene encoding kinase insert domain receptor
KOSR	KnockOut serum replacement
LGMD	Limb girdle muscular dystrophy
LIUS	Low intensity ultrasound
MACI	Matrix assisted autologous chondrocyte implantation
MEF	Mouse embryonic fibroblast
MD	Muscular dystrophy
M-MLV RT	Moloney murine leukaemia virus reverse transcriptase
MMP-13	Matrix Metalloproteinase 13
MSC	Mesenchymal stem cell
NSAIDs	Non-steroidal anti-inflammatories
NT4	Neurotrophin-4
O_2	Oxygen
OA	Osteoarthritis
OAC	Osteoarthritic chondrocyte
OAZ1	Gene encoding Ornithine Decarboxylase Antizyme 1

OCT4	Octamer-binding transcription factor 4
OP	Osteoporosis
PBS	Phosphate buffered saline
PDGF-AB	Platelet-derived growth factor-AB
PDMS	Polydimethylsiloxane
PI3K	Phosphoinositide 3-kinase
PMMA	Poly(methyl methacrylate)
PPR1	PTH/PTHrP receptor 1
PSC	Pluripotent stem cell
PTHrP	Parathyroid hormone-related protein
RT-qPCR	Real time-quantitative polymerase chain reaction
SSEA1	Stage-specific embryonic antigen 1
SOX2	Sex determining region Y-box 2
SOX9	Sex determining region Y-box 9
SSC	Skeletal stem cell
TGF-β3	Transforming growth factor-beta 3
TJR	Total joint replacement
UBC	Gene encoding Ubiquitin C
US	Ultrasound
USNCB	United States National Committee on Biomechanics
USWF	Ultrasonic standing wave field
USWT	Ultrasonic standing wave trap
Vpp	Peak-to-peak voltage
WNT3A	Wingless-type MMTV integration site family, member 3A

Chapter 1 Introduction

1.1 Socioeconomic burden of musculoskeletal disease

Non-communicable disorders affecting the musculoskeletal system are a major cause of disability and morbidity. A decline in the function of bone, muscle and joint tissues is currently an inescapable consequence of ageing. Due to improved healthcare, longevity has increased; however, whilst lifespan has improved, a corresponding increase in health span (years lived in good health) has not been achieved. As a result, the incidence of musculoskeletal disorders in a rapidly expanding ageing population is increasing (Nedergaard et al., 2013). The Global Burden of Disease study highlighted the impact of musculoskeletal disorders worldwide, and estimated that the number of disability adjusted life years (DALYs) that were attributed to musculoskeletal disorders increased by 17.7% between 2005 and 2013 (Murray et al., 2015), with osteoarthritis increasing by 23.2% from 10401.5 to 12811.1 DALYs. This has contributed to a huge financial strain on healthcare systems, as well as affected individuals. Moreover, the associated side effects of these disorders, such as intense and often chronic pain, coupled with decreased mobility, has a dramatic impact on quality of life. Current treatments are limited in their efficacy (Antebi et al., 2014; Hunter et al., 2011; Malafarina et al., 2012; Rodino-Klapac et al., 2013) . Furthermore, the subsequent progressive deterioration of the musculoskeletal system results in an increased fall and fracture risk (Dargent-Molina et al., 1996; Horlings et al., 2008; Landi et al., 2012; Wild et al., 1980). The natural healing of fractures is often poor in the older population, and carries a higher risk of mortality (Johnell and Kanis, 2004). Effective treatments for musculoskeletal disorders are therefore necessary to improve the quality of life of our ageing population, and decrease the burden placed on the healthcare system.

1.2 Osteoarthritis: Current treatment interventions and their limitations

1.2.1 Physiology and structure of Articular Cartilage

Cartilage is a flexible but strong tissue with the biological functions of forming the supporting framework for internal organs, and coating the articulating surfaces of bones. There are three distinct types of cartilage: elastic, fibrous and hyaline (Figure 1.1). Elastic cartilage, as its name suggests, contains elastic fibres with the principle protein being elastin which gives the tissue flexibility. Elastic cartilage is found in places such as the epiglottis and the ears. Fibrous, or

fibrocartilage, is found between the intervertebral discs, menisci, and the temporal mandibular joint. It contains both collagens type I and II. Hyaline cartilage is the most widespread type of cartilage and covers the ends of long bones in adults, as well as the ends of ribs and parts of the trachea. During development, bones are first formed as hyaline cartilage before endochondral ossification occurs. Hyaline cartilage matrix is more homogenous than elastic or fibrous and appears as a smooth glass-like surface.

Articular cartilage is a specialised type of hyaline cartilage that allows for smooth articulation of the joint by reducing friction and providing cushioning against impact (Sophia Fox et al., 2009). Types II, VI, IX and XI constitute the main collagens found in articular cartilage, with type II collagen being the most abundant and providing much of the tensile strength. Articular cartilage is also rich in proteoglycans, with aggrecan being the predominant type. Aggrecan consists of a protein core with negatively charged chondroitin and keratin sulfate glycosaminoglycan (GAG) chains attached. Due to the polar charge of the GAG chains, aggrecan traps water within the cartilage matrix, thus contributing to the compressibility of articular cartilage. Cartilage is monocellular and is synthesised and maintained by a population of cells called chondrocytes (Figure 1.1). These cells are low in number but provide essential roles in cartilage maintenance by forming extracellular matrix consisting primarily of collagens and proteoglycans.

Articular cartilage is formed of distinct regions with cell and tissue morphology differing between zones (Figure 1.1). The thin superficial zone protects the underlying cartilage from shear stresses and is approximately 10-20% of the total cartilage depth. Here collagen fibres (mainly type II and IX) are tightly packed and are positioned in parallel, and there exist a relatively high number of flattened chondrocytes. Beneath the superficial zone lies the middle zone, which is rich in proteoglycans and consists of approximately 40-60% of the total cartilage volume. The middle zone provides some of the resistance to compressive forces endured by articular cartilage. However, it is the deep zone that provides the greatest resistance to compression. Here, collagen fibrils are arranged perpendicular to the surface. The deep zone contains the highest proteoglycan and lowest water content.

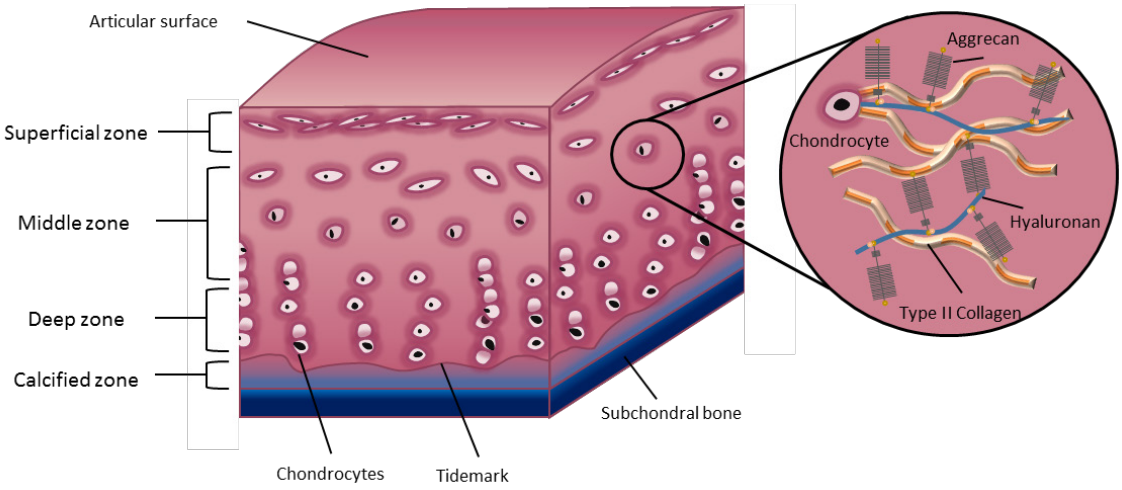

Figure 1.1 **Diagram depicting the principle structure and components of hyaline articular cartilage.**

Hyaline articular cartilage is a zonal tissue with distinct chondrocyte morphologies in the different regions. The surface is smooth and enables joint articulation. Chondrocytes are located within lacunae in the cartilage tissue. In the superficial zone the chondrocytes have a flattened morphology and align parallel to the surface of the tissue. In the middle zone chondrocytes are rounded and dispersed within the extracellular matrix. In the deep zone rounded hypertrophic chondrocytes orientate into columns perpendicular to the joint surface. The tide mark distinguishes the deep zone from the calcified cartilage, and the calcified cartilage anchors the cartilage to the subchondral bone. Principle constituents of hyaline articular cartilage are type II collagen, hyaluronan and aggrecan.

1.2.1.1 Developmental chondrogenesis and cartilage maintenance

The distinct morphologies and functions of the cartilage layers are enabled by the differences in the differentiation and proliferation of chondrocytes. This is tightly regulated by many cytokines and signalling pathways.

1.2.1.1.1 Endochondral ossification

Chondrocytes arise from mesodermal lineage cells during skeletal development and synthesise a cartilage analage that provides a template for developing bone that forms during endochondral ossification. Chondrogenesis occurs following the condensation of mesenchymal cells and differentiation of chondrogenic progenitor cells that express the cartilage specific collagens II, IX and XI. The process of endochondral ossification occurs as the resting chondrocytes at the opposing ends of bones begin to proliferate, resulting in multiple chondrocytes occupying a single lacuna (cavity within the cartilage matrix). This is then followed by maturation and hypertrophy, where chondrocytes and their lacunae increase in size and cells begin to express hypertrophy markers such as type X collagen. The chondrocytes then undergo apoptosis which enables the process of endochondral ossification whereby the calcified hypertrophic cartilage is resorbed and replaced by bone.

Following chondrocyte hypertrophy, the hypertrophic cartilage is surrounded by a fibroblastic cell layer called the perichondrium. These cells differentiate into osteoblasts, forming the periost, a highly vascularised tissue. Blood vessels from the periost invade the matrix of the terminal hypertrophic chondrocytes, which has itself become calcified, and the chondrocytes there undergo apoptosis. Osteoblasts and osteoclasts invade the tissue and replace/remodel the calcified cartilage to produce mineralised bone. Osteoblasts in the periost simultaneously produce a calcified matrix, forming the bone collar which later forms the cortical bone. A key regulator of endochondral ossification is Indian Hedgehog (IHH), which is a growth factor secreted by prehypertrophic chondrocytes. IHH signals to both proliferating chondrocytes and cells of the periosteum. IHH activates chondrocyte proliferation, particularly in the highly proliferative chondrocytes that are organised in columns. In high concentrations IHH represses the expansion of the round proliferating chondrocyte population at the distal ends of the limb, but at low concentrations favours its expansion. IHH signalling functions to maintain cartilage in conjunction with Parathyroid-related Protein (PTHrP). IHH induces PTHrP expression in the distal chondrocytes which in turn activates the PTH/PTHrP receptor (PPR1) and inhibits hypertrophic differentiation and therefore the differentiation of IHH-secreting hypertrophic cells. This negative feedback loop maintains the pool of proliferating chondrocytes and regulates the rate of proliferation.

Commitment to the chondrogenic fate requires several cell fate decisions. The transcription factor SOX9, belonging to the family of 'high-mobility group box' proteins, is a key early chondrogenic marker. SOX9 binds to sequences in the *COL2A1* and *COL11A2* genes (Bi et al., 1999), along with other chondrogenic genes, resulting in expression of these cartilage specific collagens. SOX9 expression begins during chondrocyte condensation, and expression is maintained in proliferating chondrocytes. Mutations in *SOX9* result in campomelic dysplasia, characterised by malformations of the endochondral skeleton and is often lethal in new-borns due to respiratory difficulties. It has been demonstrated that in chimeric mice carrying SOX9 mutant cells, SOX9-deficient cells are excluded from cartilage condensations in a cell autonomous manner, and $Sox9^{-/-}$ cells failed to produce cartilage in teratomas, suggesting that SOX9 is required for chondrogenesis (Bi et al., 1999). The role of SOX9 in cartilage development and maintenance is complex. Until recently it was thought that SOX9 played a key role in the initiation of chondrogenesis and in the prevention of hypertrophy. The latter was largely believed to be the case as it has been demonstrated that chondrocytes lose *SOX9* mRNA as they undergo hypertrophic differentiation and suggested that SOX9 may repress *COL10A1* (a marker of chondrocyte hypertrophy). However, it has now been reported that SOX9 is required to permit both chondrocyte proliferation and hypertrophy (Dy et al., 2012; Ikegami et al., 2011), thus driving skeletal growth, but also to inhibit cell death or osteoblast transformation, thereby inhibiting endochondral ossification (Hattori et al., 2010).

WNT (Wingless-type MMTV integration site family))-signalling also plays an important role in regulating mesenchymal condensation. Activation of WNT-signalling via the canonical pathway induces stabilisation of β-catenin which acts downstream of WNT by translocation to the nucleus leading to transcriptional changes. Stabilisation of β-catenin represses SOX9 expression, thereby inhibiting cartilage formation. Loss of β-catenin activity is required to initiate chondrogenic differentiation in mesenchyme condensations. The loss of β- catenin results in defects in osteoblast formation; the interaction between β-catenin and WNT provides a balance between chondrocyte and osteoblast differentiation.

Postnatally, chondrocytes exist in a restricted domain between the ossified regions of the developing bone called the growth plate. Proliferation and differentiation of chondrocytes within this zone enables the process of bone growth through the elongation of the epiphyseal growth plates.

1.2.1.1.2 Adult cartilage

Healthy adult cartilage is generally considered to be a stable and quiescent tissue, particularly in terms of extracellular matrix turnover. Using ^{14}C dating methods it has been shown that collagen matrix has very limited replacement in adult life in both healthy and osteoarthritic cartilage,

however GAG turnover occurs at a rate of just a few years (Heinemeier et al., 2016). This suggests that in different parts of the cartilage extracellular matrix, the rate of turnover is quite different. For example, in the proteoglycan rich pericellular matrix of chondrocytes the turnover rate is high, whilst in the collagen rich domains the turnover is comparatively low. SOX9 appears to play a key role in the normal turnover of adult cartilage. Inactivation of *Sox9* in the articular chondrocytes of *Sox9$^{fl/fl}$AcanCreER* adult mice resulted in severe depletion of proteoglycans, but did not appear to affect collagens in the cartilage matrix (Henry et al., 2012).

The maintenance and repair of articular cartilage is controlled by several signalling pathways. Prominent bioactive growth factors that are involved in these signalling pathways belong to the TGF-β (transforming growth factor-β) superfamily. Notable members of this molecular family that are considered to be anabolic for cartilage metabolism include TGFβ-1, TGFβ-3, BMP7 (bone morphogenic protein 7), IGF-1 (insulin-like growth factor-1) and FGF-2 (fibroblast growth factor-2)(Fortier et al., 2011; Gupta et al., 2011; Loeser et al., 2003). Signalling via the ALK5 (anaplastic lymphoma kinase 5) receptor results in recruitment and phosphorylation of Smad 2/3 which then form a heterocomplex with Smad 4. The Smad 2/3/4 complex is then translocated into the nucleus which results in regulated expression of the stable chondrocyte markers type II collagen, SOX9 and Aggrecan (Figure 1.2). TGFβ signalling by BMP ligands via ALK1 and ALK6 receptors results in activation of Smad 1/5/8, leading to expression of hypertrophic chondrocyte markers such as MMP-13 (matrix metalloproteinase-13) and type X collagen. As articular cartilage is stable under physiological conditions, signalling occurs predominantly via ALK5 receptors. In growth plate cartilage where chondrocytes become hypertrophic, signalling occurs through the ALK1 and 6 receptors.

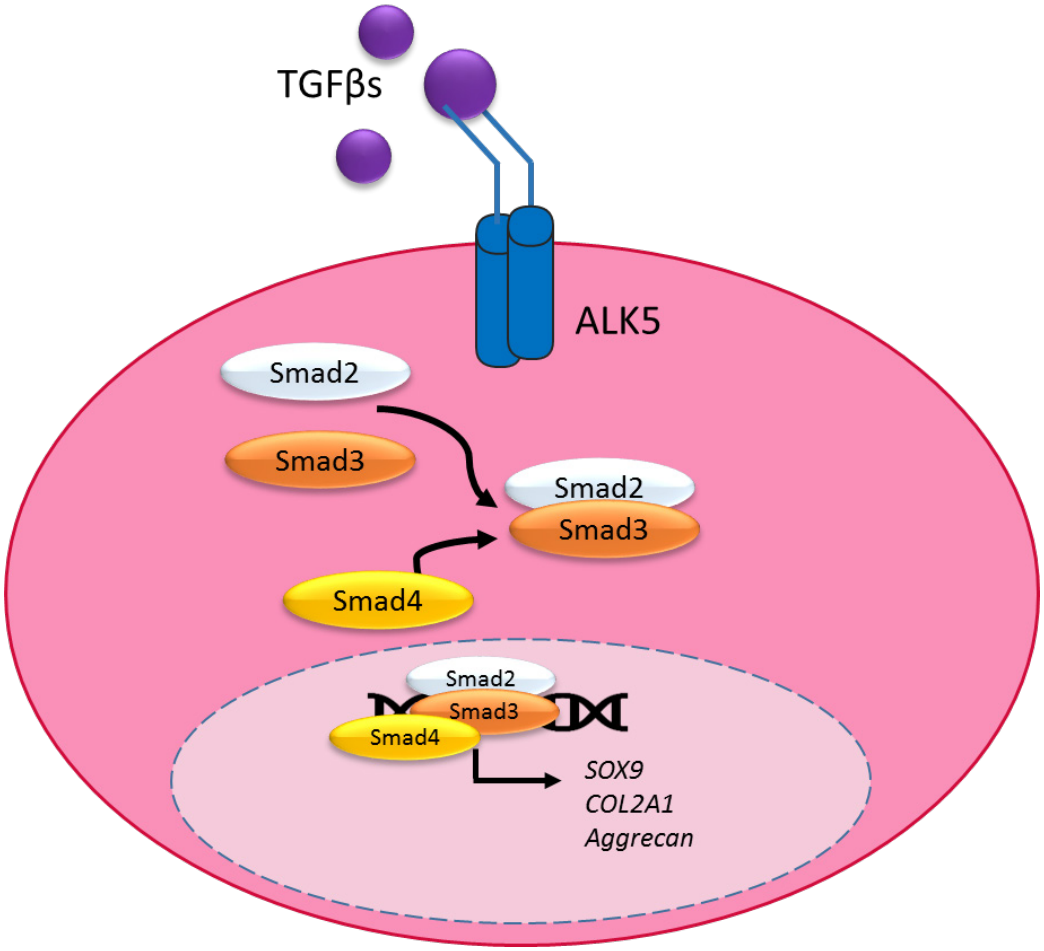

Figure 1.2 **Regulatory control of chondrocyte gene expression via SMAD signalling.** *TGFβ signalling via the ALK5 receptor results in recruitment and phosphorylation of Smad 2/3 which then form a heterocomplex with Smad 4. The Smad 2/3/4 complex is then translocated into the nucleus which results in regulated expression of the stable chondrocyte markers type II collagen, SOX9 and aggrecan.*

1.2.2 Osteoarthritis (OA)

OA is the most common joint disease amongst older adults (Control and Prevention, 2010), with OA of the knee joint estimated to have a global prevalence of 3.6% (Cross et al., 2014). Whilst the percentage of global prevalence remained constant between 1990 and 2010, the disability adjusted life years increased dramatically (Murray et al., 2015), thus demonstrating the impact of increased lifespan without a corresponding improvement in health span.

OA is caused by the degradation of hyaline articular cartilage and the abnormal remodelling of the joint tissues, which results in loss of joint function. Cartilage is avascular, aneural, has low cellularity and, therefore, a limited capacity for repair. Daily wear and tear or injury leads to the structural deterioration of articular cartilage at the joint surface. The early stages of OA are characterised by the formation of partial thickness chondral defects. If left untreated the defects will extend throughout the cartilage, forming a full thickness chondral defect, and eventually into the underlying subchondral bone, resulting in an osteochondral defect, allowing infiltration of bone marrow stem cells. The progression and characteristic hallmarks of OA are shown in Figure 1.1.3. The damage is largely irreversible, and any cartilage formed by the infiltrating stem cells is typically fibrocartilaginous rather than hyaline (Pritzker et al., 2006).

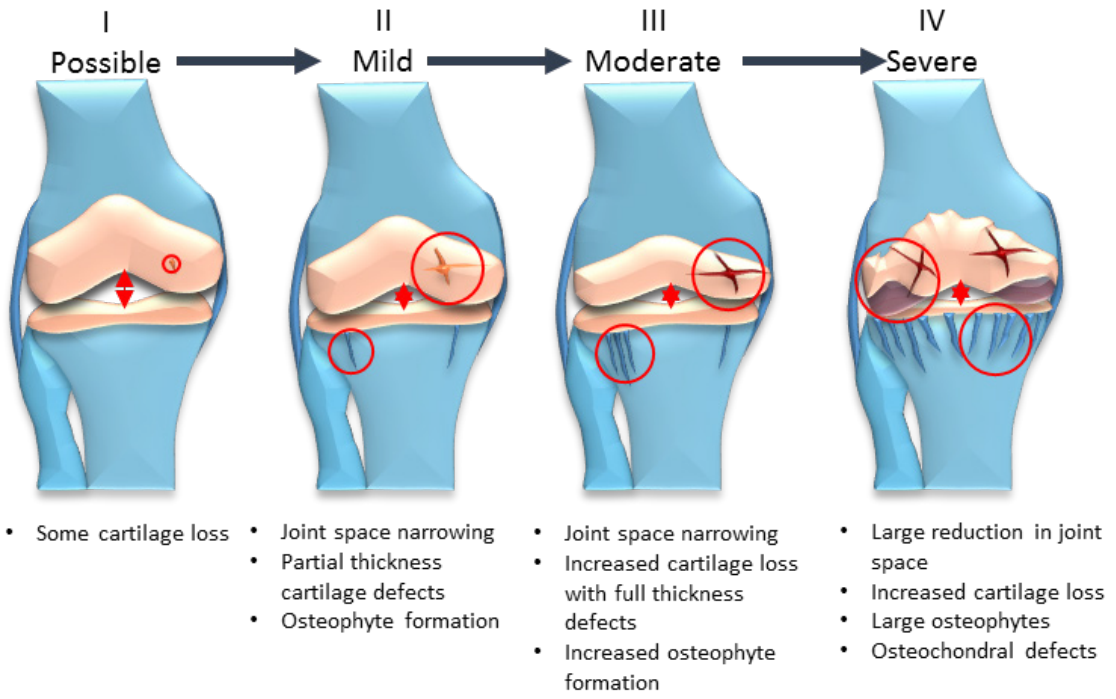

Figure 1.1.3 **Schematic diagram depicting stages of Osteoarthritis (OA) in the knee.**

OA initially manifests with small defects and low level cartilage loss. As the disease progresses the joint space begins to narrow, cartilage defects increase in size and bony ridges known as osteophytes begin to form. Further progression results in the formation of full thickness cartilage defects and increased osteophyte formation. In severe OA there is a large reduction in the joint space, widespread cartilage loss and the formation of osteochondral defects that extend through the cartilage and into the subchondral bone.

1.2.3 OA treatments

Management of OA of the hip and knee falls into three categories: non-pharmacological, pharmacological and surgical intervention. Clinical guidelines recommend a combination of pharmacological and nonpharmacological treatments before surgical options are explored (Zhang et al., 2008). Nonpharmacological treatments include lifestyle recommendations such as weight loss and exercise, whilst pharmacological treatments mainly symptomatic and include analgesics and potentially nonsteroidal anti-inflammatories (NSAIDs) (Kongtharvonskul et al., 2015).

Effective treatments for OA are currently lacking (see *Table 1.*). Whilst pharmacological treatment using NSAIDs provide temporary relief, they carry a risk of gastro-intestinal bleeding and vascular adverse events (Blandizzi et al., 2009; Mukherjee et al., 2001). Total joint replacement (TJR) surgeries are widely used, however these surgeries carry significant risks which increase with patient age (D'Apuzzo et al., 2014) and are a late stage treatment option. Early stage interventions are available and focus on initiating cell-based repair. Reparative techniques such as abrasion arthroplasty (Johnson, 2001), drilling (debridement) (Insall, 1974), and microfracture (Mithoefer et al., 2006) aim to encourage infiltration of stem cells from the underlying marrow spaces of the subchondral bone to stimulate repair of the damaged tissue. Restorative techniques such as mosaicplasty (Bentley et al., 2012) involve removing cartilage plugs from what are considered non-load bearing regions of the joint, and implanting them into the osteochondral defect site.

Another restorative surgical technique is autologous chondrocyte implantation (ACI) (Brittberg et al., 1994); here, patient-derived autologous chondrocytes are harvested from non-load bearing regions of the articular cartilage, expanded in monolayer culture and implanted at the site of damage. The procedure has significantly evolved over the last two decades. First generation ACI utilized a periosteal patch to cover the defect (Brittberg et al., 1994), but this process was associated with hypertrophy; second generation ACI therefore used a collagen patch to seal the defect (Marcacci et al., 2007); third generation ACI now involves the application of chondrocytes within a matrix and is referred to as matrix-assisted ACI (MACI) (Selmi et al., 2008). A major difference between ACI and other treatments for damaged cartilage is that ACI requires 2 stages. The first stage involves arthroscopically harvesting cartilage from non-weight-bearing regions of the joint, and monolayer expansion of the isolated chondrocyte *in vitro*. The second stage is implantation of the expanded chondrocyte population into the defect.

ACI has in the past been seen as a salvage procedure for cartilage defects in the knee following unsuccessful primary treatments by the aforementioned methods. Microfracture is often considered to be a first-line treatment due to ease of the procedure and relative low cost. Short

term outcomes for microfracture are typically good (Mithoefer et al., 2009); however, it has been suggested that long term the outcomes worsen after 5 years postoperatively (Gobbi et al., 2014). However, it is now being proposed that ACI be a first-line treatment in certain cases (Welch et al., 2016). In October 2017, NICE published guidelines that support the application of ACI for patients with symptomatic articular cartilage defects in the knee (NICE, 2017). To be eligible for treatment patients must not have had previous surgery to repair articular cartilage defects, must have only minimal osteoarthritic damage to the knee, and the defect must be larger than $2cm^2$. Recently, NICE published guidelines for the use of ACI using chondrosphere (Spherox) for treating cartilage defects of the femoral condyle and patella (NICE, 2018). Chondrosphere consists of small spheroids of neocartilage composed of the patient's culture expanded chondrocytes and extracellular matrix.

However, whilst ACI has been relatively successful compared to other techniques such as mosaicplasty (Bentley et al., 2012), the benefits over microfracture are unclear with systematic reviews finding similar improvements in clinical outcomes for patients treated with ACI and microfracture at midterm to long-term follow up (Kraeutler et al., 2018). There are also a number of drawbacks associated with the treatment (Table 1.1). One important issue is that human articular chondrocytes (HACs) are known to dedifferentiate during monolayer culture (Schnabel et al., 2002), and thus the cells that are re-implanted have lost their chondrogenic phenotype. ACI has been found to provide effective temporary relief for the symptoms of OA but frequently fails to provide an effective long term treatment (Harris et al., 2010; Redman et al., 2005) due to the sub-optimal quality of the fibrocartilaginous repair tissue (Horas et al., 2003; Redman et al., 2005). However, a study based on patient-reported outcomes of ACI procedures have been shown to perform well in terms of long-term follow up (10-20 years after implantation) (Peterson et al., 2010). It is therefore difficult to draw a clear conclusion regarding the long-term benefits of ACI.

The aforementioned treatments all involve surgical procedures that could compromise the stability of the existing joint tissue due to harvested material from healthy/non-load bearing regions of the joint. They also produce sub-standard cartilage that is typically fibrous rather than hyaline. As such, alternative methods of treatment that do not involve damaging healthy areas of cartilage are essential. Recent endorsement of ACI, and ACI using chondrosphere, by NICE clearly indicates a clinical focus on restorative techniques for cartilage treatment. The publication of guidelines regarding Chondrosphere suggest that a tissue engineering approach may be the next stage in ACI evolution.

Table 1.1 **Overview of epidemiology and treatment options for musculoskeletal diseases.**

Table adapted from (Jevons et al., 2018)

Disease	Incidence/risk	Treatments	Drawbacks
Osteoarthritis	• Worldwide incidence of knee OA estimated at 3.8%, and hip OA 0.85% (Cross et al., 2014). • Lifetime risk of developing symptomatic knee OA ~40% in men and ~47% in women, with higher risk for obese individuals (Murphy et al., 2008).	<u>NSAIDs</u> <u>Total joint replacement</u> <u>Reparative techniques</u>: • Abrasion arthroplasty (Johnson, 2001) • Debridement (Insall, 1974) • Microfracture (Mithoefer et al., 2006) <u>Restorative techniques</u>: • Mosaicplasty • Autologous chondrocyte implantation (ACI)(Brittberg et al., 1994) • MACI	Risk of gastro-intestinal bleeding and vascular adverse events (Blandizzi et al., 2009; Mukherjee et al., 2001). Carries some degree of risk (D'Apuzzo et al., 2014), late stage intervention treatment. Limited repair, and typically results in fibrocartilaginous tissue. Invasive procedure to procure chondrocytes, limited cell number, dedifferentiation during monolayer expansion, expensive (not available on the NHS), typically results in fibrocartilaginous tissue.

1.2.3.1 Immune privileged status of cartilage

Immune privilege exists where an antigen normally does not initiate an immune reaction. When developing new treatments for diseases it is important to consider the potential issue of immunogenicity. The immune privileged status of cartilage tissue is currently under some debate.

Certain tissues such as the eye, brain, ovary, testis, and pregnant uterus are well established immune privileged sites (Streilein, 1995). The mechanisms maintaining immune privilege are thought to include a lack of lymphatic drainage, the presence of a physical barrier, and the production of immunosuppressive cytokines/neuropeptides (Streilein, 1995). Cartilage is widely considered to be immune privileged due to a lack of innervation and vascularisation. However, it has been observed that implantation of allogeneic chondrocytes results in a rapid immune response whilst transplantation of osteochondral allografts has high success rates. This led to the theory that allogenic chondrocytes are indeed immunogenic, but an ECM acts to form a protective barrier around the chondrocytes, thereby shielding this immunogenicity and enabling grafts with sufficient matrix accumulation to resist immune rejection (Revell and Athanasiou, 2008).

One study investigating immunogenicity in cartilage found that donor source and lesion location were key factors. Here, scaffold-free tissue engineered cartilage constructs from either xenogeneic bovine or allogeneic leporine (rabbit) chondrocytes were implanted into defects in the patella or the trochlea of rabbits. It was hypothesized that allogeneic but not xenogeneic engineered tissue would be suitable for cartilage repair. However, it was concluded that the knee joint cartilage does not represent an immune privileged site, with strong rejection of xenogeneic but not allogeneic chondrocytes in a location-dependent fashion. The difference in survival of allogeneic tissue may be associated with proximity to the synovium (Arzi et al., 2015).

A molecular basis for immune privilege has been identified and is mediated by the expression of certain ligands, including FasL (fas ligand, or CD95) (Bellgrau et al., 1995). Interestingly, it has been shown that chondrocytes in tissue engineered cartilage express FasL, along with other markers that are associated with immune privilege (Fujihara et al., 2010). In a subcutaneous transplantation study it was observed that FasL expression on chondrocytes was induced by macrophages and conferred immune privilege to the tissue engineered construct (Fujihara et al., 2014). This may indicate that the process of *in vitro* tissue engineering may provide some protection from immunogenicity.

1.3 A tissue engineering approach to cartilage repair

Current therapies for cartilage damage have not yet demonstrated a full restoration of the damaged tissue to its original hyaline state. Some pharmacological treatments such as NSAIDs can ameliorate the symptoms, however the side effects associated with long term use make them inadequate as a therapeutic option (Table 1.1). Cell therapies such MACI have been shown to be effective; however, the long-term repair of damaged tissue remains an issue, as does the formation of fibrous rather than hyaline cartilage. A new and innovative approach for cartilage repair is required to enable damaged tissue to be replaced with new tissue that is morphologically and functionally the same as healthy native tissue, thereby enabling effective clinical applications.

Tissue engineering aims to repair, maintain, or enhance native tissue. This is enabled by cell culture with the use of growth factors, scaffolds and bioreactor systems to generate a 3D tissue construct *in vitro,* before implantation. A clear benefit is that 3D culture aims to help recapitulate the *in vivo* environment, by enabling more complex and physiological cell-cell contact in the early stages of the culture period compared to monolayer culture and allows the deposition of extracellular matrix to enable formation of 3D aggregates. It is therefore expected to allow the successful generation of musculoskeletal tissues *in vitro.* This approach ensures that suitable tissue constructs with the appropriate physiological and mechanical properties are formed, thus providing a level of control that is not possible with cell transplantation techniques. The recent publication of guidelines by NICE regarding the use of ACI with chondrosphere (NICE, 2018) indicate that the treatment of cartilage defects is leaning towards a tissue engineering approach.

The development of a clinically relevant and beneficial tissue engineering-based treatment for cartilage damage is desirable. However, it is worth noting that some tissues are, relatively, easier to replicate *in-vitro* than others. Cartilage, unlike bone and muscle, is monocellular and does not require a blood supply. Whilst this characteristic makes cartilage unable to adequately self-repair following damage, the relative simplicity does make cartilage an ideal tissue type for an *in-vitro* tissue engineering approach.

1.3.1 Scaffold-based cartilage tissue engineering

The traditional tissue engineering paradigm incorporates cells, signalling molecules and scaffolds. Exogenous scaffolds are useful as they provide a 3D structure that enables cell adherence and allows cells to proliferate and produce extracellular matrix in a more spatially relevant environment compared to monolayer cell culture. It is a requirement that scaffold materials are both biocompatible and biodegradable and provide appropriate mechanical properties for cells seeded onto the material. Biomaterial scaffolds can be classified at either synthetic or natural,

which can then be subdivided into whether they are protein or polysaccharide based. Commonly used natural protein-based scaffolds include collagen, fibrin and silk; commonly used polysaccharide based scaffolds include hyaluronic acid, chitosan, cellulose and alginate (Vinatier and Guicheux, 2016).

Natural polymers such as hyaluronic acid and type-II collagen are key constituents of hyaline articular cartilage, and therefore provide a physiologically relevant base for tissue engineered cartilage. It is therefore no surprise that these biomaterials are among those used clinically in ACI procedures. Membranes consisting of type I and II collagen are used for MACI procedures (Cherubino et al., 2003; Vinatier and Guicheux, 2016), and the hyaluronic-acid based scaffold, HYAFF-11 has also been tested in the clinic with favourable results (Nehrer et al., 2006). However, due to concerns regarding a lack of safety and efficacy data, HYAFF-11 is no longer available. Experimental approaches using ECM fragments such as fibronectin have also been shown to support hESC chondrogenesis (Cheng et al., 2018).

Different materials have inherently different characteristics such as stiffness. Cells are known to be sensitive to substrate stiffness (Engler et al., 2006), and manipulation of scaffold stiffness can therefore be exploited to direct cell behaviour and differentiation. An additional benefit of scaffold-based tissue engineering is that the scaffold can provide the mechanical integrity that may be required of the engineered tissue from an early stage of development. However, the biofunctionality, biocompatibility, degradation rates and immunogenicity of the degradation products can pose significant issues (Johnstone et al., 2013; Vacanti and Langer, 1999).

As discussed in section 1.2.1, articular cartilage is zonally defined with distinct morphological differences in each zone. Scaffold based tissue engineering has been used to mimic this unique zonal organisation. Hydrogel-based attempts have involved developing multi-layer (Kim et al., 2003; Sharma et al., 2007) and gradient hydrogels (Zhu et al., 2018) between which the biochemical and/or the mechanical properties of the material are distinct. Multi-layer hydrogels are simpler to construct in comparison to gradient gels, however they are typically weaker in comparison and contain discrete layers (Sharma et al., 2007) which can result in delamination. A persistent issue with both approaches has been that the hydrogel is nanoporous which results in cells being physically constrained within the gel leading to an delays in matrix deposition and localisation only to the pericellular region (Sharma et al., 2007; Zhu et al., 2018). As a result much of the scaffold material remains unaffected and is not easily remodelled. In an attempt to overcome many of these limitations, one group has developed spatially patterned μ-ribbons (μRB) to guide MSC-based cartilage regeneration (Gegg and Yang, 2020). They observed that by tuning μRB alignment and composition, MSCs were directed to create neocartilage with zonal

biochemical, morphological, and mechanical properties. Alignment of gelatin μRBs in the 'superficial zone' resulted in robust collagen deposition and expression of superficial zone protein when cells were cultured in the scaffold. Cell laden scaffold stained positive for the presence of proteoglycans, a key constituent of articular cartilage, following 21-days culture.

1.3.2 Scaffold-free cartilage tissue engineering

Due to the complications of incorporating exogenous scaffold materials, there has been a shift towards scaffold-free tissue engineering strategies. Tissue engineering without scaffolds refers to any platform that does not require an exogenous, 3D material for cell seeding and culture (Athanasiou et al., 2013). Scaffold-free tissue engineering requires cells to provide their own 3D framework for tissue generation and is therefore more likely to faithfully recapitulate the developmental process of tissue generation.

3D pellet culture is the current 'gold standard' for cartilage tissue engineering and has frequently been used to demonstrate the *in vitro* cartilage forming potential of chondrogenic cells (Li et al., 2015; Manning and Bonner Jr, 1967; Tare et al., 2005). This technique involves the centrifugation of cells to form a pellet which is typically cultured for 21-days. This scaffold free approach has shown to enhance cartilage formation compared to encapsulation in 'gel-like biomaterials' (Bernstein et al., 2009). Chondrocytes dedifferentiate during monolayer culture expansion (Schnabel et al., 2002). Aggregation of these cells into a 3D pellet, in the presence of chondro-inductive factors helps to restore the chondrogenic phenotype. Whilst pellet culture is generally considered the gold standard for *in vitro* cartilage generation, it is doubtful that this method would permit the generation of tissue constructs of a clinically relevant size as pellets typically measure ~1mm diameter. If larger pellets are allowed to form they typically contain necrotic cores (Li et al., 2014c; Muschler et al., 2004).

To enhance chondrogenesis, exogenous factors are routinely added to chondrogenic culture medium, typically with the aim of enhancing collagen deposition. Ascorbic acid has been shown to enhance collagen production (Hata and Senoo, 1989; Temu et al., 2010); enhanced synthesis is due to ascorbic acid being an essential component of hydroxyproline and hydroxylysine which are required for stabilizing the collagen triple helix and for intermolecular crosslinking respectively (Murad et al., 1981). Transforming growth factor- β1 (TGF-β1) and TGF-β3 are also commonly incorporated into chondrogenic media (Tang et al., 2009).. TGF-β is involved in the regulation of SOX9 by mediating phosphorylation and stabilisation via both p38 and Smad2/3 (Coricor and Serra, 2016). SOX9 is a key transcriptional regulator of chondrogenesis, and directly regulates the

expression of the type II collagen gene (*COL2A1*) (Bell et al., 1997) This allows prolonged activation of *COL2A1* and therefore enhances chondrogenesis.

Without a scaffold to impart mechanical cues such as stiffness, cells may not be receiving adequate information to enhance tissue generation. However, perfusion based bioreactor tissue culture systems (Schulz and Bader, 2007) and the incorporation of ultrasound (Li et al., 2014b) have been shown to provide mechanical cues in a scaffold free environment. This will be discussed in more detail in section 1.5.3.1.3.

1.3.3 Mechanical testing of tissue engineered cartilage constructs

The mechanical properties of tissue engineered constructs are important as they directly relate to a tissue's function. This is particularly true for musculoskeletal tissues such as cartilage, bone, and muscle, as their mechanical properties and structural integrity play fundamental physiological roles. The ability to engineer and validate tissue engineered constructs pre-implantation is therefore advantageous. This overcomes one of the pitfalls of cell therapy, which is the inability to determine specifically what sort of tissue will form subsequent to implantation, and whether it is suitable for purpose.

As mentioned in section 1.3.1, cells are known to be sensitive to substrate stiffness which can determine stem cell differentiation (Engler et al., 2006). The bioengineered cartilage tissue will therefore influence cell behaviour, making it imperative that the mechanical properties of are properly validated. Despite the importance of examining the mechanical properties of engineered cartilage, it is not commonly investigated. The elastic modulus of a substance is defined as the ratio of the force exerted upon a substance or body to the resultant deformation. Native cartilage is reported to have an elastic modulus in the range 0.45 to 0.80 MPa (Boschetti et al., 2004; Mansour, 2003).

Previously our group tested the elastic modulus of cartilage generated in an acoustofluidic perfusion bioreactor using HACs which was compared to native cartilage using indentation type-atomic force microscopy; the local elastic modulus for native cartilage was found to be approximately 1.3 MPa, and for the engineered cartilage approximately 1 MPa (Li et al., 2014b). Interestingly, other work from our group estimated the Elastic modulus of engineered and native cartilage to be in the region of 0.1-0.3MPa (Jonnalagadda et al., 2018). Here, a nanoindentation technique was used, and whilst the data suggested no significant difference between native and engineered tissue, the elastic modulus was reported as being much lower than was reported elsewhere in the literature (Boschetti et al., 2004; Mansour, 2003). Different assessment methods

appear to produce different values for E. To ensure accuracy or data interpretation it is imperative that studies test both native and engineered tissue using the same device.

Not all studies have found the elastic modulus of the engineered tissue to be equivalent to that of the native cartilage tested. For instance one study reported E for native cartilage to be approximately 1.5MPa, and approximately 0.5MPa for the engineered cartilage (Park et al., 2019). The technique used here was a variation on traditional pellet culture that involved the centrifugation of cell sheets rather than single cells to create a layered pellet. The resulting construct contained open spaces between the layers which probably resulted in the low elastic modulus as the tissue formed was not as dense as native cartilage. Note that this study was performed using rabbit cartilage, which likely accounts for the relatively high reporting for E compared to that reported in the literature for human cartilage.

1.4 Choosing the right cells for tissue engineering

The cell type used for bioengineering tissues is important, as certain cell types have inherent limitations in their ability to form new tissues.

Potency refers to the capacity to differentiate into more specialised cell types (Figure 1.4). A totipotent cell such as the zygote, has the ability to give rise to all embryonic, extraembryonic and placental tissues. Pluripotent cells such as embryonic stem cells (ESCs) are able to differentiate into cells of all three developmental lineages (endoderm, ectoderm and mesoderm). In adults, most tissues have a resident population of stem cells. These cells are multipotent and being even more lineage restricted, can differentiate into cells within a specific lineage. For example, skeletal stem cells (SSCs) can be found in the postnatal bone marrow and can give rise to bone, cartilage and adipose tissue (Bianco and Robey, 2015). The most restricted stem cell is termed unipotent and can only give rise to a single cell type, e.g. spermatogonia.

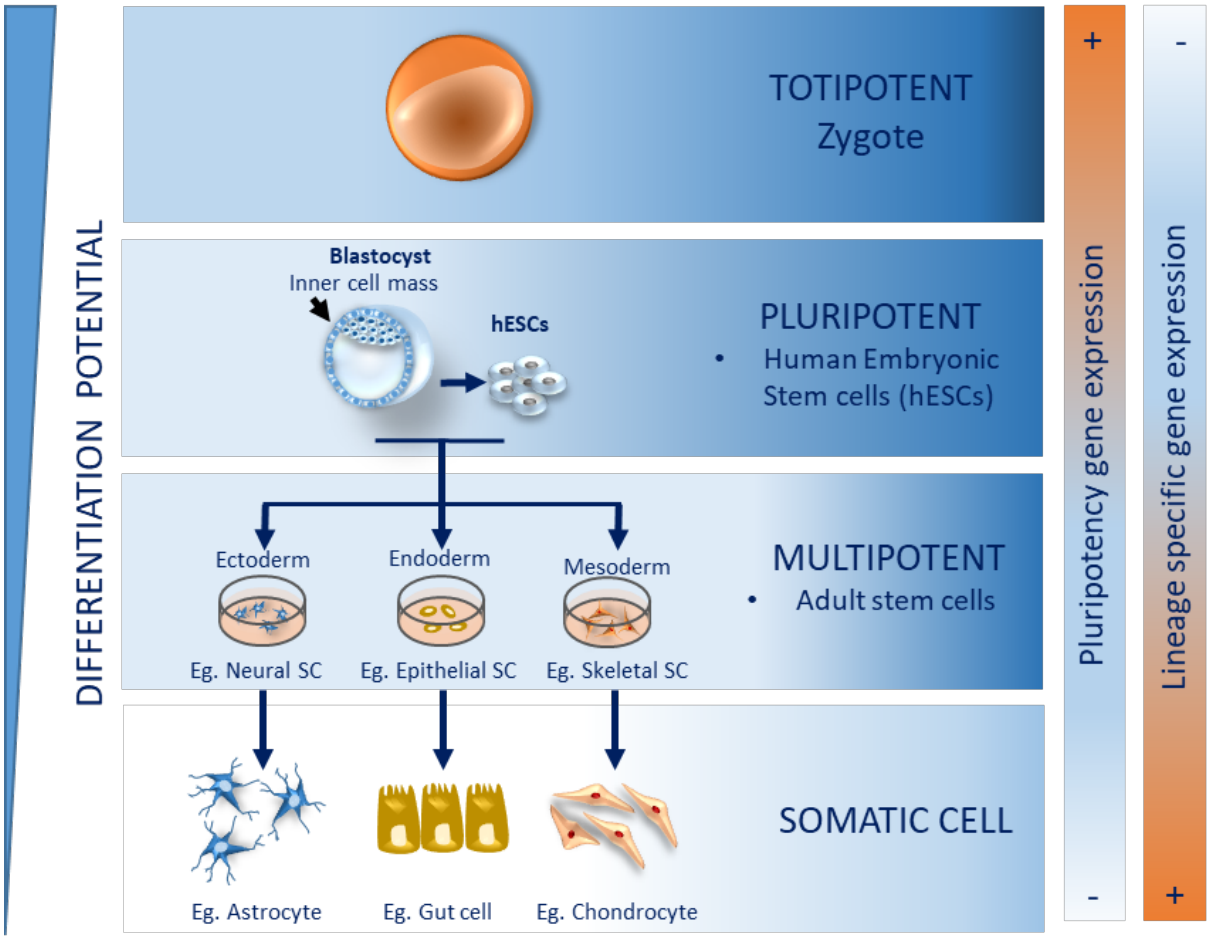

Figure 1.4 **Cell potency and lineage restriction**

Cell potency is hierarchical with the most potent being the zygote. The zygote is totipotent and has the potential to give rise to all embryonic and extraembryonic tissues. As cells begin to specialise, potency decreases; the next level of cell potency is pluripotency and refers to cells derived from the inner cell mass of the blastocyst (hESCs). Further specialisation leads lineage restriction whereby cells, eg. Adult stem cells can only differentiate into specialised cells of a specific lineage. Somatic cells are fully specialised.

1.4.1 Pluripotent stem cells (PSCs)

It is of significant clinical benefit to develop a method of restoring damaged tissue that maximises the quality of repair and minimises the risk to the patient. To this end, there has been a surge of research interest in the potential of pluripotent stem cells (PSC) for the treatment of skeletal disorders. PSC have the potential to differentiate into cells of all three germ layers (endoderm, mesoderm, ectoderm), and can therefore provide a source for any somatic cell in the body (Figure 1.5). PSCs can also proliferate indefinitely *in vitro,* without showing signs of cellular senescence. Therefore, PSCs have tremendous potential as a viable source of cells for musculoskeletal repair as they can be differentiated into cells of mesodermal origin, and subsequently used to regenerate tissues such as cartilage, bone and muscle.

There are two distinct types of PSCs, embryonic, and induced PSC (iPSCs) (Figure 1.5). Embryonic stem cells (ESCs) are derived from the inner cell mass of the blastocyst (Evans and Kaufman, 1981; Thomson et al., 1998), and were the only known source of PSC until 2006 when Yamanaka and Takahashi developed a technique for reprogramming somatic cells into iPSCs using mouse skin cells (Takahashi and Yamanaka, 2006), for which Yamanaka was awarded the 2012 Nobel Prize in medicine. iPSCs offer the potential for personalised regenerative therapy as they can be derived from the patient's own cells.

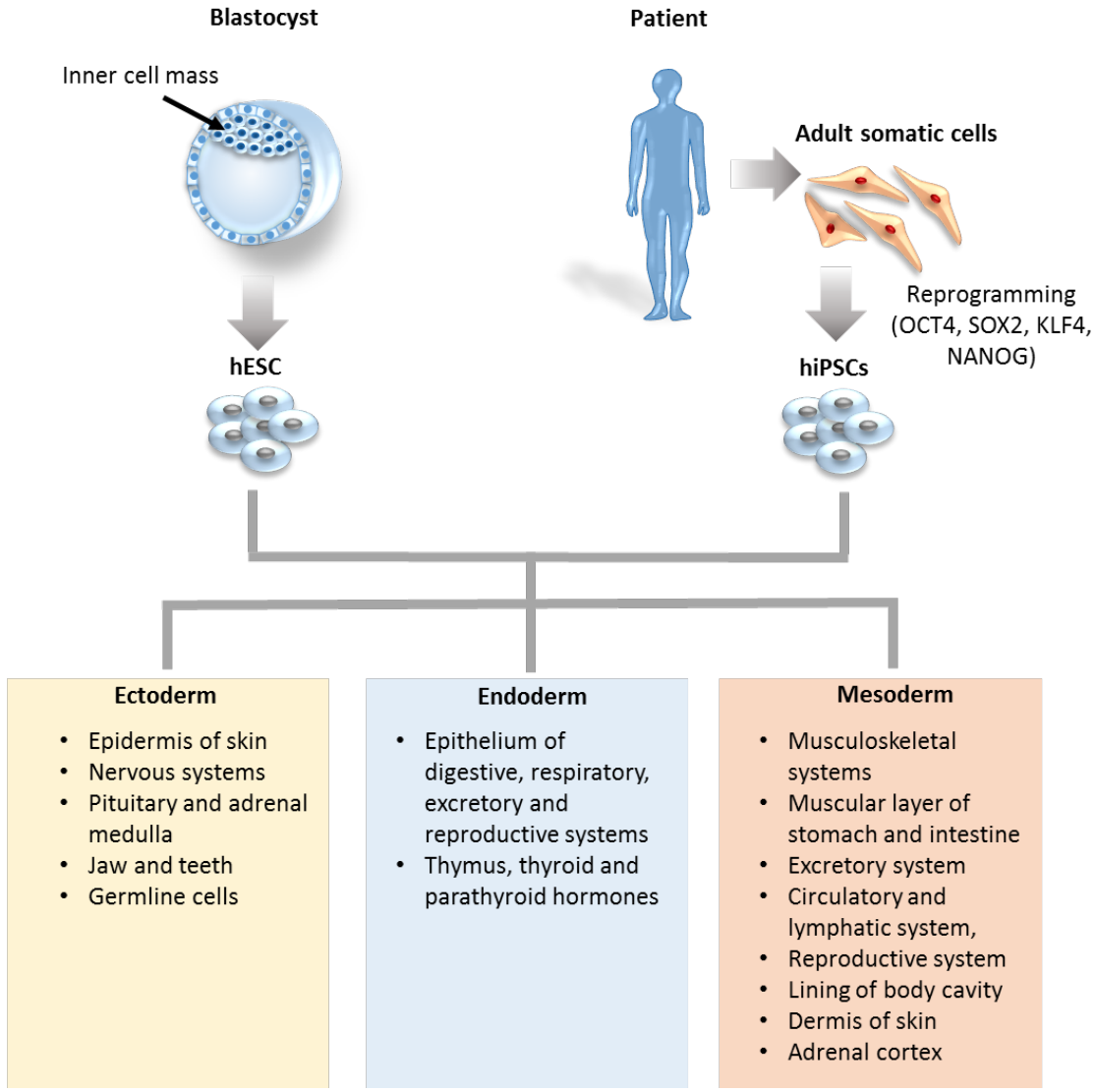

Figure 1.5 **Derivation and differentiation of pluripotent stem cells and differentiation.**

hESCs can be derived from the inner cell mass of a blastocyst at the final stage of preimplantation development. hiPSCs can be reprogrammed from somatic cells using the forced expression of OCT4, SOX2, KLF4, NANOG. These cells can subsequently be differentiated into any derivative of the three germ layers (ectoderm, endoderm, and mesoderm). (Jevons et al., 2018).

1.4.1.1 Regulation of pluripotency

Pluripotency is a cell state that exists only transiently *in vivo* during early embryonic development and can be recapitulated *in vitro* using tightly regulated culture conditions. *In vivo*, pluripotent cells first arise during the blastocyst stage of the embryo in the inner cell mass (ICM). The pluripotent state is controlled by the pluripotency gene regulatory network (PGRN) with a set of core transcription factors that serve as the PGRN hub: Octamer-binding transcription factor 4 (OCT4), SRY-box 2 (SOX2), and NANOG (derived from Tír na nÓg, Celtic for land of the young).

OCT4 is uniquely expressed in ESCs, the preimplantation embryo and primordial germ cells; it has been demonstrated to be essential for pluripotency both *in vitro*, and *in vivo* (Nichols et al., 1998; Niwa et al., 2000; Schöler et al., 1989). SOX2 is known to regulate OCT4 expression in mESCs (Masui et al., 2007), and is required for epiblast formation *in vivo* (Avilion et al., 2003). Loss of either OCT4 or SOX2 leads to trophectoderm differentiation, whereas overexpression drives differentiation of mesendoderm (OCT4) or neural ectoderm (SOX2) (Niwa et al., 2000; Thomson et al., 2011). NANOG, which has been shown to be regulated by OCT4 and SOX2 (Rodda et al., 2005), is involved in the acquisition of pluripotency in the ICM (Silva et al., 2009); however, it has been shown to be dispensable for the generation of iPSCs derived from murine cells (Schwarz et al., 2014).

Chromatin immunoprecipitation (ChIP) technology has been used to map the genomic binding sites of the core pluripotency factors. Such studies have revealed extensive OCT4, SOX2 and NANOG co-binding at multiple target sites. It has been suggested that the core pluripotency factors establish and maintain the pluripotent state by activating the expression of core ESC transcription factors whilst repressing the expression of lineage-specific genes, and by positive regulation of their own promoters and that of the other core pluripotency factors forming an interconnected auto-regulatory loop (Young, 2011). Co-localisation of these core factors provides a recruitment platform for additional regulatory factors such as co-activators, co-repressors, regulatory RNAs and epigenetic mechanisms (Li and Belmonte, 2017).

1.4.1.2 Human Embryonic Stem Cells (hESCs)

Human ESCs (hESCs) were first derived by Thomson et al. (1998). These cells originate from the preimplantation or periimplantation embryo, display prolonged undifferentiated proliferation, and stable developmental potential to form derivatives of all three embryonic germ layers even after prolonged culture (Thomson et al., 1998). This pluripotent potential can be tested *in vitro* via Embryoid Body (EB) formation, or *in vivo* via teratoma formation.

Since their discovery, hESCs have been heralded as a potential panacea for regenerative medicine. However, there has also been some debate over whether or not hESCs present an immunogenic risk. There has been evidence to suggest that hESCs trigger an immune response (Grinnemo et al., 2006), however there is also contrasting evidence to suggest that they are immune-privileged (Li et al., 2004), or have negligible immunogenicity (Araki et al., 2013). If hESCs do indeed elicit an immune response this would hinder clinical application. To resolve this it has been proposed that banks of clinical-grade hESC lines that can be HLA (human leukocyte antigen)-matched to groups of individuals could make hESCs a viable option for regenerative medicine (Nakajima et al., 2007; Taylor et al., 2005).

Based on principles used currently for organ transplantation it has been proposed that, approximately 150 consecutive blood group compatible donors, 100 consecutive blood group O donors, or ten highly selected homozygous donors could provide the maximal benefit for HLA matching (Taylor et al., 2005). The first option would produce the highest level of patient compatibility, whilst the latter two would reduce the range of compatibility but would be easier to generate. It was noted that beyond 150 blood group compatible donors conferred only a small incremental increased benefit. Using one of these methods it is therefore conceivable that HLA-banked hESC lines could be a viable option for avoiding potential issues of immune rejection.

Despite there being some controversy surrounding the therapeutic use of hESCs, just 12 years after their discovery hESCs were used in a clinical trial, run by Geron, for treatment of spinal cord injuries. However, just one year into the trial it was prematurely discontinued with only 4 of the planned 10 patients receiving treatment (Ilic et al., 2015; Scott and Magnus, 2014). Geron stated that their decision to terminate the trial would save the company at least $25 million per year, and that these resources could be used for the company's cancer programs (Scott and Magnus, 2014). Although the trial has officially been ended, Geron intends to monitor patients for a 15-year period.

Current trials are underway for the treatment of Stargardt's Macular Dystrophy and Dry Age Related Macular Degeneration and diabetes (Ilic et al., 2015; Schwartz et al., 2012). Early results for the treatment of wet age-related macular degeneration are promising, with reports of increased visual acuity after 12 months (da Cruz et al., 2018).

1.4.1.3 Human Induced Pluripotent Stem Cells (hiPSCs)

hiPSCs can be generated via the reprogramming of human somatic cells to a pluripotent state by overexpressing a set of key transcription factors: OCT3/4, SOX2, KLF4, and C-MYC (Takahashi et al., 2007). iPSCs have been found to be similar to hESCs in their morphological characteristics, self-

renewal capacity, differentiation potential, and gene expression profile (although there is some controversy regarding the latter (Doi et al., 2009)).

Reprogramming methods can be grouped into two categories: integrative systems and non-integrative systems. Integrative systems involve the integration of exogenous genetic material into the host genome; this was the first method of reprogramming used to generate iPSCs via retroviral transduction of the key factors (Takahashi et al., 2007; Takahashi and Yamanaka, 2006). However, reprogramming efficiencies are low, and the process of creating patient specific cell lines slow and costly. A further significant drawback is the potential for insertional mutagenesis which may increase the risk of tumour formation and genetic dysfunction (Takahashi et al., 2007; Yu et al., 2007).

To overcome these limitations, non-integrating adenovirus or completely DNA-free techniques have been developed (Kim et al., 2009; Yu et al., 2009). One study compared reprogramming using sendai-virus, episomal plasmids/Epi-reprogramming (use of Epstein-Barr virus-derived sequences) and mRNA reprogramming. mRNA was found to have the highest efficiency (2.1%), followed by Sendai-viral reprogramming (0.077%) and Epi-reprogramming (0.013%). They compared these techniques to lentiviral reprogramming (integrative system) and found the efficiency to be 0.27% (Schlaeger et al., 2015). Due to the relative increase in efficiency, reprogramming using mRNA may be a viable alternative to integrative methods.

The first in-human hiPSC clinical trial took place in 2014 (Li et al., 2014a). The successful implantation of hiPSC derived retinal pigment epithelium cells into a patient with age-related macular dystrophy was reported; however, the trial was prematurely suspended when it was found that the second patient's differentiated cells contained multiple mutations (Ilic et al., 2015). It remains unclear as to whether these mutations arose from the reprogramming process or were present in the patient's own somatic cells. Nevertheless, this has raised another important issue regarding the safety of hiPSCs. It has been suggested that an alternative trial using allogeneic hiPSCs may be a possibility (Ilic et al., 2015). In 2018 it was announced that a clinical trial using allogeneic hiPSCs was to be launched (Science, 2018). Researchers at Kyoto University are currently using hiPSCs to generate dopaminergic neurons and have transplanted these cells into at least one patient with Parkinson's disease so far.

The promise of hiPSCs was to develop autologous patient-specific cell-therapies, and so a conversion to allogeneic treatments arguably has no real patient benefit over the use of hESCs, although there would be no requirement for human embryos.

Whilst iPSCs display many of the characteristics of ESCs such as high proliferation under continuous culture without senescence, and the ability to form teratomas *in vivo*, there are also some fundamental differences. For example, hiPSCs have been shown to form teratomas with increased efficiency and decreased latency compared to hESCs (Gutierrez-Aranda et al., 2010). It has also been shown that miPSCs and hiPSCs, once programmed, retain the epigenetic signature of the somatic parent cell (Kim et al., 2010; Kim et al., 2011), and exhibit altered methylation patterns in some of the key pluripotency genes such as OCT4 (Doi et al., 2009). This 'epigenetic memory' can influence the behaviour of the reprogrammed cells directing them towards their lineage of origin or affecting their potency. This could potentially hinder attempts to differentiate iPSCs towards a designated lineage for clinical applications.

1.4.2 Advantages of using hESCs over hiPSCs for regenerative medicine

The advantages and disadvantages of using adult stem cells, hESCs and hiPSCs are outlined in Figure 1.6.

Whilst both hESCs and hiPSCs display the characteristic hallmarks of pluripotency, there are a number of issues associated with hiPSCs. hiPSCs would ideally be used with autologous origins. However, the process of deriving patient specific hiPSC lines would be costly and time consuming. A further issue relating to the use of hiPSCs is that they may contain somatic mutations or reprogramming-induced genetic/epigenetic defects, which would make them unsuitable candidates for regenerative medicine. The issue of epigenetic memory is also poignant in relation to regenerative therapies for musculoskeletal diseases where cells often undergo epigenetic changes during the disease process that alters cell phenotypes, as is the case in OA (Barter et al., 2012). Whilst alternative cell types could be used for reprogramming, it is worth bearing in mind that these cells themselves will probably have a specific epigenetic profile that could influence lineage specific differentiation.

hiPSCs have a huge potential for disease modelling, however their potential for use in regenerative medicine may be hindered by the aforementioned factors. With the potential for HLA matching it is feasible that banks of clinical grade hESCs could be generated to enable clinical applications of hESCs without issues of immunogenicity. There are many hESC lines currently available; The website human Pluripotent Stem Cell registry lists 739 hESC lines (hPSCreg, 2019), and as of February 2019 the US National Institutes of Health (NIH) listed 398 hESC lines for which research using these lines is eligible for NIH funding (NIH, 2019). It is likely that the 150 hESC-lines that are proposed to be required to HLA match most individuals (Taylor et al., 2005) have already been generated.

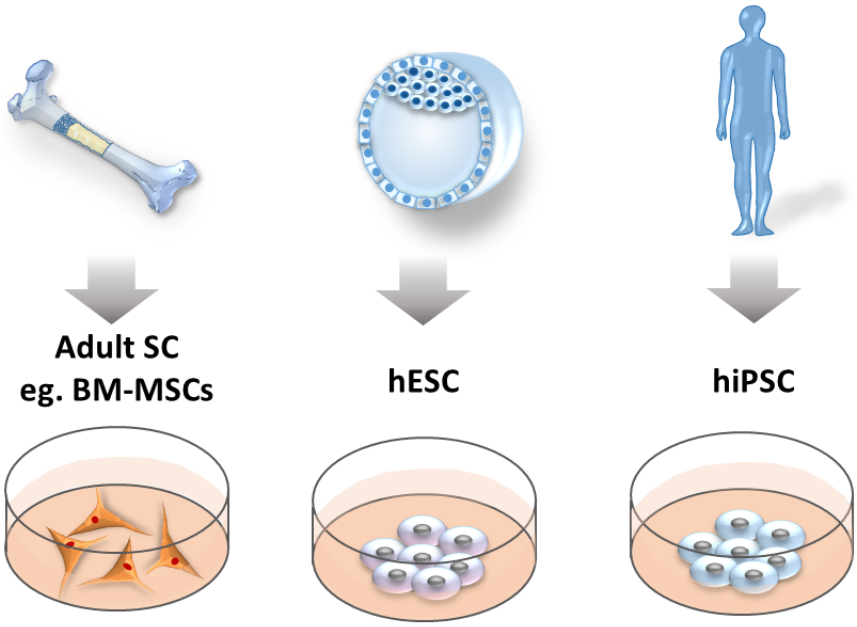

	Adult SC eg. BM-MSCs	hESC	hiPSC
Benefits	• Multipotent • Autologous • Comprehensive characterisation • Well established clinically	• Pluripotent • Allogenic • Extensive proliferation without senescence • High yield	• Pluripotent • Autologous • Extensive proliferation without senescence • High yield
Drawbacks	• Limited proliferation and differentiation capacity • Senescence • Heterogeneity • Low yields	• Possible immunogenicity • Ethical considerations • Risk of teratomas	• Low reprogramming efficiency • Epigenetic memory • Risk of teratomas

Figure 1.6 **Benefits and drawbacks of using adult stem cells and pluripotent stem cells for clinical applications.**

Comparison of the advantages and disadvantages of BM-MSCs, hESCs and hiPSCs for application in regenerative medicine (Jevons et al., 2018).

1.5 Harnessing the potential of hESCs for cartilage tissue engineering

1.5.1 Differentiation of hESCs into chondrocytes

To generate cartilage *in vitro*, first a chondrocyte population must be established. There are numerous techniques that have been developed to induce the *in vitro* differentiation of PSC into chondrocytes which have been reviewed extensively by Jevons et al. (2018).

1.5.1.1 Differentiation via Embryoid Bodies (EBs)

One of the first methods described was the generation of chondrocytes via the formation of embryoid bodies (EBs). These 3D structures share similar characteristics to the postimplantation embryo. EBs have frequently been used for targeted differentiation into certain cell types; it has been hypothesised that important signalling events take place within the 3D structure of the EB that results in a more efficient differentiation compared to 2D cultures. Kramer *et al.* demonstrated modulation of mouse EB differentiation into chondrocytes via members of the TGF-β family (Kramer et al., 2000). Here they found that application of BMP-4 or 2 acted as a stimulant for chondrogenesis, and that the effect of BMP-2 occurred in a time-dependant manner, with its inducing effects only occurring when applied to the EBs from days 2-5. Interestingly, it has been shown that some members of the TGF-β family are inhibitory of chondrogenesis during certain stages of differentiation of EBs *in vitro (Kramer et al., 2000; Toh et al., 2007; Yang et al., 2009)*, despite their pro-chondrogenic actions during mesenchymal stem cell (MSC) differentiation (Mackay et al., 1998). This highlights the distinct differences that exist between adult stem cells and ESCs in terms of chondrogenic differentiation, and gives an insight into the potential complexity of generating chondrocytes from ESCs. Nevertheless, growth factors have become a useful tool for directing EB differentiation, with key factors being applied to the EB culture medium. Furthermore chondrogenic differentiation of EBs into cartilaginous tissue has been shown via various culture methods, such as, pellet or micromass culture (Tanaka et al., 2004). These methods are also used for cartilage generation using MSCs (Zhang et al., 2010), and the effective use of these techniques to derive cartilage grafts from EBs demonstrates the suitability of ESCs for *in vitro* chondrogenesis.

As with ESCs it has been shown that iPSCs can be used to generate EBs, which could subsequently be directed to differentiate into cartilage like tissue. Wei *et al,* reprogrammed osteoarthritic-chondrocytes (OAC) to generate hiPSCs, and then differentiated the hiPSCs towards chondrocytes using supplementation with TGF-β1 (Wei et al., 2012). Cartilage markers, type II collagen, aggrecan and COMP (cartilage oligomeric matrix protein) were expressed by the OAC derived

differentiated hiPSCs. There is certainly some value in investigating how osteoarthritic chondrocytes behave, particularly as any implanted cells would be influenced by factors secreted by the resident chondrocyte population of OA sufferers. For instance, it has been shown that OAC can induce chondrogenesis in MSCs during co-culture (Aung et al., 2011). However, it is unlikely that using OAC for iPSC chondrogenesis would be a suitable alternative to current osteoarthritis treatments as patients would still have to undergo an invasive procedure, something that can be prevented with the use of hESCs, or hiPSCs derived from different tissues.

1.5.1.2 Differentiation via co-culture

An alternative method to direct differentiation via EBs is co-culture of PSC with differentiated chondrocytes. This co-culture can be either direct, or indirect.

During direct co-culture, pluripotent cells are grown and differentiated in a heterogeneous culture with mature chondrocytes; whereas during indirect co-culture, pluripotent cells are separated from chondrogenic cells via a filter. Indirect co-culture using a transwell insert was demonstrated by Vats et al. (2006): secreted factors from the adult chondrocyte population were able to diffuse across the membrane, creating an extracellular milieu that enhanced chondrogenic differentiation, thus emphasising the importance of the extracellular environment in controlling differentiation. This has since been reproduced by other groups (Hwang et al., 2008). The factors influencing chondrogenesis were unknown in these experiments, however, some of the chondrocyte secreted factors have since been identified. For example, it is now known that parathyroid hormone-related peptide (PTHrP) is secreted from mature chondrocytes and plays an important role in chondrogenesis and the prevention of hypertrophy (Fischer et al., 2010).

Fibrocartilaginous differentiation has also been shown using hESCs separated from a fibrocartilage derived chondrocyte cell layer via nylon cell strainers coated with 2% agarose; here they combined the indirect co-culture method with growth factor supplementation (BMP-4, TGF-β3), and found that this significantly improved differentiation (Hoben et al., 2009). Direct co-culture in the form of high density pellet-culture of hESCs with mature chondrocytes was also shown to enhance differentiation along chondrogenic lines (Bigdeli et al., 2009). However, clinical applications of these methods would be difficult due to the need for an adult chondrocyte population, preferably derived from the patient. Furthermore, these culture systems are difficult to scale up as larger cultures often result in poor nutrient diffusion leading to necrotic cores (Kafienah et al., 2007; Tare et al., 2005).

1.5.1.3 Differentiation via MSC-intermediates

Another technique involves differentiating hESCs, or hiPSCs, into chondrocytes via MSC intermediates. As previously mentioned MSCs can be derived from a number of sources including bone marrow and are multipotent; they can differentiate along the mesodermal lineage into cells such as cartilage, bone, muscle and adipose tissue. Bone marrow-derived MSCs (BM-MSCs) have limited proliferation and differentiation capacities *in vitro*, and expansion in culture is associated with a hypertrophic phenotype and dedifferentiation (Johnstone et al., 1998; Yoo et al., 1998). BM-MSCs from older patients also have a tendency towards decreased proliferative and differentiation potentials. However, when PSC are used to derive MSCs, these problems can be overcome. Barberi et al. (2005), showed mesenchymal differentiation in hESCs cultured on a monolayer of murine OP9 cells. The cells were analysed via FACs following 40 days of culture, and CD73+ cells were re-plated without a feeder layer. These cells were found to express adult MSC markers such as STRO-1, VCAM, ALCAM, ICAM-1, CD105, CD29, and CD44. They were subsequently successfully differentiated along chondrogenic, osteogenic, adipogenic, and myogenic lineages. However, due to the use of a feeder layer, this method of deriving ESC-MSCs is not appropriate for clinical translation due to the secretion of undefined factors into the culture medium. Clinically compliant MSCs have been derived from hESCs; these cells were cultured without a feeder-layer in serum free medium with the addition of FGF-2 and PDGF-AB (Lian et al., 2007). Cells expressed MSC antigens and gene expression profiles similar to BM-MSCs and could be differentiated into chondrocytes and osteoblast-like cells. The hESC-derived MSCs were able to proliferate *in vitro* for at least 35 population doublings without developing any karyotypic abnormalities that would normally occur in *in vitro* cultures of BM-MSCs. This suggests that hESC derived MSCs may have a much more robust karyotype than adult BM-MSCs, making this method of derivation significantly beneficial in comparison to using adult BM-MSCs.

Whilst the aforementioned methods have demonstrated success in the derivation of chondrocytes from PSCs, most of the systems were not clinically compliant or had low expansion capacities. Standard hESC culture utilises feeder layers in the form of irradiated mouse embryonic fibroblasts (MEFs), and the addition of serum (Thomson et al., 1998). This type of culture exposes the hESCs to xenoantigens, and is not chemically defined, it is therefore unsuitable for clinical applications (Martin et al., 2005). Whilst this may be generally acceptable for laboratory practice, the batch to batch variation of media components such as fetal calf serum (FCS) can affect reproducibility. To overcome these limitations culture methods that avoid using feeder layers and animal serum have been developed and are increasingly being used. An alternative to feeder layers is the use of ECM coatings such as laminin or fibronectin. hESCs have been shown to grow well *in vitro* on laminin coated tissue culture plastics; cells maintain their ESC phenotype, and are

still able to form teratomas *in vivo* (Xu et al., 2001). Feeder-free/serum-free culture systems have also been developed (Baxter et al., 2009; Chen et al., 2011; Liu et al., 2006; Ludwig et al., 2006a; Yao et al., 2006). For culture of hESCs it has become common practice to use KnockOut Serum Replacement (KSR) for routine culture; the formulation of this is proprietary information but is marketed as being free from undefined growth factors or differentiation stimuli.

1.5.1.4 Directed differentiation

For clinical applications a fully defined feeder/serum-free culture method is required. To this end, Oldershaw et al. (2010b), have developed a clinically compliant protocol for deriving chondrocytes from hESCs. This protocol is based on the sequential signalling pathways involved in the developmental process of chondrogenesis. Growth factors are used to direct differentiation of the hESCs towards chondrocytes over the course of 14 days. Cells progress through three defined developmental stages: primitive streak/mesendoderm, mesoderm, chondrocyte. The growth factors used to direct chondrogenesis were primarily members of the TGF-β superfamily (Wnt3a, Activin A, FGF2, BMP4, Follistatin, NT4 and GDF5). An 8.5-fold expansion of the cell population was reported during the differentiation protocol, and between 75% and 97% of cells were SOX9-positive based on results from four different hESC lines (Oldershaw et al., 2010b). The protocol was also applied to two iPSC lines with similar success. However, the chondrogenic potential of these cells was not tested *in vitro* in terms of cartilage generation.

To test the potential for clinical application of this technique, hESC derived chondroprogenitors embedded in a fibrin gel were transplanted into an osteochondral defect in the trochlear grooves of distal femurs in athymic RNU rats (Cheng et al., 2014). Repair tissue was identifiable at 4 weeks, and further developed by 13 weeks following implantation into the defect. Using a histomorphological scoring system, they determined that defect repair was significantly improved in defects transplanted with ESC-derived chondroprogenitors, compared to fibrin-only controls. They also used EGFP to track the transplanted cells, and to determine if they were responsible for matrix deposition; they found that at 8 weeks EGFP-positive cells were present in the defect area including at the level of subchondral bone. This suggests that there was cell survival of the transplanted population at 8-weeks, however it did not provide confirmation that these cells were responsible for matrix deposition. As an osteochondral defect model was used to assess the cells ability to form cartilage *in vivo*, the repair process was likely to have been influenced by the infiltration of resident stem cells from the subchondral bone.

The directed differentiation protocol developed by Oldershaw et al. (2010b) has since been utilised by a number of different groups, with some groups reproducing the work with little alteration (Boreström et al., 2014; Elayyan et al., 2017; Suchorska et al., 2016), and others with

more substantial modifications (Lee et al., 2015; Okada et al., 2014; Yamashita et al., 2015). Common variations of this protocol are the inclusion of 3D culture steps to generate chondrocytes.

1.5.2 Cartilage tissue engineering using PSC-derived chondrocytes

Whilst many methods have been reported for the generation of chondrocytes from PSCs, there are relatively few publications describing the generation of cartilage from these cells.

Approaches to generating cartilage from PSC-derived chondrocytes commonly utilise pellet culture or scaffolds. Often initiating chondrogenesis in an embryoid body (EB). This method of chondrocyte generation, though relatively simply, generates a mixed population of cells representative of all three developmental germ lineages and does not exclusively generate chondrocytes. Both Yodmuang et al. (2015) and Ko et al. (2014) differentiated PSCc (hESCs and hiPSCs respectively) via EB's which were then dissociated via enzymatic digestion before pellet culture. In both instances, hyaline-like cartilage with a type II collagen and proteoglycan rich matrix was generated. However, these constructs were relatively small in size, ~1mm diameter (Yodmuang et al., 2015), ~2mm diameter (Ko et al., 2014). Ko et al. (2014) also compared the pellet culture method with encapsulating cells in alginate. Both methods produced hyaline-like tissue; however, the authors noted that they preferred the alginate encapsulation method when pellets or alginate encapsulated cells were transplanted into an osteochondral defect model in rat femurs. This was because the hydrogel was amenable to minimally invasive injection via an arthroscopic procedure. Regardless, both pellets and alginate encapsulated cells initiated repair in the osteochondral defect model.

Differentiation via co-culture of hESCs with bovine chondrocytes, followed by pellet culture has also been shown to generate cartilage-like tissue with positive staining for ECM components such as proteoglycans and type II collagen (Hwang et al., 2008). However, these pellets were relatively small in size (<1mm diameter). Larger cartilaginous constructs were generated by use of a poly(ethylene glycol)-diacrylate (PEGDA) hydrogel (~5mm diameter). However, whilst PEGDA hydrogels are often used in these types of short term studies, it is widely acknowledged that the hydrolytically labile esters formed upon acrylation of the PEG diol result in slow degradation rates *in vivo* (Browning and Cosgriff-Hernandez, 2012); thus providing a barrier to clinical translation.

It is essential that further studies into cartilage generation from pluripotent stem cells overcome the translational barriers listed above (size, heterogeneous cell populations and slow degradation rates of scaffold materials). Scale-up will be particularly important as tissue-engineered cartilage will be required to fill defects larger than the scaffold-free constructs generated in the studies

discussed here. It is of note that when larger cartilage pellets are generated, these constructs often have a characteristic necrotic core (Li et al., 2014c). Diekman et al. (2012) describe the generation of chondrogenic cells from murine iPSCs by type II collagen (Col2)-driven green fluorescent protein (GFP) expression, and subsequent cartilage generation by pellet culture. The pellets generated here exceeded 2mm in diameter, however it is of note that these pellets were not homogenous throughout but lacked the proteoglycan rich ECM at the core of the pellet. This is likely due to impaired nutrient diffusion as a result of diffusion distance to the core of the pellet. This is a key issue in cartilage tissue engineering that must be overcome to enable viable clinical applications of tissue engineered cartilage.

1.5.3 Effective differentiation into chondrocytes and cartilage generation

Cell differentiation and tissue formation are complex processes that are governed by a multitude of different criteria. To successfully engineer viable tissue *in vitro* it is essential to take the *in vivo* environment into consideration. Translating characteristics of the developmental microenvironment such as O_2 tension, and mechanical cues can contribute to the successful generation of tissue engineered constructs, and should play important roles in the tissue culture process.

1.5.3.1 Importance of mechanical stimulation in tissue engineering

1.5.3.1.1 Mechanical stimulation and differentiation

Mechanobiology is the study of mechanisms by which cells are able to detect and respond to mechanical stimuli. Mechanical cues during development play important roles in the development of an organism (Lee et al., 2011a). It is well established that stem cells cultured *in vitro* are responsive to mechanical cues. It has been demonstrated that matrix elasticity (Engler et al., 2006), nanotopography (Waddell et al., 2018) and extracellular forces can direct stem cell fate *in vitro* even in the absence of biochemical stimuli (Nava et al., 2012). Whilst much of this work has been demonstrated in MSCs, this phenomenon has also been reported to occur in ESCs (Evans et al., 2009), highlighting the importance of mechanical cues early on in the process of lineage determination and cell specification. Mechanical loading in the form of cyclic compressions been shown to upregulate both TGF-β1 and TGF-β3 gene and protein expression in MSCs (Lian et al., 2010), thus demonstrating the impact of mechanical stimulation on chondrogenesis.

1.5.3.1.2 Effect of mechanical stimulation on cartilage

Functional tissue engineering is an initiative spearheaded by the United States National Committee on Biomechanics (USNCB) and proposes a set of principles and guidelines for

engineering load bearing tissues (Guilak et al., 2014). Researchers within the field of tissue engineering should take into account both the ultimate biomechanical requirements of the engineered tissue, and the potential for mechanical stimulation to enhance the generation of the desired tissue. This concept is of particular relevance for musculoskeletal tissue engineering, as these tissues have a primary biomechanical function.

Bioreactor systems have been used to culture a wide array of cell types. The design and development of bioreactor systems allows for the production of an *in vitro* culture system that provides the environmental conditions that allow the formation of functional 3D tissue constructs. For cartilage tissue engineering, perfusion flow bioreactors have demonstrated an ability to enhance ECM generation by chondrocytes (Davisson et al., 2002). Enhanced chondrogenesis has also been demonstrated in hESC-derived MSCs cultured in a perfusion bioreactor (Tığlı et al., 2011). Here, cells were cultured on a silk scaffold in chondrogenic medium in a perfusion bioreactor; results showed an increase in both proteoglycan and collagen content of the mechanically stimulated constructs, as well as increased construct stiffness. The incorporation of perfusion in such devices applies mechanical stimulation through the generation of hydrodynamic shear stresses, which improves the diffusion of both oxygen and metabolites through the engineered tissue. However, these bioreactor systems typically require the incorporation of scaffold materials onto which cells are seeded and subsequently cultured. As such, this could be a potential limiting factor in terms of clinical translation due to the issues associated with scaffold-based tissue engineering discussed in 1.2.3.1.

1.5.3.1.3 Application of ultrasound for cartilage tissue engineering

Ultrasound (US) waves are acoustic waves with a frequency equal to, or greater than 0.02MHz. US is commonly used as a non-invasive imaging tool for clinical applications. US, at low intensities, is also used as a clinical tool for aiding the repair of fractures and non-union breaks. However, it is debatable as to whether this treatment contributes to improved patient outcomes (Schandelmaier et al., 2017). Low intensity US (LIUS) has also been shown to enhance repair of cartilage in numerous animal studies (Cook et al., 2008; Cook et al., 2001).

A relatively less exploited use of ultrasound is the generation of ultrasonic standing wave fields (USWFs) for cell entrapment. When cells are introduced into an environment in which an USWF is generated, the acoustic waves scatter upon contact with the cells. Acoustic radiation forces are generated by the dispersion of an US wave, and it is these forces that spatially determine where the cells will be directed. Nodes and anti-nodes are created within the USWF, which refer to areas of relative low and high pressure respectively, forming an ultrasonic standing wave trap (USWT). Cells are directed towards pressure nodes where they aggregate and are held in levitation over

the course of the culture period within the USWT. The ability of an USWT to spatially pattern cells has been well demonstrated by Garvin et al. (2011). Here they utilised an USWT to spatially orient human umbilical vein endothelial cells (HUVECS) in a collagen gel prior to polymerisation, resulting in the generation of a vascularised cell network following culture. This has since been demonstrated using hESC-derived neuro-progenitor cells to create a layered neural network within a fibrin gel (Bouyer et al., 2016).

The aforementioned studies focussed on the ability of the USWT to temporarily trap and therefore spatially pattern cells. However long term use of USWTs has also been demonstrated in cell culture and has been shown to impart mechanical stimulation upon the cells. The successful generation of hyaline-like cartilage has been demonstrated via use of an acoustofluidic perfusion bioreactor that incorporated USWTs to levitate HACs (Jonnalagadda et al., 2018; Li et al., 2014b). These studies generated hyaline-like cartilage constructs with a type II collagen and proteoglycan rich extracellular matrix, and a cross-sectional area of approximately 1.4mm and 2.5mm respectively (Jonnalagadda et al., 2018; Li et al., 2014b), without signs of tissue necrosis. In both studies, mechanical stimulation of the cells was achieved by both media perfusion and a technique known as frequency sweeping. This involved driving the bioreactor between ranges of frequencies that encompassed the resonant frequency of the device, this being the frequency at which the USWT was optimally generated. By employing this technique, cells were continuously being driven towards the pressure nodes when the resonant frequency was excited and being essentially released from the USWT when the signal generator was out of range. They also discussed the phenomenon that by using a sweep repetition rate of 50Hz there was less cell displacement than when driven at 1Hz, and thus the relative amount of mechanical stimulation could be manipulated (Jonnalagadda et al., 2018).

These studies have demonstrated the effective application of USWFs for the generation of hyaline-like cartilage explants of monolayer-expanded HACs without the use of scaffolds, and thus has great translational potential for the generation of clinically viable tissue engineered constructs. However, due to the requirement for multiple invasive surgeries, low yields, and dedifferentiation of HACs during culture, an alternative cell source is required. Levitation of mouse ESCs in an USWT has been demonstrated (Bazou et al., 2011), and the successful generation of chondrocytes from hESCs may provide a valuable alternative cell source for the scaffold-free generation of cartilage constructs using an ultrasound-based bioreactor system.

1.5.3.1.4 The role of hypoxia in hESC culture and cartilage tissue engineering

Decreasing spontaneous differentiation and promoting self-renewal are critical for maintaining a healthy hESC population. There is substantial evidence demonstrating that this could be

supported by culturing cells under more physiological conditions (Ezashi et al., 2005; Forristal et al., 2010; Ludwig et al., 2006b; Westfall et al., 2008).

hESC culture is routinely carried out under 20% (atmospheric) O_2 tension. However, there is substantial evidence to demonstrate that hESCs retain pluripotency and proliferation capacity more efficiently when cultured under hypoxic conditions (5% O_2)(Forristal et al., 2013; Forristal et al., 2010; Petruzzelli et al., 2014); this is most likely because the *in vivo* environment of the preimplantation embryo is characterised by low oxygen tension (hypoxia) (Fischer and Bavister, 1993). Culture at 5% O_2 increases hESC proliferation and the expression of pluripotency markers SOX2, NANOG and OCT4 compared to 20% O_2, an effect regulated by HIF2α (Forristal et al., 2010; Petruzzelli et al., 2014). Environmental O_2 also regulates energy metabolism, and is intrinsic to the self-renewal of hESCs (Arthur et al., 2019; Christensen et al., 2015; Forristal et al., 2013).

Being avascular, cartilage resides in a hypoxic niche. Culturing human cartilage tissue explants under hypoxic conditions has been shown to significantly up-regulate both the mRNA and protein expression of the key chondrogenic regulator SOX9, as well as downregulate the expression of cartilage-degrading enzymes (Thoms et al., 2013). This demonstrates a protective effect of hypoxia on cartilage anabolism. It has been reported that HIF1α plays an important role in extracellular matrix production by epiphyseal chondrocytes, with significantly reduced aggrecan mRNA and protein levels in HIF1α-null chondrocytes, and increased type II collagen production in wild-type cells subjected to just 44 hours of hypoxia (Pfander et al., 2003). This effect is due to the binding of HIF1α to the *Sox9* promoter (Amarilio et al., 2007). HIF1α has also been shown to play a role in the regulation of collagen synthesis in chondrocytes (Stegen et al., 2019), further highlighting the role of hypoxia in cartilage generation. Not only does hypoxia play a role in extracellular matrix synthesis, but it also inhibits hypertrophy in MSCs and chondrocytes (Lee et al., 2013; Markway et al., 2013).

Hypoxic culture clearly plays important roles in both the maintenance of pluripotency, and during chondrogenesis. It is therefore likely that hypoxic culture will be both beneficial and influential for the generation of chondrocytes from hESCs, and subsequent tissue generation using tissue engineering.

1.6 Summary

Currently there is a lack of effective early intervention treatments for OA that provide long-term patient benefit. Autologous Chondrocyte Implantation (ACI) has been reported to relieve pain and improve joint function, however long-term amelioration of the condition is not always achieved. Furthermore, the repair tissue is typically fibrous rather than hyaline. To address these issues, a

tissue engineering approach using an alternative cell source such as hESCs could be employed. ACI has evolved substantially over the last two decades, and the recent publication of the NICE guidelines for use of ACI and ACI with chondrosphere (NICE, 2017; NICE, 2018) indicate that we are moving towards a tissue engineering based treatment strategy for OA. This would provide a quality control system, whereby 3D explants that are generated can be assessed in terms of their morphological, mechanical and physiological properties prior to implantation.

1.7 Hypothesis

hESCs are capable of generating hyaline-like cartilage constructs *in vitro* that are mechanically and morphologically similar to native cartilage, and can be scaled up to generate large constructs that have the potential to treat clinically relevant cartilage lesions.

1.8 Project aims and objectives

The aim of this study is to generate 3D hyaline-like neocartilage constructs from hESC-derived chondrocytes that are analogous to native cartilage by using scaffold-free culture techniques, namely culture in an acoustofluidic bioreactor and static pellet culture.

1. To generate a population of hESC-derived chondrocytes using a modified Directed Differentiation Protocol (DDP).
2. To bioengineer cartilage in an acoustofluidic bioreactor using Human Articular Chondrocytes (HACs) as a positive control.
3. To generate robust hyaline-like cartilage from hESC-derived chondrocytes that is morphologically and mechanically similar to native cartilage.
4. To repair partial thickness chondral defects using hESC-derived cartilage in an *ex vivo* organotypic defect model.

Chapter 2 Materials and Methods

2.1 Human Embryonic Stem Cell (hESC) culture

2.1.1 Derivation of Mouse Embryonic Fibroblasts (MEFs)

12.5-day pregnant mice (MF-1) were euthanized via cervical dislocation, and the embryonic sac removed. Embryos were dissected from the embryonic sac, decapitated and the liver removed. The remaining parts of the embryo were washed twice with sterile phosphate buffered saline (PBS pH 7.4) before being transferred to a Petri dish. Embryos were finely shredded with a razor blade and transferred into 50 ml tubes (9 embryos per tube) and digested with 15 ml Trypsin-EDTA (0.05%) (Gibco) for 15 minutes at 37°C with agitation by pipetting every 5 minutes. 200 µl of DNAse (stock 10 mg/ml) was added to 15 ml of MEF media (High glucose DMEM containing 1% Penicillin/Streptomycin, 10% foetal bovine serum (FBS)), which was combined with the digesting embryos. This mixture was incubated at 37°C until it appeared as liquid throughout. Once a homogenous liquid mixture had been achieved, the volume was made up to 50 ml with MEF media and centrifuged at 200 x*g* for 5 minutes. Following centrifugation, supernatant was removed, and pellet was re-suspended in 15 ml MEF media. This cell suspension was divided between 3x T175 tissue culture flasks, with approximately 3 embryos per flask. Media was changed after 24 hours, and when flasks reached confluence each flask was frozen into 9 cryovials using freezing media (10% DMSO in FBS), and the temperature slowly reduced to -80°C using a Mr Frosty.

2.1.2 Culturing and irradiating MEFs

For culture expansion, vials of un-irradiated MEF were thawed in a water bath and added to 10 ml of MEF media. The cell suspension was centrifuged at 450 x*g* for 4 minutes, re-suspended in MEF media, and the cell suspension introduced into a T175 flask. Cells were incubated at 37°C in a humidified incubator with 5% CO_2. Confluent cells were washed with PBS and dissociated using Trypsin-EDTA (0.05%) at 37°C. Once the cells had detached the Trypsin-EDTA (0.05%) was neutralised using MEF media. The cell suspension was transferred to a 50 ml tube and centrifuged as above. Following centrifugation, the cell pellet was re-suspended in MEF media and passaged at a ratio of 1:4 in T175 flasks containing 20 ml MEF media. This process was repeated with a passage ratio of 1:3.

Once the sub-cultured flasks of cells reached ~90% confluence, the cells were dissociated and 12 T175 flasks were combined. The cell suspension was centrifuged as above, and the 4 cell pellets

were re-suspended in 10 ml of MEF media which were combined into 1x50 ml tube with a total volume of 40 ml. The cell suspension was γ-irradiated at 50G to mitotically inactivate the MEFs. Following the irradiation procedure, cells were centrifuged as above, and cell pellet was re-suspended in 12 ml freezing media (10% DMSO in FBS). The cell suspension was divided between 12 cryovials and the temperature slowly reduced to -80°C using a Mr Frosty. Frozen irradiated MEFs (iMEFs) were transferred to liquid nitrogen for long term storage.

2.1.3 Culture of HUES7 hESCs on feeder layers

HUES7 hESCs (Male; Harvard, USA) were cultured on a layer of iMEFs maintained in hESC media (knockout DMEM, supplemented with 15% knockout serum replacement, 1x non-essential amino acids, 1x penicillin/streptomycin, 1x L-glutamax, 50 µM β-mercaptoethanol and 10 ng/ml basic fibroblast growth factor (bFGF)). Cells were maintained at 37°C, 5% CO_2, and either 20 or 5% O_2. Cells underwent at least 3 passages at 5% O_2 before being used for experiments. Cells were routinely passaged at a ratio of 1:2 or 1:3. Cells were incubated with collagenase IV (160U/ml in knockout DMEM) at 37°C for 4 minutes, the collagenase was removed and hESC media was added. Using a cell scraper and gentle pipetting, cells were passaged onto fresh iMEFs and allowed to adhere overnight. Media changes were carried out every 24 hours using hESC media, and cells were passaged every 2-4 days at a ratio of 1:2 or 1:3.

For immunocytochemistry cells were plated onto chamber slides at a similar density to cells plated on 6-well plates, and allowed to adhere overnight. Actual cell numbers have not been determined as cells are passaged as colonies.

2.1.4 Feeder free culture of HUES7 hESCs

For feeder-free culture of HUES7 hESCs, cells were passaged using the above method and plated onto Matrigel (Corning) coated tissue culture plates. Matrigel is a solubilized basement membrane preparation extracted from the Engelbreth-Holm-Swarm (EHS) mouse sarcoma, and is rich in ECM proteins such as laminin, collagen IV, heparin sulfate proteoglycans, nidogen. Cells were maintained at 5% O_2 and passaged as in section 2.1.3. Feeder free hESCs underwent at least 3 passages to eliminate MEF carryover before being used for experiments.

2.2 Directed differentiation of HUES7 hESCs into chondrocytes

A directed differentiation protocol (DDP) based on that of Oldershaw et al. (2010a), was used to differentiate hESCs into chondrocytes. This protocol aims to recapitulate the developmental pathway that directs hESCs to become chondrocytes by facilitating their progression through the following three stages (Figure 2.1):

- Stage 0: Pluripotent cells (hESCs)
- Stage 1: Primitive streak-mesendoderm
- Stage 2: Mesoderm
- Stage 3: Chondrocyte

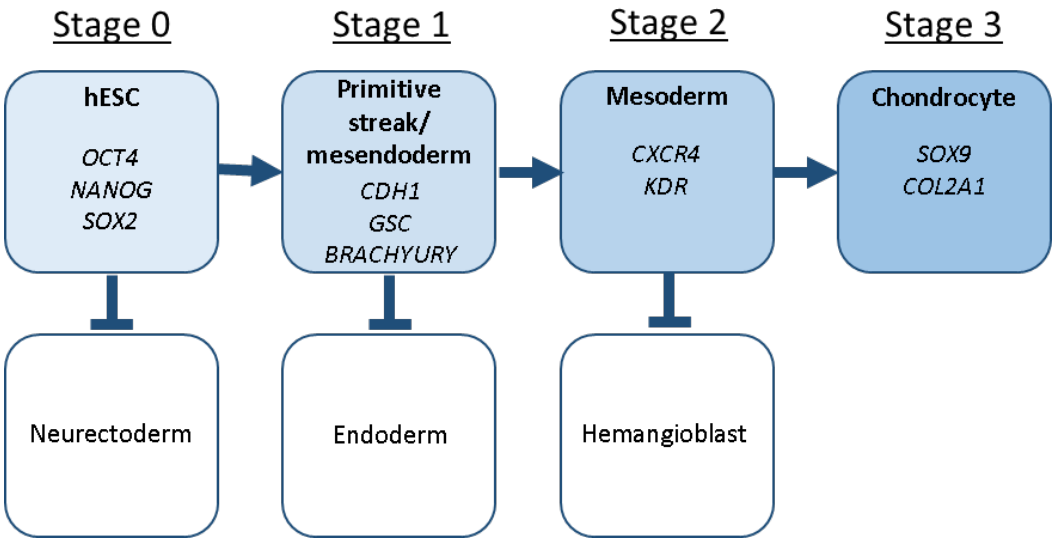

Figure 2.1 **Schematic representation of DDP.**

The developmental stages through which the cells are directed to progress along with stage specific genes used for RT-qPCR analysis, and lineage inhibition depicted by flat ended arrows.

Directed differentiation was achieved by adding growth factor cocktails to the cell culture media, at varying concentrations over the course of 14 days. Growth factors were added to a serum free medium, referred to as Directed Differentiation Protocol Basal Medium (DMEM: F12 (Gibco) supplemented with 1x NEAA (Gibco), 1x B27 supplement (Gibco), 1x ITS (Gibco) and 90 µm β-mercaptoethanol (Sigma)), in defined concentrations and combinations over the course of 13 days.

The DDP described here deviates from the original by the addition of the TGF-β3 from day 9 onwards (Table 2.1), a growth factor that was not originally included. Also, here cells were cultured on Matrigel coated plates, and were routinely cultured at 5% O_2 prior to initiating the DDP. Cells derived from the DDP were termed hESC-derived chondrocytes.

Table 2.1 **Growth factor concentrations for the directed differentiation of hESCs into chondrocytes.**

Stage	Days	WNT3A (R&D) (ng ml^{-1})	ACTIVIN-A (Peprotech) (ng ml^{-1})	FGF2 (Invitrogen) (ng ml^{-1})	BMP4 (Peprotech) (ng ml^{-1})	Follistatin (Sigma) (ng ml^{-1})	GDF5 (Peprotech) (ng ml^{-1})	NT4 (Peprotech) (ng ml^{-1})	TGFß-3 (Peprotech) (ng ml^{-1})
1	1	25	50						
	2	25	25	20					
	3	25	10	20	40				
2	4-7			20	40	100		2	
	8			20	40			2	
3	9			20	20		20	2	10
	10			20	20		20	2	10
	11-13			20			40	2	10
	14		**END**	**OF**	**PROTOCOL**				

2.3 Human Articular Chondrocyte (HAC) cell culture

2.3.1 Isolation of HACs

Femoral head samples were obtained from 9 haematologically normal osteoarthritic individuals (8 female, mean age: 66 years; male aged 82 years) undergoing hip replacement surgery. Only tissue that would have been discarded was used in this study with approval of the Southampton and South West Hampshire Research Ethics Committee (REC210/01).

Femoral heads were sprayed with 70% ethanol to remove excess blood and tissue debris. Full thickness sections of cartilage were removed using a scalpel and covered with PBS (Lonza) to prevent the tissue from drying out. The cartilage was washed twice with PBS, and chopped into small sections (<1mm^2), transferred into a 50 ml tube and incubated with 3 ml of Trypsin-EDTA (0.05%) (Gibco) at 37°C for 30 minutes, and shaken by hand every 10 minutes. Trypsin-EDTA (0.05%) was discarded, and the cartilage pieces were washed with PBS. Samples were incubated with 3 ml of Hyaluronidase (Sigma) (1 mg/ml in PBS, sterile filtered using 0.22 µm filter) at 37°C for 15 minutes, and shaken half way through. The hyaluronidase was discarded and the cartilage pieces washed in PBS. The cartilage was incubated with 2.5 ml of collagenase B (Roche) (10 mg/ml in α-MEM (Lonza)) overnight (9-15 hours) at 37°C, with constant agitation using an SI50 orbital shaker incubator (Stuart Scientific).

10 ml of α-MEM was added to the digested cartilage suspension, passed through a cell strainer (70 µm, Fisher scientific) and centrifuged at 400 x*g* for 5 minutes and the cell pellet resuspended in 10 ml of HAC medium (DMEM/F12 (Gibco) containing 5% filtered FBS, 1x ITS (Gibco), 100 µM Ascorbate-2-phosphate (Sigma)). Cells were counted and seeded into flasks at densities between 3.5x10^4 1.7x10^4 cells per cm^2. HACs were cultured in a humidified incubator at 37°C, 5% CO_2 in air.

2.3.2 HAC maintenance and culture

The first media change was performed on day 6 of culture after isolated cells had adhered firmly to tissue culture plastic.

Cells were passaged at approximately 70-90% confluency. HAC medium was removed from the flasks, and cells were washed with PBS. HACs were incubated with collagenase IV (Gibco) (160 U/ml in α -MEM (Lonza)) for 30-45 minutes. The collagenase IV was removed, and the cells washed in PBS. Cells were incubated with Trypsin-EDTA (0.05%) until cells began to detach and α-MEM containing 10% FCS was used to neutralise the Trypsin-EDTA (0.05%). The cell suspension

was pipetted up and down against the inner surface of the flask to remove any remaining cells before being transferred into a 50 ml tube. The cell suspension was centrifuged at 400 x*g* for 5 minutes and the cell pellet resuspended in 10 ml of HAC medium. The cell suspension was divided between new flasks containing HAC medium, and incubated at 37°C, 5% CO_2. Cells were routinely passaged at a ratio of 1:3, or 1:4 for continued culture.

Cells used for experiments were between P0 and P2.

2.4 Gene expression analysis

2.4.1 Isolation of total RNA

For lysis of cells and tissue for RNA extraction, peqGOLD TriFast™ reagent was used. 1 ml of peqGOLD TriFast™ reagent was added to each sample and a cell scraper was used to remove cells from the well of the tissue culture plate. Samples were stored in screwcap microcentrifuge tubes at -80°C until required or progressed directly to RNA isolation.

For RNA isolation, samples were allowed to thaw and incubated at room temperature for 10 minutes. 200µl of chloroform was added to each sample (1 ml volume) followed by 15 seconds of vigorous shaking to produce a phase separation. Samples were incubated at room temperature for 5 minutes. To fully separate the RNA from DNA and phenol contaminants the samples were centrifuged at 17,000 x*g* at 4°C for 30-45 minutes.

Samples were placed on ice whilst the upper aqueous phase was carefully transferred into a fresh RNAse free 1.5ml Eppendorf tube. To precipitate the RNA ½ the sample volume of isopropanol was added, along with 50 µl Glycogen (Invitrogen) followed by vigorous shaking for 15 seconds before being incubated at room temperature for 10 minutes and stored at -80°C for at least 10 minutes to precipitate the RNA. Samples were allowed to thaw before being centrifuged at 17,000 x*g* 4°C for 20-40 minutes.

Following centrifugation, samples were kept on ice for the desalting process. First, the RNA pellets were washed with 1 ml of ice cold 100% EtOH followed by 5 minutes centrifugation at 17,000 x*g*, 4°C. The EtOH was removed carefully, avoiding the RNA pellet, and the pellet was washed with 1ml ice cold 75% EtOH followed by 5 minutes centrifugation at 17,*000* x*g*, 4°C. The EtOH was carefully removed, avoiding the RNA pellet, before being centrifuged for a short burst to remove any residual liquid. Pellets were left to air dry on ice with the lids open. Once the RNA pellets had become translucent, 20-30 µl of DEPC treated H_2O was added to dissolve the RNA pellet and 1 µl

of RNasin (RNase inhibitor) (Promega) was added to prevent RNA degradation. Samples were left on ice for 30 minutes for the RNA pellets to dissolve.

Assessment of RNA purity and concentration was carried out using a NanoDrop 1000. 1 µl of sample was used for each test, and each sample was measured at least in duplicate to ensure precise quantification. A 260/280 ratio was used to assess RNA purity, with a ratio of approximately 2 reflecting a pure sample.

2.4.2 cDNA synthesis

1 µg of total RNA was used for cDNA synthesis.

1 µl of DNAse I and 1 µl of 10x DNAse reaction buffer (Invitrogen) was added to 1 µg RNA in 8 µl of DEPC water, briefly centrifuged and incubated at room temperature for 15 minutes. To terminate the reaction, 1 µl of 25mM EDTA (Invitrogen) was added and the samples heated at 65°C for 10 minutes before cooling on ice.

For first strand synthesis, 3 µl of DEPC treated H_2O and 1 µl of random primers were added to each sample, heated at 70°C for 10 minutes, immediately cooled on ice and briefly centrifuged. For the reverse transcription, the following was added to each sample:

- 8 µl M-MLV RT-5X buffer (Invitrogen)
- 5 µl 10mM dNTPs (premixed) (Invitrogen)
- 1 µl M-MLV reverse transcriptase (Invitrogen)
- 11 µl DEPC H_2O

The samples were heated at 42°C for 60 minutes, immediately cooled on ice and briefly centrifuged.

cDNA samples were either stored at -20°C for future use, tested for genomic DNA contamination, or used for real-time quantitative PCR (RT-qPCR) (2.4.4).

2.4.3 PCR to confirm lack of genomic DNA contamination

PCR (polymerase chain reaction) was used to confirm the lack of genomic DNA contamination. 1 µl of cDNA was used for each PCR reaction, and the following was added to each sample: 0.5 µl 10 mM dNTPs, 5 µl GO Taq buffer, 0.5 µl of each primer at 5 µM (OAZ1, forward primer 5'-GGCGAGGGAATAGTCAGAGG-3', reverse primer 5'-GGACTGGACGTTGAGAATCC-3'), 0.375 µl GO Taq polymerase, 17.125 µl DEPC H_2O. A no cDNA control was used for each run (substituting cDNA for 1 µl of H_2O). The samples were briefly centrifuged before being placed in a thermocycler (G-Storm) on the following program:

1. 94°C, 2 minutes.
2. 94°C, 1 minute.
3. 58°C, 1 minute (annealing).
4. 72°C, 1 minute (extending).
5. Step 2-4, 40x repeat.
6. 72°C, 10 minutes.
7. 4°C, hold.

Samples were either stored at 4°C overnight or run on an agarose gel.

For agarose gel electrophoresis a 2% Agarose gel was used (2 g Agarose in 100 ml of 1xTAE buffer (Gibco, pH 8.3)). 5 µl of Nancy-520 (Sigma) (a double stranded DNA binding dye) was added to the 2% Agarose/TAE solution which was poured into a tray, a comb inserted, and allowed to set. Once the gel had formed it was placed in the running module and covered with 1X TAE buffer (pH 8.3), the combs removed and 25 µl of samples added to the wells. 5 µl of QuickLoad® 100 bp ladder (New England Biolabs) was loaded into the first well to determine molecular weight of detected bands. The gel was run at 80 mV for 30-60 minutes.

The gel was imaged under UV light using Syngene gel imager. A single band at approximately 122 bp confirmed a lack of gDNA contamination, whilst a band at 373 bp indicated gDNA contamination.

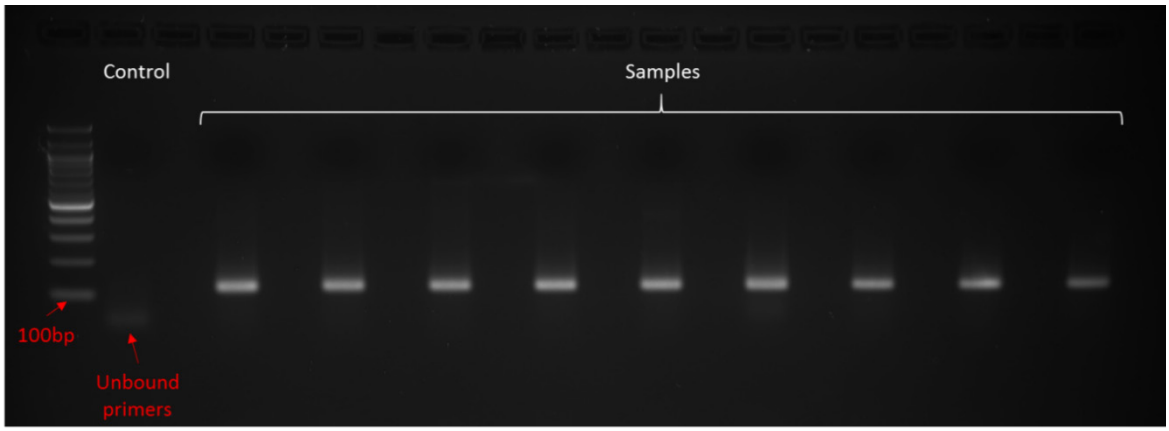

Figure 2.2 **Representative image of a PCR gel imaged under UV light.**
Presence of a single band of OAZ1 cDNA at 122 bp confirmed lack of gDNA contamination. Band in control lane shows unbound primers.

2.4.4 Taqman® quantitative real time-PCR (RT-qPCR)

2.4.4.1 RT-qPCR set up and amplification

RT-qPCR was set up in 96 well plates, with 20 µl reaction volumes consisting of:

- 10 µl TaqMan® Universal PCR Master Mix
- 8 µl DEPC treated H_2O
- 1 µl TaqMan® probe (Table 2.2)
- 1 µl cDNA

Reactions were performed in duplicate, and run on an ABI 7500 Real Time PCR system. The following cycling parameters were used for amplification:

1. 50°C, 2 minutes.
2. 95°C, 10 minutes.
3. 95°C, 15 seconds.
4. 60°C, 1 minute.
5. Steps 3-4, 45x repeat.
6. 10°C, hold

Table 2.2 **List of Taqman probes used for RT-qPCR**

Target	Catalogue number
OCT4 (POU5F1)	Hs04260367_gH
SOX2	Hs00602736_s1
NANOG	Hs02387400_g1
UBC	Hs00824723_m1
GSC2	Hs00906630_g1
CDH1	Hs01023894_m1
Brachyury (T)	Hs00610080_m1
CXCR4	Hs00607978_s1
KDR	Hs00911700_m1
SOX9	Hs01001343_g1
COL2A1	Hs00264051_m1
COL10A1	Hs00166657_m1

2.4.4.2 $2^{-\Delta\Delta CT}$ method

For relative quantification of RT-qPCR C_T values the 2-ΔΔCT method was used.

$$\Delta C_T = C_{T(\text{target gene})} - C_{T(\text{UBC})}$$

$$\Delta\Delta C_T = \Delta C_{T(\text{sample})} - \Delta C_{T(\text{control})}$$

$$2^{-\Delta\Delta CT} = \text{Fold Change}$$

For stage specific gene expression analysis of DDP cultures all samples of interest were compared to a paired stage 0 sample which acted as a control and was itself normalised to 1. Ubiquitin C (UBC) was used as a housekeeping gene.

2.5 Histology

2.5.1 Fixation, processing and embedding of fixed tissue

Tissue samples were fixed overnight in 4% paraformaldehyde. Following fixation, samples were washed in PBS and either processed immediately, or stored in PBS at 4°C for up to 4 days before being processed.

Samples were transferred to glass bijou tubes and stained in 1% Eosin in dH_2O for 5 minutes. Samples progressed through the following stages under agitation:

1. 30 minutes in 50% EtOH
2. 30 minutes in 90% EtOH
3. 30 minutes in 100% EtOH
4. 30 minutes in 100% EtOH
5. 30 minutes in a 50:50 mix of 100% EtOH and histoclear
6. 30 minutes in 100% histoclear
7. 30 minutes in 100% histoclear

Histoclear was removed, and samples were incubated at 60°C in molten paraffin wax for 45 minutes. The wax was removed and replaced with fresh wax, the sample was incubated again at 60°C in 45 minutes.

Samples were embedded in fresh paraffin wax using a metal tray and cassette, and allowed to set for approximately 30 minutes on a cooling stage (2°C). Tissue blocks were stored at 4°C until sectioning.

2.5.2 Sectioning

Tissue sections were cut to 5 µm thickness using a microtome. Sections were placed in a water bath set to 40°C before being attached to glass slides (1-3 sections per slide). Slides were allowed to dry flat on a heater set at 37°C for 1-2 hours before being placed in a slide rack and being dried vertically overnight in a drying oven set at 37°C. Slides were wrapped in foil and stored at 4°C until used for staining.

2.5.3 Safranin O staining

Safranin O stains proteoglycans and glycosaminoglycans (GAGs).

Slides were warmed at 37°C for 30-60 minutes in a warming oven. Slides were cleared and rehydrated by the following procedure:

1. 7 minutes in 100% histoclear
2. 7 minutes in 100% histoclear
3. 2 minutes in 100% EtOH
4. 2 minutes in 90% EtOH
5. 2 minutes in 50% EtOH

Slides were placed into dH_2O until ready to start staining. Cells were placed on a metal staining tray and covered with Wiegert's Haematoxylin working solution (1:1 parts A & B (part A: 10 g Haematoxylin in 1 L 100% EtOH, allowed to mature for at least 4 weeks; part B: 6 g Ferric chloride in 500ml dH_2O, with 5 ml concentrated HCl) for 10 minutes in the dark. Slides were washed in running tap water for 10 minutes to remove excess haematoxylin. Following this, slides were dipped 3 times in acid-alcohol (1% HCl/70% EtOH) and rinsed in 1% Acetic acid/dH_2O for 15 seconds. Slides were stained in Safranin O (0.1% Safranin O/dH_2O) for 15 minutes and dipped in dH_2O to remove any excess.

Slides were dehydrated and cleared by the following procedure:

1. 30 seconds in 50% EtOH
2. 30 seconds in 90% EtOH
3. 30 seconds in 100% EtOH
4. 30 seconds in 100% EtOH
5. 30 seconds in 100% Histoclear
6. 30 seconds in 100% Histoclear

Slides were mounted in resinous media (DPX) and sealed with glass cover slips. Slides were boxed and stored at room temperature.

Slides were imaged using a Zeiss inverted microscope.

2.5.4 Immunostaining

Slides were incubated at 37°C for 30-60 minutes. Slides were cleared and rehydrated as in section 2.5.3. Slides were then rinsed gently in running tap water, placed in to dH_2O.

For SOX9 and Aggrecan antibodies, heat mediated antigen retrieval was performed. Slides were placed in a black plastic staining rack and into a sealed plastic box containing 10 mM Citrate Buffer in dH_2O (pH 6) which had been heated to 95°C. Slides were incubated for 30 minutes at 95°C in a water bath. Immediately after incubation slides were dipped in dH_2O which was immediately replaced with fresh dH_2O and placed in PBS.

Slides were placed on a metal staining tray and sections were covered with 3% H_2O_2 in dH_2O and incubated at room temperature for 5 minutes. During this step, any endogenous peroxidase activity was quenched to reduce background staining.

For type I and II collagen antibodies, enzyme mediated antigen retrieval was performed. Slides were placed on a black plastic staining tray and sections were covered with Hyaluronidase (520

U/ml) in 1% BSA in PBS for 20 minutes at 37°C. Following incubation, slides were rinsed in tap water.

Blocking was performed using 1% BSA in PBS. Slides were placed on a black plastic staining tray and sections were covered with the blocking buffer and incubated for at least 5 minutes at 4°C.

The blocking buffer was removed by dipping the slides in dH_2O and slides were placed on a black plastic staining tray. Sections were separated by use of a hydrophobic pen and were covered in the primary antibody dilution (Table 2.3) (~30 µl per section). Slides were incubated overnight (~17 hours) at 4°C.

Table 2.3 **List of antibodies used for immunostaining.**

Primary Antibody	Secondary Antibody
Anti-Type II Collagen, Rabbit (1:500) (Calbiochem)	Anti-Rabbit, biotinylated (1:100) (Sigma)
LF67 Anti-Type I Collagen, Rabbit (1:300) (Gift from Dr Larry Fisher)	Anti-Rabbit, biotinylated (1:100) (Sigma)
Anti-Type X Collagen, Mouse (1:300) (Gift from Dr Gary Gibson)	Anti-Mouse, biotinylated (1:100) (Sigma)
Anti-SOX9, Rabbit (1:150) (Millipore)	Anti-Rabbit, biotinylated (1:100) (Sigma)
Anti-Aggrecan, Goat (1:240) (R&D)	Anti-Goat, biotinylated (1:400) (Sigma)
Anti-MMP-13, Rabbit (1:100)(Abcam)	Anti-Rabbit, biotinylated (1:100) (Sigma)
Anti-Ki67, Rabbit (1:240)(Abcam)	Anti-Rabbit, biotinylated (1:100) (Sigma)
Anti-Connexin-43, Rabbit (1:150)(Abcam)	Anti-Rabbit, biotinylated (1:100) (Sigma)

Following incubation with the primary antibody, slides were dipped in dH_2O, placed in a metal staining rack, and 3 x5 minute washes in 0.05% Tween-20 in PBS were carried out. Slides were dipped in dH_2O, allowed to drain, and placed on the black plastic staining tray. Sections were covered with the diluted secondary antibody solution (Table 2.3) and incubated for 60 minutes at room temperature. Secondary antibodies used for immunostaining were biotin conjugated.

Following incubation with the secondary antibody solution slides were dipped in dH_2O, placed in a metal staining rack, and 3 x5 minute washes in 0.05% Tween-20 in PBS were carried out. Slides were dipped in dH_2O, allowed to drain, and placed on the black plastic staining tray. Slides were covered in ExtrAvidin Peroxidase (Sigma) diluted 1:50 in 1% BSA in PBS and incubated for 30

minutes at room temperature. Avidin has a strong affinity for biotin, and the ExtrAvidin Peroxidase acts as a tertiary antibody.

Slides were rinsed gently in the running water bath and 3 x5 minute washes in 0.05% Tween-20 in PBS were carried out. Slides were dipped in dH_2O and placed on the black plastic staining tray. Sections were covered in 3-amino-9-ethylcarbazole (AEC) working solution (Table 2.5) and were left until a colour reaction took place.

Table 2.4 **AEC Stock recipe.**

AEC stock solution	
AEC (Sigma)	0.01g
Dimethylformamide (VWR)	1250µl

Table 2.5 **AEC working solution recipe.**

AEC working solution	
AEC stock solution (Table 2.4)	500µl
Acetate buffer pH 5.0	9500µl
30% H_2O_2	5µl

Following incubation with the AEC working solution, slides were first dipped in dH_2O, and placed in the running water bath to terminate the reaction. For all antibodies, other than Aggrecan, sections were counterstained using Alcian Blue (0.5% Alcian Blue 8GX in dH_2O) for 90 seconds. Excess Alcian Blue stain was removed by gently washing in running water bath.

Slides were mounted using Hydromount.

Slides were imaged using a Zeiss inverted microscope.

2.6 Image analysis

Quantitative analysis of Safranin O and immunohistochemical stained images was performed using the FIJI/ImageJ software.

2.6.1.1 Quantitative image analysis of Safranin O and immunohistochemical staining

To enable comparative quantitation, any samples that would be compared were stained at the same time. Images were taken using a Zeiss inverted microscope using the same objective (5x). Microscope settings remained constant between slides.

2.6.1.1.1 Safranin O density (intensity) measurements

Sections were stained as described 2.5.3.

Images were opened on FIJI/ImageJ, inverted and the area of interest (AOI) of the sample was mapped out to select the sample (Figure 2.3). Where folding of the section had occurred, these regions were not selected in the AOI. Area and density measurements were taken for the AOI. Density measurements calculate the mean grey value over the AOI, area accounted for the entirety of the AOI.

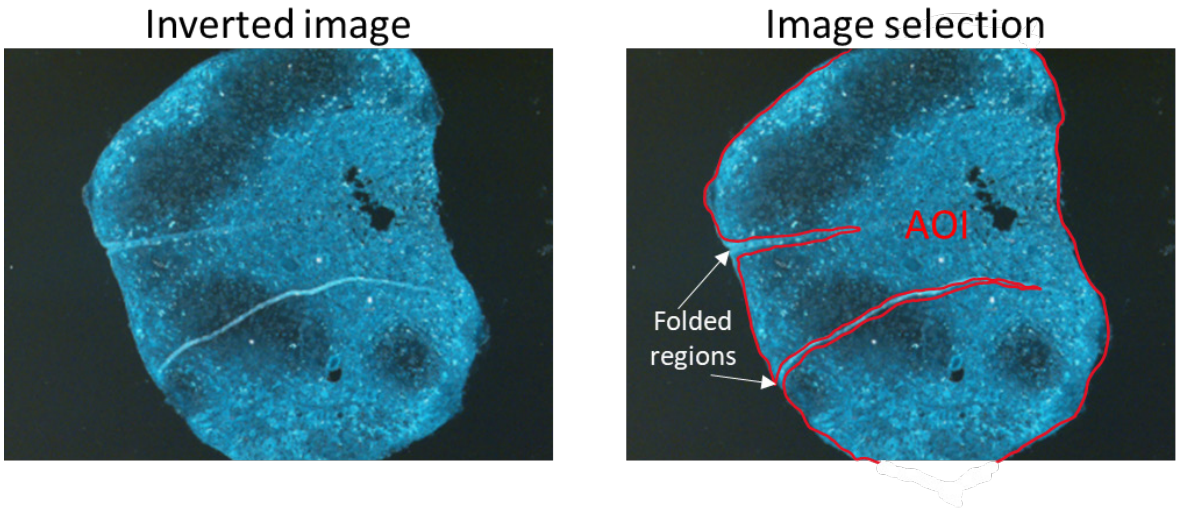

Figure 2.3 **Area of interest (AOI) selection for image analysis.**
To analyse staining intensity via integrated density analysis using the Imagej/FIJI software, images were first inverted and then the AOI was selected. AOI is defined by a red border. Regions of section folding were omitted from the AOI.

To account for differences in area of the AOI between samples, density measurements were normalised to area to give a density per unit area value.

$$\frac{density}{area} = Density\ per\ unit\ area\ (DA)$$

Values were then normalised to the highest density per unit area value and an average for each group was taken.

2.6.1.1.2 Immunohistochemistry density measurements

Staining was performed as described in section 2.5.4, however for the purposes of image analysis sections were not counterstained in Alcian Blue.

For immunostaining, measurements were taken from both positively stained sections and negative controls; measurements were made as in section 2.6.1.1.1 for both. To account for non-specific staining/background, density per unit area values were normalised by the following equation:

$$sample\ DA - control\ DA = Normalised\ density$$

Chapter 3 Differentiation of hESCs into Chondrocytes

3.1 Introduction

hESCs provide a source for any somatic cell type in the human body as they have the potential to differentiate into cells from any of the three germ layers (endoderm, mesoderm, ectoderm). hESCs are an allogeneic source of cells for humans, and are widely assumed to be immune-privileged, or to possess negligible immunogenicity (Li et al., 2004). As a precaution it has been proposed that by using HLA antigen matching the potential for immunogenicity could be avoided as a hESC bank would enable accurate HLA matching for many patients (Nakajima et al., 2007; Taylor et al., 2005). hESCs therefore provide a promising cell source for regenerative medicine.

Hypoxia plays an important role in the maintenance of pluripotency in hESCs. Standard culture for hESCs is performed at 20% O_2. However, much work has highlighted the benefits of maintaining hESCs under hypoxic conditions with culture at 5% O_2 resulting in enhanced self-renewal, decreased spontaneous differentiation and increased proliferation (Forristal et al., 2013; Forristal et al., 2010; Petruzzelli et al., 2014).

Chondrogenic differentiation of hESCs has been demonstrated using a variety of different protocols, reviewed by Jevons et al. (2018). Many utilise 3D embryoid body (EB) culture to initiate differentiation (Toh et al., 2007; Yodmuang et al., 2015). However, differentiation via EBs results in heterogeneity with a population of cells derived from each of the three developmental germ layers, typically with low chondrocyte yields (Kawaguchi et al., 2005; Oldershaw et al., 2010b). Cell sorting techniques can then be used to isolate chondrocytes from the final population, however this additional step requires EB dissociation and cell labelling which may provide additional stresses to the cells. Other techniques involve co-culture of hESCs with mature differentiated chondrocytes (Hwang et al., 2008; Vats et al., 2006); however as this technique requires a secondary cell population of primary chondrocytes patients must undergo an invasive surgery. Co-culture of hESCs and chondrocytes also results in the transfer of unknown factors from the primary chondrocytes to the differentiating stem cells. These differentiation techniques are often unsuitable for therapeutic applications as they are not clinically compliant due to the use of animal products such as serum media supplements or animal derived growth factors.

A directed differentiation protocol developed by Oldershaw et al. (2010b) goes some way towards overcoming issues such as clinical compliance and heterogeneous cell populations. The chemically defined protocol aims to recapitulate the developmental progression of chondrogenesis by directing cells through the states of primitive streak/mesendoderm, mesoderm before

differentiation into chondrocytes. The protocol involves treating hESCs with different growth factor cocktails over the course of 14 days. Using this protocol differentiation of hESCs towards chondrocytes was demonstrated in three hESC lines (Oldershaw et al., 2010b).

The scalable and chemically defined protocol developed by (Oldershaw et al., 2010b) provides a useful starting framework for the differentiation of hESCs into chondrocytes. Modifications to the protocol to further refine the chondrocyte yield and chondrogenic profile of the cells will aid clinical translation.

3.2 Aims and objectives

- To reproducibly generate a robust population of hESC-derived chondrocytes.
- To characterise hESC-derived chondrocytes by analysing expression of chondrogenic markers using RT-qPCR, immunocytochemistry and Western Blotting.
- To investigate the effects of oxygen tension on the differentiation of hESCs into chondrocytes.

3.3 Methods

3.3.1 Immunocytochemistry

hESCs cultured on MEFs, or hESC-derived chondrocytes cultured on MG were fixed at room temperature for 15 minutes in 4% paraformaldehyde in PBS, washed with PBS, and incubated with 100 mM Glycine in PBS for 10 minutes (all stages carried out at room temperature) before being permeabilised in for 10 minutes with 0.2% Triton X-100 for intracellular proteins. This step was omitted for surface markers and extracellular matrix proteins. All samples were blocked in 10% FBS in PBS for 30 minutes before incubating in primary antibodies diluted in 0.6% BSA in PBS (see Table 3.1 for dilutions) for 90 minutes.

The cells were washed twice with PBS for 5 minutes each in the dark. The PBS was removed, and cells incubated with the relevant secondary antibody diluted in 0.6% BSA in PBS for 60 minutes in a humidified container in the dark (see Table 3.1 for dilutions). The cells were washed twice in PBS for 5 minutes each in the dark, followed by a 5 minute wash with dH_2O and covered with a thin layer of VECTASHIELD® Antifade Mounting Medium with DAPI (Vector Laboratories). The cells were covered with a glass coverslip and sealed using nail varnish, and well plates were sealed with Parafilm. Slides and plates were covered with foil to protect from light, and stored at 4°C.

A Zeiss Axiovert fluorescence microscope was used to image the cells as soon as possible following labelling.

Table 3.1 **List of antibodies used for immunocytochemistry**

Primary Antibody	Secondary Antibody
Anti-OCT4 Mouse IgG2b (1:100), (Santa Cruz)	Goat anti-Mouse IgG FITC (Sigma) (1:100)
Anti-SOX2, Rabbit (1:200) (Cell Signalling Technology)	Goat anti-rabbit IgG Alexa Fluor 488 (1:700) (Invitrogen)
Anti-NANOG, Rabbit (1:100) (AbCam)	Goat anti-rabbit IgG Alexa Fluor 488 (1:700) (Invitrogen)
Anti-TRA-1-60 Mouse IgM (1:100) (Santa Cruz)	Goat anti-Mouse IgM FITC (1:200) (Molecular Probes)
Anti-SSEA1 Mouse IgM (1:100) (Santa Cruz)	Goat anti-Mouse IgM FITC (1:200)(Molecular Probes)
Anti-Type II Collagen, Rabbit (1:500) (Calbiochem)	Goat anti-rabbit IgG Alexa Fluor 488 (1:700) (Invitrogen)
Anti-SOX9, Rabbit (1:150) (Millipore)	Goat anti-rabbit IgG Alexa Fluor 488 (1:700) (Invitrogen)

3.3.2 Directed differentiation of hESCs to chondrocytes and stage-specific gene expression analysis

The Directed Differentiation Protocol (DDP) was carried out as outlined in section 1.1. At each stage of progression along the chondrogenic lineage a sample of cells were analysed for the expression of stage-specific genes. hESCs of the same passage that were not exposed to growth factors associated with the DDP were used as Stage 0 controls for gene expression analysis.

Feeder-free HUES7 hESCs cultured on Matrigel at 5% O_2 tension for at least 3 passages were used for these experiments. Upon initiation of the DDP, cells were cultured at 5% O_2 or 20% O_2. Day 1 of the DDP was initiated when cells were approximately 80% confluent, and 1-3 ml of growth factor containing DDP-basal medium was added to each well of a 6-well plate. Cells were passaged as in section 2.1.3 when cells were 60-80% confluent resulting in an average of 2 passages during each DDP.

In some experiments, following termination of the DDP, hESC-derived chondrocytes were cultured in HAC medium (DMEM/F12 (Gibco) containing 5% FBS, 1xITS (Gibco), 100 µM Ascorbate-2-phosphate (Sigma)), 'day-14' medium (DDP-BM containing day 11-13 growth factors (Table 2.1), or chondrogenic media (Table 3.2).

Table 3.2 **Chondrogenic media preparation**

Supplements	Stock concentration	Volume added	Final concentration
α-MEM (Lonza)		48.6 ml	
Ascorbate-2-phosphate (Sigma)	50 mM	100 µl	100 µM
ITS (100x) (Gibco)	insulin 1 mg/ml transferrin 0.55 mg/ml, sodium selenite 0.67 µg/ml	500 µl	insulin 10 µg/ml transferrin 5.5 µg/ml, sodium selenite 6.7 ng/ml
rh TGF-β3 (Peprotech)	2 ng/µl	250 µl	10 ng/ml
Dexamethasone (Sigma)	10 µM	50 µl	10 nM
L-proline (Sigma)	35 mM	500 µl	0.35 mM

3.3.3 Western Blotting

Western Blotting was used to quantify the expression of proteins in hESCs compared to hESC-derived chondrocytes.

3.3.3.1 Protein isolation

Cells at each stage of the DDP were washed in PBS and lysed by the addition of 100 µl ice cold radioimmunoprecipitation assay (RIPA) buffer (Sigma). Cells were scraped from the wells and cells in RIPA buffer were transferred to a clean Eppendorf. Samples were incubated for 20 minutes on ice before sonicating for 30 seconds and the supernatants collected and stored at -80°C.

3.3.3.2 Protein quantification

The protein concentration of samples was quantified using the Bradford assay. BSA standards were prepared (1.25-20 µg/ml) and 180 µl of each standard was added to a 96-well plate, blanks were also included (dH_2O). Samples were diluted 1:1000 in dH_2O and 180 µl of sample was added to the 96-well plate. Standards and samples were plated in duplicate. 20 µl of Bradford reagent (Biorad) was added to each well and mixed thoroughly by pipetting. Absorbance at 595nm was measured using a FLUOstar optima BMG Spectrophotometer and Optima software. Based on the absorbance readings a standard curve was generated and used to determine protein concentration of samples (Figure 3.1).

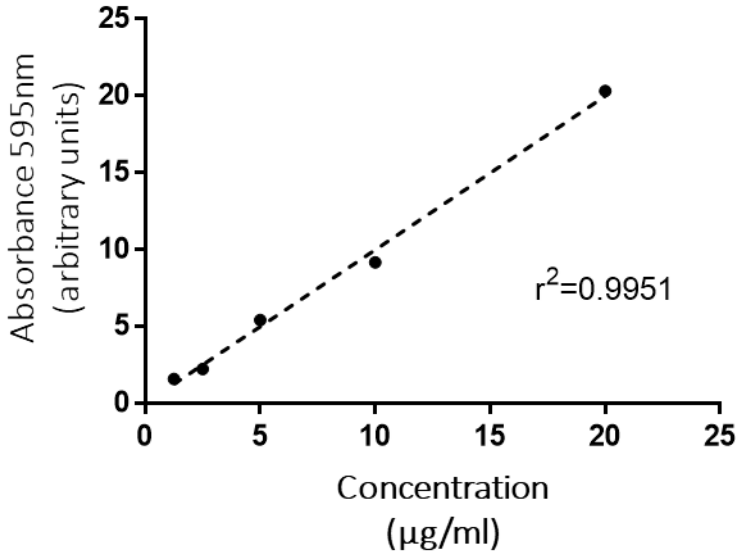

Figure 3.1 **Representative BSA standard curve used to calculate sample protein concentrations.**

3.3.3.3 SDS polyacrylamide gel electrophoresis (SDS-PAGE)

Protein samples were resolved on a 10% or 12% SDS bisacrylamide gel with a 5% stacking gel with a thickness of 0.75 mm (Table 3.3), alongside 5 µl EZ-Run Pre-stained Protein Ladder (Fisher). 20-50 µg protein lysate was loaded per sample along with 7.5 µl 4X Nu-PAGE LDS-sample buffer (Invitrogen), 7.5 µl 1M DL-dithiothreitol (DTT) (Sigma) and RIPA buffer to make a total volume of 25 µl. Prepared samples were incubated at 95°C for 5 minutes prior to loading. The electrophoresis 5x running buffer was diluted to make a 1x solution (pH 8.3) which was used to fill the electrophoresis tank (Biorad) (Table 3.4). Electrophoresis was performed at a constant rate of 55 mA until the ladder had run an appropriate distance through the gel.

Table 3.3 **Preparation of bis-acrylamide gels used for electrophoresis.**
Table provides information required to make either a 10% or a 12% gel. Volumes given are for 2x0.75 mm gels.

	Resolving gel		Stacking gel
Reagent	10%	12%	5%
1.5M Tris pH8.8 (Sigma)	4 ml	2.5 ml	-
10% SDS (Sigma)	160 µl	100 µl	50 µl
40% Acrylamide-bis (Sigma)	4 ml	3 ml	625 µl
dH_20	7.7 ml	5 ml	3.63 ml
1M Tris pH6.8	-	-	695 µl
10% ammonium persulphate (Sigma)	160 µl	100 µl	50 µl
TEMED (Fisher)	16 µl	7.5 µl	7.5 µl

Table 3.4 **Preparation of buffers for Western Blotting.**

Reagent	5x running buffer	Transfer buffer
Tris	15.1 g	-
Glycine	94 g	2.93 g
dH_20	900 ml	-
10% SDS	50 ml	-
1.5M Tris pH8.3	-	32 ml
Methanol	-	200 ml
	Make up to 1 L with dH_20 and pH to 8.3	Make up to 1 L with dH_20

3.3.3.4 Gel transfer and detection of proteins

Proteins were electroporated onto a nitrocellulose membrane (GE Healthcare) at 250 mA for 2 hours in chilled transfer buffer (Table 3.4).

Following transfer membranes were blocked for one hour at room temperature with 5% milk in either PBST (PBS containing 0.1% Tween-20 (pH ~7.4)) or 5% milk in TBST (Tris buffered saline (200 mM Tris and 1.5 M NaCl solution with 0.1% Tween-20 (pH ~7.4)) with constant agitation (SSM1 mini orbital shaker, Stuart). Membranes were then incubated overnight at 4°C in blocking buffer containing the relevant primary antibody with constant agitation (Table 3.5).

The membranes were washed three times (5 minutes each) in either PBST or TBST with constant agitation before incubation with the relevant HRP conjugated secondary antibody prepared in the same blocking buffer as the primary antibody (Table 3.5). Membranes were incubated for one hour at room temperature with constant agitation. Membranes were then washed as above before the addition of 1 ml electrochemiluminescence (ECL) detector (GE Healthcare) per membrane for 5 minutes in the dark. The membranes were transferred to light excluding cassettes and exposed to films. The exposure time varied between antibodies and samples. Films were developed in GBX developer/replenisher solution (Kodak) (diluted 1:5 in dH_20) until bands appeared. Films were then washed in water and fixed in GBX fixer/replenisher solution (Kodak) (diluted 1:5 in dH_20) were washed in water and allowed to dry.

After detection of the primary antibody, membranes were washed three times in PBST (5 minutes each) with constant agitation and incubated with an anti-β-actin-HRP antibody (Table 3.5) in 5% Milk/PBST for one hour at room temperature with constant agitation. Membranes were washed as previously described and ECL was added for 5 minutes in the dark.

β-actin was developed by the same method described for primary antibodies.

Table 3.5 **Antibodies used for Western Blotting.**

All primary and secondary antibodies used for Western Blotting are shown, along with the % gel on which they were run, and the relevant blocking buffer.

Primary antibody	% gel	Dilution	Blocking buffer	Secondary antibody
Mouse-IgG2b anti-OCT4 (Santa Cruz)	12	1:1000	5% Milk/PBST	Anti-mouse IgG HRP (1:100.000) (Sigma)
Rabbit-IgG anti-SOX2 (Cell Signalling Technology)	12	1:3000	5% Milk/TBST	Anti-rabbit IgG HRP (1:35,000) (GE Healthcare)
Rabbit-IgG anti-NANOG (AbCam)	12	1:500	5% Milk/PBST	Anti-rabbit IgG HRP (1:35,000) (GE Healthcare)
Rabbit IgG anti-SOX9	12	1:850	5% Milk/PBST	Anti-rabbit IgG HRP (1:35,000) (GE Healthcare)
Rabbit Anti-Type II Collagen (Calbiochem)	10	1:1500	5% Milk/PBST	Anti-rabbit IgG HRP (1:35,000) (GE Healthcare)
Mouse-IgG1 anti-β-actin-HRP (Sigma)	-	1:50,000	5% Milk/PBST	Anti-rabbit IgG HRP (1:35,000) (GE Healthcare)

3.3.3.5 Densitometry

Films were scanned and high resolution .Tiff format images were used for quantification. Images were opened on FIJI/ImageJ, inverted, and the integrated density of the bands was measured, as was the integrated density of the background. Background integrated density was deducted from the integrated density of the band of interest, and the process was repeated for the relevant β-actin bands. Relative expression of the protein of interest was calculated by dividing the background deducted integrated measurement by the background deducted integrated density of β-actin to give relative expression of the protein of interest.

3.3.4 Statistics

3.3.4.1 RT-qPCR analysis

A Shapiro-Wilk normality test was used to confirm normal distribution. Once normal distribution was determined a Student's t-test was used (paired or unpaired depending on data), assuming equal variance (2 sample t-test).

3.3.4.2 Western Blot analysis

A Shapiro-Wilk normality test was used to confirm normal distribution. For data where two conditions were compared a paired Student's t-test was used, assuming equal variance (2 sample t-test). For data where more than 2 conditions were compared a one-way Anova followed by Tukey's post-hoc multiple comparisons test was used. Protein expression was normalised to β-actin and the results made relative to 1 for the highest value.

3.4 Results

3.4.1 Characterisation of HUES7 hESCs

HUES7 hESCs were cultured on a MEF feeder layer, either at 20% (normoxia) or 5% (hypoxia) O_2 tension. It is known that hESCs are sensitive to O_2 tension, and express key pluripotency genes (*OCT4, SOX2, NANOG*) at higher levels when cultured at 5% O_2 tension compared to 20% O_2 (Forristal et al., 2010). As routine hESC culture is currently carried out at 20% O_2 tension, the expression of key pluripotency proteins was confirmed at both 20% and 5% O_2. Immunocytochemistry was performed on cells cultured at either 20% or 5% O_2.

HUES7 hESCs cultured at both 20% and 5% O_2 formed distinct colonies with clearly defined borders (Figure 3.2). MEFs can be seen surrounding the cells in phase contrast images. Colonies of cells cultured at 5% O_2 appeared larger and more tightly packed compared to 20%, and the colony borders were typically better defined. This is in line with what has been reported in the literature (Forristal et al., 2010).

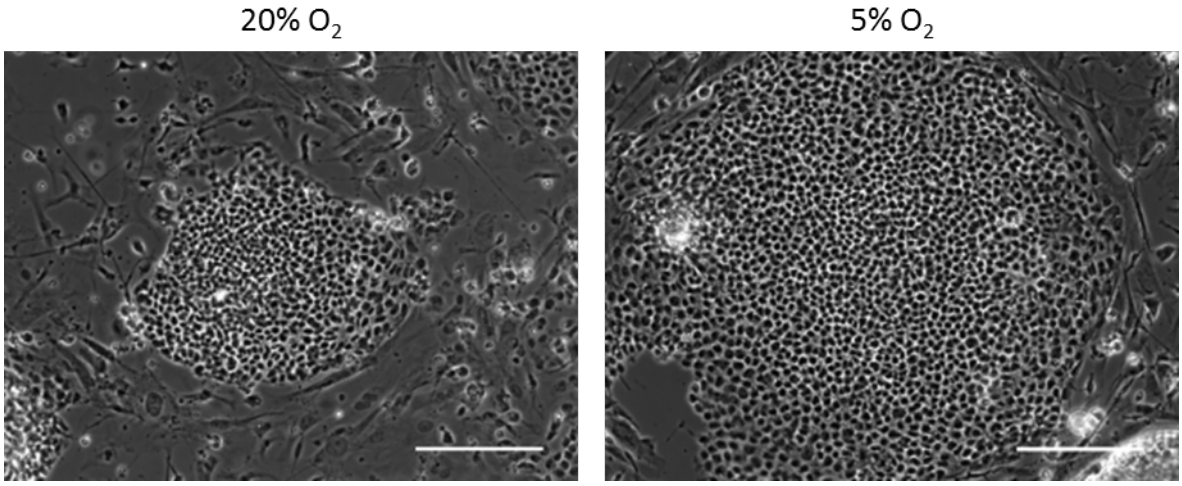

Figure 3.2 **HUES7 hESCs cultured at 20% or 5% O_2 form tightly packed colonies.**
HUES7 hESCs were cultured on a MEF feeder layer at 20% and 5% O_2. Representative phase contrast images were taken for comparison of colony morphology. Scale bars, 200 µm.

The pluripotency markers OCT4, SOX2 and NANOG were all clearly expressed in the nuclei of cells cultured at 20% (Figure 3.3 & Figure 3.4) and 5% O_2 (Figure 3.5 & Figure 3.6), and the co-localisation of the FITC labelled proteins and DAPI demonstrates nuclear localisation of these transcription factors. There was no detectable difference in expression levels of OCT4, SOX2 or NANOG by immunocytochemistry between 20% and 5% O_2 tension.

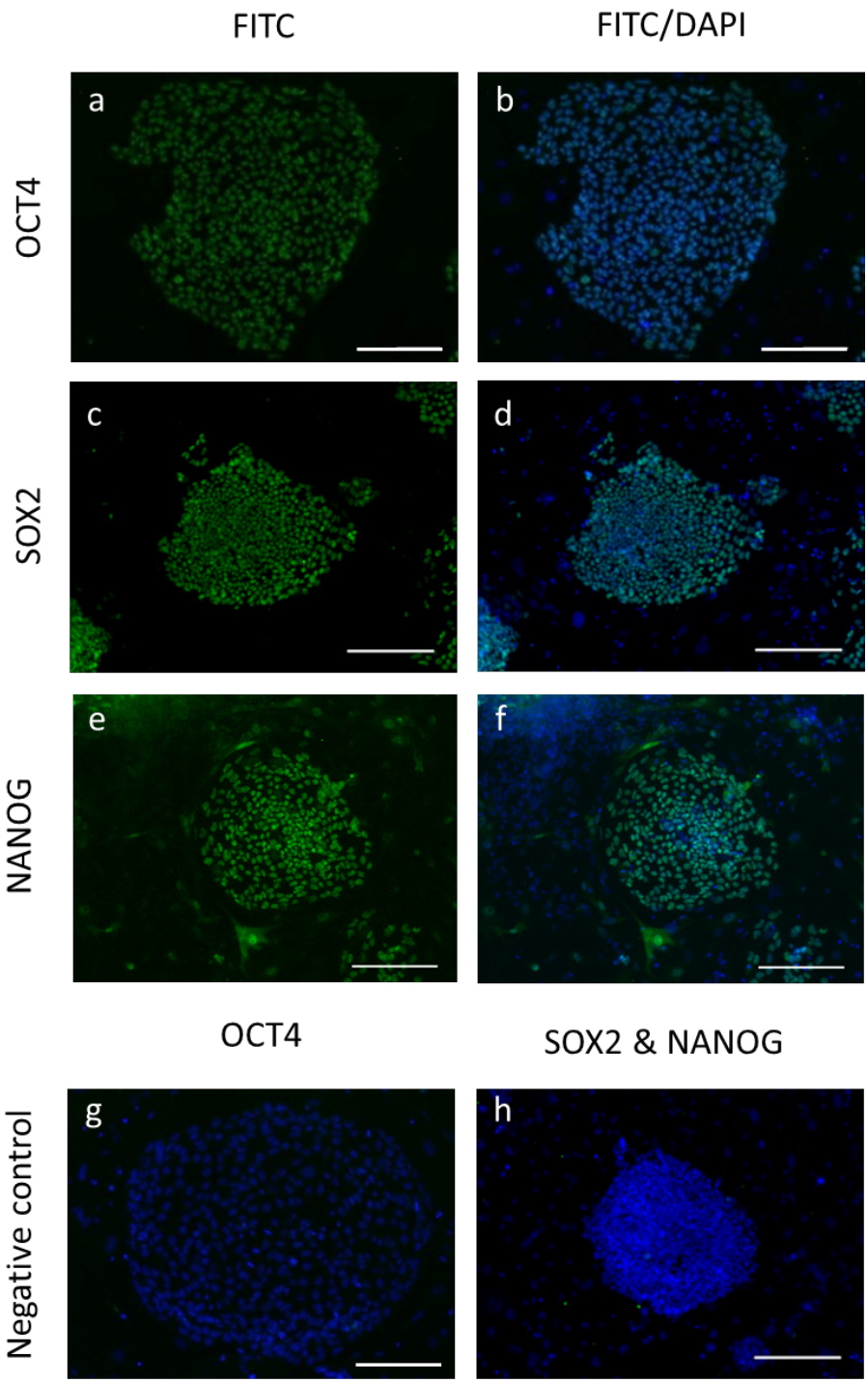

Figure 3.3 **HUES7 hESCs cultured at 20% oxygen tension express key intracellular pluripotency markers.**

HUES7 hESCs were cultured on MEFs at 20% O_2. Immunocytochemistry was performed, and cells were labelled for the pluripotency markers OCT4 (a, b), SOX2 (c, d), and NANOG (e, f) using a FITC conjugated secondary antibody. DAPI was used as a nucleus specific label. Secondary antibody only negative controls shown g and h. Scale bars, 200 µm.

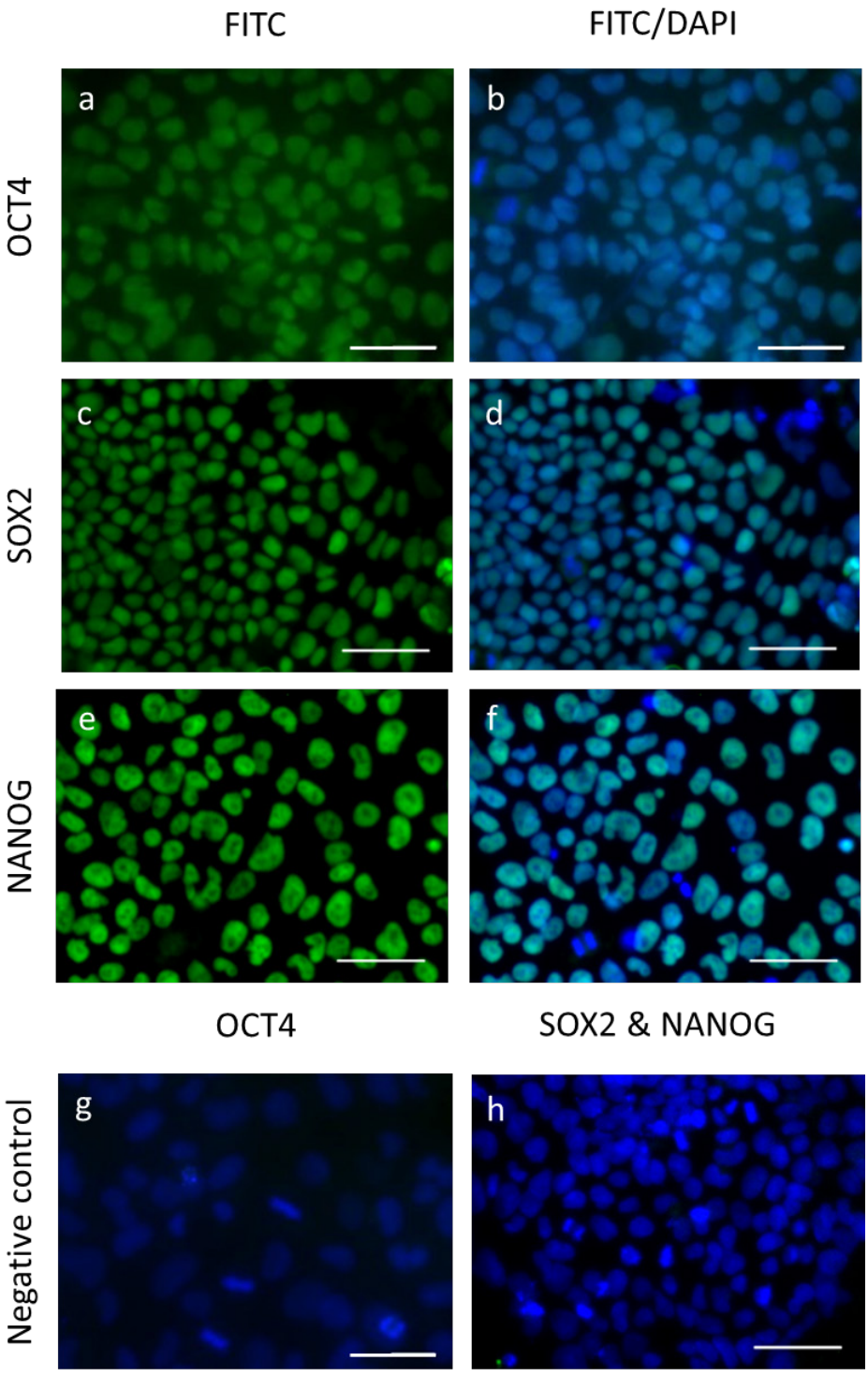

Figure 3.4 **Localisation of HUES7 hESCs cultured at 20% oxygen tension express key intracellular pluripotency markers.**

HUES7 hESCs were cultured on MEFs at 20% O_2. Immunocytochemistry was performed, and cells were labelled for the pluripotency markers OCT4 (a, b), SOX2 (c, d), and NANOG (e, f) using a FITC conjugated secondary antibody. DAPI was used as a nucleus specific label. Secondary antibody only negative controls shown g and h. Scale bars, 50 µm.

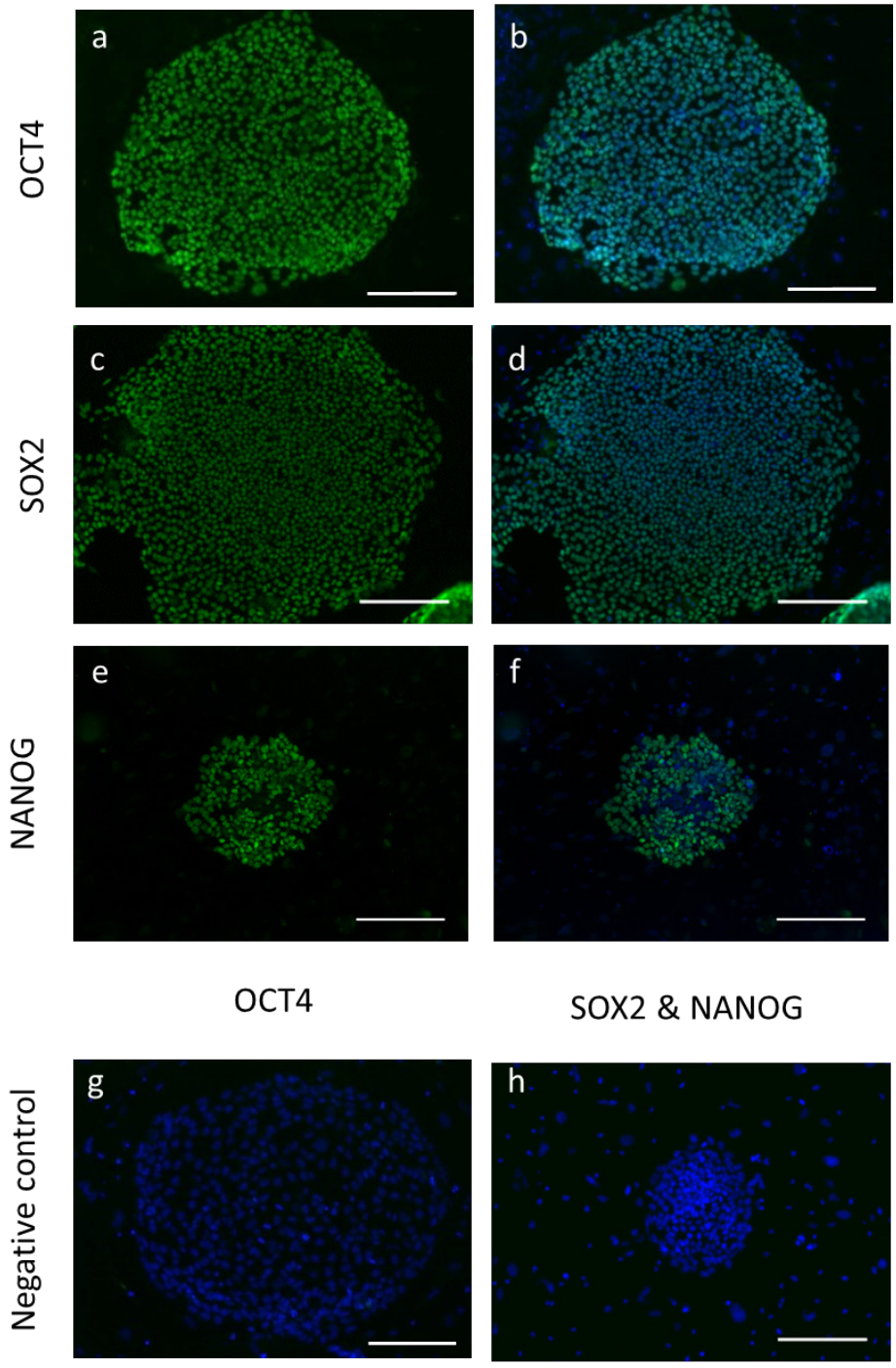

Figure 3.5 **HUES7 hESCs cultured at 5% oxygen tension express key intracellular pluripotency markers.**

HUES7 hESCs were cultured on MEFs at 5% O_2. Immunocytochemistry was performed, and cells were labelled for the pluripotency markers OCT4 (a, b), SOX2 (c, d), and NANOG (e, f) using a FITC conjugated secondary antibody. DAPI was used as a nucleus specific label. Secondary antibody only negative controls shown g and h. Scale bars, 200 µm.

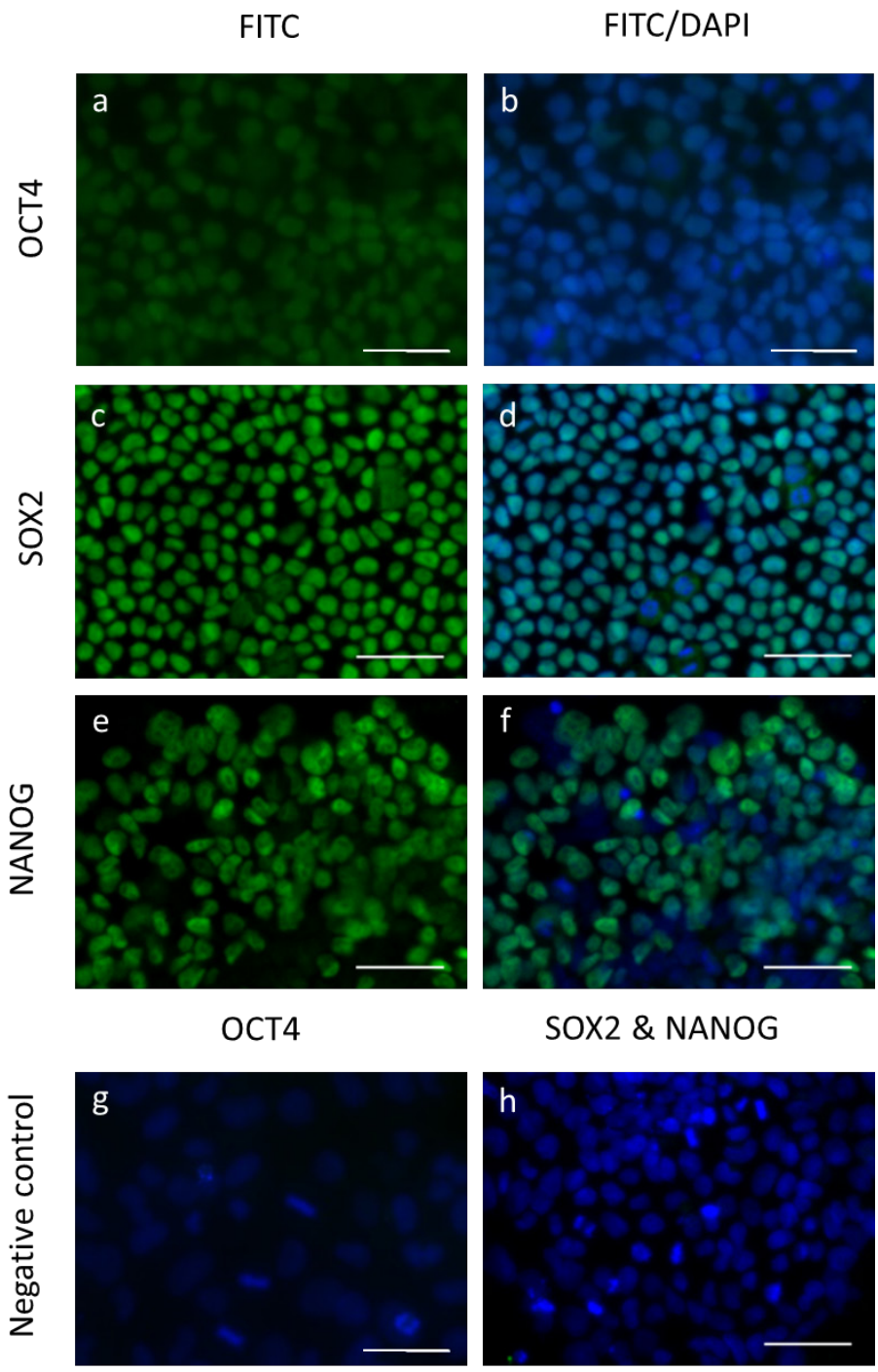

Figure 3.6 **Localisation of HUES7 hESCs cultured at 5% oxygen tension express key intracellular pluripotency markers.**

HUES7 hESCs were cultured on MEFs at 5% O_2. Immunocytochemistry was performed, and cells were labelled for the pluripotency markers OCT4 (a, b), SOX2 (c, d), and NANOG (e, f) using a FITC conjugated secondary antibody. DAPI was used as a nucleus specific label. Secondary antibody only negative controls shown g and h. Scale bars, 50 µm.

Cells were also labelled for the surface markers TRA-1-60 (pluripotency) and SSEA1 (early differentiation). Cells cultured at 20% (Figure 3.7 and Figure 3.8) and 5% O_2 (Figure 3.9 and Figure 3.10) showed expression of TRA-1-60. Cells cultured at 20% O_2 showed some limited expression of the early differentiation marker SSEA1 (Figure 3.7 c, d), which was not detected in cells maintained at 5% O_2 (Figure 3.9 c, d).

For all subsequent experiments cells cultured at 5% O_2 were used.

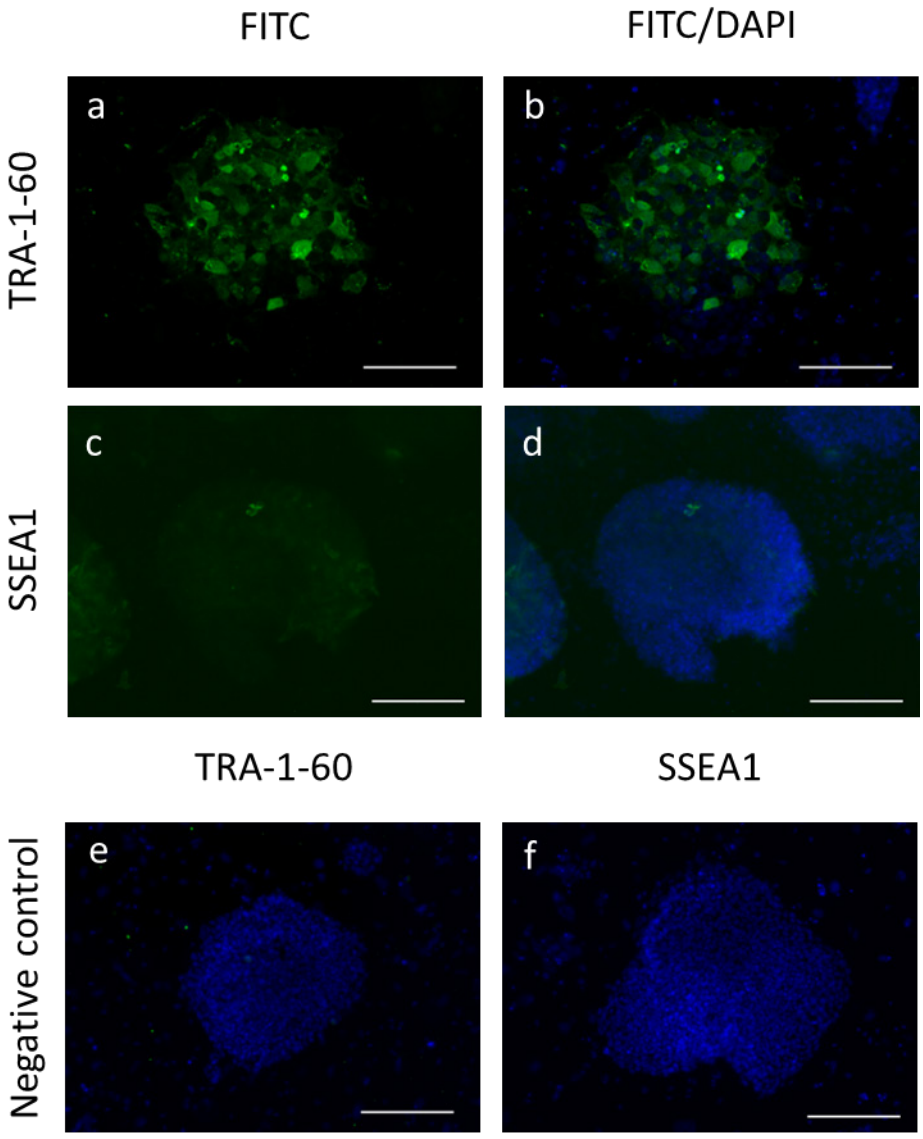

Figure 3.7 **HUES7 hESCs cultured at 20% oxygen tension express the cell surface marker TRA-1-60 but not SSEA1.**

HUES7 hESCs were cultured on MEFs at 20% O_2. Immunocytochemistry was performed, and cells were labelled for the pluripotency marker TRA-1-60 (a, b), and the early differentiation marker SSEA1 (c, d) using a FITC conjugated secondary antibody. DAPI was used as a nucleus specific label. Secondary antibody only negative controls shown e and f. Scale bars, 200 µm.

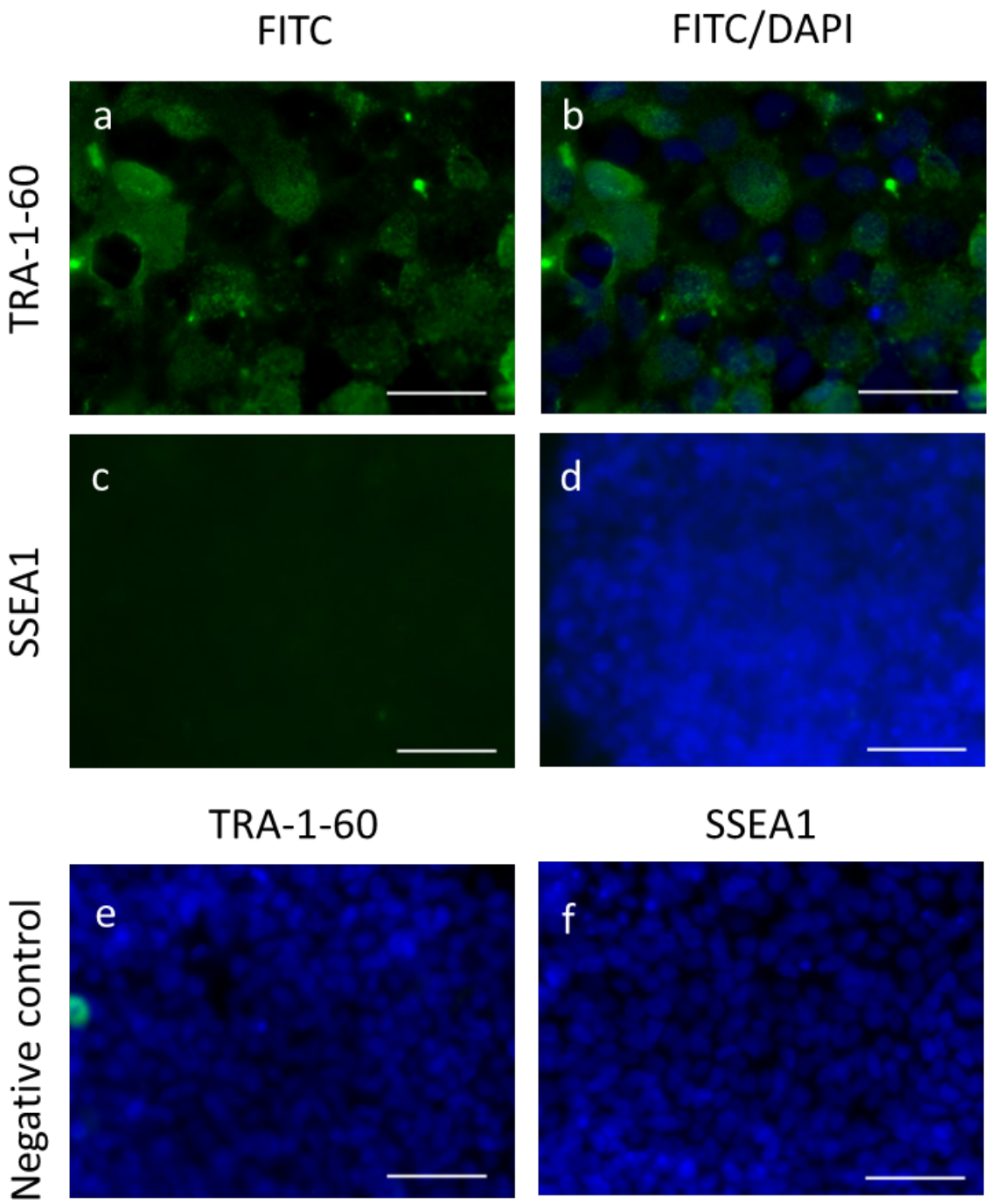

Figure 3.8 **Localisation of HUES7 hESCs cultured at 20% oxygen tension express the cell surface marker TRA-1-60 but not SSEA1.**

HUES7 hESCs were cultured on MEFs at 20% O_2. Immunocytochemistry was performed, and cells were labelled for the pluripotency marker TRA-1-60 (a, b), and the early differentiation marker SSEA1 (c, d) using a FITC conjugated secondary antibody. DAPI was used as a nucleus specific label. Secondary antibody only negative controls shown e and f. Scale bars, 50 µm.

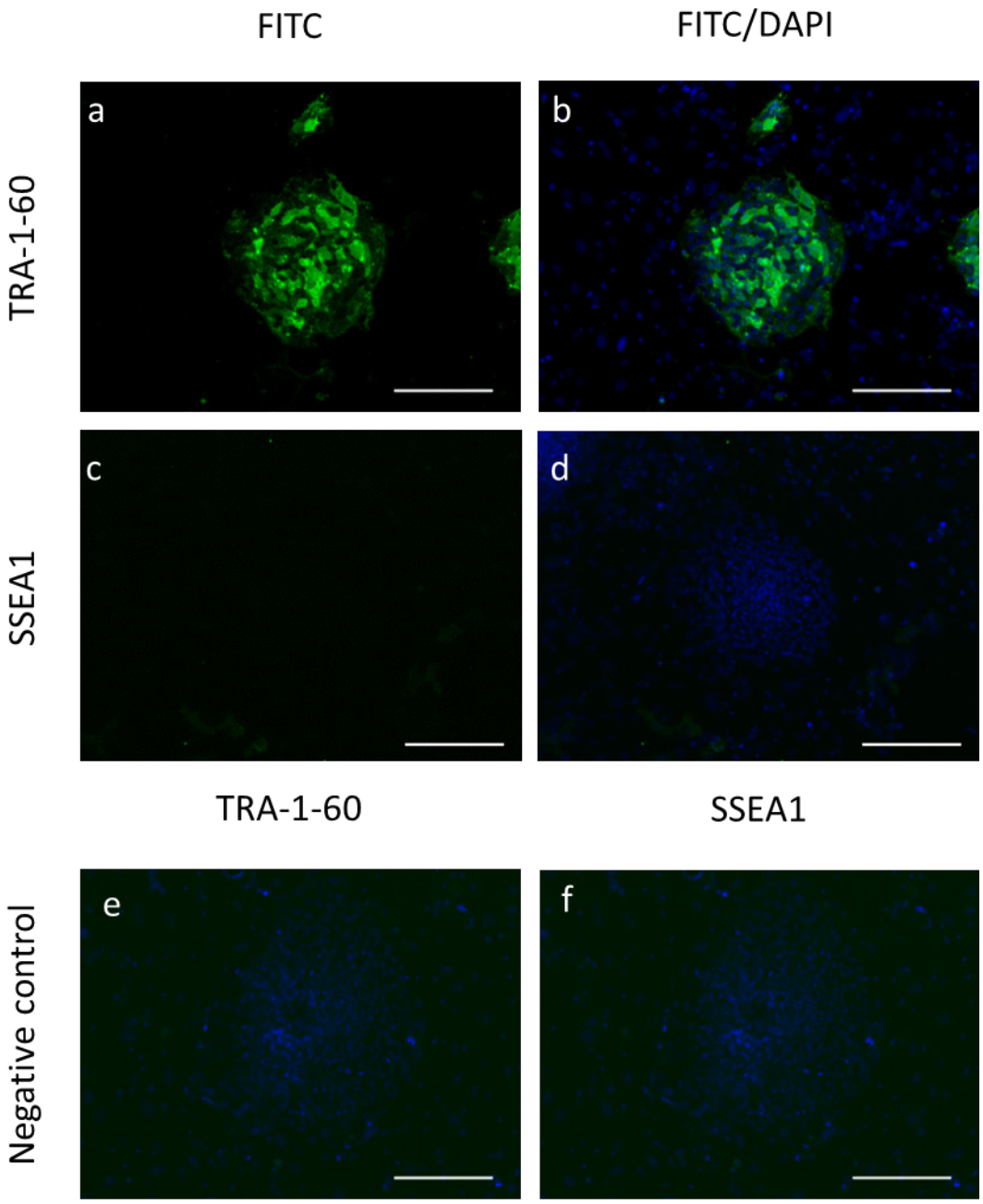

Figure 3.9 **HUES7 hESCs cultured at 5% oxygen tension express the cell surface marker TRA-1-60 but not SSEA1.**

HUES7 hESCs were cultured on MEFs at 5% O_2. Immunocytochemistry was performed, and cells were labelled for the pluripotency marker TRA-1-60 (a, b), and the early differentiation marker SSEA1 (c, d) using a FITC conjugated secondary antibody. DAPI was used as a nucleus specific label. Secondary antibody only negative controls shown e and f. Scale bars, 200 µm

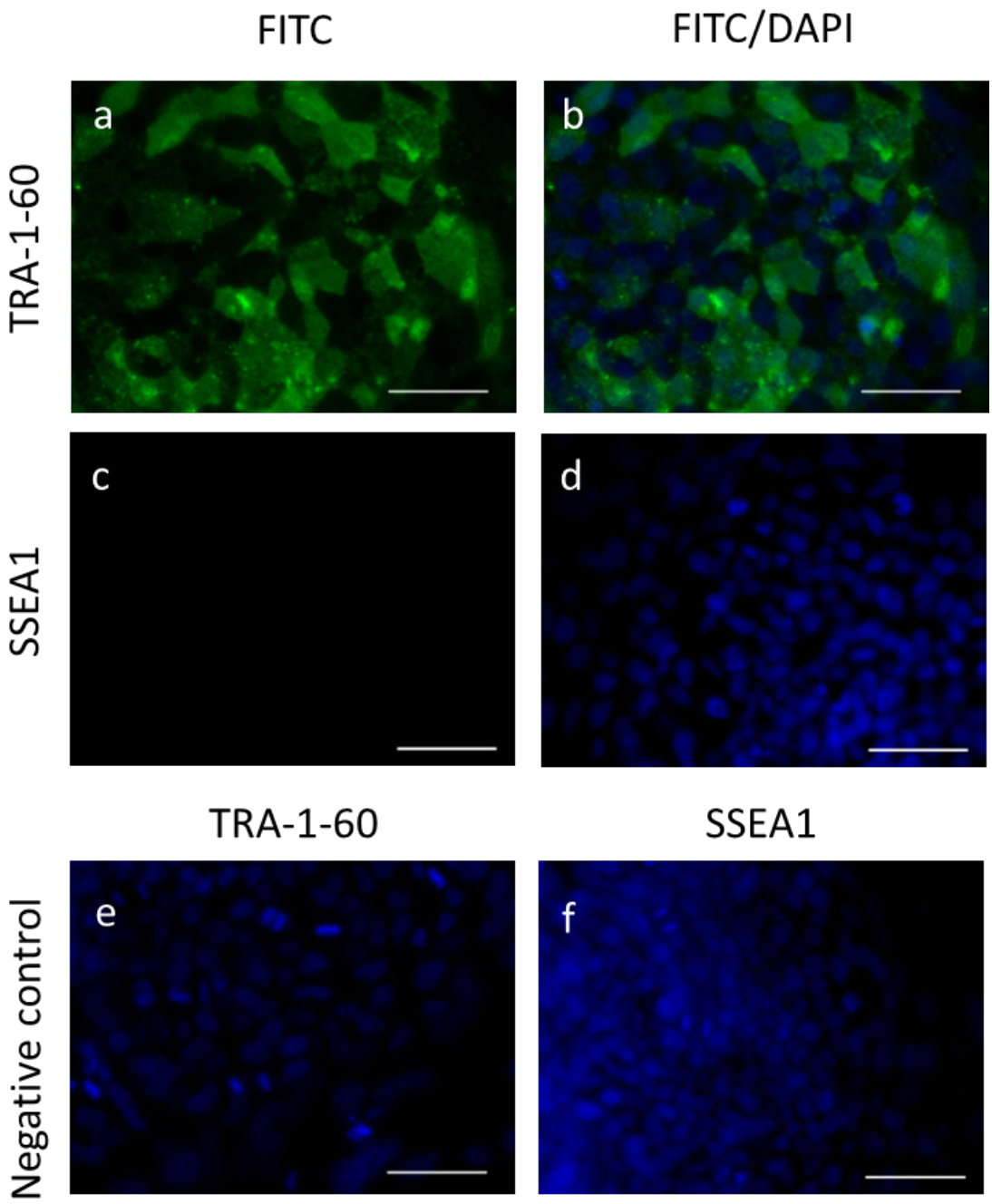

Figure 3.10 **Localisation of HUES7 hESCs cultured at 5% oxygen tension express the cell surface marker TRA-1-60 but not SSEA1.**

HUES7 hESCs were cultured on MEFs at 5% O_2. Immunocytochemistry was performed, and cells were labelled for the pluripotency marker TRA-1-60 (a, b), and the early differentiation marker SSEA1 (c, d) using a FITC conjugated secondary antibody. DAPI was used as a nucleus specific label. Secondary antibody only negative controls shown e and f. Scale bars, 50 µm.

3.4.2 Directed differentiation of hESCs towards chondrocytes

3.4.2.1 Cells exhibit morphological changes throughout the DDP

A modified directed differentiation protocol (DDP) based on that of Oldershaw et al. (2010b), was used to differentiate hESCs into chondrocytes (Figure 3.11). This protocol aims to recapitulate the signalling events that occur during embryonic development and cartilage generation; this is achieved by using a chemically defined growth factor-based culture, thereby promoting differentiation towards chondrogenesis. The protocol directs cells through primitive streak/mesendoderm, to mesoderm and finally towards chondrocytes (Figure 3.11).

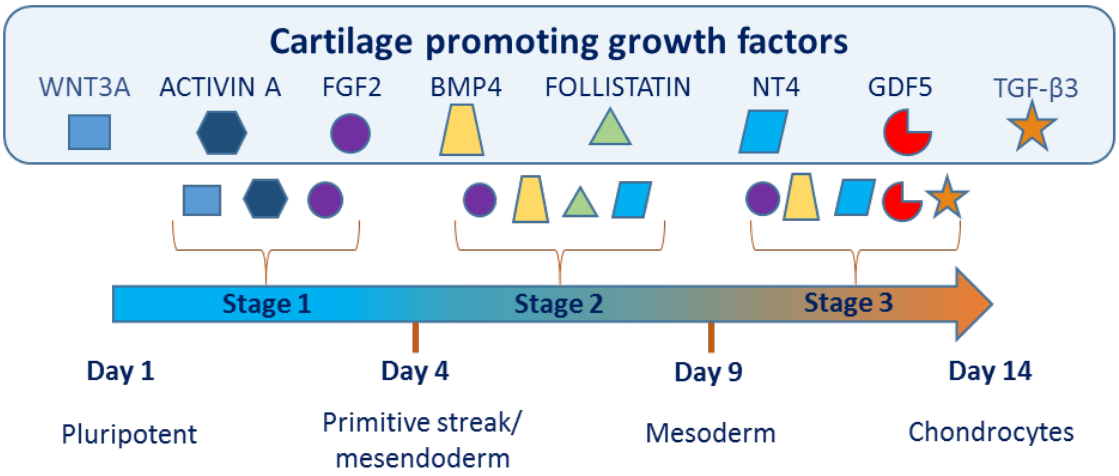

Figure 3.11 **A directed differentiation protocol to generate chondrocytes from hESCs.**

A 3-stage Directed Differentiation Protocol (DDP) was developed to differentiate hESCs into chondrocytes. Growth factor cocktails were used to direct pluripotent hESCs through 3 stages: Primitive streak/Mesendoderm (Stage 1), Mesoderm (Stage 2) and Chondrocytes (Stage 3).

HUES7 hESCs were cultured on Matrigel at 5% O_2 tension. The DDP was initiated on hESCs cultured under feeder free conditions on Matrigel 3 days post passage and was termed stage 0. At stage 0, the cells displayed typical hESC 'cobblestone' morphology and formed large compact colonies, with well-defined borders (Figure 3.12a, e and (Figure 3.13a, e). Upon initiation of the DDP, cells were either cultured at 20% O_2 (5-20% O_2) (Figure 3.12), or maintained at 5% O_2 (5-5% O_2) (Figure 3.13). Under both conditions, distinct changes in cell morphology were observed during the DDP. The initial stage of the DDP involved treating the cells with combinations of the growth factors WNT3A, ACTIVIN A and FGF2. These growth factors were used to drive the hESCs towards the primitive streak-mesendoderm lineage (Figure 3.11). At stage 1, cellular morphology was unaltered, however due to extensive proliferation, 5-20% O_2 cells were highly confluent relative to 5-5% O_2 cells (Figure 3.12b, f and Figure 3.13b, f).

Between stages 1 and 2, cells were treated with a combination of FGF2, BMP4, FOLLISTATIN and NT4. This combination of growth factors aimed to direct cells towards mesoderm (Figure 3.11). At stage 2 cells showed distinctly altered morphology. Under both differentiation conditions individual cells were less rounded and had elongated, gaining a more fibroblastic morphology. Cells had also organised to form rosette like structures (Figure 3.12c, g and Figure 3.13c, g).

The final phase of the DDP directed the differentiation of cells from mesoderm to chondrocytes (Figure 3.11). Cells were treated with combinations of FGF, GDF5 and TGF-β3 throughout, and BMP4 up to day 10. At stage 3, cells cultured under the 5-20% O_2 condition had lost the comparatively fibroblastic morphology seen at stage 2 and had formed loosely packed colonies with a less compact cobblestone morphology than observed in stage 0 hESCs (Figure 3.12d, h). Individual cells under 5-5% O_2 conditions shared similar morphology with those cultured under the 5-20% O_2 condition, however by Stage 3 cells had formed a confluent monolayer (Figure 3.13d, h) whereas 5-20% O_2 cells were relatively sparse (Figure 3.12d, h). At stage 3, cells were termed hESC-derived chondrocytes.

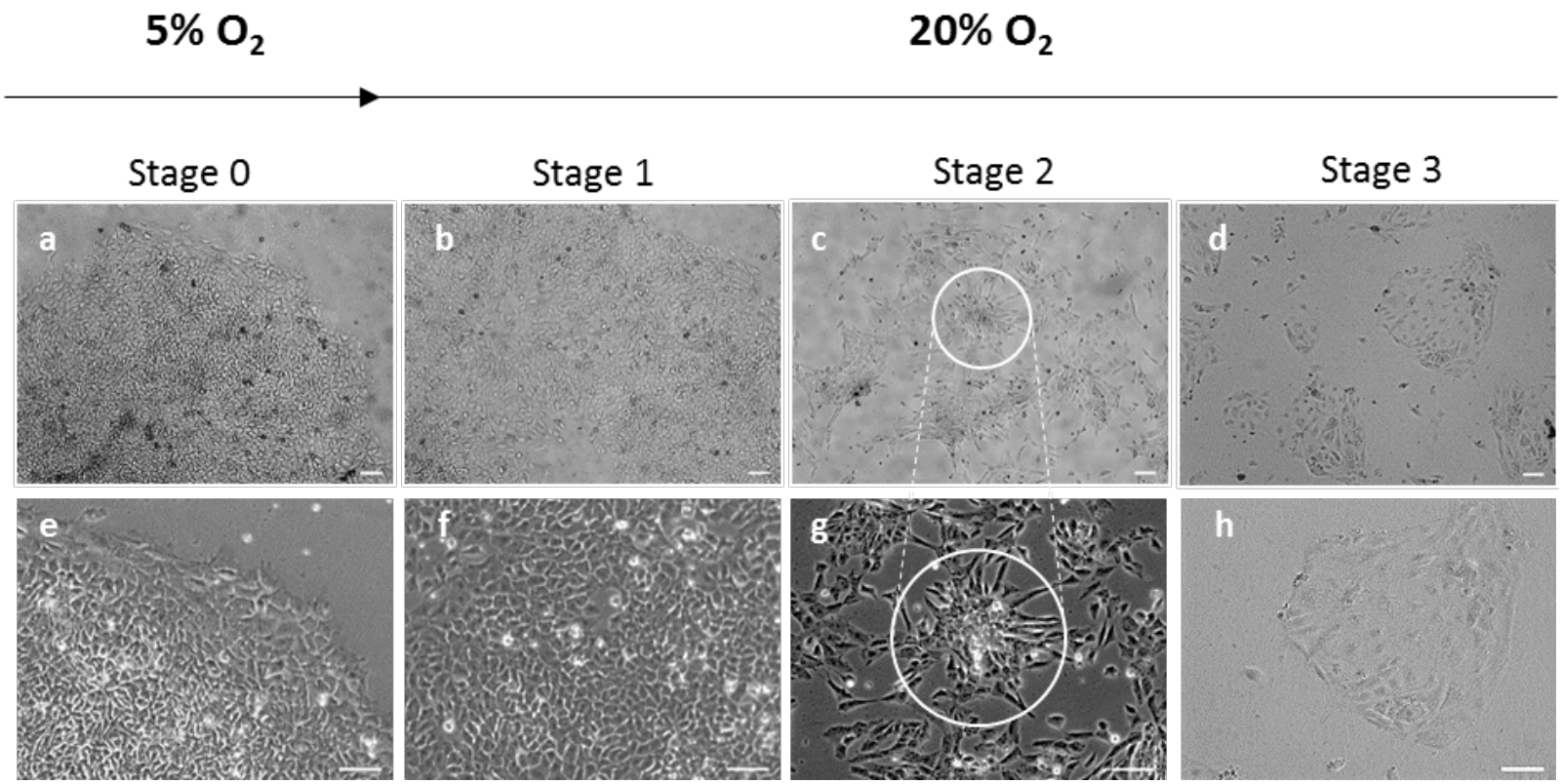
5% O_2
20% O_2
Stage 0
Stage 1
Stage 2
Stage 3
a
b
c
d
e
f
g
h

Figure 3.12 **hESCs cultured at 5% O_2 and differentiated at 20% O_2 (5-20% O_2) exhibit morphological changes over the course of the DDP.**

hESCs were cultured at 5% O_2. Upon initiation of the DDP, cells were transferred to 20% O_2 (5-20% O_2). Feeder free pluripotent HUES7 colony with round tightly packed morphology with distinct borders (a, e). Stage 1 (day 4) cultures with cells appearing like day 0 cells, but at a higher confluency (b, f). Stage 2 (day 9) cultures show cells developing an altered morphology and forming 'rosette-like' clusters (circled) (c, g). Stage 3 (day 14) (d, h) cells forming distinct colonies of cells with cobblestone morphology (d, h). Scale bars, 100 µm.

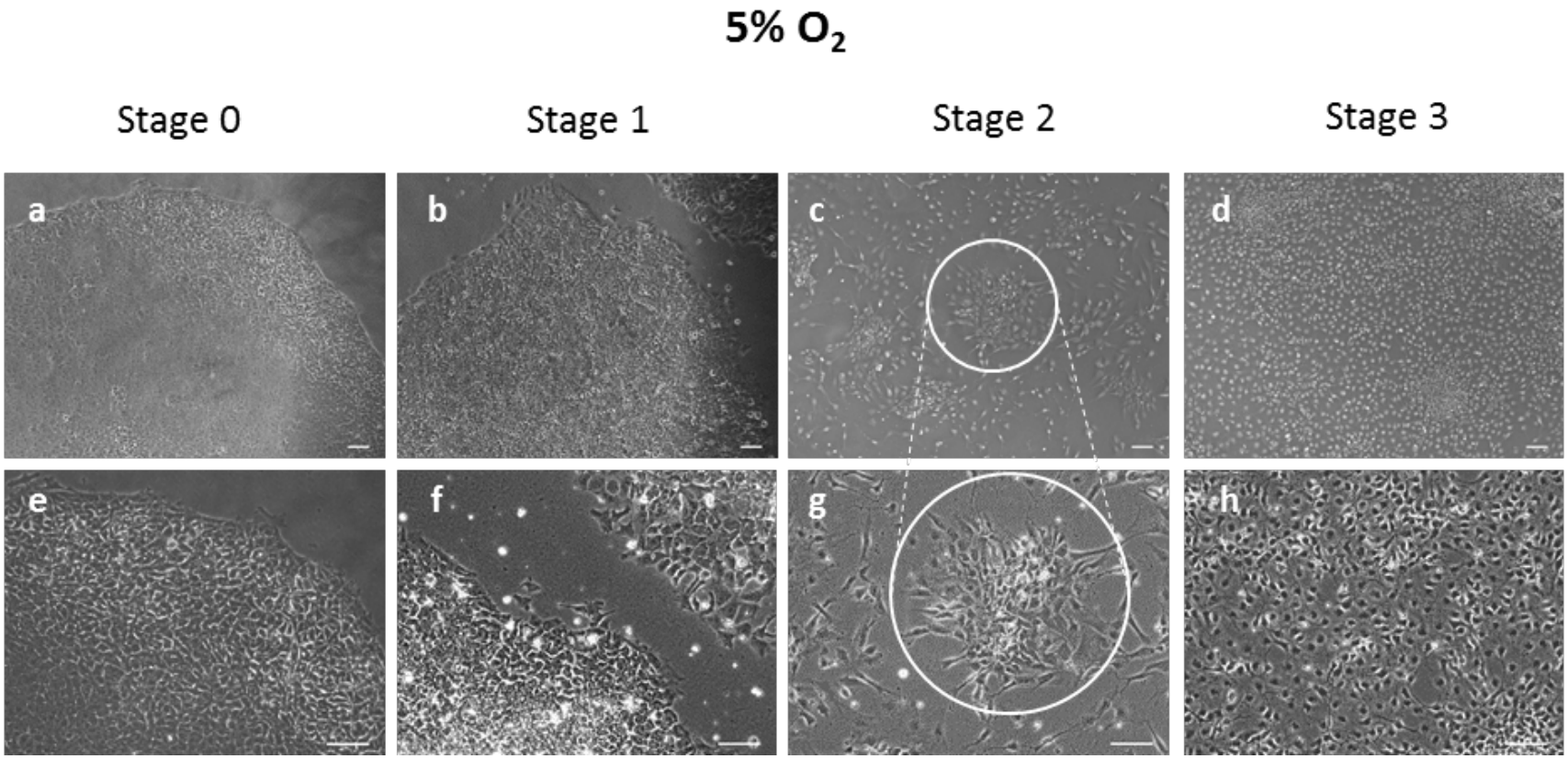
5% O_2
Stage 0
Stage 1
Stage 2
Stage 3
a
b
c
d
e
f
g
h

Figure 3.13 **hESCs cultured and differentiated at 5% O_2 (5-5% O_2) exhibit morphological changes over the course of the DDP.**

hESCs were cultured and differentiated at 5% O_2 (5-5% O_2). Feeder free pluripotent HUES7 colony with round tightly packed morphology with distinct borders (a, e). Stage 1 (day 4) cultures with cells appearing like day 0 cells (b, f). Stage 2 (day 9) cultures show cells developing an altered morphology and forming 'rosette-like' clusters (circled) (c, g). Stage 3 (day 14) cells forming a confluent monolayer of cells with cobblestone morphology (d, h). Scale bars, 100 µm.

3.4.2.2 Hypoxic differentiation is beneficial for generation of hESC-derived chondrocytes

hESC-derived chondrocytes were successfully generated by differentiation under both the 5-20% O_2 and 5-5% O_2 conditions, however cell numbers were noticeably lower when differentiation was performed at 20% O_2. To ascertain which condition yielded the most robustly chondrogenic cell expression of chondrogenic markers was compared between the two groups.

SOX9 expression was unchanged between the two conditions, however there was a significant increase (~15-fold) in the level of *COL2A1* mRNA transcripts in cells differentiated at 5% O_2, compared to cells differentiated at 20% O_2 ($p<0.05$) (Figure 3.14).

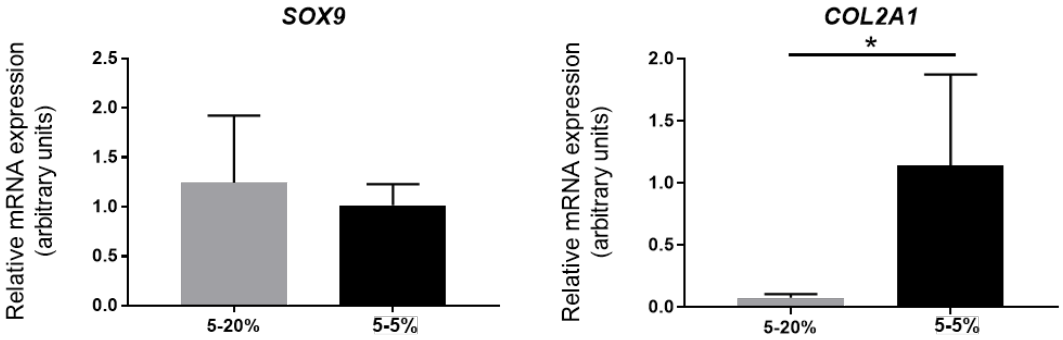

Figure 3.14 **Stage 3 cells differentiated at 5% O_2 express the chondrogenic marker *COL2A1* at a higher level than cells differentiated at 20% O_2.**

*DDPs were performed on HUES7 hESCs at either 20% O_2 (5-20% O_2) or 5% O_2 (5-5% O_2). Samples were collected at stage 3 of the DDP and RT-qPCR was performed to compare mRNA expression of SOX9 and COL2A1. Gene expression was normalised to UBC. Values represent mean ± SD. *$p<0.05$ according to unpaired t test. n=4 for each group.*

hESC-derived chondrocytes differentiated at either 20% (5-20% O_2) or 5% O_2 (5-5% O_2) were immunolabelled for SOX9 (Figure 3.15) and type II collagen (Figure 3.16). Under both conditions cells exhibited robust nuclear expression of the transcription factor SOX9 (Figure 3.15), and deposited a network of the extracellular matrix protein type II collagen (Figure 3.16). Despite a difference in *COL2A1* mRNA expression, no clear differences in protein expression between cells 5- 20% or 5-5% O_2 was observed. The expression of the pluripotency marker OCT4 was not detectable by immunocytochemistry in hESC-derived chondrocytes differentiated at 20% or 5% O_2 (Figure 3.17a, b).

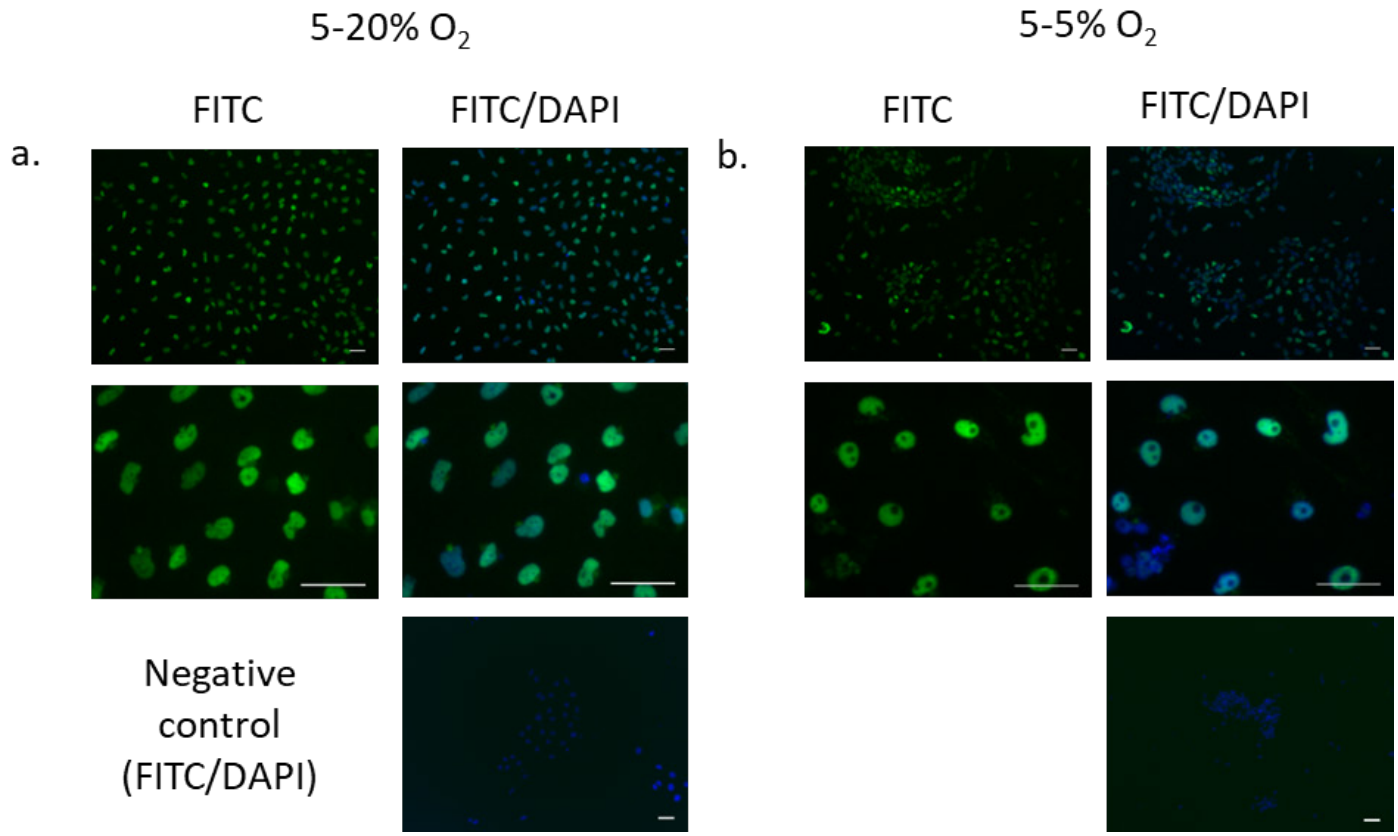

Figure 3.15 **hESC-derived chondrocytes differentiated at both 20% and 5% O_2 express the chondrogenic marker SOX9.**

Immunocytochemistry was performed on hESC-derived chondrocytes following differentiation at either 20% (5-20% O_2) (a) or 5% O_2 (5-5% O_2) (b). Samples were imunolabelled for SOX9 using a FITC conjugated secondary antibody. DAPI was used as a nucleus specific label. Secondary antibody only negative controls were included. Scale bars, 50 µm.

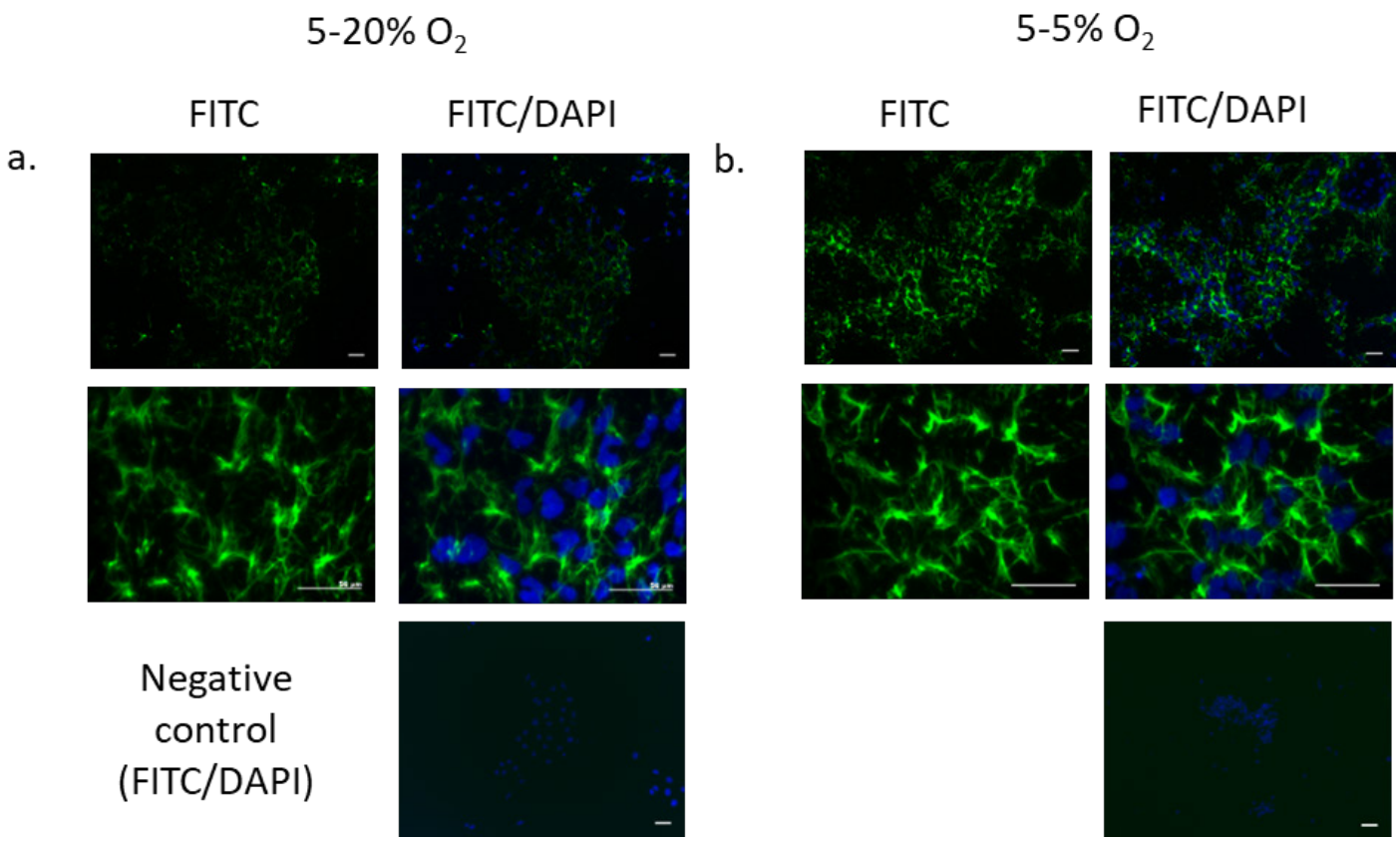

Figure 3.16 **hESC-derived chondrocytes differentiated at both 20% and 5% O_2 deposit the extracellular matrix protein type II collagen**

Immunocytochemistry was performed on hESC-derived chondrocytes following differentiation at either 20% (a) or 5% O_2 (b). Samples were imunolabelled for type II collagen using a FITC conjugated secondary antibody. DAPI was used as a nucleus specific label. Secondary antibody only negative controls were included. Scale bars, 50 µm.

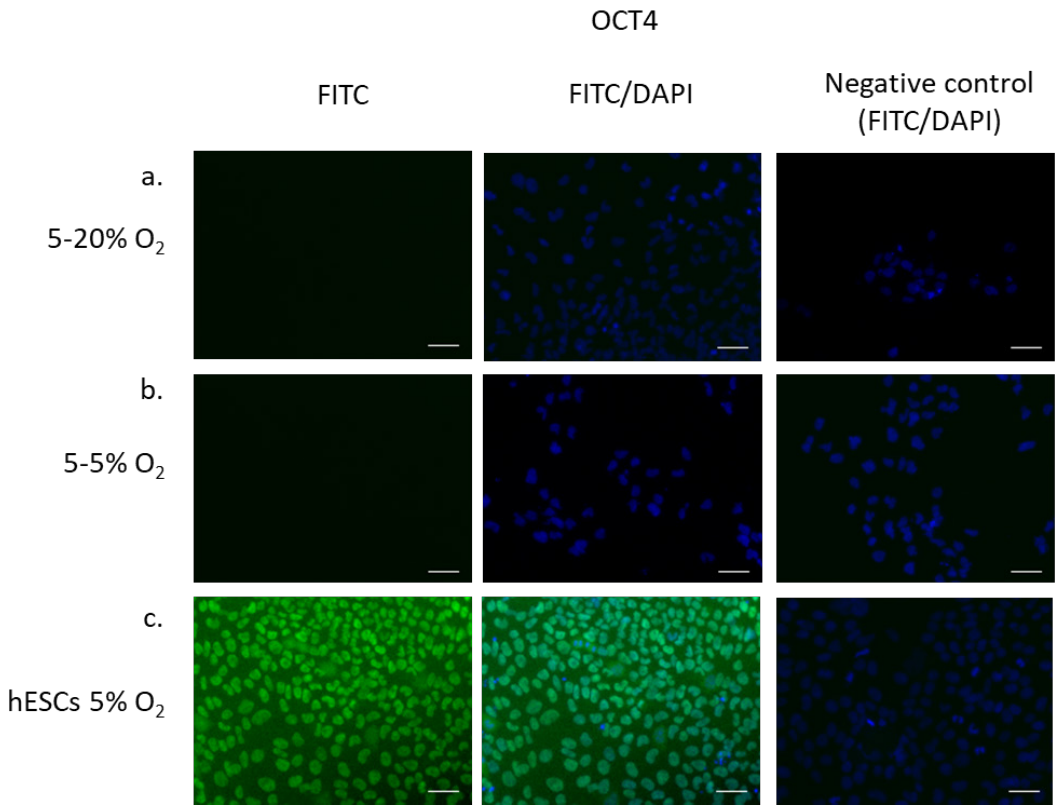

Figure 3.17 **OCT4 is no longer detectable by immunocytochemistry in hESC-derived chondrocytes.**

Immunocytochemistry was performed on hESC-derived chondrocytes following differentiation at either 20% (5-20% O_2) (a) or 5% O_2 (5-5% O_2) (b). Samples were imunolabelled for OCT4, using a FITC conjugated secondary antibody. DAPI was used as a nucleus specific label. hESCs cultured at 5% O_2 were used as a positive control (c). Secondary antibody only negative controls were included. Scale bars, 50 µm.

The success of differentiation under each condition was determined by the percentage of differentiation experiments that yielded enough cells for use in further experiments. A sufficient number of cells was regarded as at least $3x10^5$, as this is the minimum number required for pellet culture. It was found that when cells were differentiated at 20% O_2 cell numbers were typically low (as observed in Figure 3.12d, h), and frequently differentiation did not yield a sufficient number of cells for subsequent experiments. The success rate (percentage of experiments yielding $>3x10^5$ cells) for differentiation experiments at 5% O_2 was 95.3% compared to just 72.7% for differentiation experiments at 20% O_2 (Table 3.6).

Table 3.6 **DDPs performed under hypoxia were more successful than those performed at 20% O_2.**

Cells were differentiated at either 20% O_2 (5-20% O_2) or 5% O_2 (5-5% O_2). Percentage success refers to DDPs that had enough cells for subsequent experiments. 5-20% n=11, 5-5% n=43.

Condition	% success
5-20% O_2	72.7
5-5% O_2	95.3

3.4.2.3 Developmental stage-specific changes in gene expression during differentiation

Due to the higher rate of success of DDPs performed at 5% O_2 (5-5% O_2) relative to 20% O_2 (5-20% O_2) (Table 3.6), along with higher expression of *COL2A1* (Figure 3.14), all experiments from this point onwards utilised hESC-derived chondrocytes generated via DDPs performed at 5% O_2.

To further investigate cell differentiation at each stage of the DDP performed at 5% O_2, RT-qPCR was performed. The expression at stages 1, 2, and 3 were compared to Stage 0. Stage specific gene expression analysis discussed here is for cells differentiated at 5% O_2.

The effects of the DDP on the expression of the key pluripotency genes *OCT4*, *SOX2*, and *NANOG* were investigated (Figure 3.18a). *OCT4* expression decreased significantly at stages 1 and 2 relative to stage 0 ($p<0.01$) (Figure 3.18a i and ii). Between stages 0 and 2 *OCT4* expression had decreased by 75% (Figure 3.18a ii). By stage 3 *OCT4* was not significantly different from stage 0

(Figure 3.18a iii). *SOX2* expression was significantly decreased at stages 1 and 2 relative to stage 0 ($p<0.001$) (Figure 3.18a iv and v), with expression decreasing by 82% by stage 2 (Figure 3.18a v. There was no significant difference in *SOX2* expression between stages 0 and 3 (Figure 3.18a vi). *NANOG* expression remained unchanged between Stages 0 and 1 (Figure 3.18a vii). By Stage 2 mRNA expression was significantly downregulated ($p<0.001$) (Figure 3.18a viii), and by Stage 3 expression had decreased by 83% relative to Stage 0 ($p<0.1$) (Figure 3.18a ix).

The effect of the DDP on the expression of stage 1 specific genes (*Brachyury, CDH1, GSC2)* was also investigated (Figure 3.18b). *BRACHYURY* expression increased ~50-fold relative to Stage 0 ($p<0.05$) (Figure 3.18b i). By Stage 2 there was no significant difference in expression relative to Stage 0 (Figure 3.18b ii), but by Stage 3 expression had decreased by ~99% relative to Stage 0 ($p<0.001$) (Figure 3.18biii). *CDH1* showed no significant changes in mRNA expression between Stages 0-3 (Figure 3.18b iv-vi). *GSC2* showed no significant differences in expression at any stage relative to stage 0, however there was a trend towards increased expression (Figure 3.18b vii-ix).

The effect of the DDP on the expression of stage 2 specific genes (*CXCR4, KDR)* was also investigated (Figure 3.18c). Whilst there were no significant changes in expression of either gene, *CXCR4* expression increased non-significantly by ~8-, ~28- and ~12-fold at Stages 1, 2 and 3 respectively (Figure 3.20c i-iii), whilst *KDR* mRNA increased non significantly by ~3-, ~10- and ~5-fold at Stages 1, 2 and 3 respectively (Figure 3.18c iv-vi).

Finally, the effect of the DDP on the expression of stage 3 specific genes (*SOX9, COL2A1)* was investigated (Figure 3.18 d). There was no significant difference in *SOX9* mRNA expression between stage 0 and stage 1 (Figure 3.18d iv), however by stage 2 expression was ~20-fold greater than at Stage 0 ($p<0.05$) (Figure 3.18d ii). There was no significant difference between *SOX9* expression at stage 3 (Figure 3.18d iii). *COL2A1* expression did not show any statistically significant changes in expression during the DDP, however there was a trend towards increased expression with fold changes ~12 and ~180 at Stages 2 and 3 respectively (Figure 3.18d iv-vi).

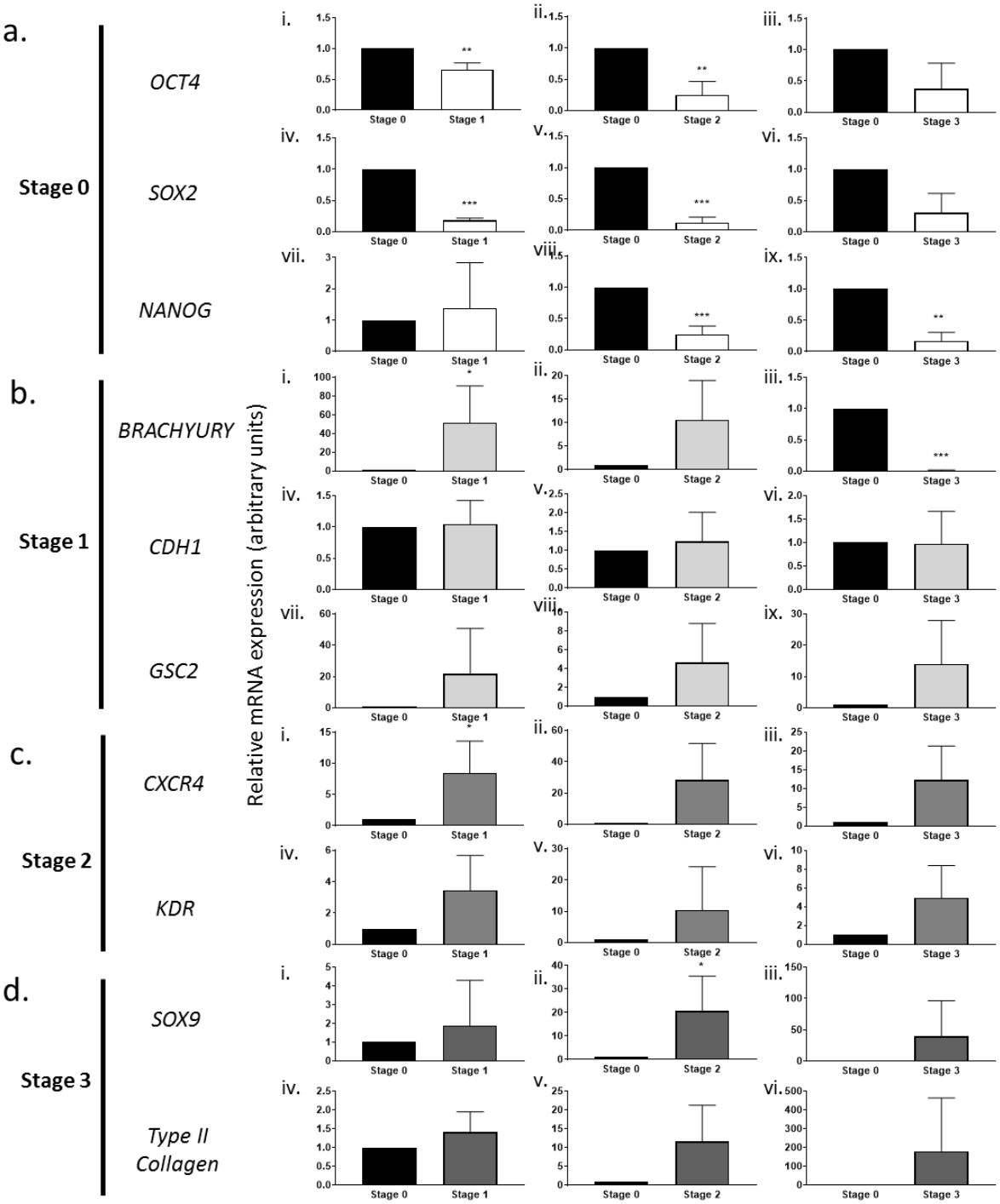

Figure 3.18 **Stage-specific changes in gene expression of cells differentiated at 5% O_2 (5-5% O_2).** *RT-qPCR was performed on samples from HUES7 hESCs at stage 0 (day 0), stage 1 (day 4), stage 2 (day 9), and stage 3 (day 14) of the DDP performed at 5% O_2. Genes associated with pluripotency (a), primitive streak-mesendoderm (b), mesoderm (c), and chondrocytes (d) were investigated. Gene expression was normalised to UBC and set at 1 for Stage 0. Undetermined CT values were set at 40. Values represent mean ± SD. Significance is given relative to Stage 0. *p<0.05, **p<0.01, ***p<0.001. Stage 0 (n=12), stage 1 (n=7), stage 2 (n=4), stage 3 (n=5).*

To more easily visualise temporal expression patterns in stage specific genes, the data plotted in Figure 3.18 was also plotted in line graph format (Figure 3.19). Statistical significance was not detailed on this graph as the data set had already been analysed in Figure 3.18 by use of student's T-test, the results of which do not translate onto the line graphs in Figure 3.19 due to their being more than 2 groups on each graph.

Figure 3.19a demonstrates an overall decrease in expression of the Stage 0 specific genes between Stages 0 and 1. *Nanog*, unlike *OCT4* and *SOX2* was found to increase expression at Stage 1 compared to stage 0. The expression of Stage 1 specific genes *Brachyury* and *GSC2* showed a peak in expression at Stage 1, whereas *CDH1* expression did not appear to change at any stage (Figure 3.19b). Stage 2 specific genes, *CXCR4* and *KDR* showed a peak in expression at Stage 2, with a subsequent decrease at Stage 3 (Figure 3.19c). The Stage 3 specific genes *SOX9* and *COL2A1* increased expression at Stage 2 relative to Stage 0, and continued to increase at Stage 3 (Figure 3.19d).

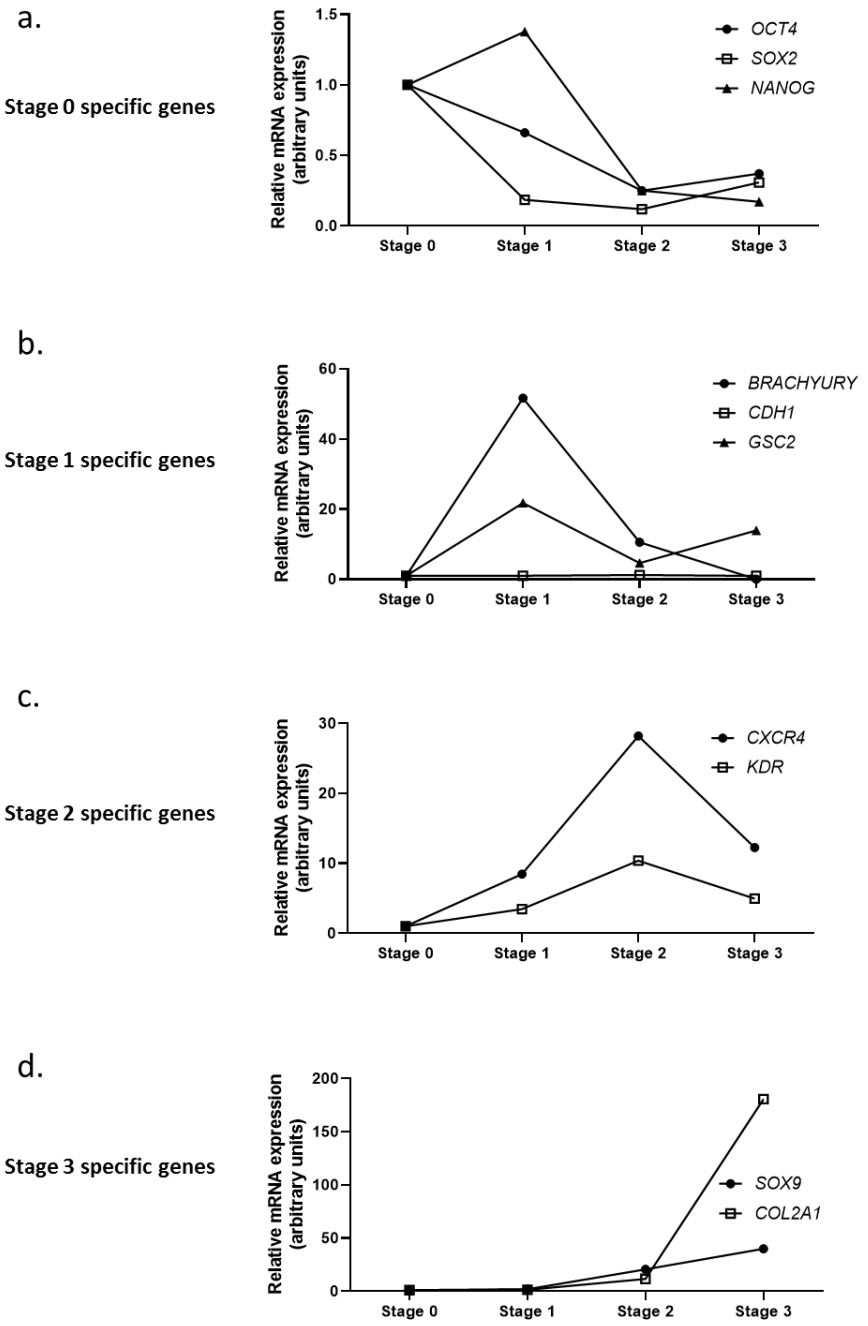

Figure 3.19 **Line graphs depicting temporal expression patterns of stage-specific genes in cells differentiated at 5% O_2 (5-5% O_2).**

RT-qPCR was performed on samples from HUES7 hESCs at stage 0 (day 0), stage 1 (day 4), stage 2 (day 9), and stage 3 (day 14) of the DDP performed at 5% O_2. Genes associated with pluripotency (a), primitive streak-mesendoderm (b), mesoderm (c), and chondrocytes (d) were investigated. Gene expression was normalised to UBC and set at 1 for Stage 0. Undetermined CT values were set at 40. Values represent mean. Stage 0 (n=12), stage 1 (n=7), stage 2 (n=4), stage 3 (n=5).

3.4.2.4 Western blot analysis of pluripotency and chondrogenic marker expression in hESC-derived chondrocytes

To quantitatively analyse changes in the expression of pluripotency and chondrogenic proteins during the DDP (5-5% O_2), Western Blotting was performed on cells obtained at stage 0 and stage 3 (Figure 3.20a). Between stages 0 and 3 the OCT4 expression decreased by ~97% between stage 0 and stage 3 ($p<0.001$) (Figure 3.20b i), SOX2 decreased by ~79% ($p<0.01$) (Figure 3.20b ii) and NANOG decreased by ~92% ($p<0.001$) (Figure 3.20b iii). The expression of key chondrogenic transcription factor, SOX9 increased by ~84% between stage 0 and stage 3 ($p<0.001$) (Figure 3.20b iv), and expression of the cartilage extracellular matrix protein Type II Collagen increased by 68% ($p<0.05$) (Figure 3.20b v).

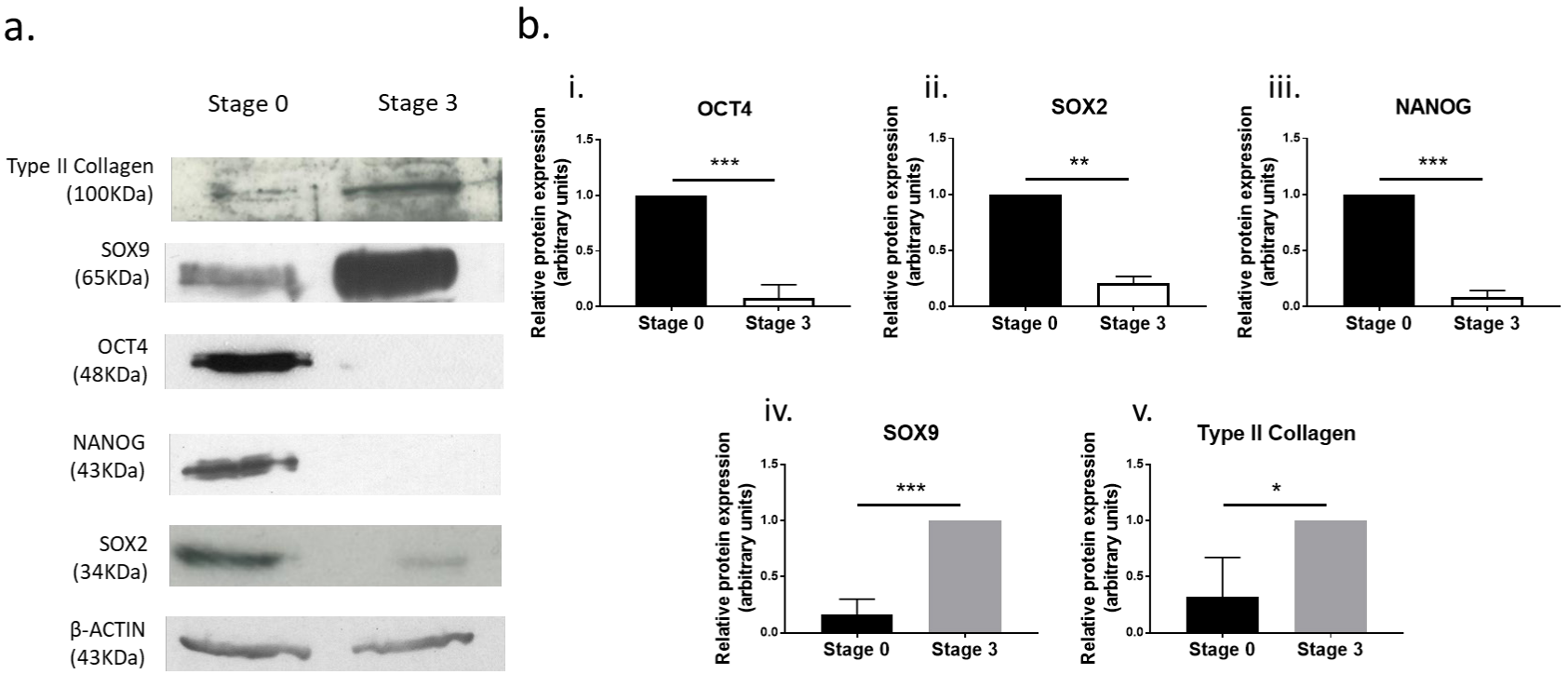

Figure 3.20 **hESC-derived chondrocytes differentiated at 5% O_2 exhibit negligible pluripotency marker expression and robust expression of chondrogenic markers.**

*hESCs were differentiated at 5% O_2. (a) Representative western blot of paired protein samples taken at stage 0 (hESCs) and stage 3 (hESC-derived chondrocytes) of chondrogenic differentiation. Target protein expression was normalised to β-Actin. Differences in expression of the pluripotency markers OCT4 (n=4), SOX2 (n=3) and NANOG (n=4) are shown in bi-iii; chondrogenic markers SOX9 (n=5) and type II collagen (n=4) are shown in biv and bv. Values represent mean ± SD, *p<0.05, **p<0.01 and ***p<0.001.*

3.4.2.5 Expression of SOX9 and type II collagen in hESC-derived chondrocytes maintained under different conditions

To establish which medium would best support the maintenance of the hESC-derived chondrocytes, the cells differentiated at 5% O_2 were cultured for 7 days in either Human Articular Chondrocyte (HAC) medium, Chondrogenic medium or Stage 3 differentiation medium (Day-14 medium). Expression of SOX9 and type II collagen was investigated via immunocytochemistry (Figure 3.21, Figure 3.22) and Western Blot (Figure 3.23).

Differential expression of SOX9 was observed between the different media groups via immunocytochemistry. SOX9 expression was detected in most cells cultured with day-14 medium (Figure 3.21a, c) and chondrogenic medium (Figure 3.21I, k). However, cells cultured in HAC medium were heterogeneous in their expression of SOX9 with large colonies of cells negative for SOX9 expression (Figure 3.21e), and other colonies with robust SOX9 expression (Figure 3.21g). Interestingly, some cells cultured in day-14 medium showed strong SOX9 expression and axial alignment (Figure 3.21c).

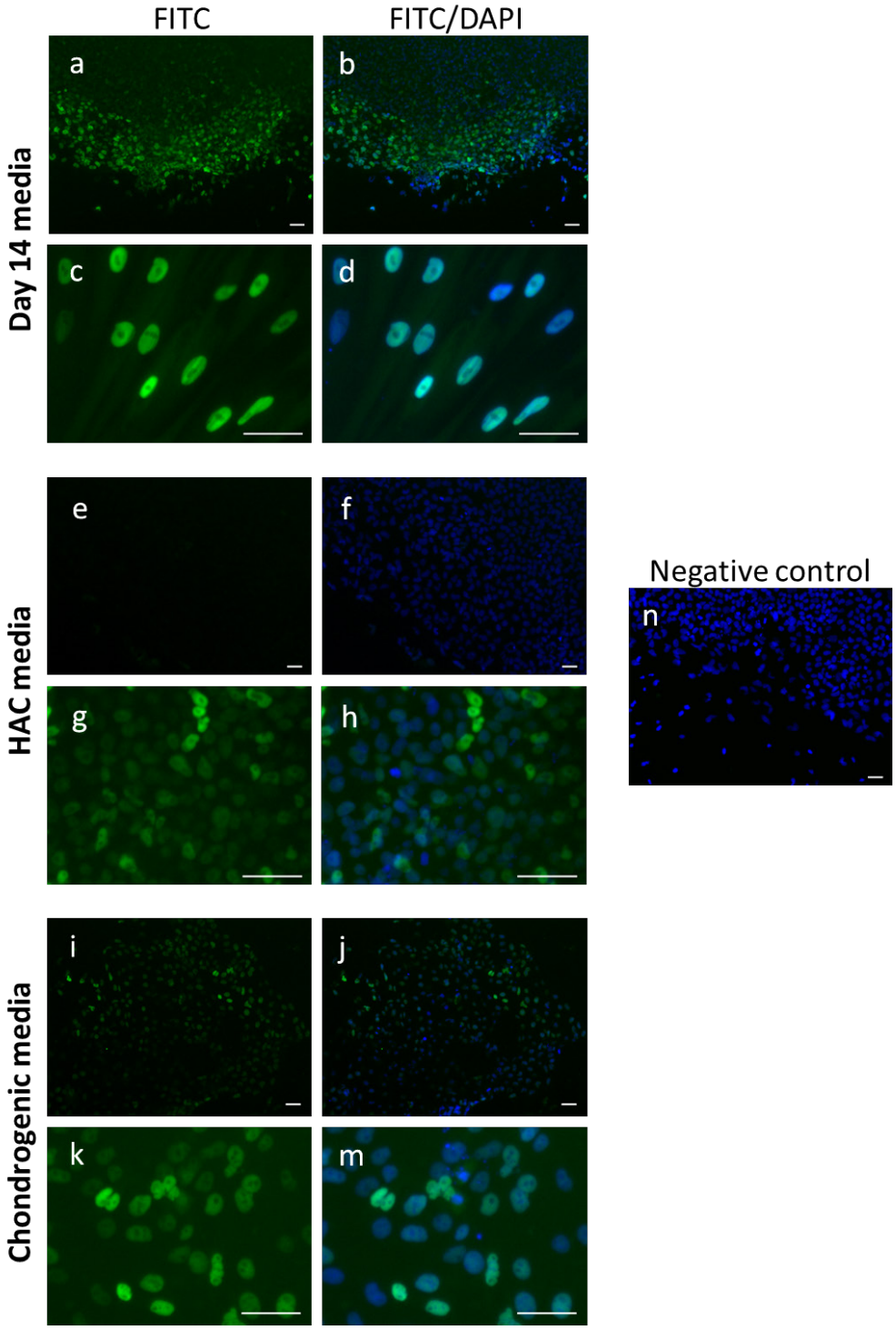

Figure 3.21 **Differential expression of SOX9 in hESC-derived chondrocytes differentiated at 5% O_2 and maintained at 5% O_2 for 7 days in different media.**

hESC-derived chondrocytes were generated from a DDP carried out at 5% O_2 tension. Cell culture was continued using either day-14 medium (a-d), HAC medium (e-h) or Chondrogenic medium (i-m). After 7 days, cells were used for immunocytochemistry. Cells were labelled for SOX9 using a FITC conjugated secondary antibody. DAPI was used as a nucleus specific label. Secondary antibody only negative control shown in n. Scale bars 50 µm.

Type II collagen was present in cells cultured in all the three media groups. In cells cultured in Day-14 medium (Figure 3.22d) and HAC medium (Figure 3.22g, h), there were regions where type II collagen appeared to be localised to single cells rather than forming a large interwoven matrix. This was not observed in cells cultured in chondrogenic medium (Figure 3.22i-m). This pattern of deposition was most evident in cells cultured in HAC medium with large numbers of cells distinct from colonies with expression of type II collagen appearing close to the nuclei (Figure 3.22g). Overall, type II collagen deposition patterns were similar between groups, with the formation of complex interwoven and interconnected type II collagen networks forming around and within large colonies (Figure 3.22a-g).

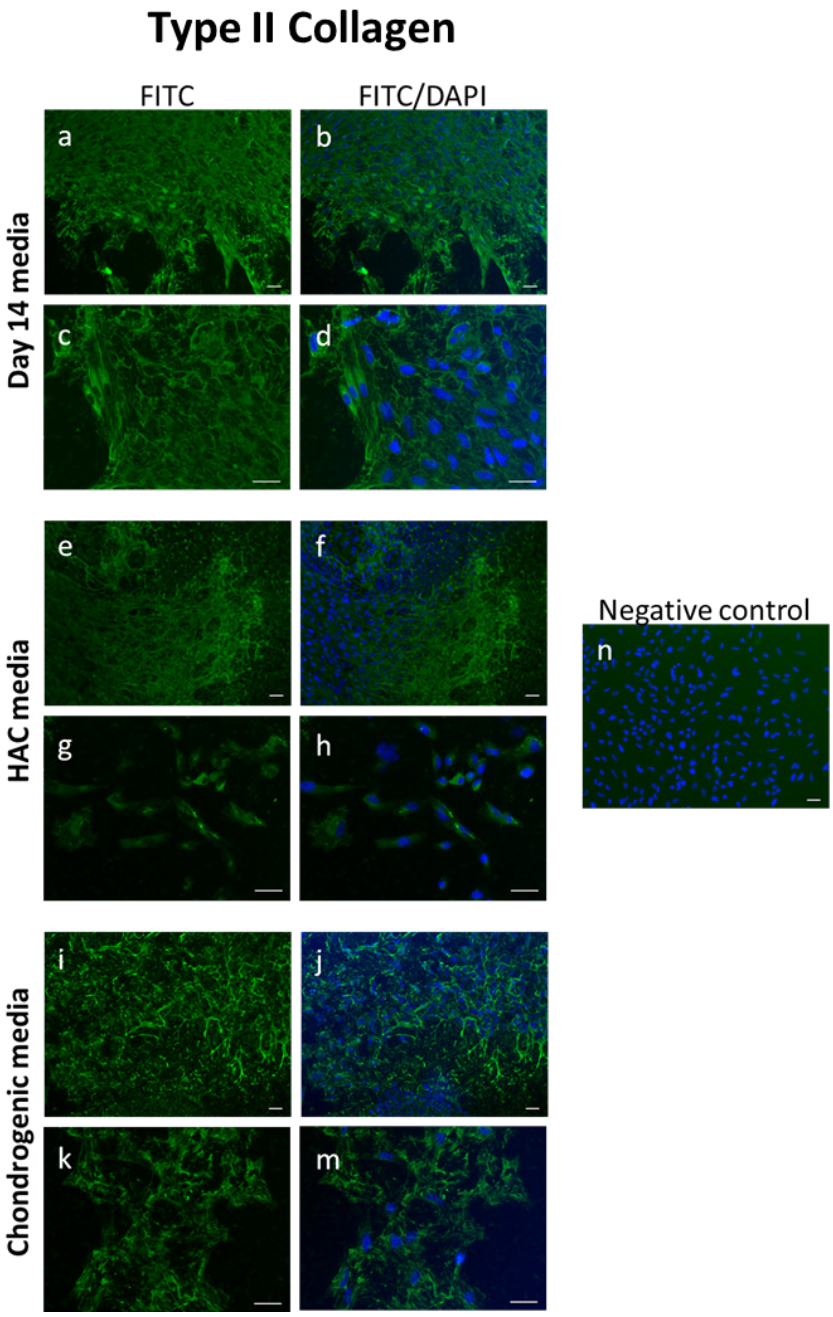

Figure 3.22 **hESC-derived chondrocytes differentiated at 5% O_2 and cultured at 5% O_2 for 7 days in different culture media maintained type II collagen expression.**

hESC-derived chondrocytes were generated from a DDP carried out at 5% O_2 tension. Cell culture was continued at 5% O_2 tension using either day-14 medium (a-d), HAC medium (e-h) or chondrogenic medium (i-m). After 7 days, cells were used for immunocytochemistry. Cultures were labelled for type II collagen using a FITC conjugated secondary antibody. DAPI was used as a nucleus specific label. Arrow in d indicates intracellular localisation. Secondary antibody only negative control shown in n. Scale bars 50 µm.

Expression of the chondrogenic proteins SOX9 and type II collagen was investigated by Western Blot (Figure 3.23).

Although it appeared that Day 14-medium doubled the expression of SOX9 protein there was no significant difference between any of the media conditions (Figure 3.23a, b). Similarly, culture medium did not alter the expression of type II collagen (Figure 3.23c, d).

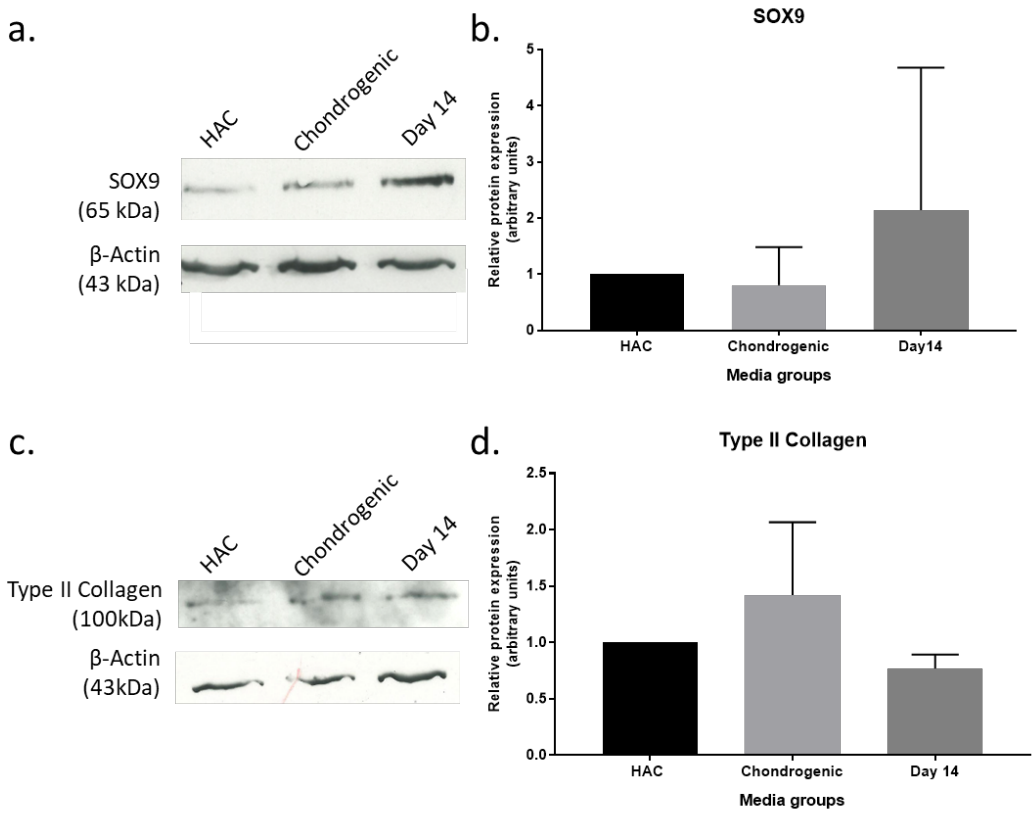

Figure 3.23 **No significant difference in expression of SOX9 and type II collagen in hESC-derived chondrocytes differentiated at 5% O_2 and cultured at 5% O_2 in different media for 7 days.**

Representative Western Blots of protein samples from hESC-derived chondrocytes differentiated at 5% O_2 and cultured in HAC, Chondrogenic or Day-14 medium for 7 days following DDPs performed at 5% O_2. Target protein expression was normalised to β-Actin. Differences in expression of SOX9 (b) and type II collagen (d). SOX9 n=3, type II collagen n=4. Values represent mean ± SD.

3.5 Discussion

The potential to generate any type of somatic cell from hESCs provides a powerful tool for regenerative medicine. Multiple protocols exist to differentiate hESCs into chondrocytes, however work is required to optimise and refine these methods. This chapter demonstrates the benefits of hypoxic culture on the generation of hESC-derived chondrocytes.

For this study, experiments were performed using HUES7 hESCs cultured for a minimum of 3 passages on Matrigel at 5% O_2 tension prior to initiation of the DDP. Hypoxic culture of hESCs is known to be beneficial for the maintenance of pluripotency, with key regulatory transcription factors being upregulated in cells cultured at 5% O_2 compared to cells cultured at 20% O_2 (Forristal et al., 2010). Hypoxic culture is also known to influence colony morpholgy, with hESCs cultured at 5% O_2 exhibiting an ~50% increase in colony diameter and cell number compared to hESCs cultured at 20% O_2 Forristal et al. (2010). Representative images of colonies cultured at both 5% and 20% O_2 reflect the findings of Forristal et al. (2010), with the hESC colony cultured at 5% O_2 appearing larger than the colony cultured at 20% O_2 (Figure 3.2). Whilst the benefits of hypoxia on hESC culture are well known, routine hESC culture is typically carried out at 20% O_2. Here it was confirmed that cells cultured at both 20% and 5% O_2 both express the self-renewal markers OCT4, SOX2, NANOG and TRA-1-60.

The differentiation protocol used here (referred to as the DDP), directs cells through successive developmental stages from pluripotent cells to chondrocytes using growth factor cocktails over 14-days. This directed approach was chosen due to reportedly high yields of chondrocyte-like cells at the end of the DDP, scalability, and developmental approach to differentiation which was demonstrated to yield cells analogous to articular chondrocytes (Oldershaw et al., 2010b). In the protocol published by Oldershaw et al. (2010b) hESCs were maintained and differentiation was performed at 20% O_2. For the work described here. it was initially hypothesised that due to the increased self-renewal and decreased spontaneous differentiation of hESCs cultured at 5% O_2 compared to 20% O_2, hESCs routinely cultured under hypoxic conditions would have an increased initial capacity for differentiation. Furthermore, the transition to 20% O_2 for the differentiation protocol would encourage a loss of pluripotency and better facilitate differentiation than if the DDP was performed at 5% O_2, whilst also replicating the differentiation conditions described in the literature (Oldershaw et al., 2010b). This was investigated by either transferring cells from 5% O_2 to 20% O_2 (5-20% O_2) upon initiation of differentiation or maintaining them at 5% O_2 (5-5% O_2) throughout.

In addition to oxygen tensions, other modifications to the original protocol include culture on Matrigel coated plates rather than fibronectin and gelatine and the addition of the chondrogenic growth factor TGF-β3 from day 9 of the DDP, which was not part of the original protocol. Both TGF-β1 and TGF-β3 are potent inducers of chondrogenesis. TGF-β3 was chosen as it has been shown that TGF-β1 treatment increases the expression of osteogenic, hypertrophic and chondrogenic genes in hMSCs (Li et al., 2010), and has also been shown to induce hypertrophy in human chondrocytes (Chen et al., 2017).

During the differentiation process cell morphology was altered in line with that reported by Oldershaw et al. (2010b), specifically with the emergence of rosette-like structures by Stage 2, suggesting that despite modifications to the protocol differentiation progressed as expected. However, stage 3 cells were observed to be more confluent in the 5-5% O_2 group than 5-20% O_2, a condition that frequently resulted in unsuccessful experiments where cell numbers were insufficient for subsequent experiments (pellet culture). Success rates of the DDP were determined by the outcome of having enough cells to generate pellets of $3x10^5$ cells; when differentiation was carried out at 5% O_2 tension the success rate was 95.3% compared to just 72.7% at 20% O_2. Therefore, differentiating cells at 20% O_2, as described in Oldershaw et al. (2010b), failed to reproducibly generate a usable population of hESC-derived chondrocytes, suggesting modification to this original protocol was required.

The media used throughout the DDP is serum free. A lack of serum in the cell culture media during the DDP could have contributed to declining cell numbers observed under the 5-20% O_2 condition. It has been reported that hypoxia can induce resistance to apoptosis induced by serum withdrawal in rat pheochromocytoma PC12 cells (Alvarez-Tejado et al., 2001). It is therefore possible that differentiation under hypoxic conditions (5% O_2 tension) prevented cell loss observed during differentiation at 20% O_2. Another contributing factor may have been that starting population of hESCs had acclimatised to culture at 5% O_2 tension and possibly did not adapt well to reoxygenation. Work investigating the effects of hESC reoxygenation found that 72h following reoxygenation there was an upregulation in the expression of NANOG and an euchromatic chromatin state, which was proposed to be a protective mechanism in place to promote cell survival during ischaemia reperfusion injury (Petruzzelli et al., 2014). These genetic changes may have been incompatible with differentiation and resulted in cell loss.

In addition to regulating the maintenance of pluripotency in hESCs, hypoxia is also be beneficial for culturing chondrocytes. Adult cartilage is avascular, making the cartilage microenvironment hypoxic. Hypoxia has been shown to enhance chondrogenesis (Robins et al., 2005) and prevent terminal differentiation through anti-apoptotic pathways regulated by PI3K/Akt/FoxO (Lee et al.,

2013). Gene expression analysis indicated that stage 3 cells differentiated at 5% O_2 may be more chondrogenic than cells differentiated at 20% O_2. When mRNA expression of *SOX9* and *COL2A1* was compared between cells differentiated at 20% or 5% O_2 there was a ~15-fold increase in *COL2A1* expression in cells differentiated at 5% O_2 ($p<0.05$), however *SOX9* remained unchanged. This may indicate that differentiation under hypoxic conditions increases the efficiency at which SOX9 can induce *COL2A1* mRNA expression. Importantly, robust expression of SOX9 and Type II Collagen protein was observed in stage 3 cells differentiated at 5% O_2, alongside a loss of OCT4 expression.

Stage-specific gene expression analysis of cells differentiated at 5% O_2 revealed changes in the expression of some genes that was in line with the developmental progression of hESCs towards chondrocytes via primitive streak/mesendoderm and mesoderm. The pluripotency genes *OCT4, SOX2* and *NANOG* exhibited a significant decrease in gene expression by stage 1. Interestingly, Oldershaw et al. (2010b) did not detect a significant decrease in the expression of these genes until stage 2, perhaps suggesting that the modifications presented here increased the rate at which the pluripotent state is lost. The stage 1 specific marker *Brachyury* is transiently expressed during differentiation but expression was captured in Stage 1 samples and was significantly decreased by stage 3. Stage 2 specific genes *CXCR4* and *KDR* are expressed during embryonic development in mesoderm (Cortés et al., 1999; McGrath et al., 1999), and increases in expression are indicative that cells had become developmentally similar to mesoderm. Whilst cells differentiated at 5% O_2 did not show statistically significant changes in expression of *CXCR4* and *KDR* there was a consistent trend towards increased expression.

The transcription factor SOX9 is a potent activator of the chondrocyte-specific enhancer of the pro alpha1 (II) collagen gene *COL2A1* (Lefebvre et al., 1997), and has been shown to be required for cartilage formation (Bi et al., 1999). SOX9 and Type II Collagen are therefore considered to be the two main chondrogenic markers. Interestingly, whilst there appeared to be a trend towards upregulation of both of these stage 3 genes the difference in expression was only statistically significant for *SOX9* at stage 2. A key consideration in the interpretation of these results is that the majority of functional properties of a gene occur at the protein level, and that there is a now well established discrepancy between gene and protein expression which is the result of post-transcriptional and post-translational regulation (Gygi et al., 1999; Maier et al., 2009). Another important consideration relating to this gene expression analysis is that the time points chosen for analysis were artificially designated in what is an essentially a continuous differentiation process, and it is therefore possible that peak gene expression is not captured in these results.

Western Blot analysis demonstrated significant decreases in the expression of pluripotency markers and significant increases in the expression of SOX9 and Type II Collagen in hESC-derived chondrocytes differentiated at 5% O_2. Oldershaw et al. (2010b) based the success of their DDP on the percentage of SOX9 positive cells. Whilst SOX9 is a key early chondrogenic marker, it is also expressed in multiple other tissues. Here, the expression of SOX9 and Type II Collagen, a key constituent of hyaline cartilage, have been quantified by western blot. Quantitative analysis at the protein level was not performed in the original publication (Oldershaw et al., 2010b), however in subsequent work investigating the effects of using recombinant ECM fragments to support chondrogenesis an increase in SOX9 expression of ~3.5-fold was reported between stage 0 and stage 3 (Cheng et al., 2018). The results presented here show a ~6-fold increase in SOX9 expression between Stage 0 and Stage 3, suggesting a more robust chondrogenic phenotype. Type II collagen expression was also quantified by western blot, and a ~3-fold increase was detected between stage 0 and stage 3. In culture these cells were observed to form a complex, interwoven, Type II Collagen matrix, providing compelling evidence for the chondrogenic capacity of these cells.

To investigate whether hESC-derived chondrocytes could be maintained post-DDP cells were cultured for 7 days in HAC medium, chondrogenic medium or Day 14-medium. HAC medium refers to the medium used to culture human articular chondrocytes (HACs) following isolation from articular cartilage, chondrogenic medium is used to stimulate cells to form cartilage *in vitro* and Day-14 medium refers to the medium used during the final stage of differentiation via the DDP. Both chondrogenic and Day-14 medium are serum free and are supplemented with TGFβ3, whilst HAC medium contains FBS and no TGFβ3. The optimum condition could not easily be established as there was no significant differences in the expression of SOX9 or Type II Collagen protein between the three groups. Robust expression of Type II Collagen in hESC-derived chondrocytes may be indicative of a stable chondrogenic phenotype. However, this should be accompanied by stable SOX9 expression; in HAC medium SOX9 was not homogenously expressed with large cell clusters appearing negative for SOX9. Continued culture of hESC-derived chondrocytes in day-14 medium or chondrogenic medium did not result in the detrimental loss/partial loss of SOX9 expression observed in cells cultured in HAC medium and are therefore more appropriate options for continued culture media. It has been demonstrated that TGF-β is involved in the regulation of SOX9 by mediating the proteins' phosphorylation and stabilisation via both p38 and Smad2/3 (Coricor and Serra, 2016). TGF- β3 is included in Day-14 and Chondrogenic medium, but not HAC medium. Whilst culture in HAC medium appeared to result in a mature chondrocyte phenotype, the lack of stable SOX9 is not ideal. This suggests that Day-14 or chondrogenic medium may be more beneficial for maintaining the desired chondrocyte

phenotype. Maintenance of hESC-derived chondrocytes beyond day-14 of the DDP has not been previously demonstrated. The results presented here may enable the generation of a larger population of cells from individual experiments, thereby facilitating scale up in a more cost-effective manner than increasing the starting population for differentiation.

In conclusion, whilst the protocol described in Oldershaw et al. (2010b) did yield a small population of chondrogenic cells, significant modifications to the DDP were required before a robust population of hESC-derived chondrocytes that were sufficient in number for downstream experiments were generated. Hypoxia, was demonstrated to play a key role in the generation of a robust chondrogenic population of hESC-derived chondrocytes with increased expression of the chondrogenic gene *COL2A1* following hypoxic differentiation. The improved success rate (number of experiments generating >3x10^5 cells) that resulted from hypoxic differentiation enabled the use of these hESC-derived chondrocytes for downstream experiments, something that was limited when differentiation was performed at 20% O_2 as described in Oldershaw et al. (2010b). The addition of the potent chondrogenic growth factor TGFβ3 was probably also a key contributor to the success of this protocol. Thus, the aims of this chapter have been met resulting in the generation of a robust, consistent and reproducible protocol for the differentiation of hESCs into chondrocytes. This cell population provides a powerful tool for the bioengineering of cartilage *in vitro*.

Chapter 4

Cartilage generation using an Acoustofluidic Bioreactor

4.1 Introduction

Tissue engineering aims to repair, maintain, or enhance native tissue. This is enabled by cell culture with the use of growth factors, scaffolds and bioreactor systems to generate a 3D tissue construct *in vitro,* before implantation. A clear benefit of 3D culture is that it aims to recapitulate the *in vivo* environment, by enabling more complex and physiological cell-cell contact in the early stages of the culture period compared to monolayer culture and allowing the deposition of extracellular matrix to form 3D aggregates.

Ultrasound (US) waves are acoustic waves with frequencies higher than the upper audible limit of human hearing, which is usually equal to, or greater than 0.02MHz. The generation of ultrasonic standing wave fields (USWF) enables cell entrapment, and manipulation of culture parameters can enable mechanical stimulation (Li et al., 2014b). When cells are exposed to USWF, the acoustic waves scatter upon contact with the cells. Acoustic radiation forces are generated by the dispersion of an US wave, and it is these forces that spatially determine where the cells are directed. Nodes and anti-nodes are created within the USW field, which refer to areas of relative low and high pressure respectively, forming an ultrasonic standing wave trap (USWT) (Figure 4.1a). Cells are directed towards pressure nodes where they aggregate and are held in levitation over the course of the culture period within the USWT.

The successful generation of hyaline-like cartilage has been demonstrated by our group via use of an acoustofluidic perfusion bioreactor that incorporated USWTs to levitate and aggregate HACs (Jonnalagadda et al., 2018; Li et al., 2014b). Here mechanical stimulation of the cells was achieved by media perfusion (Li et al., 2014b) and a technique known as frequency sweeping (Jonnalagadda et al., 2018; Li et al., 2014b). This involved driving the bioreactor through a range of frequencies that encompassed the resonant frequency of the device, this being the frequency at which the USWT was optimally generated. By employing this technique, cells were continuously being driven towards the pressure nodes when at the resonant frequency and being essentially released from the USWT when the signal generator was out of range (Figure 4.1c-d). It was also observed that by using a sweep repetition rate of 50Hz there was less cell displacement than when driven at 1Hz, and thus the relative amount of mechanical stimulation could be manipulated (Jonnalagadda et al., 2018).

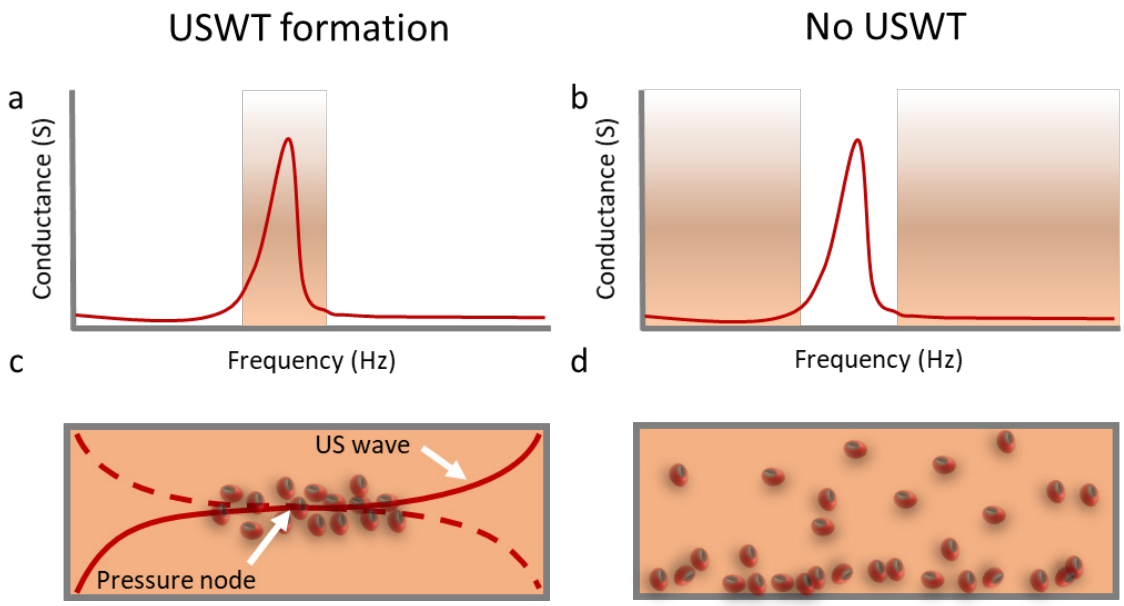

Figure 4.1 **Ultrasonic standing wave trap formation (USWT) results in cell aggregation at pressure nodes**

Ultrasound waves can be used to generate an USWT (a, c). When cells are not exposed to the ultrasonic standing wave field (USWF) they disperse freely and will begin to settle on the bottom of the chamber (b, d), when the USWF is generated cells will be directed to pressure nodes and an USWT is formed (c). Shaded regions refer to the frequency in range. When the resonant frequency is in range cells levitate within the USWT. When frequency sweeping is used the USWT will be formed when the resonant frequency of the device is met (a), but when the resonant frequency is out of range the USWT is not generated (b). Conductance is measured in Siemens, and frequency in Hertz.

Importantly, these studies demonstrated effective tissue generation without the use of scaffolds. The basis of this system therefore has huge translational potential for the generation of clinically useable tissue engineered constructs. These studies utilised primary HACs for *in vitro* cartilage generation, however, this is not the optimal cell type for regenerative medicine due to the requirement for multiple invasive surgeries, low yields, and dedifferentiation of cells during culture. The ability to consistently generate a robustly chondrogenic population of hESC-derived chondrocytes has been demonstrated, and I propose that these hESC-derived chondrocytes could provide a valuable alternative cell source for the scaffold-free generation of cartilage constructs using an ultrasound-based bioreactor system.

4.2 Aims and objectives

- To fabricate acoustofluidic bioreactors suitable for cell culture.
- To generate cartilage from HACs using an acoustofluidic bioreactor.
- To generate cartilage from hESC-derived chondrocytes using an acoustofluidic bioreactor.

4.3 Methods

4.3.1 Fabrication of bioreactor devices

A second generation acoustofluidic bioreactor, developed by a previous PhD student in the group (Jonnalagadda et al., 2018), was modified for use in this project.

All devices were hand assembled. Piezoelectric transducers (Ferroperm) were cut to size (10mm x 12mm) using a glass cutter and scalpel (Figure 4.2a). The edges of the transducers were sanded down (Figure 4.2b), and discontinuity was induced between the electrodes using a scalpel (Figure 4.2c). The protective outer coating on the continuous side of the transducer was removed by scraping with a scalpel blade, as were the areas where copper wire would later be soldered (Figure 4.2d). Using conductive silver paint, the two faces of the transducer were connected. A multimeter was used at each stage to check connectivity/discontinuity.

Prepared transducers were adhered to a double-width glass slide (Corning, 75 x 50 x 1 mm) using epoxy (Epotek) at 70°C for 1 hour. Each slide was prepared with 4 transducers, with the slide functioning as the carrier layer. Microscope slides were cut to 13 mm x 25 mm x 1 mm and functioned as a reflector layer. The reflector layer was adhered to 2 x strips of Polycarbonate film (500µm thickness) (Cadillac Plastics), one on each side of the reflector side using a thin film of PDMS (Polydimethylsiloxane) (1:10 curing agent:monomer) (Dow Corning). This was positioned above the transducer and adhered to the glass slide; the polycarbonate strips acted as spacers to create a cavity of approximately 0.56 mm in height for cell levitation during the culture period between the carrier and reflector layers above the transducer. The cavity is referred to as the fluid layer. PDMS was cured at 70°C for 1 hour to solidify. An air backing layer was created by adhering laser cut poly(methyl methacrylate) (PMMA) square spacers to the reflector, and sealing the top with a glass slide using PDMS at 70°C for 1 hour. The role of the air backing is to enhance reflection of the US wave by creating a layer that is acoustically different to the fluid cavity.

The acoustic device shown in Figure 4.2f is the same as the device published in Jonnalagadda et al. (2018), however the manifold that housed the device was modified for this project. Plastic manifolds were designed using the SolidWorks software and laser cut from sheets of PMMA. The

base was designed to fit the double-width glass slide in grooves that were etched during laser cutting to allow the plate to be sealed in using PDMS (Figure 4.3a). A walled divider was also laser cut to separate the four devices, and create wells to hold cell culture media (Figure 4.3b). This was adhered to the plate once it had been placed in the base, and the PDMS was cured at 70°C for 1 hour. This was something not originally included in the bioreactor design. This enabled the simultaneous culture of cells from different patients without media exchange between cells from different patients, and thereby increased throughput. An easily removable lid was also designed that slotted over the walls of the manifold (Figure 4.3c).

A circuit board was screwed onto one side of the base. This was equipped with a switch that allowed for each transducer to be connected individually. Each transducer was soldered to the circuit board using copper wire.

Each transducer coupled with the carrier, fluid, and air backing layers were referred to as resonators (Figure 4.2f); the device that combines 4 resonators on a single plate was referred to as a bioreactor.

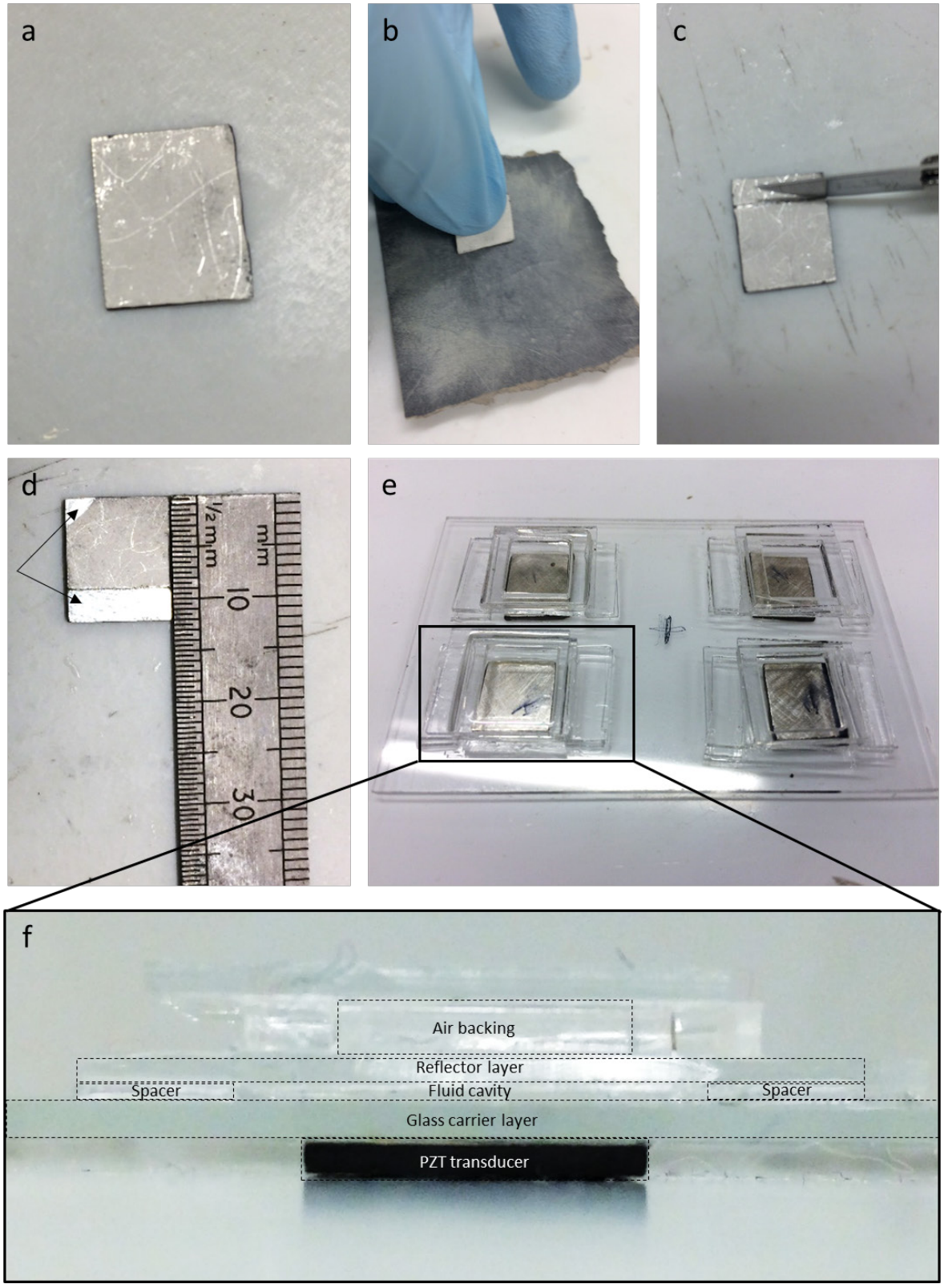

Figure 4.2 **Acoustofluidic bioreactor fabrication**.

Piezoelectric transducer is shown in a, sanding of the transducer in b, inducing discontinuity in c, a prepared transducer in d with arrows to indicate soldering points, an assembled plate in e, and a transverse view of a single resonator in f.

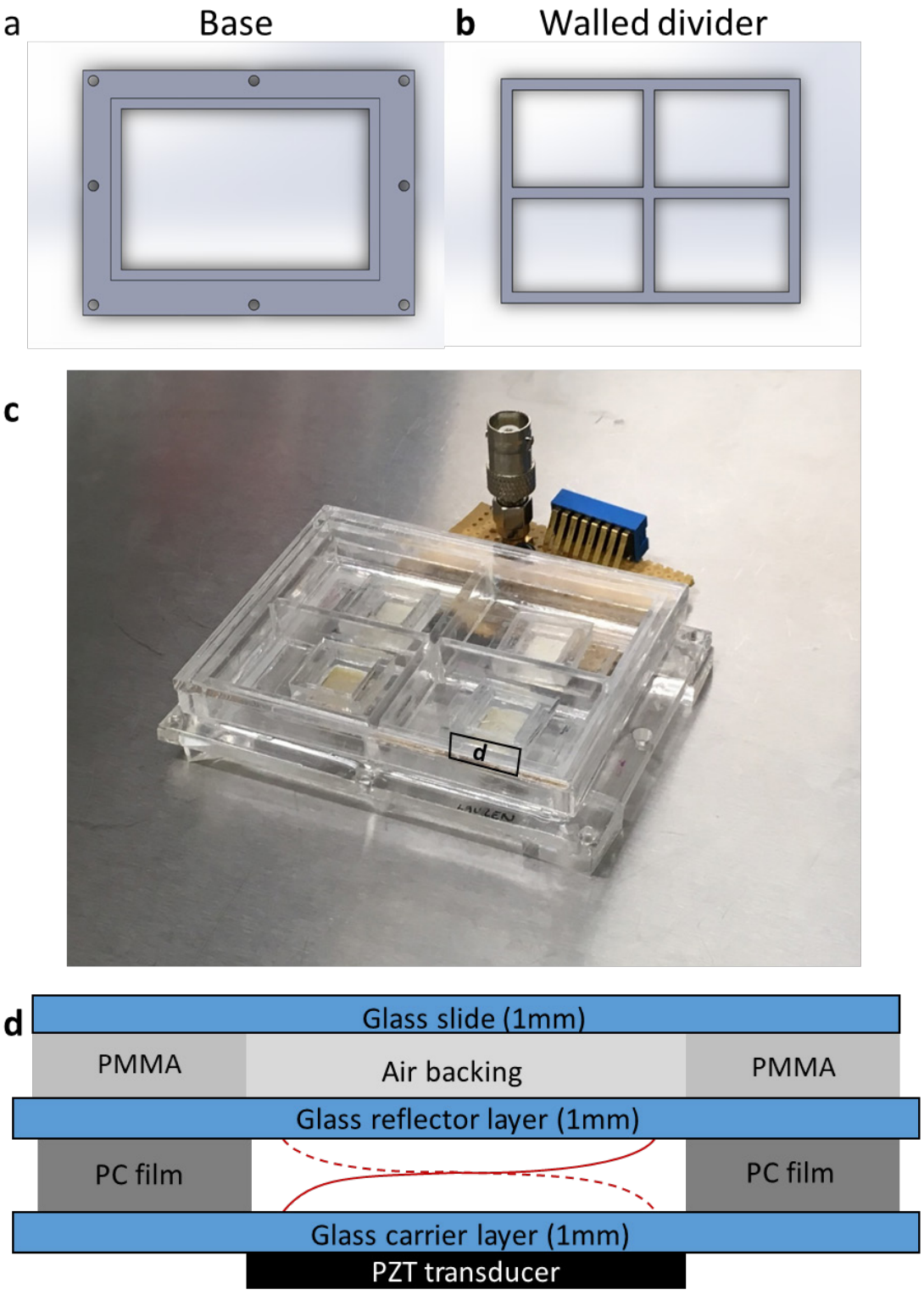

Figure 4.3 **Components of assembled acoustofluidic bioreactor.**

The base onto which the bioreactor is plate is secured is shown in a, and the multi-walled divider that separated each resonator in b. A completely assembled bioreactor is shown in c, where the label d indicates the planar view for the schematic shown in d. Schematic (d) shows a transverse view through a resonator, red lines represent an US wave with a central pressure node.

4.3.2 Culture of cells in an acoustofluidic bioreactor

Bioreactors were sterilised by washing in 70% EtOH, followed by PBS, before being UV sterilised for at least 2 hours.

HACs were dissociated as in section 2.3.2. Following cell counting, cells were centrifuged at 400 x*g* for 5 minutes, and the pellet was resuspended in a volume containing ~$1x10^6$ cells per 100 µl.

The bioreactor was connected to the signal generator (Figure 4.6a), which was run from a battery source for the set up, and the peak-to-peak voltage (Figure 4.4) was set to approximately 14 Vpp.

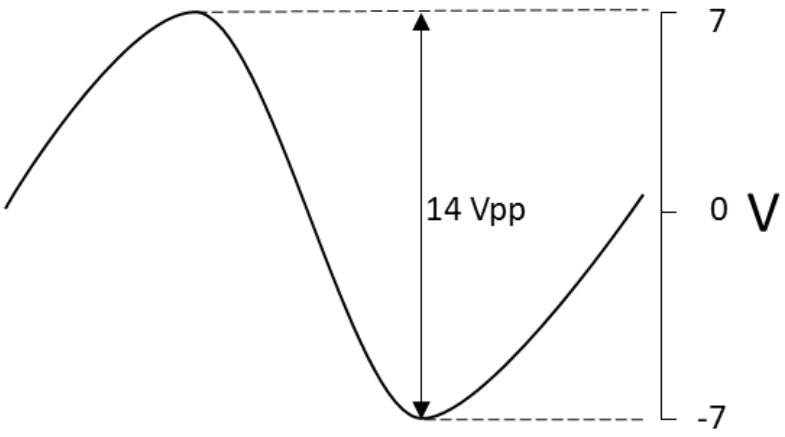

Figure 4.4 **Schematic depiction of the peak-to-peak voltage (Vpp) of a sinusoidal wave**. *Acoustofluidic bioreactors are run at 14V pp during set up. Vpp refers to the difference between the maximum positive and maximum negative amplitudes of the sinusoidal wave and is indicated by the arrow.*

An oscilloscope was used to visualise the signal generated (Figure 4.6b). Each transducer was tested for output by turning on and off the individual switches and visualising the waveform on the oscilloscope. Using a Pasteur pipette the cell suspension was flushed into the cavity to create the fluid layer. Care was taken to avoid air bubble formation within the cavity. The cell suspension was allowed 10-15 minutes to form aggregates at the pressure node before the outside of the chamber was flooded with media (Figure 4.6c). The bioreactor was then carefully transported to the incubator.

Once the bioreactor was situated within the incubator, the Vpp was reduced to approximately 10 Vpp to reduce the power being sent to the bioreactor and prevent heating. The ultrasound signal was applied constantly over the culture period. Frequency sweeping over a 0.2 MHz range was employed enabling the excitation of the resonant frequencies of all four transducers of the bioreactor (Figure 4.5).

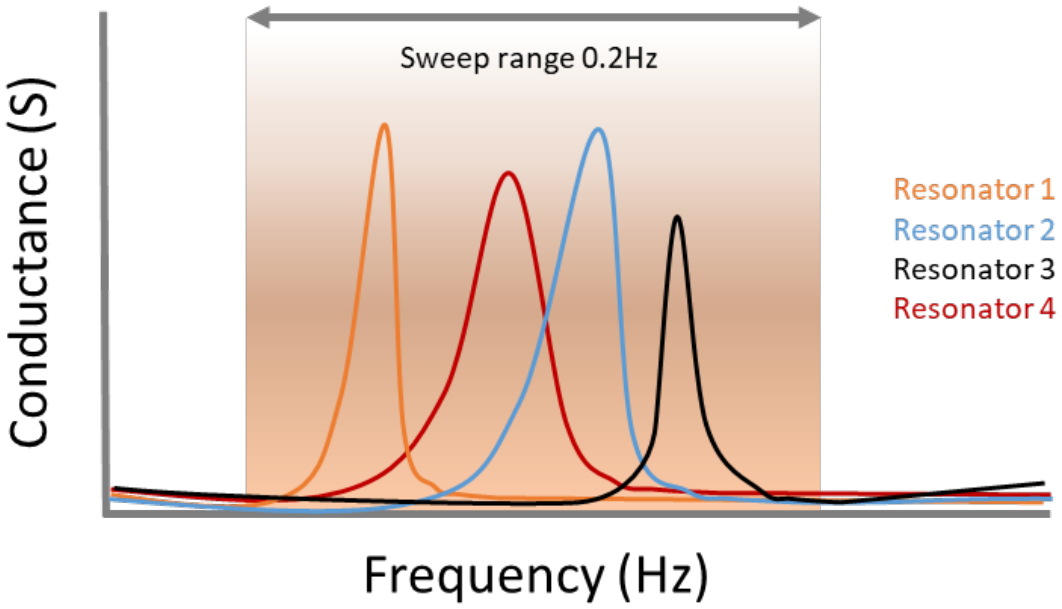

Figure 4.5 **Schematic representation of frequency sweeping.**

During acoustofluidic bioreactor culture the Arduino board within the signal generator was programmed to cycle through a range of frequencies (0.2 Hz). This ensured that the resonant frequencies (maxima of curve) of each of the four resonators was targeted during the sweep. Frequency sweeping occurred at a rate of 2 Hz (2 cycles per second). Conductance is measured in Siemens, and frequency in Hertz.

Cells were incubated in a humidified atmosphere containing 5% CO_2, 5% O_2 in balanced N_2 for 10 or 21 days. Media changes took place every 3-4 days and involved transporting the bioreactor into the tissue culture hood. During transport the Vpp was increased to approximately 14 Vpp. The resultant cell aggregates were fixed in 4% PFA and used for histology.

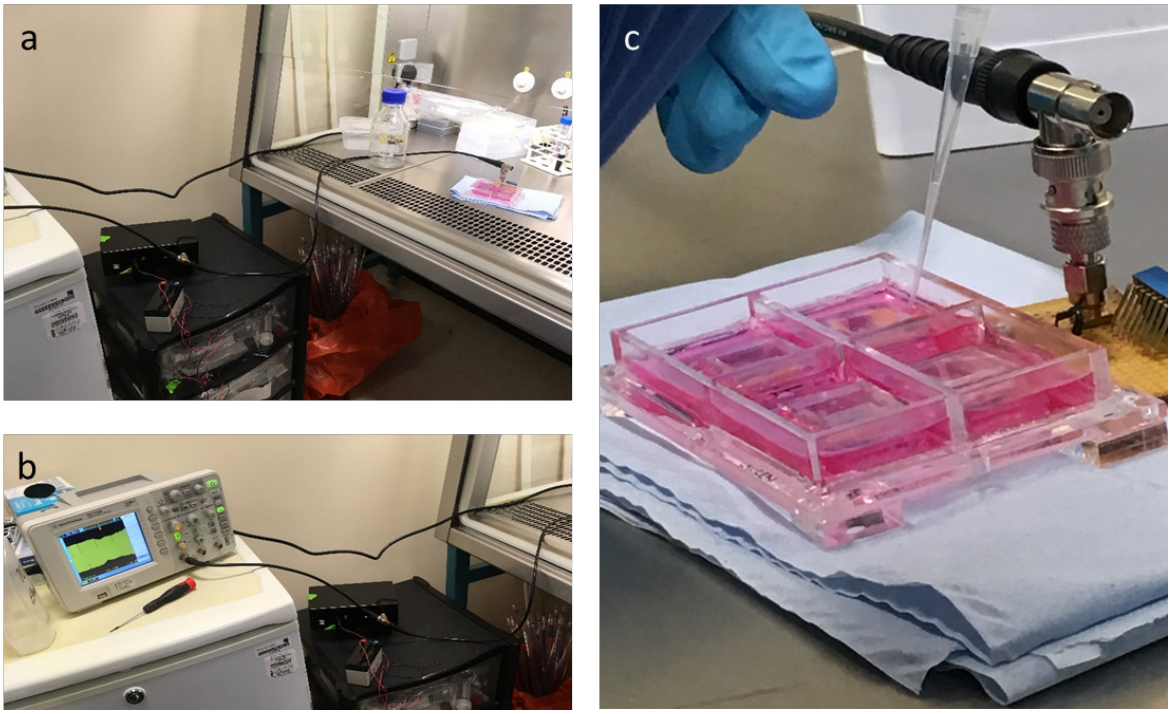

Figure 4.6 **Set up of the acoustofluidic bioreactor for cell culture.**

Signal generator is shown in a, an oscilloscope for visualising the signal in b, and injection of cells into the fluid cavity in c.

4.3.3 Whole mount staining hESC-derived chondrocyte bioreactor constructs using Safranin O

A construct generated in the acoustofluidic bioreactor from hESC-derived chondrocytes was too small to process, embed and section as detailed in section 2.5. Instead, the sample was fixed overnight in 4% PFA at 4°C, washed in PBS and stained for 15 minutes in a 96-well plate with 0.1% Safranin O. The sample was then washed with dH_2O and DPX mounting media added to the well, covering the sample.

4.4 Results

4.4.1 Conductance testing

Once the plate had been sealed and the transducers connected in a circuit, the resonant frequency (that at which an USWT is established within the fluid cavity (Figure 4.7a)) of each transducer was tested using a Cypher Instruments C-60 impedance-amplitude-phase analyser (Figure 4.7b). Each transducer was tested with a cavity filled with PBS.

The results from the conductance testing were used to set the parameters between which frequency sweeping would take place. The signal generator was set to cycle at sweep ranges of 200 kHz that encompassed the resonant frequencies of the four transducers. For the device depicted in Figure 4.7 the range was set as 1.3-1.5 MHz as this encompassed the resonant frequencies of all four devices as depicted by the peaks in Figure 4.7b. Frequency sweeping was run at a rate of 2 Hz (2 cycles per second).

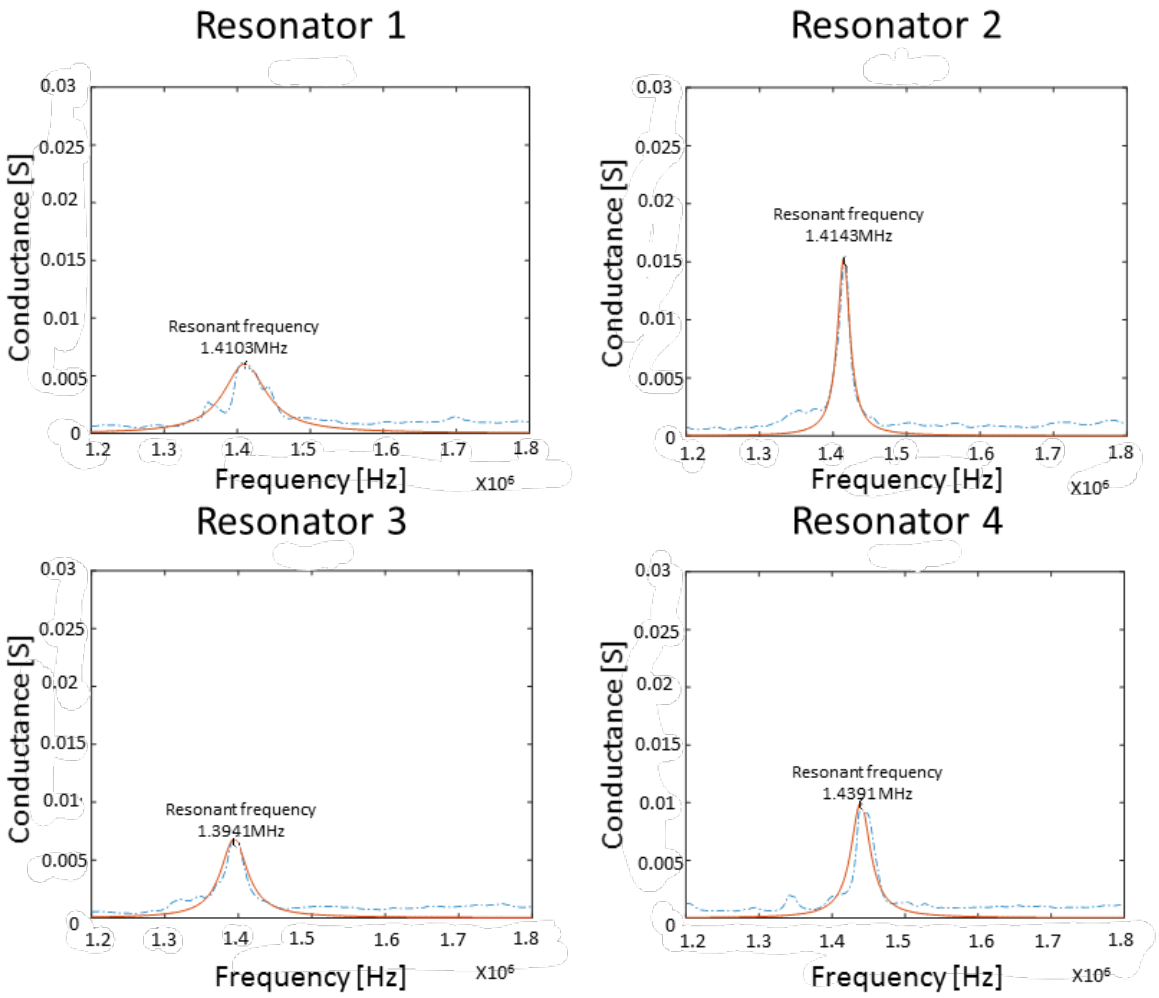

Figure 4.7 **Resonant frequencies and conductance plots of each resonator on an acoustofluidic bioreactor.**

Example conductance plots of 4 resonators tested in PBS are shown in b. Raw values are shown as a doted blue line, a line of best fit is shown as an orange line. Resonant frequencies for each resonator are described by the curve maxima and are recorded on each graph.

4.4.2 HACs form hyaline-like cartilage following 21-day bioreactor culture

A modified second generation bioreactor, described in Jonnalagadda et al. (2018), was used to generate cartilage from HACs.

Cartilage was generated in acoustofluidic bioreactors from two individual patients: Patient 1 (Female; age 67), Patient 2 (Male; age 82). Individual culture chambers were found to yield multiple constructs of variable dimensions.

Patient 1 generated 3 constructs which ranged in size from 0.8 to 1.6 mm in diameter (Figure 4.9 and Figure 4.10). Patient 1, construct 1 had hyaline cartilage-like morphology, characterised by numerous chondrocytes and lacunae. Sections were stained with haematoxylin and Safranin O to visualise cells and proteoglycan accumulation in the matrix respectively. Safranin O staining was intense and indicative of proteoglycan accumulation (Figure 4.8a).

Immunohistochemistry was performed to analyse the expression of SOX9, the key chondrogenic transcription factor, type II collagen, the primary collagen in hyaline cartilage, type I collagen, the bone/fibrocartilage-specific collagen and Aggrecan, the predominant proteoglycan in cartilage matrix. Alcian blue was used as a counter stain for proteoglycans in the construct matrix for all antibodies with the exception of Aggrecan. Counterstaining with Alcian blue showed results consistent with Safranin O staining in terms of staining intensity and distribution. Construct 1 demonstrated robust intracellular expression of SOX9 (Figure 4.8b), and type II collagen deposition mainly localised to the peripheral regions of the construct (Figure 4.8c). Type I collagen was not detected with sections appearing no different to the control (Figure 4.8d). Robust staining for the proteoglycan Aggrecan was observed throughout the construct (Figure 4.8e).

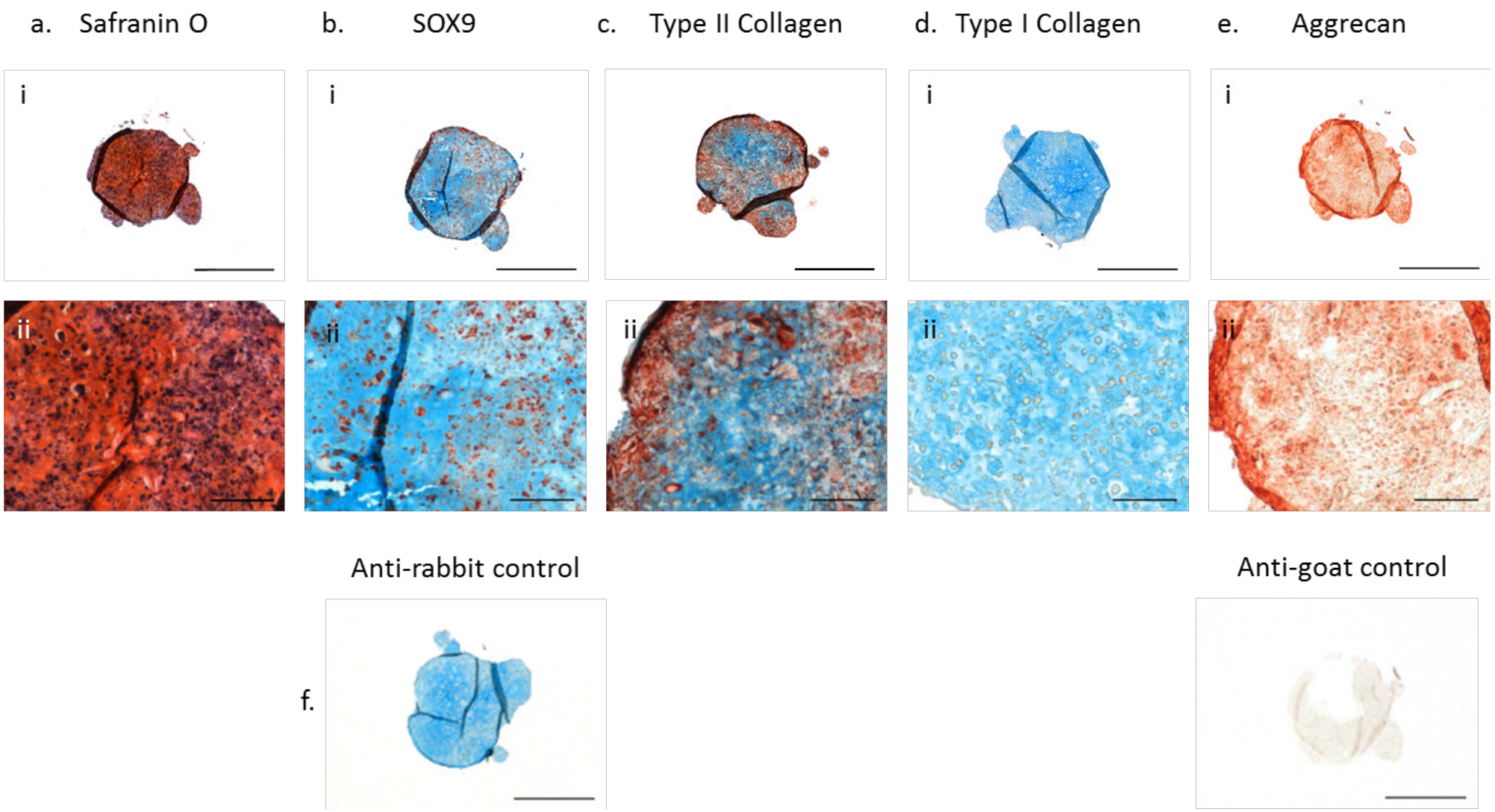
a. Safranin O
b. SOX9
c. Type II Collagen
d. Type I Collagen
e. Aggrecan
i
ii
Anti-rabbit control
f.
Anti-goat control

Figure 4.8 **Patient 1 generated hyaline-like cartilage following 21-days culture in an acoustofluidic bioreactor (construct 2).**

HACs were isolated from Patient 1 (Female; age 67) and cultured for 21 days in an acoustofluidic bioreactor in chondrogenic medium. Day 21 constructs were used for histology. Proteoglycans were detected using Safranin O staining (a i-ii), and expression of SOX9 (b i-ii) type II collagen (c i-ii), type I collagen (d i-ii) and Aggrecan (e i-ii) was investigated using immunohistochemistry. Secondary antibody only negative controls were included in the immunohistochemistry protocols (f); anti-rabbit control corresponds to SOX9, type I collagen and type II collagen, anti-goat control corresponds to Aggrecan. High magnification, 500 µm, low magnification, 100 µm.

Patient 1, construct 2 had hyaline cartilage-like morphology, characterised by numerous chondrocytes and lacunae. Sections were stained with haematoxylin and Safranin O to visualise cells and proteoglycan accumulation in the matrix respectively. Safranin O staining was positive for proteoglycan accumulation (Figure 4.9a). Counterstaining with Alcian blue showed results consistent with Safranin O staining in terms of staining intensity and distribution. Construct 2 demonstrated robust intracellular expression of SOX9 (Figure 4.9b), and type II collagen deposition mainly localised to the peripheral regions of the construct (Figure 4.9c). Type I collagen staining was negligible (Figure 4.9d). Robust staining for the proteoglycan Aggrecan was observed throughout the construct (Figure 4.9e).

a. Safranin O

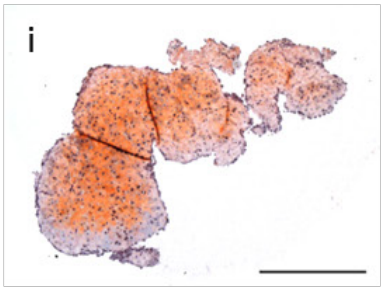

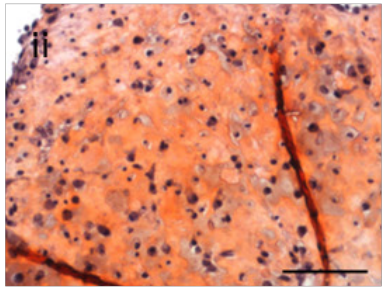

b. SOX9

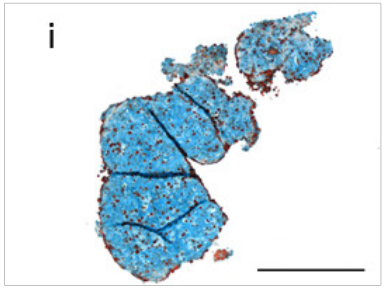

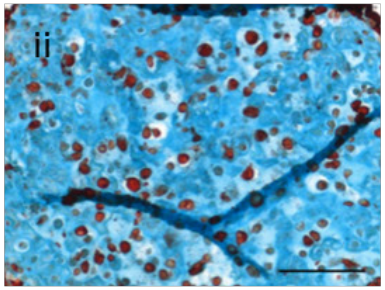

c. Type II Collagen

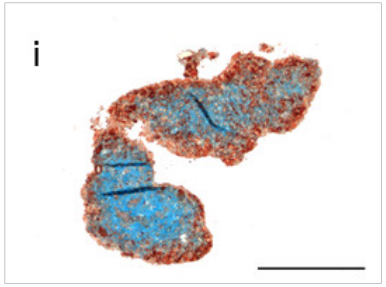

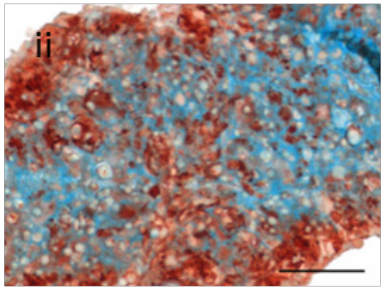

d. Type I Collagen

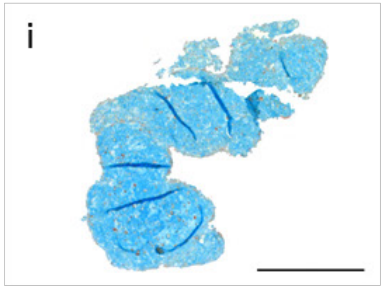

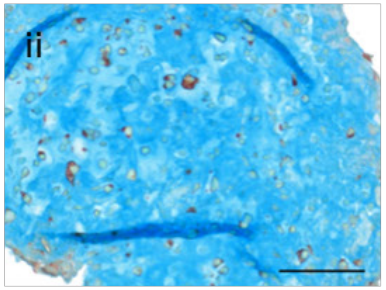

e. Aggrecan

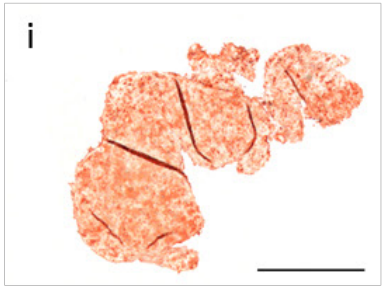

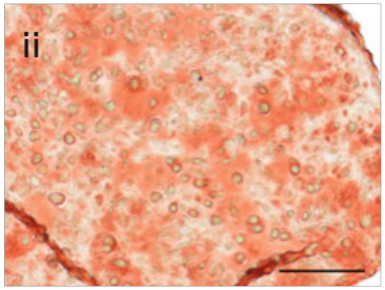

f. Anti-rabbit control

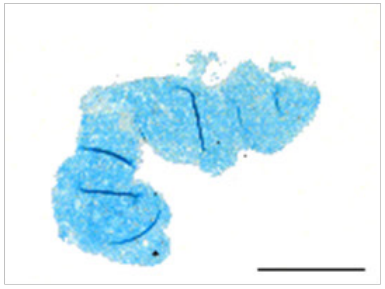

Anti-goat control

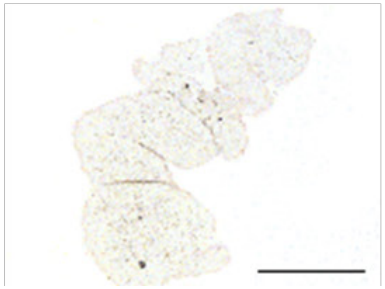

Figure 4.9 **Patient 1 generated hyaline-like cartilage following 21-days culture in an acoustofluidic bioreactor (construct 2).**

HACs were isolated from Patient 1 (Female; age 67) and cultured for 21 days in an acoustofluidic bioreactor in chondrogenic medium. Day 21 constructs were used for histology. Proteoglycans were detected using Safranin O staining (a i-ii), and expression of SOX9 (b i-ii) type II collagen (c i-ii), type I collagen (d i-ii) and Aggrecan (e i-ii) was investigated using immunohistochemistry. Secondary antibody only negative controls were included in the immunohistochemistry protocols (f); anti-rabbit control corresponds to SOX9, type I collagen and type II collagen, anti-goat control corresponds to Aggrecan. High magnification, 500 µm, low magnification, 100 µm.

Patient 1, construct 3 had hyaline cartilage-like morphology, characterised by numerous chondrocytes and lacunae. Sections were stained with haematoxylin and Safranin O to visualise cells and proteoglycan accumulation in the matrix respectively. Safranin O staining was positive for proteoglycan accumulation (Figure 4.10a). Counterstaining with Alcian blue showed results consistent with Safranin O staining in terms of staining intensity and distribution. Construct 3 demonstrated robust intracellular expression of SOX9 (Figure 4.10b), and limited type II collagen deposition mainly localised to the peripheral regions of the construct (Figure 4.10c). Type I collagen was not detected with sections appear similar to the control (Figure 4.10d). Robust staining for the proteoglycan Aggrecan was observed throughout the construct (Figure 4.10e).

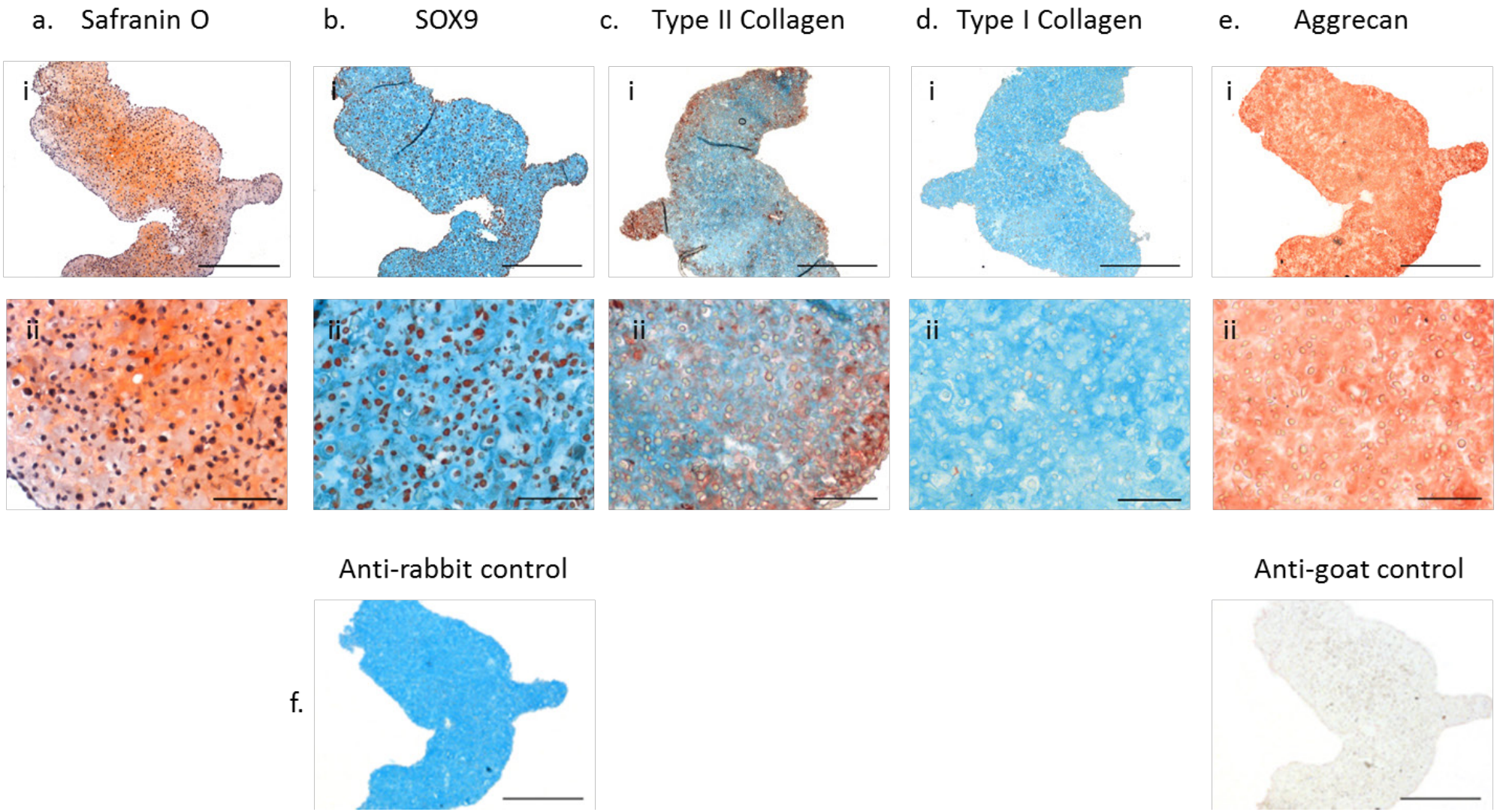
a. Safranin O
b. SOX9
c. Type II Collagen
d. Type I Collagen
e. Aggrecan
i
ii
Anti-rabbit control
Anti-goat control
f.

Figure 4.10 **Patient 1 generated hyaline-like cartilage following 21-days culture in an acoustofluidic bioreactor (construct 3).**

HACs were isolated from Patient 1 (Female; age 67) and cultured for 21 days in an acoustofluidic bioreactor in chondrogenic medium. Day 21 constructs were used for histology. Proteoglycans were detected using Safranin O staining (a i-ii), and expression of SOX9 (b i-ii) type II collagen (c i-ii), type I collagen (d i-ii) and Aggrecan (e i-ii) was investigated using immunohistochemistry. Secondary antibody only negative controls were included in the immunohistochemistry protocols (f); anti-rabbit control corresponds to SOX9, type I collagen and type II collagen, anti-goat control corresponds to Aggrecan. High magnification, 500 µm, low magnification, 100 µm.

Constructs generated from Patient 2 ranged from 1.6 to 1.7 mm in diameter (Figure 4.11 and Figure 4.12). Patient 2, construct 1 had hyaline cartilage-like morphology, characterised by numerous chondrocytes and lacunae. Sections were stained with haematoxylin and Safranin O to visualise cells and proteoglycan accumulation in the matrix respectively. Safranin O staining was intense and indicative of proteoglycan accumulation (Figure 4.11a). Counterstaining with Alcian blue showed results consistent with Safranin O staining in terms of staining intensity and distribution. Construct 1 demonstrated weak but homogenous intracellular expression of SOX9 (Figure 4.11b), and type II collagen deposition mainly localised to the peripheral regions of the construct (Figure 4.11c). Type I collagen was not detected with sections appear similar to the control (Figure 4.11d). Robust staining for the proteoglycan Aggrecan was observed throughout the construct (Figure 4.11e).

a. Safranin O

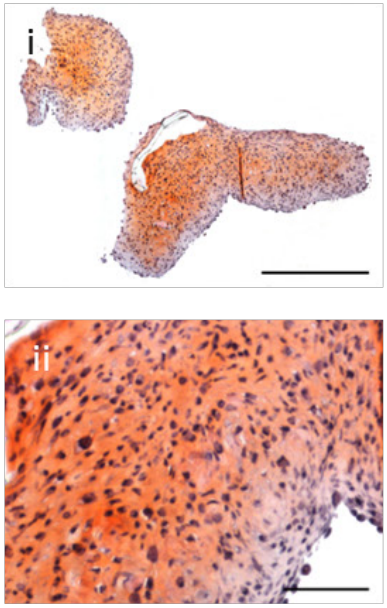

b. SOX9

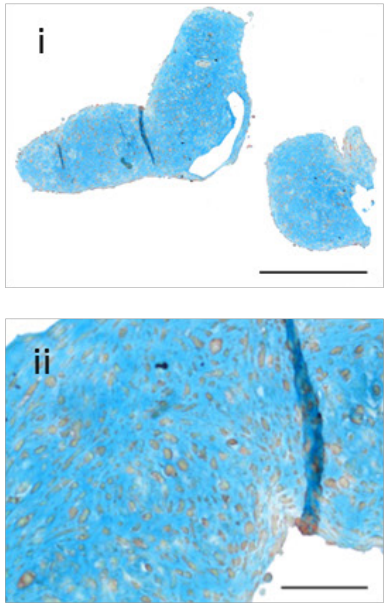

c. Type II Collagen

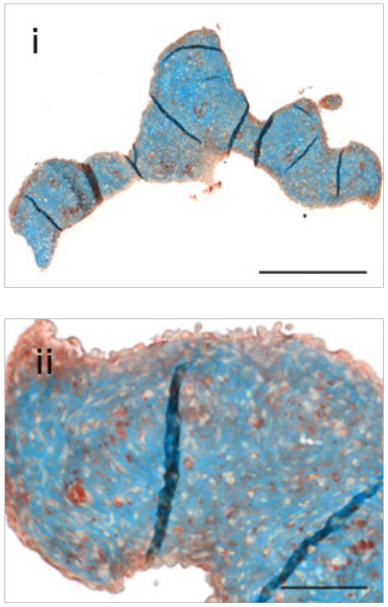

d. Type I Collagen

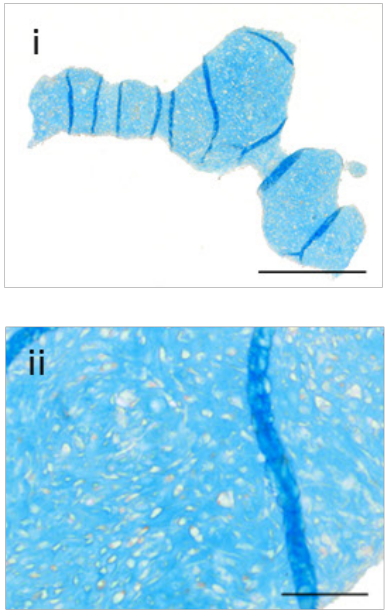

e. Aggrecan

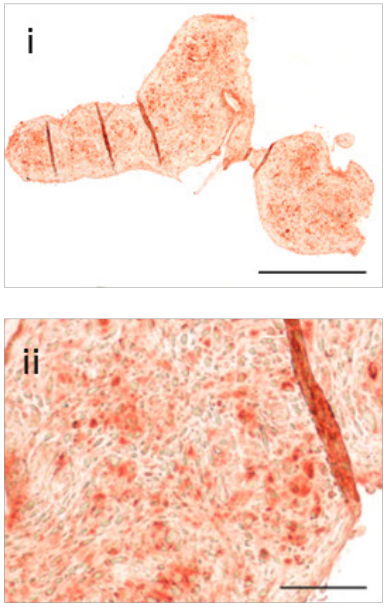

f. Anti-rabbit control

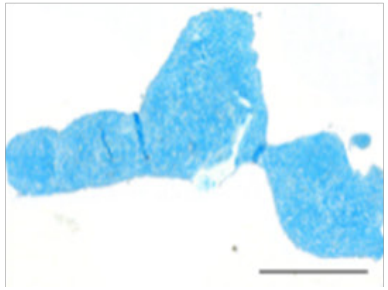

Anti-goat control

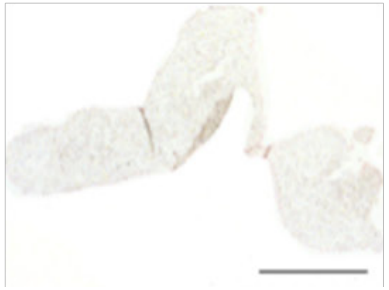

Figure 4.11 **Patient 2 generated hyaline-like cartilage following 21-days culture in an acoustofluidic bioreactor (construct 1).**

HACs were isolated from Patient 2 (Male; age 82) and cultured for 21 days in an acoustofluidic bioreactor in chondrogenic medium. Day 21 constructs were used for histology. Proteoglycans were detected using Safranin O staining (a i-ii), and expression of SOX9 (b i-ii) type II collagen (c i-ii), type I collagen (d i-ii) and Aggrecan (e i-ii) was investigated using immunohistochemistry. Secondary antibody only negative controls were included in the immunohistochemistry protocols (f); anti-rabbit control corresponds to SOX9, type I collagen and type II collagen, anti-goat control corresponds to Aggrecan. High magnification, 500 µm, low magnification, 100 µm.

Patient 2, construct 2 had hyaline cartilage-like morphology, characterised by numerous chondrocytes and lacunae. Sections were stained with haematoxylin and Safranin O to visualise cells and proteoglycan accumulation in the matrix respectively. Safranin O staining was intense and indicative of proteoglycan accumulation (Figure 4.12a). Construct 2 had weak but positive staining for SOX9 (Figure 4.12b), and type II collagen deposition concentrated at peripheral regions of the construct but with staining also present in more central regions (Figure 4.12c). Type I collagen was negligible (Figure 4.12d). Robust staining for the proteoglycan Aggrecan was observed throughout the construct (Figure 4.12e).

a. Safranin O

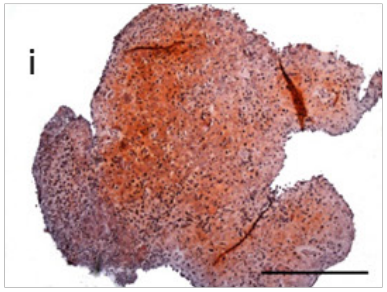

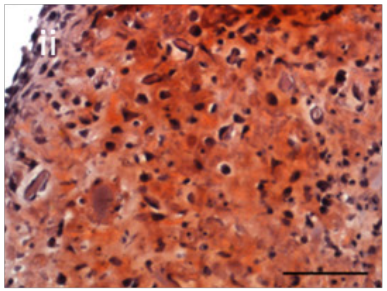

b. SOX9

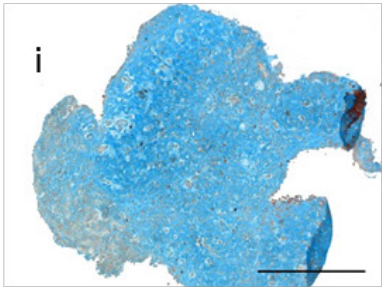

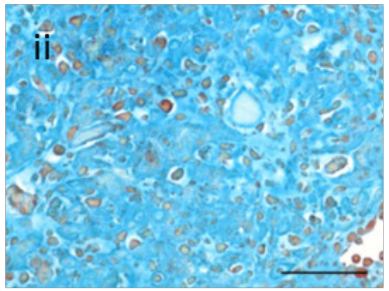

c. Type II Collagen

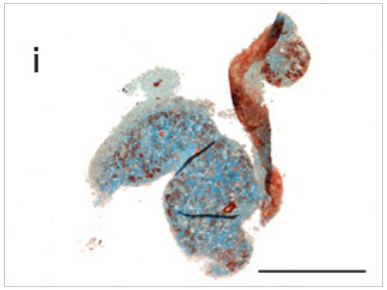

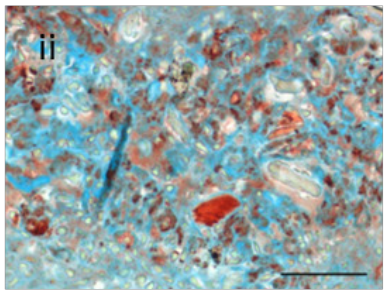

d. Type I Collagen

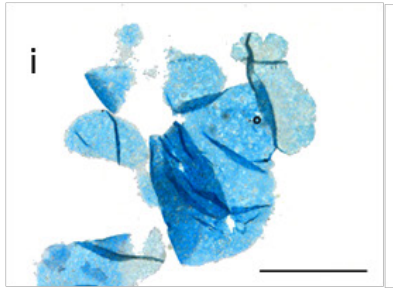

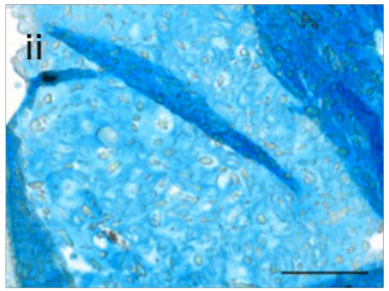

e. Aggrecan

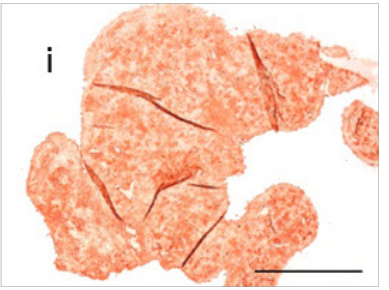

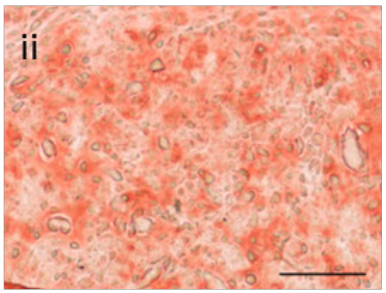

f. Anti-rabbit control

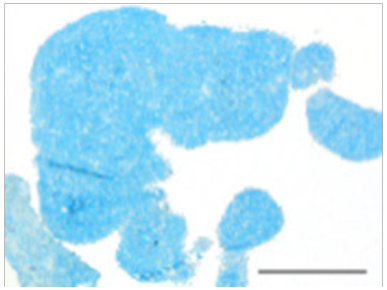

Anti-goat control

Figure 4.12 **Patient 2 generated hyaline-like cartilage following 21-days culture in an acoustofluidic bioreactor (construct 2)**

HACs were isolated from Patient 2 (Male; age 82) and cultured for 21 days in an acoustofluidic bioreactor in chondrogenic medium. Day 21 constructs were used for histology. Proteoglycans were detected using Safranin O staining (a i-ii), and expression of SOX9 (b i-ii) type II collagen (c i-ii), type I collagen (d i-ii) and Aggrecan (e i-ii) was investigated using immunohistochemistry. Secondary antibody only negative controls were included in the immunohistochemistry protocols (f); anti-rabbit control corresponds to SOX9, type I collagen and type II collagen, anti-goat control corresponds to Aggrecan. High magnification, 500 µm, low magnification, 100 µm.

Safranin O staining intensity of bioreactor constructs generated from HACs derived from patient 1 and 2 was investigated (Figure 4.13). Images were inverted (Figure 4.13a) and density analysis was performed using the ImageJ/FIJI software (Figure 4.13b and c). Figure 4.13b shows small variations in staining density between pellets from the same patient, however when the data was combined there was found to be no significant difference in Safranin O staining intensity between patients (Figure 4.13c).

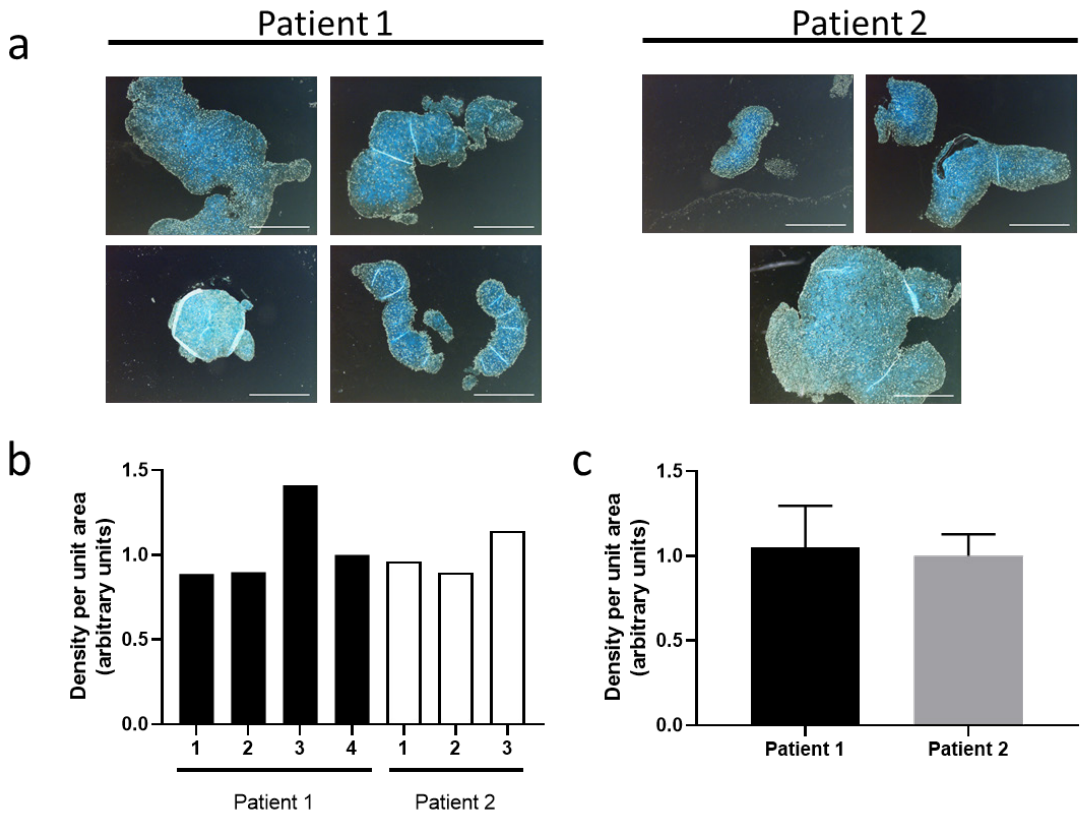

Figure 4.13 **Image analysis of Safranin O staining performed on HACs cultured in an acoustofluidic bioreactor for 21-days.**

HAC's were isolated from donors F67 (Patient 1) and M82 (Patient 2) and cultured in an acoustofluidic bioreactor for 3 weeks in chondrogenic medium. Constructs were used for histology and stained with Safranin O. Images were inverted (a) for use in density analysis using the ImageJ/FIJI software (b-c). Density for individual pellets is shown in b, and average in c (error bars represent mean ± SD). Scale bars in a, 500µm. patient 1, n=4; patient 2, n=3.

4.4.3 hESC-derived chondrocytes do not generate hyaline-like cartilage following bioreactor culture.

Following the success of HAC culture in the acoustofluidic bioreactor, hESC-derived chondrocytes were also cultured in the bioreactor for 21-days. However, unlike the HACs which formed large constructs within the resonator chamber, hESC-derived chondrocytes typically did not produce any tissue after 21-days and the resonator chambers were found to be empty. On one occasion 3 small (<200µm diameter) constructs were found following 21-days (Figure 4.14). The constructs were too small to effectively process and section and so one was fixed and whole mount staining was performed with Safranin O.

The sample appeared to stain with Safranin O, however due to the whole mount staining technique used it is not possible to confirm whether this staining is specific for proteoglycans in the matrix, or if the Safranin O was simply 'sticking' to the untreated sample.

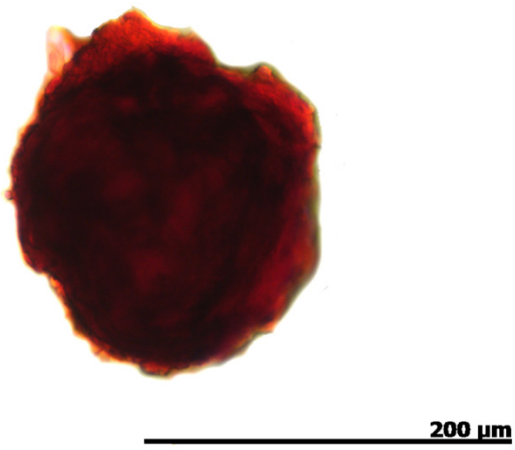

Figure 4.14 **Whole mount Safranin O staining of hESC-derived chondrocytes cultured in an acoustofluidic bioreactor for 21-days.**

hESC-derived chondrocytes were cultured in an acoustofluidic bioreactor for 21-days. Whole mount Safranin O staining was performed on the construct generated. Scale 200 µm.

4.5 Discussion

The aim of this project is to engineer viable cartilage from hESC-derived chondrocytes that is morphologically and mechanically similar to native hyaline articular cartilage. Introduction of hESC-derived chondrocytes into an acoustofluidic bioreactor is hoped to facilitate cartilage formation by allowing the self-assembly of levitating cells in an USWT, and subjecting cells to mechanical stimulation induced via the application of frequency sweeping.

Here a modified second generation bioreactor was used, based on the first and second generation bioreactors published in Li et al. (2014b) and Jonnalagadda et al. (2018), respectively. In contrast to the bioreactor design described by Li et al. (2014b) and Jonnalagadda et al. (2018), this modified second generation bioreactor is capable of supporting culture of four independent cell populations without the exchange of media between groups. The modified manifold with the four-way divider increases throughput of the bioreactor device which is advantageous for research purposes and also clinical translation. The culture parameters such as Vpp and sweep rate were standardised and determined by Jonnalagadda et al. (2018).

Conventional static tissue engineering techniques, such as pellet culture, are less complex in comparison to bioreactor culture. However, they are associated with numerous caveats such as an inability to generate large constructs due to tissue necrosis and suboptimal tissue formation that occurs due to poor nutrient mass transfer rates and oxygen diffusion (Li et al., 2014c; Muschler et al., 2004). As a result, techniques such as pellet culture utilise relatively low cell numbers and produce small tissue constructs. One study found that when pellet culture was initiated with a starting population of $1x10^6$ cells the resultant pellet had a necrotic core (Li et al., 2014c). Here, using a starting population of $1x10^6$ HACs it was possible to generate large hyaline-like cartilage constructs (up to 1.7 mm diameter) without tissue necrosis using an acoustofluidic bioreactor.

Single resonators were found to be capable of forming multiple constructs. This may be the result of the nodal configuration in the device. The device generates a single planar node in the fluid cavity (Jonnalagadda et al., 2018) at which cells aggregate in a sheet-like formation when first introduced into the device. As the cells begin to form connections during culture they start to form a 3D aggregate; it is possible that as the large planar aggregate becomes more 3D the cellular connectivity in some regions is unable to be maintained as parts of the aggregate are being forced into regions of higher pressure. As a result, the forming tissue breaks into multiple aggregates of various size. The cartilage constructs generated here stained strongly for chondrogenic markers such as proteoglycans, primarily Aggrecan, SOX9 and type II collagen. Expression of type I collagen in chondrocytes is usually associated with the cells acquiring a more

fibroblastic phenotype that is associated with dedifferentiation that results from monolayer expansion (Benya et al., 1978; Benya and Shaffer, 1982). This phenotype is usually repressed when chondrocytes are cultured in 3D (Benya and Shaffer, 1982). Here negligible expression of type I collagen was observed. The constructs generated here are similar in both size and morphology to those generated by Li et al. (2014b) and Jonnalagadda et al. (2018) using previous iterations of the acoustofluidic bioreactor. Similar to articular cartilage, the tissue generated in the bioreactor was hyaline in appearance with a proteoglycan and type II collagen rich matrix, with cells expressing the key chondrogenic marker SOX9. The tissue morphology resembled that of articular cartilage with cells existing within distinct lacunae.

When constructs generated from patient's 1 and 2 were compared in terms of proteoglycan content (using image analysis of Safranin O stained sections), there was no significant difference in staining density between the two patients, suggesting no difference in chondrogenic potential. This is despite the patients differing in both age and sex (F67 and M82). However, as this study examined constructs generated from only one male and one female patient, a much sample size would be required to determine sex-related differences in chondrogenic potential. Slight variations in staining density were observed between individual constructs from each patient; this could be related to the constructs relative positions within the resonator, where multiple constructs formed within the same cavity. Interestingly, Barbero et al. (2004) found high variability in the chondrogenic potential (measured in terms of GAG content) of HAC pellets from various donors. This was reportedly not age related and was instead attributed to factors such as previous drug treatments, life style, sports activities and the potential for different subpopulations in different cartilage biopsies. If HACs from a larger range of patients were cultured in the bioreactor, it is possible that this reported patient-patient variability would be observed. However, it is also possible that this inherent variability ay be in some way compensated for by the environment within the acoustofluidic bioreactor.

HACs are the most frequently used cell type for cartilage tissue engineering. This is because they can generate hyaline-like cartilage *in vitro* and are used clinically for treatments such as ACI. However, there are several drawbacks associated with HACs such as dedifferentiation during monolayer culture, low cell numbers from small tissue biopsies, cellular senescence and the requirement for patients to undergo multiple invasive surgeries for treatment. The hESC-derived chondrocytes generated here have the potential to circumvent the issues associated with HACs as the starting population of hESCs can grow indefinitely *in vitro* without undergoing cellular senescence and can therefore give rise to an unlimited number of progenitor cells that can be differentiated into chondrocytes via the DDP. Having demonstrated that these cells have a chondrogenic phenotype following differentiation in monolayer, I next chose to explore whether

culture of hESC-derived chondrocytes in an acoustofluidic bioreactor could generate cartilage of a similar quality to that generated by HACs. Unfortunately, this was not the case using the pre-determined driving parameters. Despite multiple attempts, using seven different bioreactors, devices were unable to generate high quality cartilage from hESC-derived chondrocytes using the same parameters used for HAC culture.

Whilst bioreactors did generate a few small (~150 µm diameter) spheroids following 21-days culture in the bioreactor. One of the small hESC-derived chondrocyte constructs was found to stain with Safranin O; however, due to the whole mount staining technique used it is difficult to determine if this staining is specific for proteoglycans as the tissue morphology could not be examined. To determine if the Safranin O staining was specific, a negative control of treating one of the samples with chondroitinase to digest proteoglycans before staining would have been beneficial. Regardless, the small size and low number of constructs generated render them useless for clinical application. It is of note that seeding the same number of cells, and maintaining them in the same culture conditions led to distinctly different results from HACs and hESC-derived chondrocytes. HACs produced multiple large hyaline-like cartilage constructs from single resonators, whereas hESC-derived chondrocytes were typically unable to generate anything, with the exception of a few very small constructs. It is possible that the driving parameters used here are not suitable for hESC-derived chondrocytes. The Vpp and sweep frequency were standardised for use with HACs, and it is possible that different cell types require different driving parameters.

With further standardisation of driving parameters it is possible that hESC-derived chondrocytes could be successfully cultured in the device to generate cartilage. However, due to time constraints focus shifted to investigating other culture methods to generate cartilage from hESC-derived chondrocytes. With regards to HAC culture, whilst the modifications to the bioreactor discussed here allowed higher throughput of patients by the introduction of a four-way divider into the bioreactor manifold, culture is still constrained by the bioreactor having only 4 small resonator chambers on each device. It is possible to increase the number of resonators on each bioreactor device, but the small fluidic cavity limits construct size. An increase in the cavity depth would, with the current parameters, result in the generation of a multi node device. This may enable the generation of even more constructs in each resonator chamber. It is also possible that by then modifying the driving parameters to once again generate a single node within the chamber, it may be possible to generate tissue with even larger dimensions than those reported here.

Chapter 5 Pellet Culture

5.1 Introduction

The traditional tissue engineering paradigm incorporates cells, signals and scaffolds. Exogenous scaffolds are useful as they provide a 3D structure that enables cell adherence and allows cells to proliferate and produce extracellular matrix in a more spatially relevant environment compared to monolayer cell culture. Commonly used scaffold materials include natural polymers such as hyaluronic acid, chitosan, alginate and collagens and synthetic polymers such as PLA (Lee and Shin, 2007). However, the biofunctionality, biocompatability, degradation rates and immunogenicity of the degradation products can pose significant issues (Johnstone et al., 2013; Vacanti and Langer, 1999). Due to the complications of incorporating exogenous scaffold materials, there has been a shift towards scaffold-free tissue engineering strategies. Scaffold-free tissue engineering requires cells to provide their own 3D framework for tissue generation and is therefore more likely to faithfully recapitulate the developmental process of tissue generation.

Chondrocytes dedifferentiate during monolayer culture expansion (Schnabel et al., 2002). Aggregation of these cells into a 3D pellet, in the presence of chondro-inductive factors helps to restore the chondrogenic phenotype. 3D pellet culture is the current 'gold standard' for cartilage tissue engineering and has frequently been used to demonstrate the *in vitro* cartilage forming potential of chondrogenic cells (Li et al., 2015; Manning and Bonner Jr, 1967; Tare et al., 2005). This scaffold free approach has shown to enhance cartilage formation compared to encapsulation in 'gel-like biomaterials' (Bernstein et al., 2009).

To enhance chondrogenesis, exogenous factors are routinely added to chondrogenic culture medium, typically with the aim of enhancing collagen deposition. Ascorbic acid is a common component of chondrogenic media as it has been shown to enhance collagen production (Hata and Senoo, 1989; Temu et al., 2010); enhanced synthesis is due to ascorbic acid being an essential component of hydroxyproline and hydroxylysine which are required for stabilizing the collagen triple helix and for intermolecular crosslinking respectively (Murad et al., 1981). Members of the transforming growth factor-β family such as TGF-β1 and TGF-β3 are also commonly incorporated into chondrogenic media (Tang et al., 2009). SOX9 is a key transcriptional regulator of chondrogenesis, and directly regulates the expression of the type II collagen gene (*COL2A1*) (Bell et al., 1997). TGF-β is involved in the regulation of SOX9 by mediating phosphorylation and stabilisation via both p38 and Smad2/3 (Coricor and Serra, 2016). This allows prolonged activation of *COL2A1* and therefore enhances chondrogenesis.

Cartilage tissue engineering has so far focussed on the chondrogenic potential of autologous human articular chondrocytes (HACs) and skeletal stem cells (SSCs). However, limitations such as the requirement for patients to undergo multiple surgeries, low cell numbers, cell senescence and dedifferentiation hinder use of these cells for regenerative therapies. hESCs are allogeneic and are widely considered to be immune-privileged (Araki et al., 2013; Li et al., 2004). This aspect coupled with their capacity for unlimited self-renewal, ability to differentiate into any somatic cell type, and the capacity to generate high numbers of cells makes hESCs an ideal candidate for cartilage tissue engineering.

A fundamental concept in cartilage tissue engineering is the replacement of damaged or missing cartilage with an engineered tissue construct that has the properties that mimic the physiology of native cartilage. The quality of the cartilage generated should be investigated in terms of composition and mechanical properties prior to *in vivo* studies and clinical application. This type of quality assessment is made possible by the generation of the tissue *in vitro*, rather than transplanting cells directly *in vivo* and allows spatial confinement of the implanted tissue which is not possible with cell injection. The work by Oldershaw et al. (2010b) and Cheng et al. (2014) did not investigate the capacity for the chondroprogenitors to form cartilage *in vitro*, but instead the cells were injected directly into an osteochondral defect created in the patellar groove of athymic RNU rats. Surprisingly, these investigators did not test ability of the chondroprogenitors to form cartilage *in vitro* prior to implantation. Moreover, due to the use of an osteochondral, rather than a chondral or partial thickness defect it is possible that cells from the bone marrow infiltrated the defect site and contributed to the defect repair. Thus, it is important not only to assess the morphology and biofunctionality of any tissue engineered construct but also to carefully assess which animal model and defect type is best to test the efficacy of bioengineered cartilage *in vivo*.

5.3 Aims and objectives

- To generate cartilage from hESC-derived chondrocytes using pellet culture.
- To assess the quality of the cartilage generated using qualitative and quantitative histological analyses.
- To assess the biomechanical properties of the cartilage generated.

5.4 Methods

5.4.1 HAC pellet culture

HACs at 70-90% confluency were dissociated as in section 2.3.2, pelleted and resuspended in chondrogenic medium (Table 3.2) containing 300,000 cells/ml. The cell suspension was divided into conical based Universal tubes (1 ml per tube), centrifuged at 400 x*g* for 5 minutes and the cell pellet resuspended in 1 ml of chondrogenic medium. Once the pellets had been centrifuged for a second time they were incubated at 37°C, 5% O_2 in air.

Pellet cultures were performed for 3-5 weeks, with a medium change performed every 2-4 days.

5.4.2 hESC-derived cartilage pellet culture

hESC-derived chondrocytes at Stage 3 (day 14) were dissociated by first incubating with collagenase IV for 4 mins, followed by Trypsin-EDTA (0.05%) until cells began to detach. α-MEM containing 10% FCS was used to neutralise the Trypsin-EDTA (0.05%). The cell suspension was pipetted up and down against the base of the well before being transferred into a 50 ml tube. The cell suspension was centrifuged at 400 x*g* for 5 minutes and the cell pellet resuspended in chondrogenic medium (Table 3.2) containing 300,000 cells/ml.

The cell suspension was divided into conical base Universal tubes (1 ml per tube), centrifuged at 400 x*g* for 5 minutes and the cell pellet resuspended in 1 ml of chondrogenic medium. Once the pellets had been centrifuged for a second time they were incubated at 37°C, 5% O_2 in air.

Pellet cultures were performed for 3-19 weeks, with a medium change performed every 2-4 days.

5.4.3 Alkaline Phosphatase staining

Samples were fixed in 70% EtOH for Alkaline Phosphatase (ALP) staining, and processed as in section 2.5.1.

Sections were rehydrated as in section 2.5.3 and briefly washed in tap water. Slides were incubated in activating buffer (Table 5.1) overnight at room temperature.

Table 5.1 **Activation buffer recipe.**

Stock A: Tris Maleate	Stock B: Sodium Hydroxide	**Activating Buffer (pH 7.4)**
12.1 g Tris	4 g NaOH	**75 ml Stock A**
11.6 g Maleic acid	500 ml dH_2O	**81 ml Stock B**
500 ml dH_2O	-	**144 ml dH_2O**
-	-	600 mg Magnesium Chloride

Slides were then incubated with filtered AS-B1/Fast Violet (Table 5.2) at 37°C for 2 hours.

Table 5.2 **AS-B1/Fast Violet recipe.**

Naphthol AS-B1 Stock: part A (pH 8.3)	Naphthol AS-B1 Stock: part B (pH 8)	Naphthol AS-B1 stock	**AS-B1/Fast Violet staining solution**
4.36 g Tris	25 mg Naphthol AS-B1 Phosphate	Naphthol AS-B1 Stock: part A	**70 ml Naphthol AS-B1 stock**
180 ml dH_2O	10 ml Dimethyl Formamide	Naphthol AS-B1 Stock: part B	**140 mg Fast Violet Salt**
-	10 ml dH_2O	300 ml dH_2O	-

Slides were then washed in a running water bath for a few minutes and counterstained in Alcian Blue as in section 2.5.4. Slides were mounted in Hydromount.

5.4.4 Isolation of RNA from pellet cultures

HAC pellets were cultured for 3 weeks and hESC-derived cartilage pellets for 4 weeks before being harvested for RNA.

Pellets were washed with sterile PBS and incubated in 1 ml collagenase IV in α-MEM in a humidified incubator at 37°C for 45 minutes. Pellets were washed again with sterile PBS and transferred into screwcap RNA tubes. 2-6 pellets from the same patient (HACs) or experiment (DDP) were pooled for RNA isolation. 1 ml of TriFast reagent was added to each sample followed by homogenization using an Ultra-turrax homogenisation probe. Probe was cleaned with 70% EtOH, RNase Away, and Trizol before homogenisation of the sample, and washing was repeated

between samples. Following homogenisation samples were either stored at -80°C or progressed directly to RNA isolation as in section 2.4.1.

5.4.5 Mechanical testing

A purpose-built mechanical testing rig was used to compress samples between two flat metal plates (compression plate and baseplate) (Figure 5.1). The device generated force and displacement readings that were used to determine the Young's elastic modulus (E) for each sample. For native cartilage, 5 mm^2 samples of full thickness articular cartilage were harvested from the non-load bearing region of the femoral head. hESC-derived cartilage pellets were tested following 4 or 19 weeks culture.

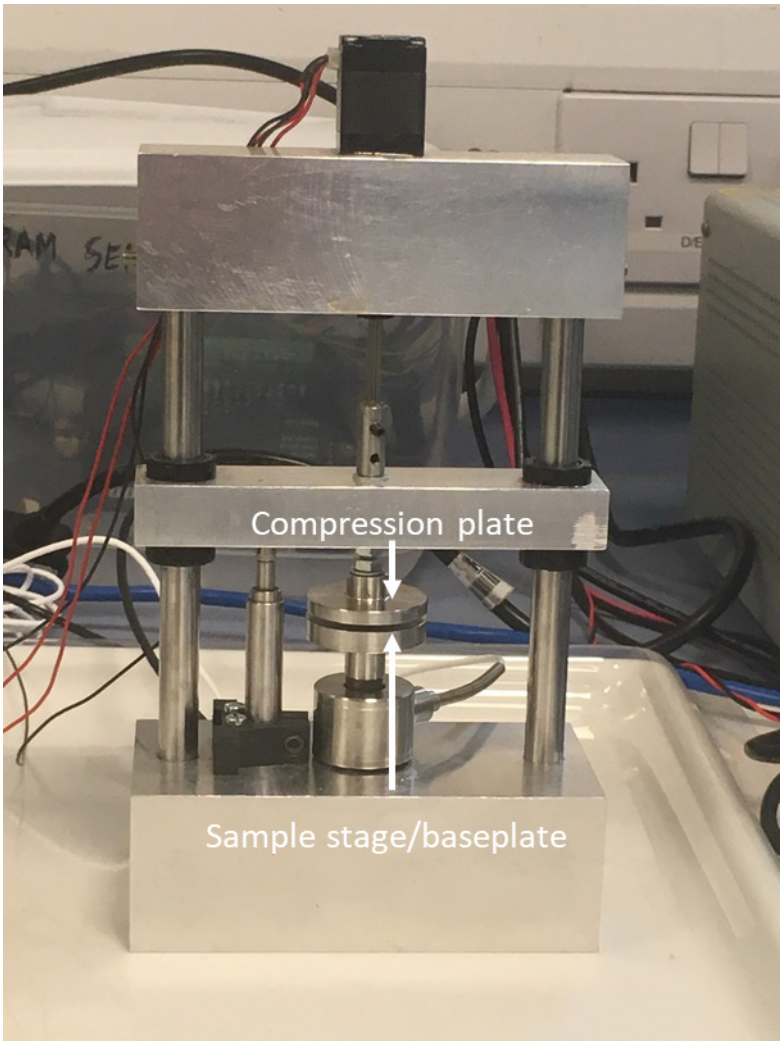

Figure 5.1 **Mechanical testing rig used for compression of native cartilage and cartilage pellets.**

For mechanical testing of native cartilage and cartilage pellets, samples were placed on the sample stage/baseplate. During the test the compression plate slowly lowered towards the baseplate and force readings were measured.

5.4.5.1 Native cartilage

A Mathematica code was developed by Katherine Arnold (project student with Rahul Tare) to determine E for each sample (see section 7.3 for Mathematica code). The following equations were used:

$$E = \frac{\sigma}{\varepsilon}$$

Where σ represents stress, and ε strain, which were calculated using the following equations:

$$\sigma = \frac{F}{A} \qquad \varepsilon = \frac{\Delta l}{l}$$

Where F represents force, A contact area, Δl change in length, and l original length.

To determine E, only the initial linear region of compression was analysed based on the principle of Hooke's Law that strain in a solid is proportional to the applied stress within the elastic limit of that solid. The equation used to generate the Young's Elastic modulus assumes a linear relationship between stress and strain which can only be applied to the linear (and not the exponential) region of a stress strain graph. The linear region was determined by mapping the stress strain curve of the tested sample against one modelled by the equation that accounted for the dimensions of the sample tested (Figure 5.2). The region that best fit the model was chosen as the linear region and was then used to calculate E.

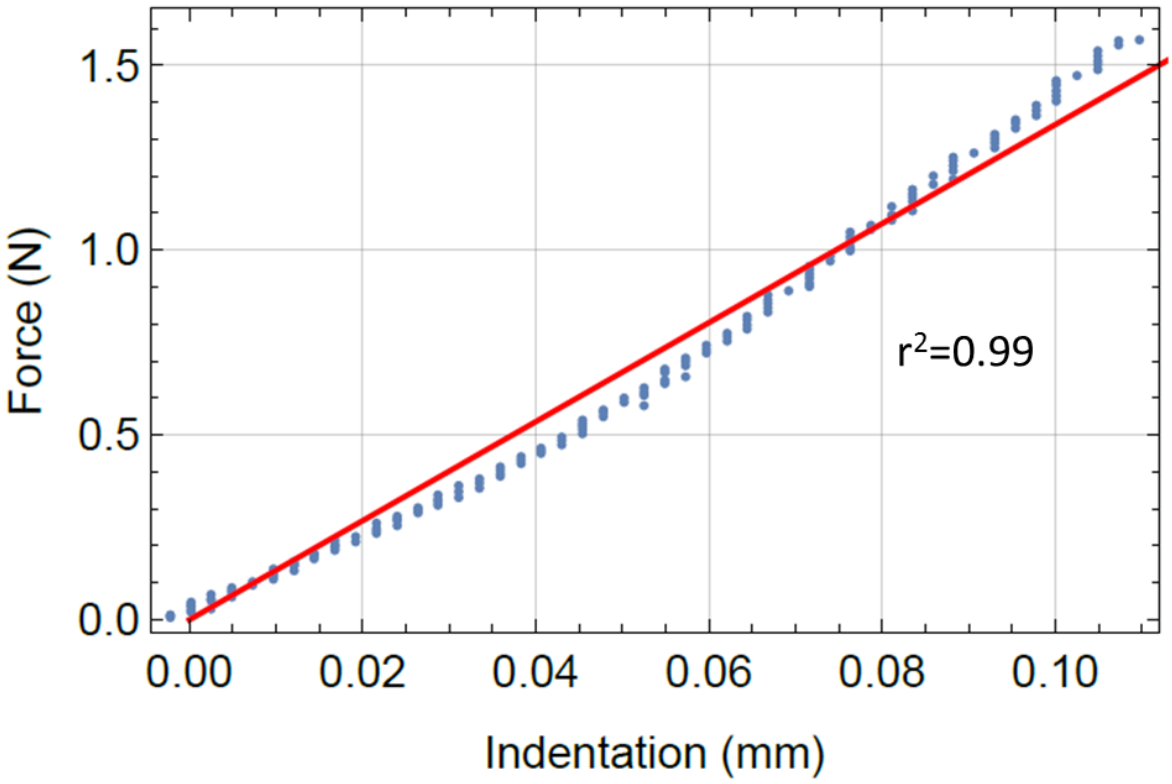

Figure 5.2 **Representative curve mapping graph generated by Mathematica code for mechanical testing of full thickness cartilage.**

Using a Mathematica code, force-indentation data from tested samples of human articular cartilage was mapped onto a model programmed with the same dimensions as the sample (red line). The number of data points selected for determining elastic modulus was determined by curve mapping; r^2 values of ~0.99 were considered to be a good fit to the model.

5.4.5.2 Cartilage pellets

Due to the change in contact area during compression of pellets the equation used to determine E for native cartilage was not appropriate. A Mathematica code based on Hertzian Theory was developed by Katherine Arnold (project student with Rahul Tare) to determine E for each sample (see section 7.4 for Mathematica code). The code also involved curve mapping as described in section 5.4.5.1 (Figure 5.3).

Hertzian theory of contact stresses allows modelling of complex situations such as those of spherical objects and flat surfaces (half planes). This considers the changing shape of the pellet and can be used to calculate the stresses involved. The general equation for Hertzian theory between two spheres is:

$$a = \sqrt[3]{\frac{3F\left[\frac{1-\nu_1^2}{E_1}+\frac{1-\nu_2^2}{E_2}\right]}{4\left(\frac{1}{R_1}+\frac{1}{R_2}\right)}}$$

a = radius of contact area [m]
F = force at contact surface [N]
E = Young's Modulus of respective materials [Pa]
v = Poisson's ratio for respective materials
R = Radius of respective surfaces [m]

For the mechanical testing of pellets, there is one sphere and a half-plane rather than two spheres. To reflect this, the radius of sphere 2 is set to infinity, as is the Poisson's ratio (the ratio of the proportional decrease in a lateral measurement to the proportional increase in length in a sample of material that is elastically stretched) and E. As the plates are stainless steel, their stiffness is much higher than that of the pellets. Comparatively, this means the Poisson's ratio and stiffness can be modelled as infinite.

Rearranging this equation for F leads to:

$$F = \frac{4}{3R} \times a^3 \times \frac{E}{(1-\nu^2)}$$

Another equation allows calculation of the contact area of a sphere under compression by a half plane:

$$a = \sqrt{\frac{Rd^i}{2}}$$

The division by 2 considers that the pellet is being compressed both top and bottom, and so the displacement (d^i) is split between the two surfaces.

This leads to the final equation for Hertzian force:

$$F = \frac{4E}{3R(1-\nu^2)} \times \left(\frac{Rd^i}{2}\right)^{3/2}$$

When applying this equation, the Poisson's ratio is assumed to be 0.4 (Jin and Lewis, 2004). This assumption takes the value for mature cartilage.

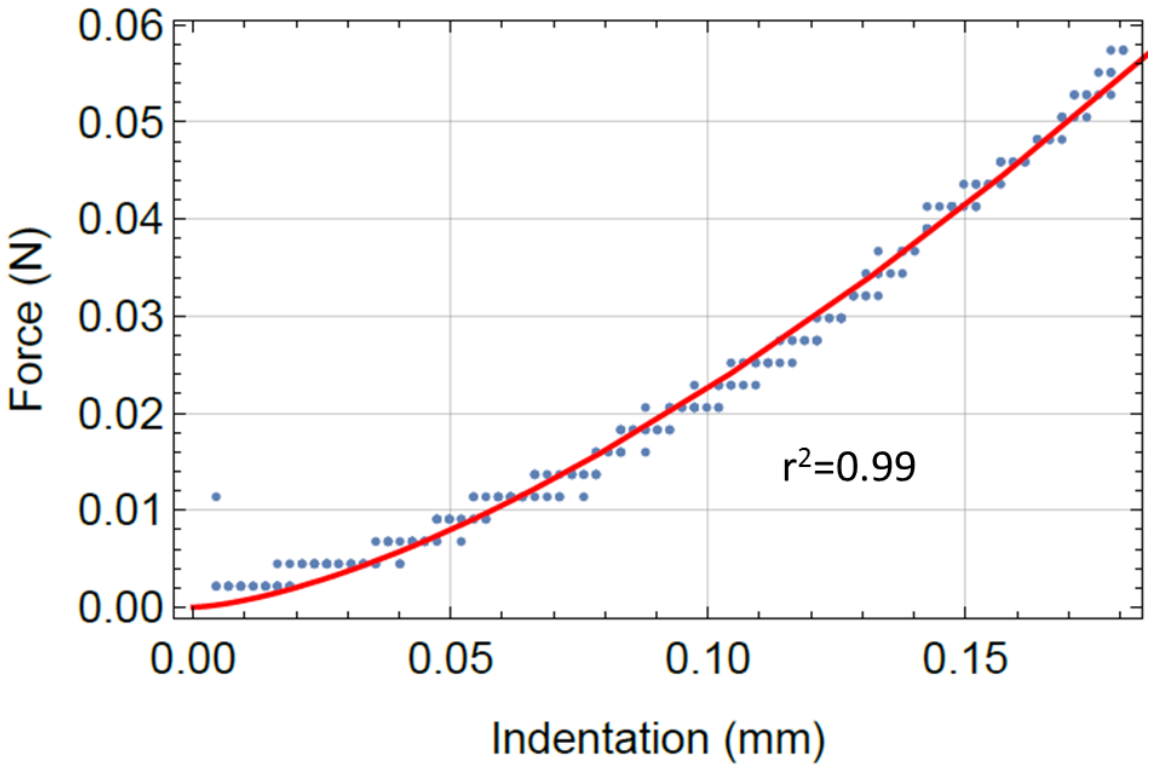

Figure 5.3 **Representative curve mapping graph generated by Mathematica code for mechanical testing of pellets.**

Using a Mathematica code, force-indentation data from tested cartilage pellets was mapped onto a model programmed with the same dimensions as the sample (red line). The number of data points selected for determining elastic modulus was determined by curve mapping; r^2 values of ~0.99 were considered to be a good fit to the model.

5.4.6 Statistical analysis

5.4.6.1 Image analysis and mechanical testing

A Shapiro-Wilk normality test was used to confirm normal distribution. A one-way Anova followed by Tukey's post-hoc multiple comparisons test was applied.

5.4.6.2 RT-qPCR analysis

A Shapiro-Wilk normality test was used to confirm normal distribution. Once normal distribution was determined an unpaired Student's t-test was used, assuming equal variance (2 sample t-test).

5.6 Results

5.6.1 HAC pellet culture

Human Articular Chondrocytes (HACs) were isolated from the femoral heads of patients undergoing hip replacement surgery. HACs were cultured as pellets in chondrogenic media, the gold standard method for *in vitro* cartilage generation.

5.6.1.1 HACs form hyaline cartilage in pellet culture

Pellets were generated using monolayer-expanded HACs from 4 donors (F65, F56, F58 and F94), cultured for 3 weeks and analysed using histology (Figure 5.4). Pellets generated from all donors were of similar dimensions and had comparable morphology.

Sections were stained with haematoxylin and Safranin O to visualise cells and proteoglycan accumulation in the matrix respectively (Figure 5.4a i-iv). Pellets exhibited hyaline cartilage-like morphology, characterised by numerous chondrocytes in distinct lacunae that were embedded in extracellular matrix composed of proteoglycans stained with Safranin O.

Immunohistochemistry was performed to analyse the expression of SOX9 (Figure 5.4b i-iv), the key chondrogenic transcription factor, type II collagen (Figure 5.4c i-iv), the primary collagen in hyaline cartilage, type I collagen (Figure 5.4d i-iv), the bone/fibrocartilage-specific collagen and Aggrecan (Figure 5.4e i-iv), the predominant proteoglycan in cartilage matrix. Alcian blue was used as a counter stain for proteoglycans in the pellet matrix for all antibodies with the exception of Aggrecan. Counterstaining with Alcian blue showed results consistent with Safranin O staining in terms of proteoglycan density and distribution.

Robust intracellular expression of SOX9 was observed in the pellets from the 4 donors (Figure 5.4b i-iv). SOX9 expression appeared more robust in patients F58 and F94 (Figure 5.4b iii and iv). Type II collagen was also present in pellets from all 4 patients, with variation in deposition between patients (Figure 5.4c i-iv). Pellets from donors F65 and F56 (Figure 5.4c i and ii) had the most intense staining with the greatest distribution; pellets from donors F58 and F94 had less intense type II collagen staining (Figure 5.4c iii and iv). Type I collagen deposition was negligible in pellets from all patients (Figure 5.4d i-iv) with sections appearing similar to controls (Figure 5.4f). Robust staining for Aggrecan was observed in pellets from all donors (Figure 5.4e).

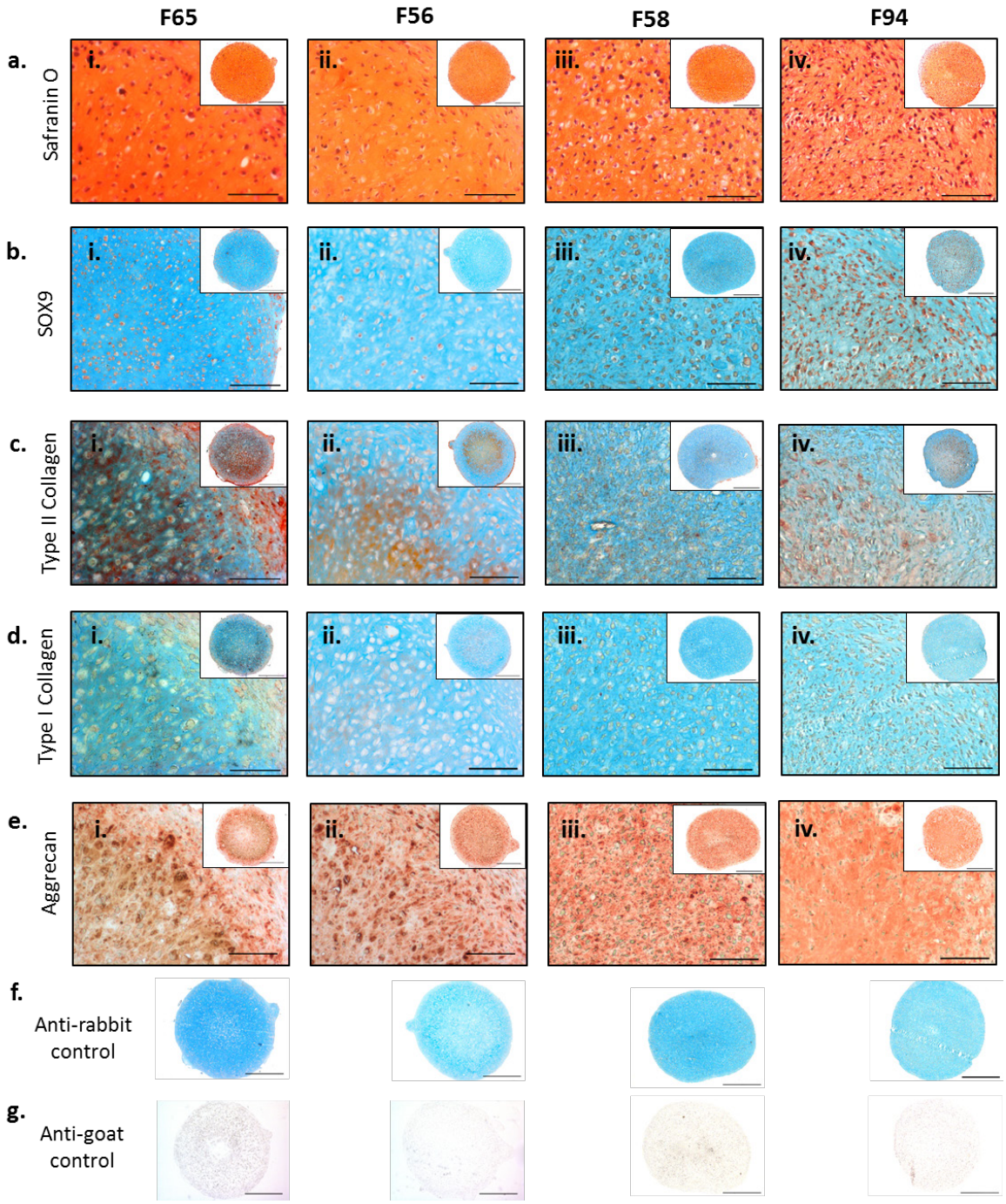

Figure 5.4 **HAC pellet culture.**

HACs were isolated from donors F65, F56, F58 and F94 and cultured as pellets for 21 days in chondrogenic medium. Day 21 pellets were used for histology. Proteoglycans were detected using Safranin O staining (a i-iv), and expression of SOX9 (b i-iv) Type II collagen (c i-iv), type I collagen (d i-iv) and Aggrecan (e i-iv) was investigated using immunohistochemistry. Secondary antibody only negative controls were included in the immunohistochemistry protocols (f and g). Anti-rabbit controls correspond to SOX9, type I collagen and type II collagen; anti-goat control corresponds to Aggrecan. High magnification, 500 µm, low magnification, 100 µm.

5.6.1.2 Cartilage formation is not enhanced by extended culture

Standard culture time for HAC pellets is reported to be 3 weeks. Here HACs were cultured as pellets for 3, 4 and 5 weeks and image analysis performed on Safranin O staining and type II collagen immunostaining.

Pellet area appeared to increase modestly with extended culture (Figure 5.5a), however this was not found to be statistically significant (Figure 5.5b).

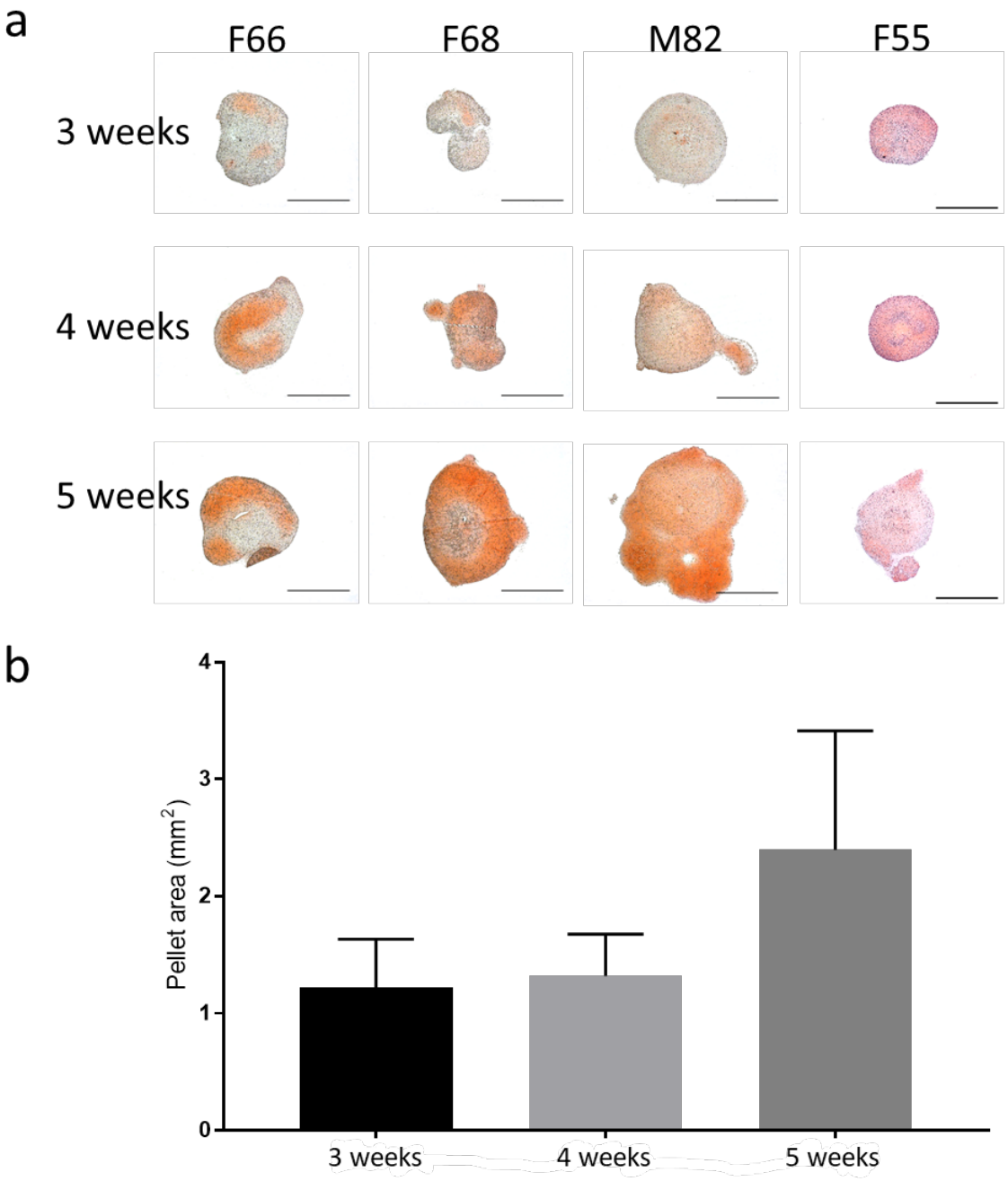

Figure 5.5 **Extended culture did not increase pellet area.**

HAC's were isolated from donors F66, F68, M82 and F55 and cultured as pellets for 3, 4 or 5 weeks in chondrogenic medium. Pellets were used for histology and stained with Safranin O. Images used to measure pellet area are shown in a, scale 1 mm. Quantitative analysis of pellet area is shown in b. Bars represent mean ± SD, n=4 per group.

Safranin O staining intensity of pellets at 3, 4 and 5 weeks was investigated (Figure 5.6). Images were inverted and density analysis was performed using the ImageJ/FIJI software. Inverted images appear to show an increase in proteoglycans over time (Figure 5.6a) however this was not statistically significant (Figure 5.6b).

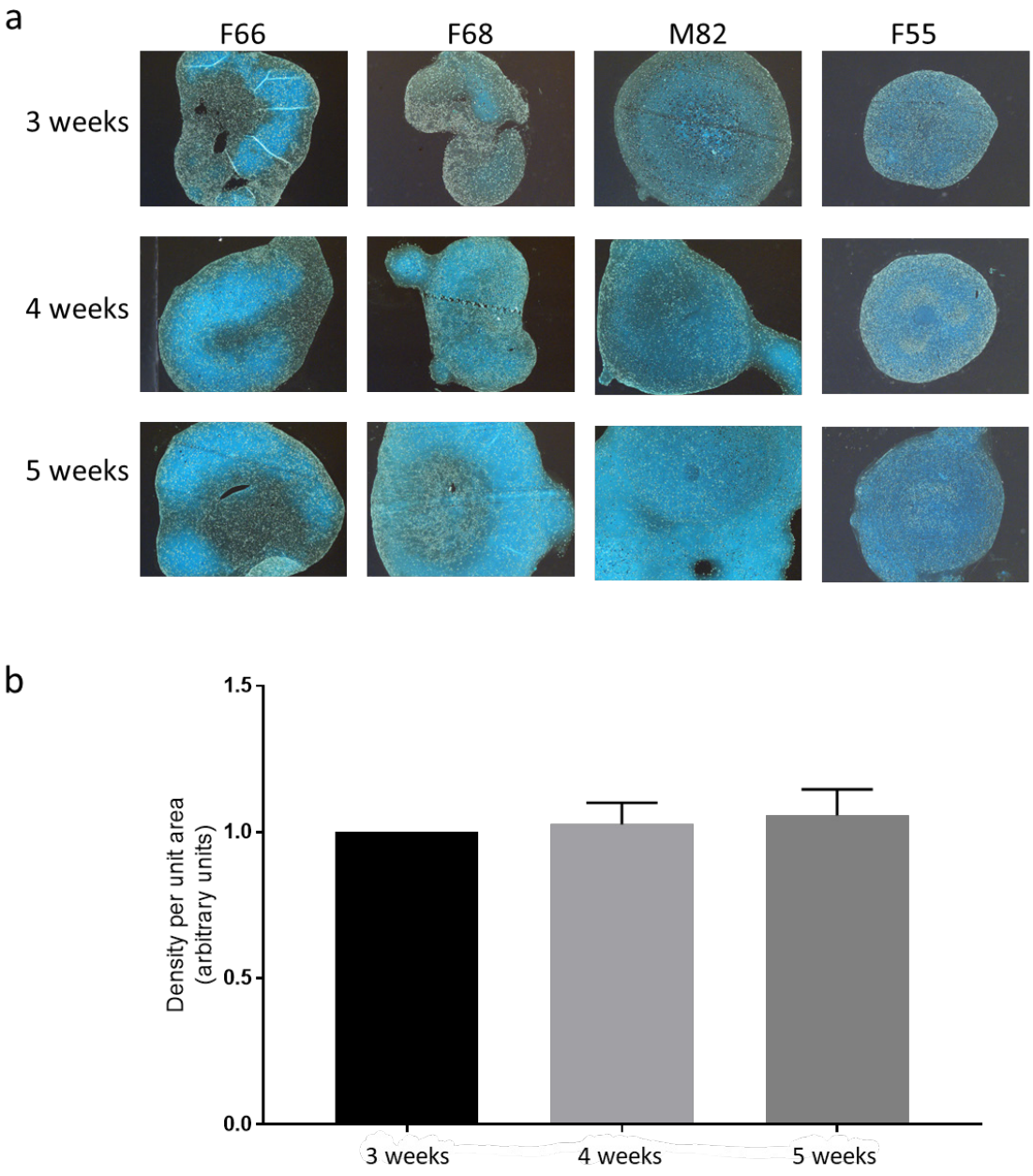

Figure 5.6 **Extended culture did not increase Safranin O staining intensity.**

HAC's were isolated from donors F66, F68, M82 and F55 and cultured as pellets for 3, 4 or 5 weeks in chondrogenic medium. Pellets were used for histology and stained with Safranin O. Images were inverted (a) for use in density analysis using the ImageJ/FIJI software. Scale bar 500µm. Bars represent mean ± SD, n=4 per group.

Type II collagen immunostaining intensity of pellets at 3, 4 and 5 weeks was investigated (Figure 5.7). Images were inverted and density analysis was performed using the ImageJ/FIJI software. Inverted images do not appear to show changes in intensity type II collagen Figure 5.6staining (Figure 5.7a), which is reflected by no significant difference in staining intensity (Figure 5.7b).

No significant differences were found between pellet size or the intensity of proteoglycan staining or type II collagen immunostaining in pellets cultured for 3, 4 or 5 weeks. It was therefore concluded that extended culture did not enhance cartilage formation by HACs and that 3 weeks was therefore the optimum culture period of those tested.

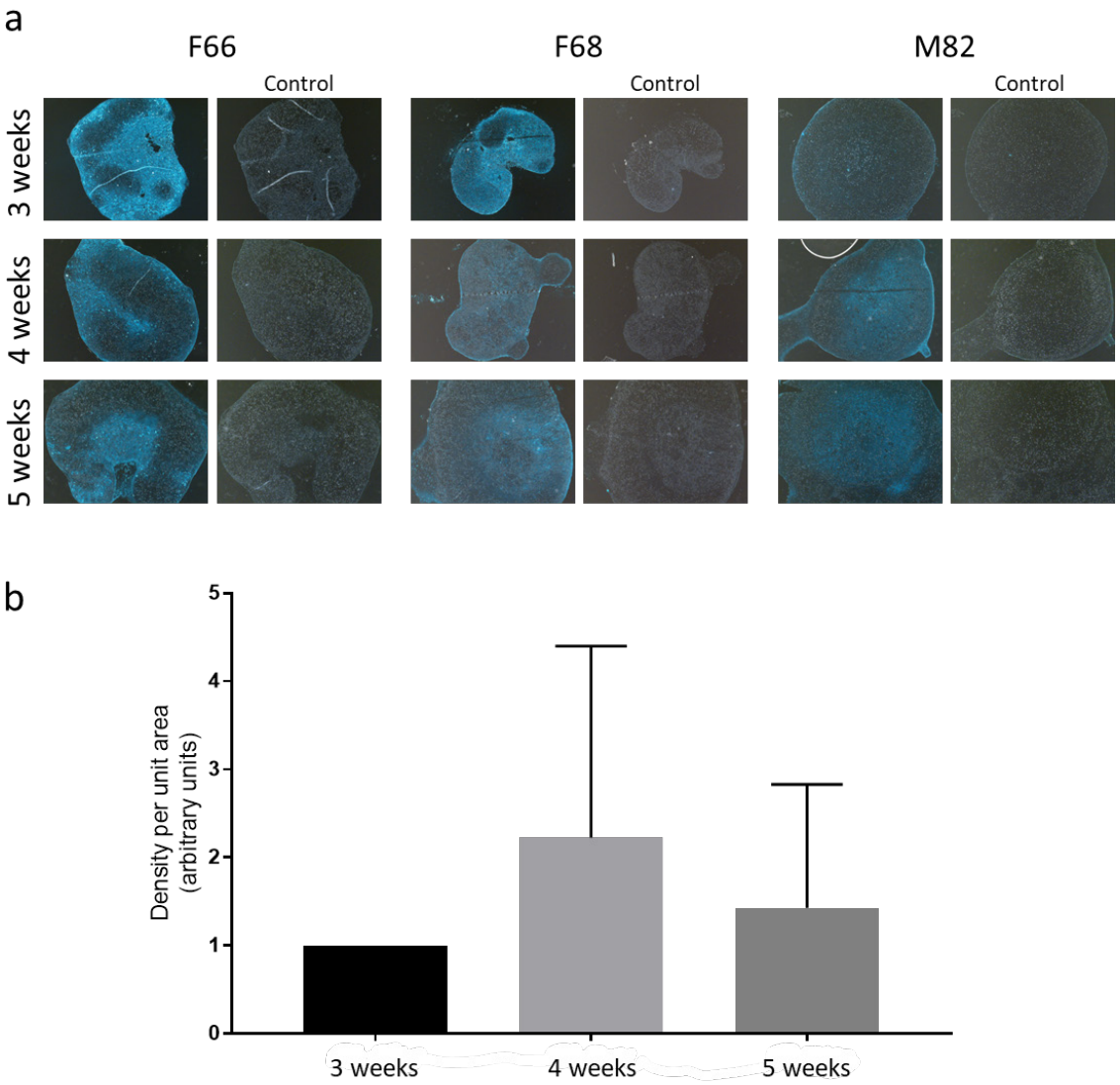

Figure 5.7 **Extended culture did not increase type II collagen staining intensity.**

HAC's were cultured as pellets for 3, 4 or 5 weeks in chondrogenic medium. Pellets were used for histology and immunostained for type II collagen. Secondary antibody only controls were included in the immunostaining protocol. Images were inverted for density analysis (a) which was performed using the ImageJ/FIJI software. Data in b represents density per unit area of stained sample minus density per unit area of control. Bars represent mean ± SD, n=3 per group.

5.6.2 hESC-derived cartilage pellet culture

5.6.2.1 hESC-derived chondrocytes form cartilage with a type II collagen rich matrix

To test the cartilage forming abilities of hESC-derived chondrocytes, cells were cultured as pellets for 3, 4 or 5 weeks in chondrogenic medium. At the end of the designated culture periods pellets were white and opaque in appearance with a diameter of approximately 1mm (Figure 5.8). Pellet size did not appear to increase within the selected timeframe of 3-5 weeks.

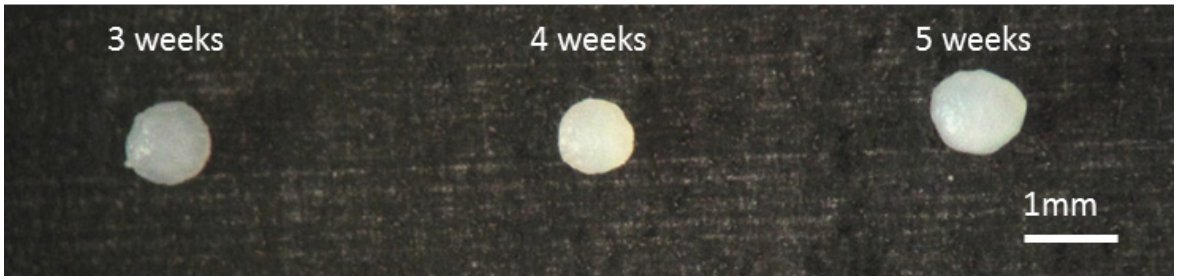

Figure 5.8 **Photographs of hESC-derived cartilage pellets cultured for 3, 4 or 5 weeks.** *hESC-derived chondrocytes were cultured as pellets for 3, 4 or 5 weeks in chondrogenic medium. Images were taken prior to fixation. Scale bar 1 mm.*

In the previous chapter it was established that hESC-derived chondrocytes express SOX9 and deposit type II collagen during 2D monolayer culture. Next, the expression of these, and other chondrogenic markers was investigated in 3D pellet cultures of hESC-derived chondrocytes cultured for 3, 4 or 5 weeks.

hESC-derived cartilage pellets generated in experiment 1 had very low proteoglycan content at all time points, as demonstrated by weak staining for Safranin O (Figure 5.9a). Aggrecan staining was undetectable (Figure 5.9e). There was however weak Alcian Blue counter staining which may indicate the presence of some proteoglycans, (Figure 5.9b-d and f).

hESC-derived cartilage pellets exhibited robust nuclear expression of SOX9 (Figure 5.9b) and an absence of the bone specific type I collagen (Figure 5.9d). There were variations in staining intensity of type II collagen with staining appearing more intense at 3 and 5 weeks. An overall improvement in pellet morphology was observed between weeks 3 and 4 with pellets becoming more uniform and rounder with more defined lacunae (Figure 5.9).

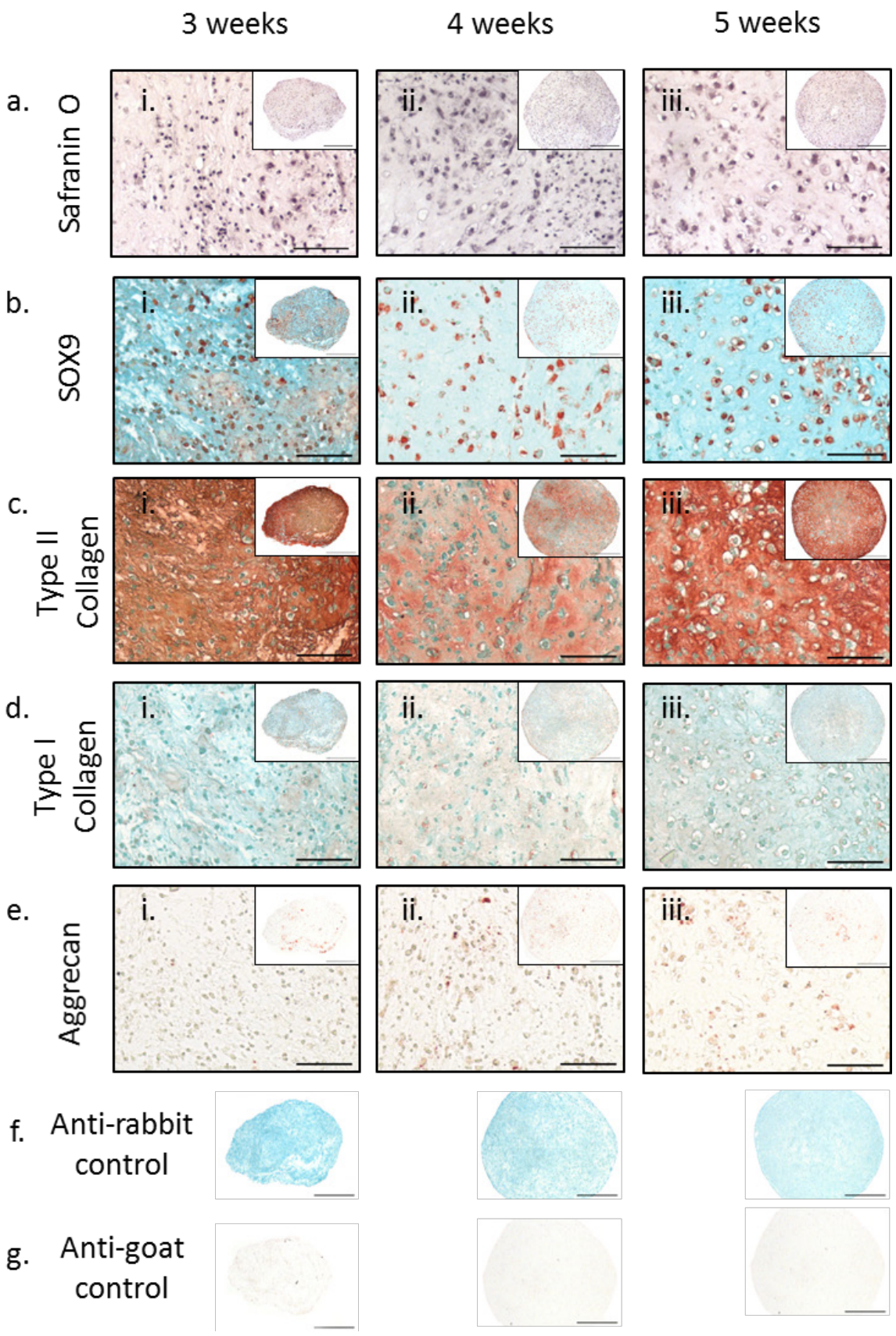
3 weeks
4 weeks
5 weeks
a.
Safranin O
i.
ii.
iii.
b.
SOX9
i.
ii.
iii.
c.
Type II Collagen
i.
ii.
iii.
d.
Type I Collagen
i.
ii.
iii.
e.
Aggrecan
i.
ii.
iii.
f.
Anti-rabbit control
g.
Anti-goat control

Figure 5.9 **hESC-derived cartilage pellets cultured for 3, 4 or 5 weeks, experiment 1.**

hESC-derived chondrocytes were cultured as pellets for 3, 4 or 5 weeks in chondrogenic medium. Pellets were used for histology. Proteoglycans were detecting using Safranin O staining (a), and expression of SOX9 (b), type II collagen (c), type I collagen (d) and Aggrecan (e) was investigated via immunohistochemistry (IHC). Sections used for SOX9, type II collagen and type I collagen IHC were counterstained with alcian blue. Secondary antibody only negative control (f and g). Anti-rabbit controls correspond to SOX9, Type I collagen and Type II collagen; anti-goat control corresponds to Aggrecan. High magnification, 500 µm, low magnification, 100 µm.

hESC-derived cartilage pellets generated in experiment 2 had very low proteoglycan content at all time points, as demonstrated by weak staining for Safranin O (Figure 5.10a). Weak Aggrecan staining was observed at all time points (Figure 5.10e), with the most robust staining at 4 weeks (Figure 5.10eii). There was however weak Alcian Blue counter staining which may indicate the presence of some proteoglycans, (Figure 5.10b-d and f).

hESC-derived cartilage pellets exhibited robust nuclear expression of SOX9 (Figure 5.10b) and an absence of the bone specific type I collagen (Figure 5.10d). There were variations in staining intensity of type II collagen with staining appearing more intense at 4 weeks. An overall improvement in pellet morphology was observed between weeks 3 and 4 with pellets becoming more uniform and rounder with more defined lacunae (Figure 5.10).

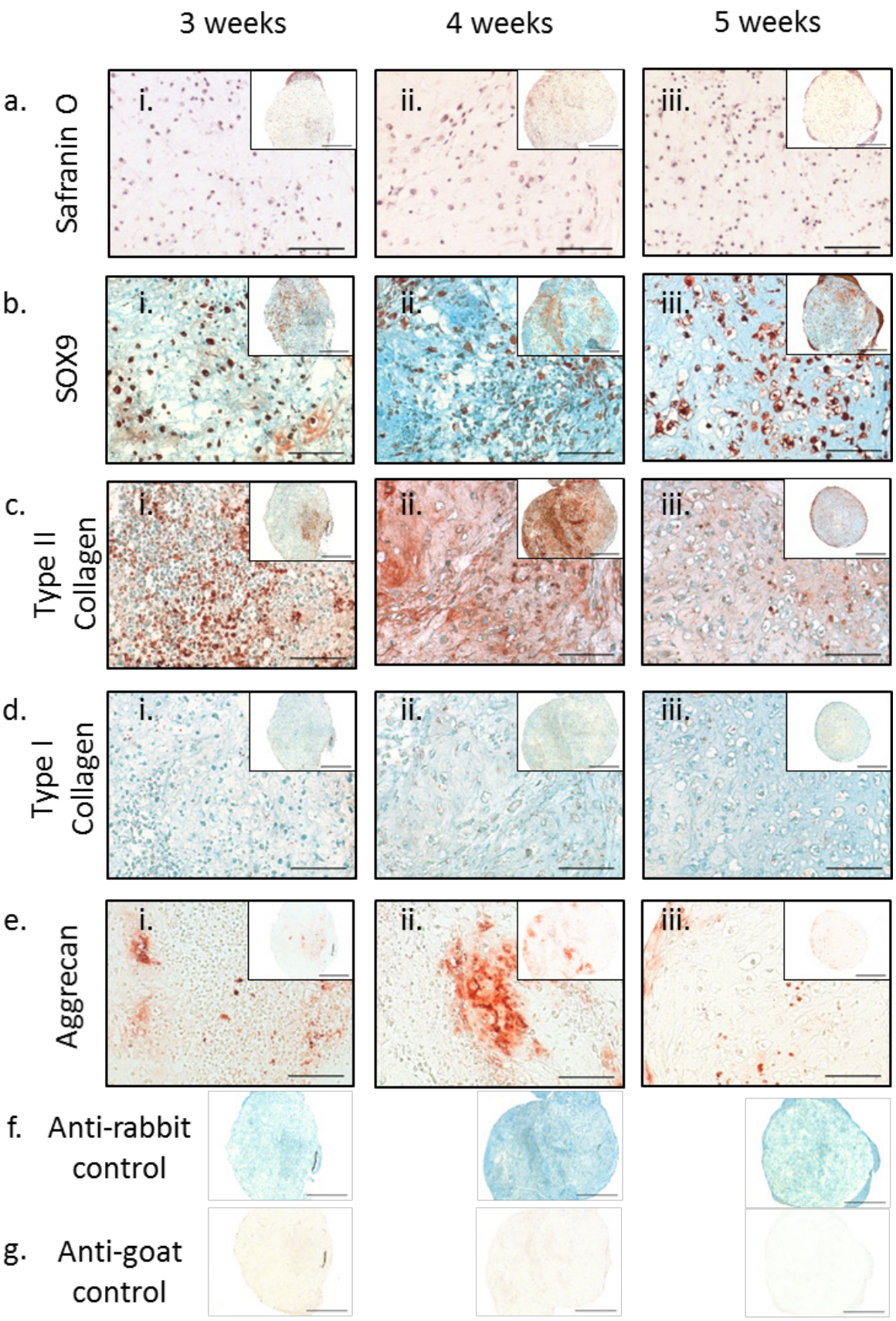
3 weeks
4 weeks
5 weeks
a.
Safranin O
i.
ii.
iii.
b.
SOX9
i.
ii.
iii.
c.
Type II Collagen
i.
ii.
iii.
d.
Type I Collagen
i.
ii.
iii.
e.
Aggrecan
i.
ii.
iii.
f. Anti-rabbit control
g. Anti-goat control

Figure 5.10 **hESC-derived cartilage pellets cultured for 3, 4 or 5 weeks, experiment 2.**

hESC-derived chondrocytes were cultured as pellets for 3, 4 or 5 weeks in chondrogenic medium. Pellets were used for histology. Proteoglycans were detecting using Safranin O staining (a), and expression of SOX9 (b), type II collagen (c), type I collagen (d) and Aggrecan (e) was investigated via immunohistochemistry (IHC). Sections used for SOX9, type II collagen and type I collagen IHC were counterstained with alcian blue. Secondary antibody only negative control (f and g). Anti-rabbit controls correspond to SOX9, type I collagen and type II collagen; anti-goat control corresponds to Aggrecan. High magnification, 500 µm, low magnification, 100 µm.

hESC-derived cartilage pellets generated in experiment 3 had very low proteoglycan content at all time points, as demonstrated by weak staining for Safranin O (Figure 5.11a). Aggrecan staining was undetectable (Figure 5.11e). There was however weak Alcian Blue counter staining which may indicate the presence of some proteoglycans, (Figure 5.11b-d and f).

hESC-derived cartilage pellets exhibited robust nuclear expression of SOX9 (Figure 5.11b) and an absence of the bone specific type I collagen (Figure 5.11d). Weak type II collagen staining was present at all time points. An overall improvement in pellet morphology was observed between weeks 3 and 4 with pellets becoming more uniform and rounder with more defined lacunae (Figure 5.11).

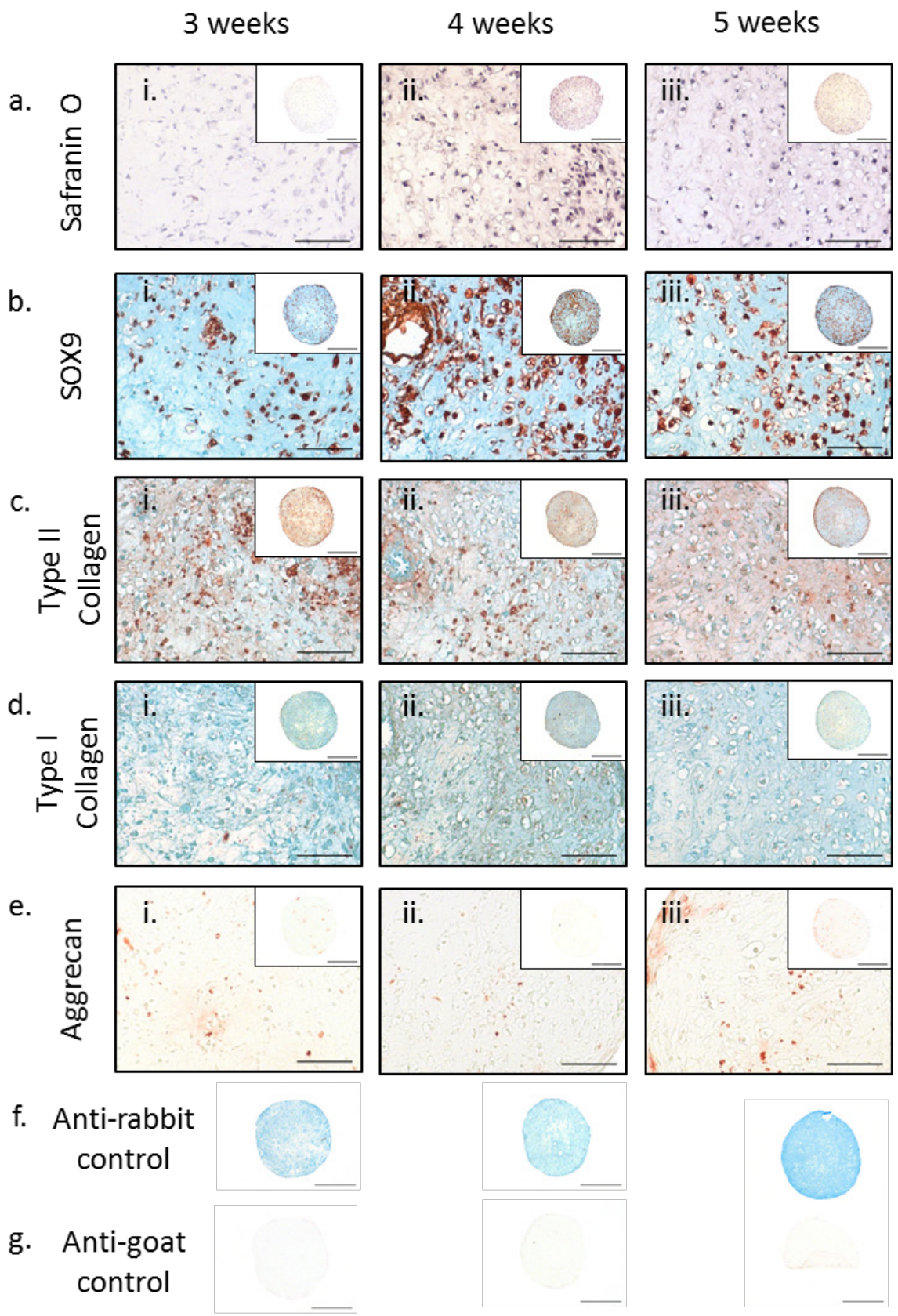
3 weeks
4 weeks
5 weeks
a.
Safranin O
b.
SOX9
c.
Type II Collagen
d.
Type I Collagen
e.
Aggrecan
i.
ii.
iii.
f.
Anti-rabbit control
g.
Anti-goat control

Figure 5.11 **hESC-derived cartilage pellets cultured for 3, 4 or 5 weeks, experiment 3.**

hESC-derived chondrocytes were cultured as pellets for 3, 4 or 5 weeks in chondrogenic medium. Pellets were used for histology. Proteoglycans were detecting using Safranin O staining (a), and expression of SOX9 (b), type II collagen (c), type I collagen (d) and Aggrecan (e) was investigated via immunohistochemistry (IHC). Sections used for SOX9, type II collagen and type I collagen IHC were counterstained with alcian blue. Secondary antibody only negative control (f and g). Anti-rabbit controls correspond to SOX9, Type I collagen and Type II collagen; anti-goat control corresponds to Aggrecan. High magnification, 500 µm, low magnification, 100 µm.

hESC-derived cartilage pellets generated in experiment 4 had low proteoglycan content at all time points, as demonstrated by weak staining for Safranin O (Figure 5.12a). Aggrecan staining was undetectable at 3 and 5 weeks but weak staining appeared at 4 weeks (Figure 5.12e). There was weak Alcian Blue counter staining which may indicate the presence of some proteoglycans, (Figure 5.12b-d and f).

hESC-derived cartilage pellets exhibited robust nuclear expression of SOX9 at all time points (Figure 5.12b) and an absence of the bone specific type I collagen (Figure 5.12d). Type II collagen staining was present at all time points; however, staining was weaker at 3 weeks compared to 4 and 5 weeks. An overall improvement in pellet morphology was observed between weeks 3 and 4 with pellets becoming more uniform and rounder with more defined lacunae (Figure 5.12).

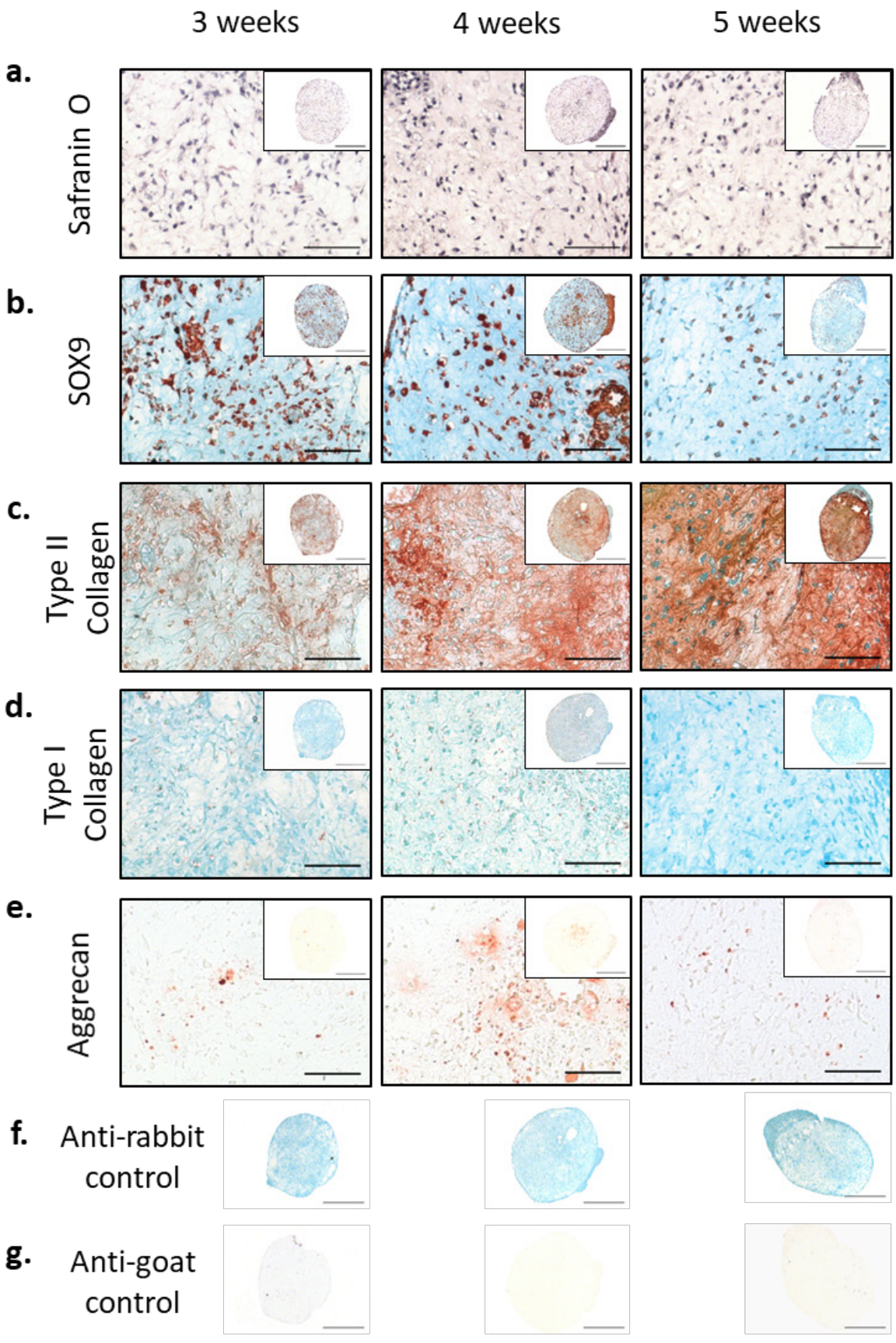
3 weeks
4 weeks
5 weeks
a.
Safranin O
b.
SOX9
c.
Type II Collagen
d.
Type I Collagen
e.
Aggrecan
f.
Anti-rabbit control
g.
Anti-goat control

Figure 5.12 **hESC-derived cartilage pellets cultured for 3, 4 or 5 weeks, experiment 4.**

hESC-derived chondrocytes were cultured as pellets for 3, 4 or 5 weeks in chondrogenic medium. Pellets were used for histology. Proteoglycans were detecting using Safranin O staining (a), and expression of SOX9 (b), type II collagen (c), type I collagen (d) and Aggrecan (e) was investigated via immunohistochemistry (IHC). Sections used for SOX9, type II collagen and type I collagen IHC were counterstained with alcian blue. Secondary antibody only negative control (f and g). Anti-rabbit controls correspond to SOX9, type I collagen and type II collagen; anti-goat control corresponds to Aggrecan. High magnification, 500 µm, low magnification, 100 µm.

5.6.2.3 Optimum culture period for hESC-derived chondrocytes is 4 weeks

To help determine the optimum culture period for hESC-derived cartilage pellets from those tested (3, 4 or 5 weeks), image analysis of type II collagen immunostaining was performed. Staining density was normalised to controls (Figure 5.13) and compared to HAC pellets cultured for 3 weeks as a positive control (Figure 5.13a). Type II collagen staining density in HAC pellets and hESC-derived cartilage pellets cultured for the same length of time (3 weeks) was not found to differ significantly. However, when hESC-derived cartilage pellets were cultured for 4 or 5 weeks type II collagen density was found to be significantly greater than that observed in HAC pellets. No significant difference was observed between hESC-derived chondrocytes cultured for 3, 4 or 5 weeks (Figure 5.14).

Having found a significant increase in type II collagen density between HAC pellets and hESC-derived cartilage pellets cultured for 4 weeks, but no significant difference between hESC-derived chondrocytes cultured for 4 or 5 weeks, 4 weeks was designated as the optimum culture period to be used for further experiments.

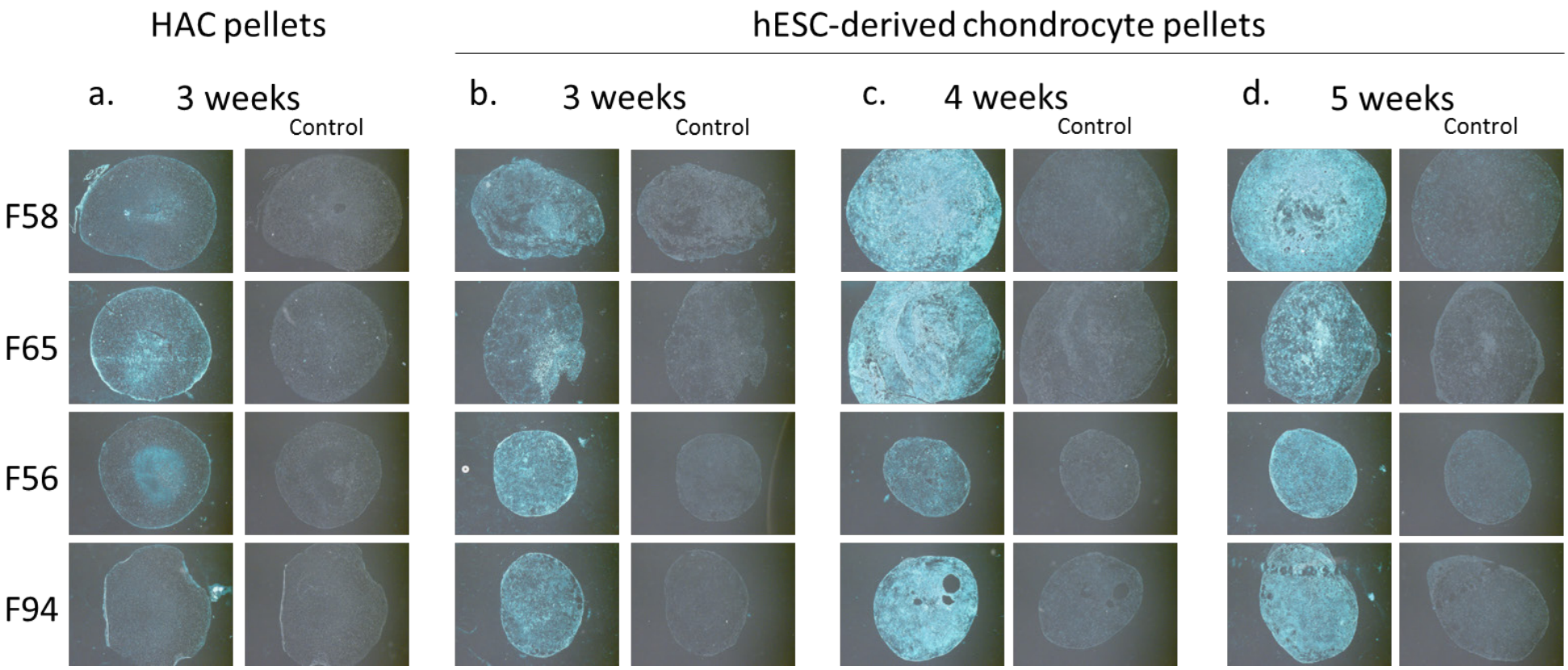

Figure 5.13 **Type II collagen staining of HAC pellets and hESC-derived cartilage pellets used for image analysis.**

HAC's were isolated from donors F58, F65, F56 and F94 and cultured as pellets for 3 weeks (a). hESC-derived chondrocytes were cultured as pellets for 3 (b), 4 (c) or 5 weeks (d). Pellets were used for histology and immunostained for type II collagen. Images were inverted for use in density analysis. On the left shows positively stained sections, and the right shows secondary antibody only negative controls.

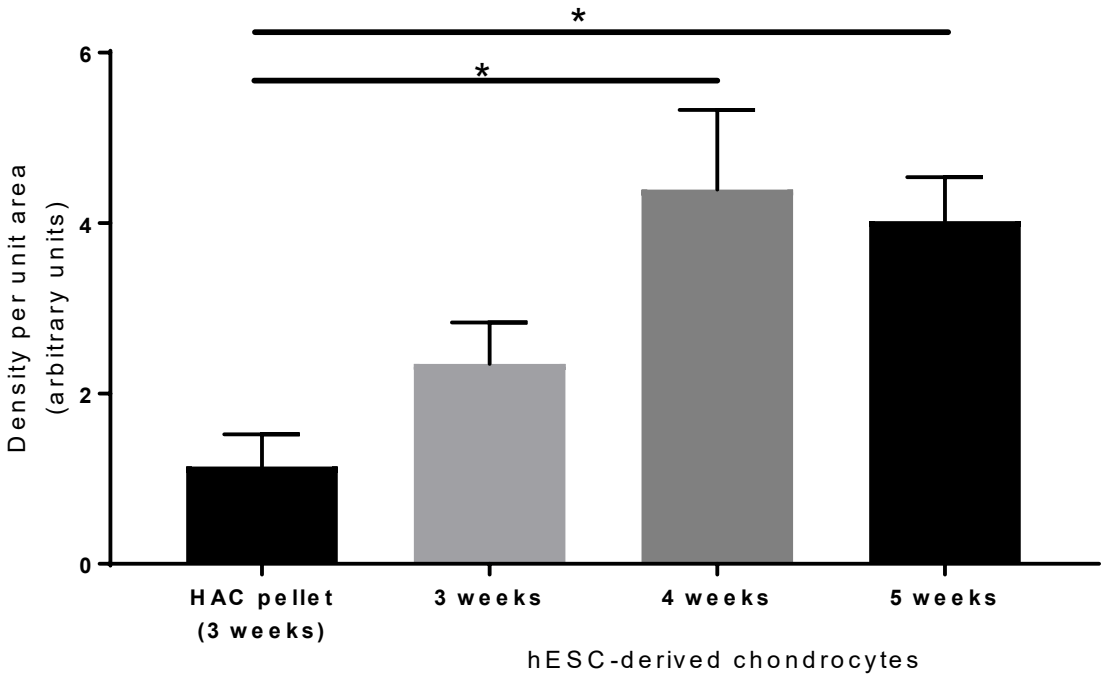

Figure 5.14 **Image analysis of type II collagen staining performed on HAC and hESC-derived cartilage pellets.**

*HAC's were cultured as pellets for 3 weeks, hESC-derived chondrocytes were cultured as pellets for 3, 4 or 5 weeks. Pellets were used for histology and immunostained for type II collagen. Staining density was measured using the FIJI/ImageJ software. Data in represents density per unit area of stained sample minus density per unit area of control. Bars represent mean ± SD, n=4 for all groups. *p<0.05.*

5.6.2.4 hESC-derived cartilage pellet gene expression analysis

It was necessary to assess the expression of the key pluripotency transcription factors OCT4, SOX2 and NANOG in hESC-derived cartilage pellets as expression of these proteins is undesirable in differentiated tissues. Without a suitable positive control for histological analysis I opted to assess mRNA expression in hESC-derived cartilage pellets (4 weeks culture) and compare expression to HUES7 hESCs (Stage 0 samples).

A significant decrease in mRNA expression was detected in the expression of all three pluripotency markers (Figure 5.15). *OCT4* expression decreased ~100 fold ($p<0.01$), *SOX2* ~8 fold ($p<0.01$) and *NANOG* ~80-fold ($p<0.01$).

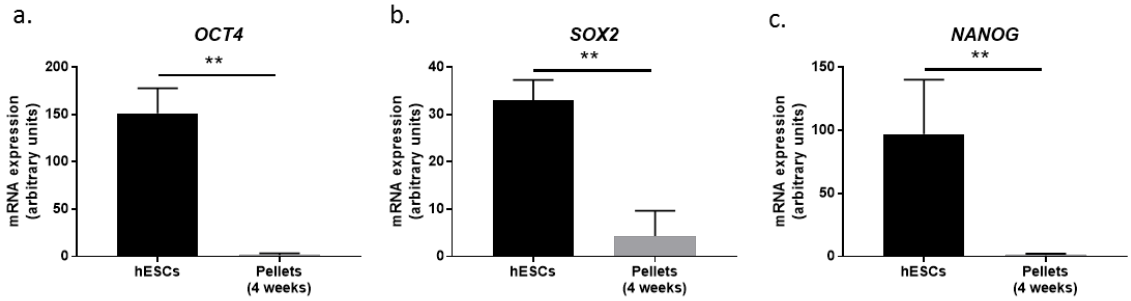

Figure 5.15 **Gene expression analysis of pluripotency genes in hESCs and hESC-derived cartilage pellets.**

*HUES7 hESCs were cultured at 5% O_2 for at least 3 passages and RNA was collected. hESC-derived chondrocytes were cultured as pellets for 4 weeks and RNA was collected. RT-qPCR was performed on samples from hESCs and pellets, and the mRNA expression of the pluripotency genes OCT4 (a), SOX2 (b) and NANOG (c) was examined. Gene expression was normalised to UBC. Values represent mean ± SD. *$p<0.01$ according to unpaired t-test. n=5 for each group.*

Whilst there was a significant loss of pluripotency marker expression in hESC-derived cartilage pellets, transcripts were still detectable, albeit at very low levels (CT values ~30). Therefore, it was investigated whether mRNA for *OCT4*, *SOX2* and *NANOG* was detectable in HAC pellets. These genes were indeed expressed in HAC pellets (Figure 5.16a-c). There was no significant difference in the expression of *OCT4* or *NANOG* mRNA between HAC and hESC-derived cartilage pellets (Figure 5.16a and c). *SOX2* expression was significantly greater in hESC-derived cartilage pellets compared to HAC pellets ($p<0.05$) (Figure 5.16b).

Expression of the chondrogenic genes *SOX9* and *COL2A1*, and the expression of the chondrocyte hypertrophy gene *COL10A1* was also examined. No significant difference was found in the expression of *SOX9*, *COL2A1* or *COL10A1* between HAC and hESC-derived cartilage pellets (Figure 5.16f).

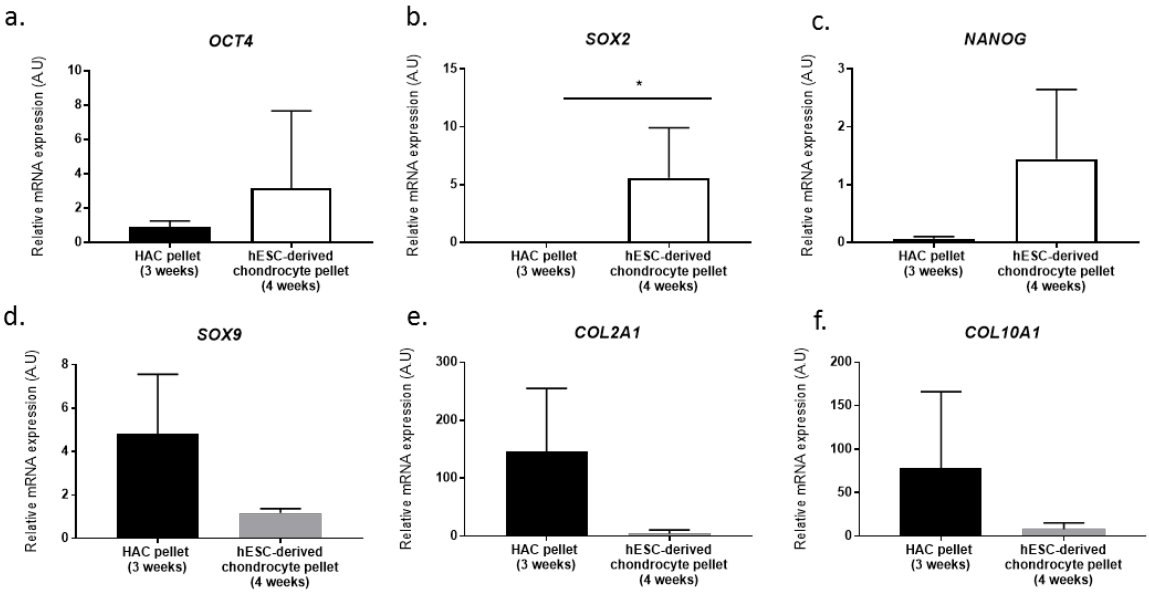

Figure 5.16 **Gene expression analysis of pluripotency and chondrogenic genes expressed in HAC and hESC-derived cartilage pellets.**

*HAC's and hESC-derived cartilage pellets were cultured for 3 or 4 weeks respectively. RNA was isolated from pellets and RT-qPCR was performed to compare mRNA expression of OCT4 (a), SOX2 (b), NANOG (c), SOX9 (d), COL2A1 (e) and COL10A1 (f). Gene expression was normalised to UBC. Values represent mean ± SD. *p<0.05 according to unpaired t-test. HAC pellets n=4, hESC-derived cartilage pellets n=3. Bars represent mean ± SD.*

5.6.2.5 Pellets generated from HACs and hESC-derived chondrocytes are not undergoing hypertrophy.

Hypertrophy is undesirable in tissue engineered cartilage. Alkaline Phosphatase (ALP) activity is a marker for hypertrophy and was therefore used to establish whether hypertrophy occurred in pellet cultures. hESC-derived cartilage pellets (4 weeks culture) and HAC pellets (3 weeks culture) were fixed in EtOH and ALP staining was performed. ALP activity was not detected in pellets generated from hESC-derived chondrocytes (Figure 5.17a) or HACs (Figure 5.17b).

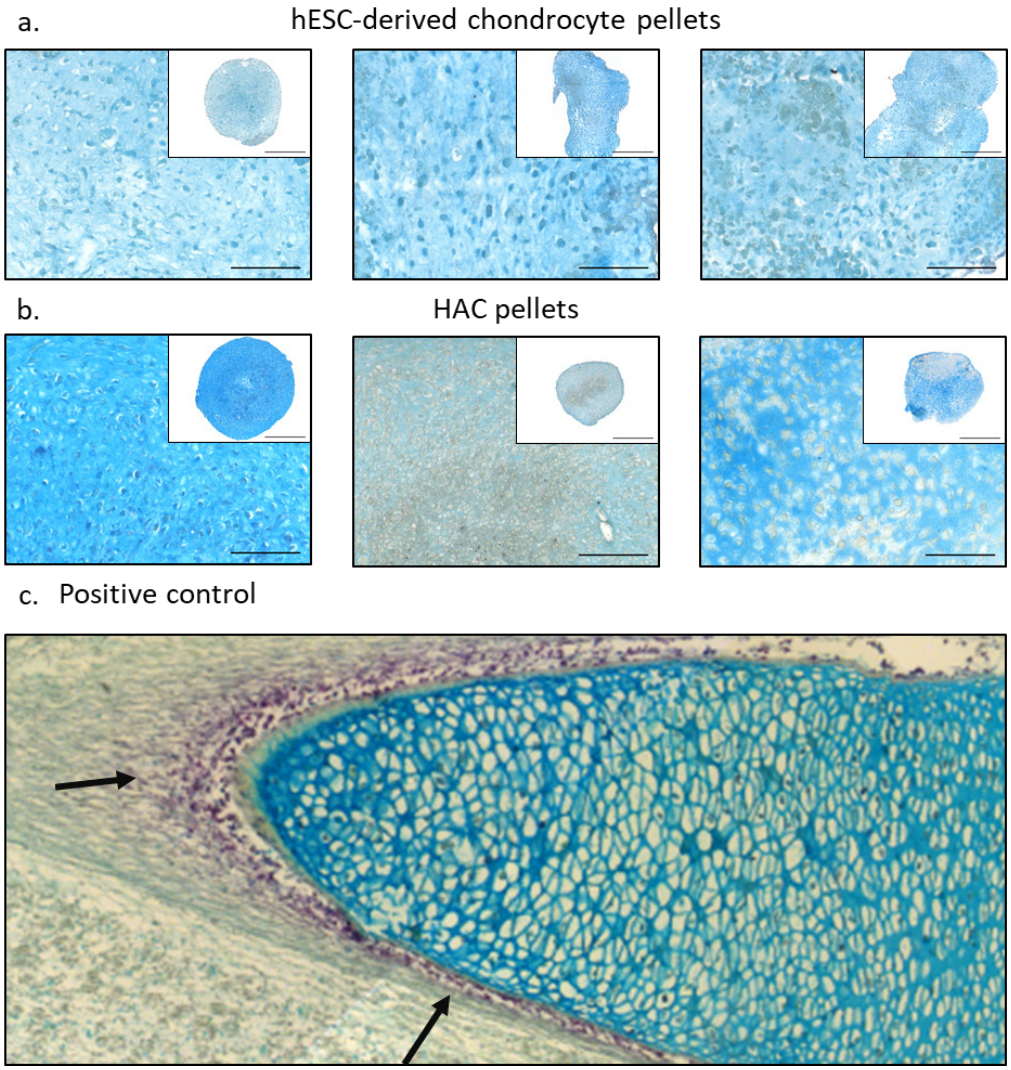

Figure 5.17 **ALP staining of hESC-derived chondrocyte and HAC pellets.**

hESC-derived cartilage pellets were cultured for 4 weeks, and HAC pellets were cultured for 3 weeks in chondrogenic medium and fixed in EtOH. Alkaline Phosphatase (ALP) staining was performed on n=3 pellets hESC-derived cartilage pellets (a), n=3 HAC pellets (b) and a foetal femur was used as a positive control (c). Arrows indicate band of positive ALP staining in the perichondrium. Low magnification scale bar 500 µm, high magnification scale bar 100 µm.

5.6.2.6 Extended culture enhances cartilage generation in hESC-derived cartilage pellets

As previously mentioned, standard culture time for HAC pellets is 3 weeks. hESC-derived chondrocytes were therefore cultured for 3-5 weeks. However, as this culture period did not result in the accumulation of proteoglycans I decided to investigate how long it would take to achieve proteoglycan accumulation in hESC-derived cartilage pellets. Pellets were cultured for 13, 16 and 19 weeks and assessed cartilage formation histologically.

13 weeks of culture generated a hESC-derived cartilage pellet with a longitudinal diameter of 4mm and a whitish appearance (Figure 5.18a). Proteoglycan expression was detectable in a discrete region of the pellet (Figure 5.18b) which is indicative of the cartilage tissue becoming more hyaline-like.

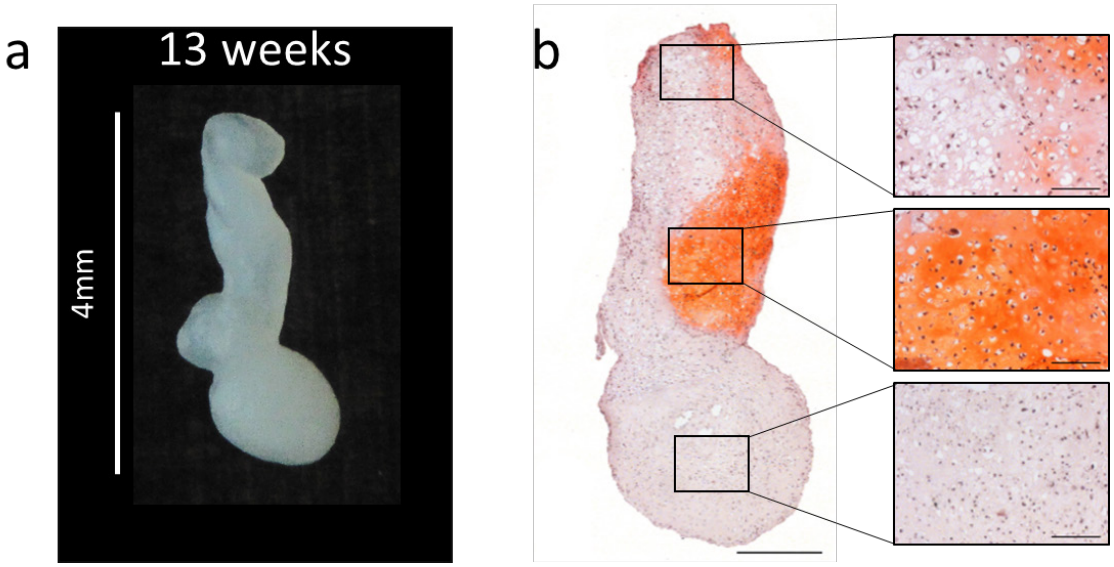

Figure 5.18 **Limited expression of proteoglycans in a hESC-derived** cartilage **pellet cultured for 13 weeks.**

hESC-derived chondrocytes were cultured as a pellet for 13 weeks. The pellet measured 4mm in length (a). Proteoglycans were detected via Safranin O staining (b). Low magnification 500 µm, high magnification 100 µm.

After 13 weeks culture the hESC-derived cartilage pellet exhibited robust *SOX9* expression (Figure 5.19a), mainly localised to areas with the weakest proteoglycan expression. Type II collagen staining was detected in the pellet matrix and was also most intense in regions lacking proteoglycans (Figure 5.19b). Type I collagen was also detected in regions lacking proteoglycans but was not present in the proteoglycan rich region of the pellet (Figure 5.19c). In line with Safranin O staining, Aggrecan expression was detected in a discrete region of the pellet where the tissue had a more hyaline-like morphology (Figure 5.19d).

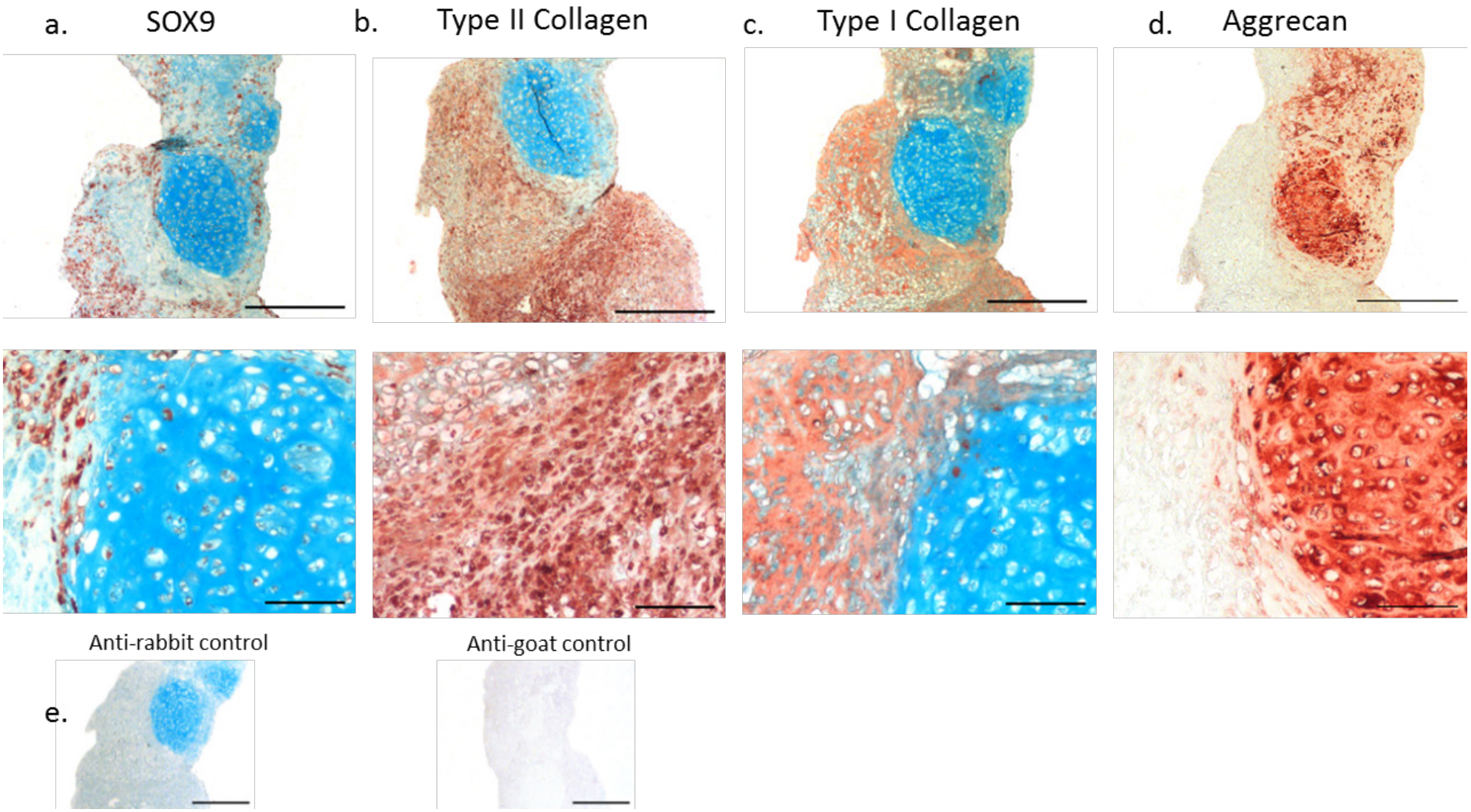
a. SOX9
b. Type II Collagen
c. Type I Collagen
d. Aggrecan
Anti-rabbit control
Anti-goat control
e.

Figure 5.19 **hESC-derived cartilage pellet cultured for 13 weeks expresses chondrogenic markers.**

hESC-derived chondrocytes were cultured as a pellet for 13 weeks. Chondrogenic markers were detected via immunostaining: SOX9 (a), type II collagen (b), type I collagen (c) and Aggrecan (d). Secondary antibody only negative controls are shown e. Anti-rabbit control corresponds to SOX9, type II collagen and type I collagen, anti-goat controls corresponds to Aggrecan. Low magnification 500 µm, high magnification 100 µm.

The expression of the matrix remodelling enzyme matrix metalloproteinase-13 (MMP-13), the proliferation marker Ki67 and the gap junction protein Connexin-43 was also investigated.

MMP-13 expression was detected at 13 weeks and was localised to the region lacking proteoglycans (Figure 5.20a). A similar pattern of staining was observed for both Ki67 and Connexin-43 (Figure 5.20b and c respectively), however there were some Ki67 and Connexin-43 positive cells in regions with high proteoglycan content.

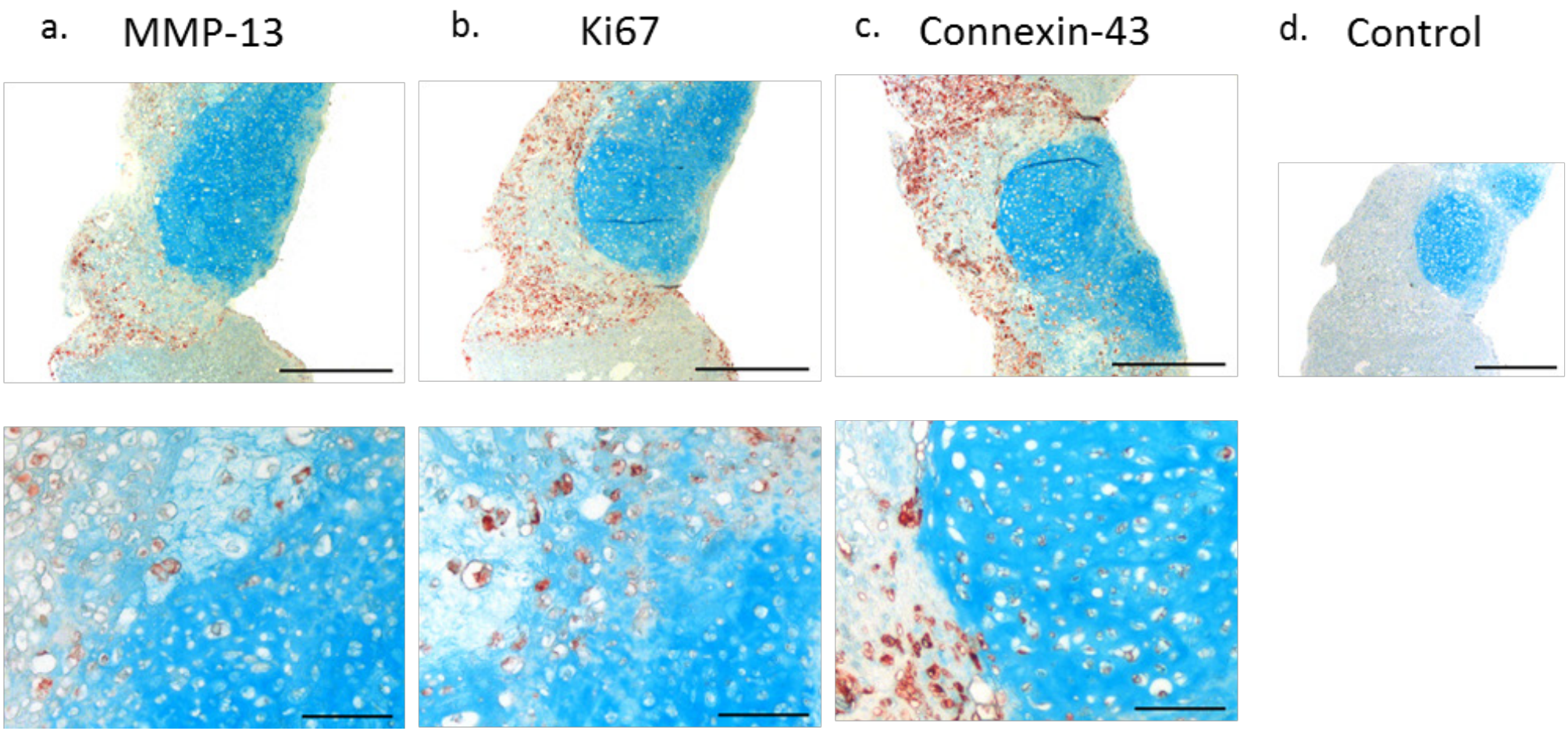
a. MMP-13
b. Ki67
c. Connexin-43
d. Control

Figure 5.20 **Remodelling of hESC-derived cartilage pellets cultured for 13 weeks.**

hESC-derived chondrocytes were cultured as a pellet for 13 weeks. Markers or matrix remodelling and proliferation were detected via immunostaining: MMP-13 (a), Ki67 (b) and Connexin-43 (c). Secondary antibody only negative controls are shown d. Low magnification 500 µm, high magnification 100 µm.

16 weeks of culture generated a hESC-derived cartilage pellet with a longitudinal diameter of 2.5mm and a whitish appearance (Figure 5.21a). Proteoglycan expression was detectable in a discrete region of the pellet (Figure 5.21b) which is indicative of the cartilage tissue becoming more hyaline-like.

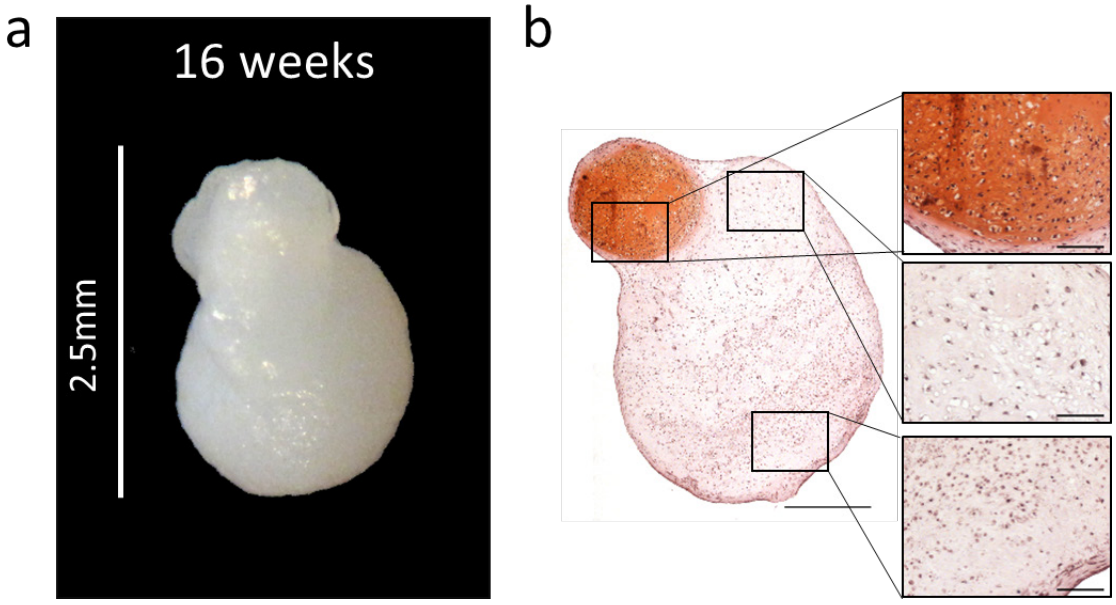

Figure 5.21 **Limited expression of proteoglycans in a hESC-derived cartilage pellet cultured for 16 weeks.**

hESC-derived chondrocytes were cultured as a pellet for 16 weeks. The pellet measured 2.5mm in length (a). Proteoglycans were detected via Safranin O staining (b). Low magnification 500 µm, high magnification 100 µm.

As observed with the 13 weeks pellet, after 16 weeks culture the hESC-derived cartilage pellet also exhibited robust *SOX9* expression (Figure 5.22a), mainly localised to areas with the weakest proteoglycan expression. Type II collagen staining was detected in the pellet matrix and was also most intense in regions lacking proteoglycans (Figure 5.22b). Type I collagen was also detected in regions lacking proteoglycans but was not present in the proteoglycan rich region of the pellet (Figure 5.22c). In line with Safranin O staining, Aggrecan expression was detected in a discrete region of the pellet where the tissue had a more hyaline-like morphology (Figure 5.22d).

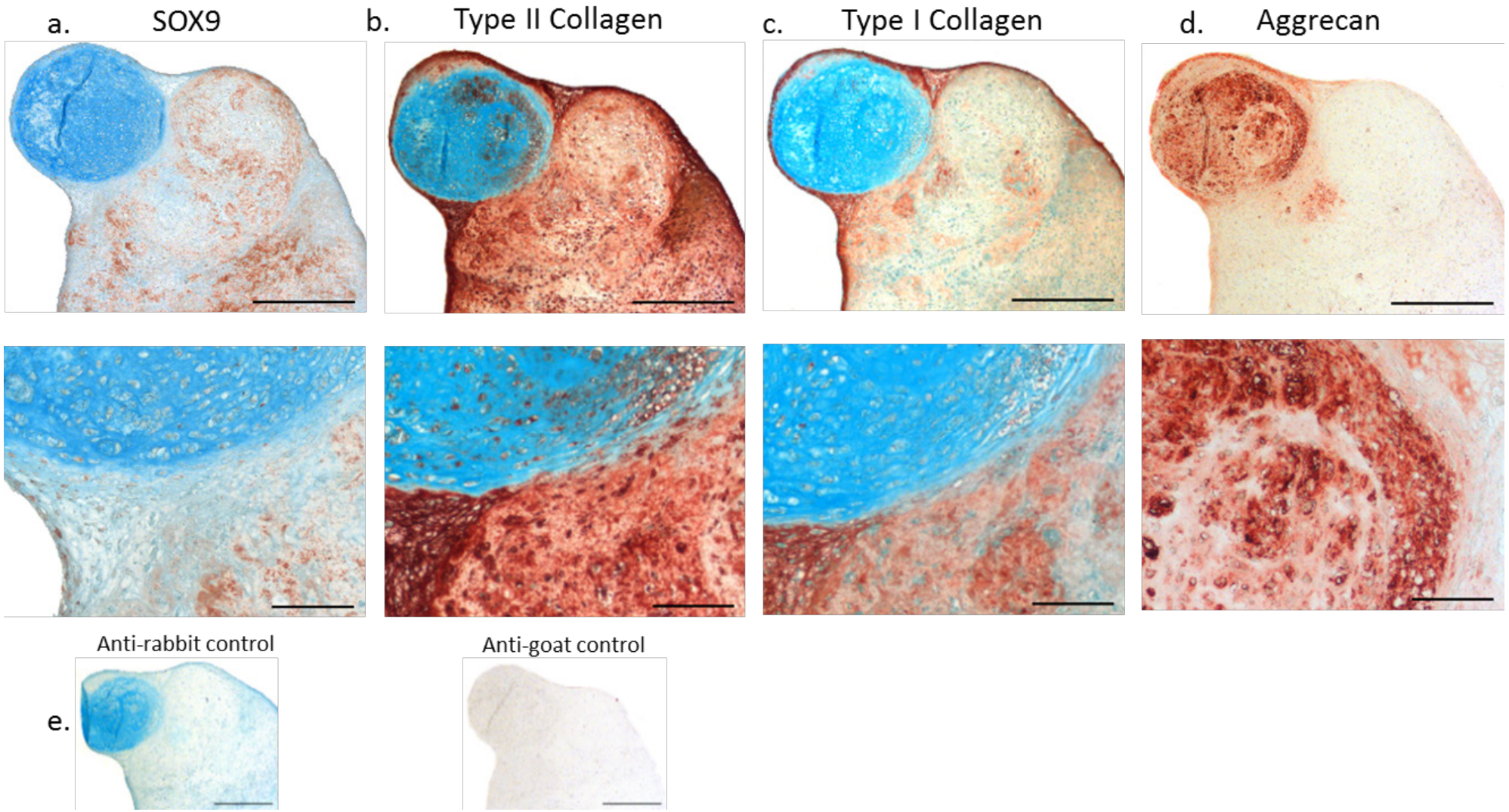
a.
SOX9
b.
Type II Collagen
c.
Type I Collagen
d.
Aggrecan
Anti-rabbit control
Anti-goat control
e.

Figure 5.22 **hESC-derived cartilage pellet cultured for 16 weeks expresses chondrogenic markers.**

hESC-derived chondrocytes were cultured as a pellet for 16 weeks. Chondrogenic markers were detected via immunostaining: SOX9 (a), type II collagen (b), type I collagen (c) and Aggrecan (d). Secondary antibody only negative controls are shown e. Anti-rabbit control corresponds to SOX9, type II collagen and type I collagen, anti-goat control corresponds to Aggrecan. Low magnification 500 µm, high magnification 100 µm.

MMP-13 expression was still detectable at 16 weeks and was again mainly localised to the region lacking proteoglycans, however some positive staining was observed in the hyaline region, though this was proportionally much lower (Figure 5.23a). A similar pattern of staining was observed for both Ki67 and Connexin-43 (Figure 5.23b and c respectively); positively stained cells were concentrated in the immature tissue however there were some Ki67 and Connexin-43 positive cells in regions with high proteoglycan content also.

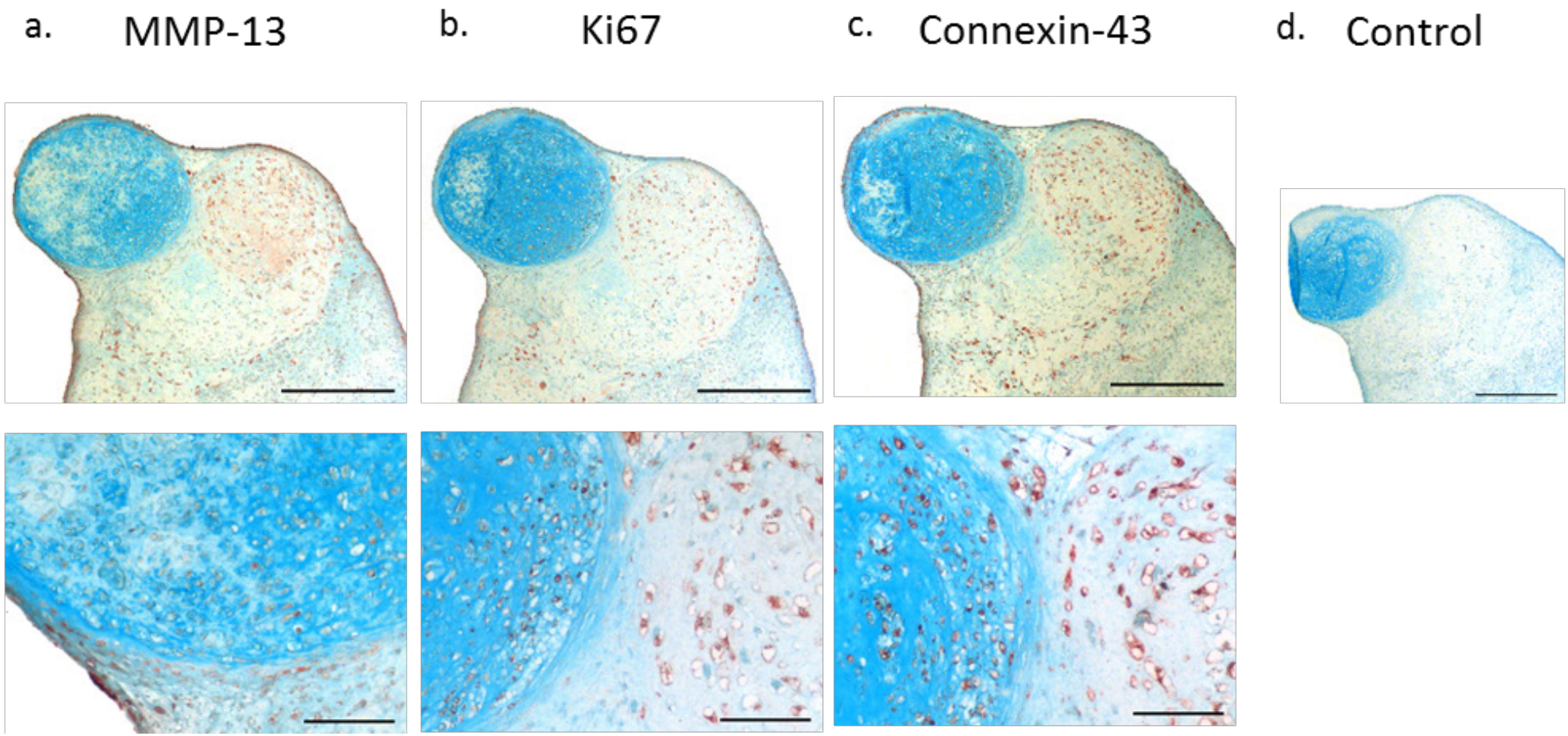
a.
MMP-13
b.
Ki67
c.
Connexin-43
d.
Control

Figure 5.23 **Remodelling of hESC-derived cartilage pellets cultured for 16 weeks.**

hESC-derived chondrocytes were cultured as a pellet for 16 weeks. Markers or matrix remodelling and proliferation were detected via immunostaining: MMP-13 (a), Ki67 (b) and Connexin-43 (c). Secondary antibody only negative controls are shown d. Low magnification 500µm, high magnification 100 µm.

19 weeks of culture generated a hyaline-like hESC-derived cartilage pellet with a longitudinal diameter of 3mm and a glossy whitish appearance (Figure 5.24a). Robust proteoglycan expression was detected throughout the pellet with the most intense staining located in central regions (Figure 5.24b).

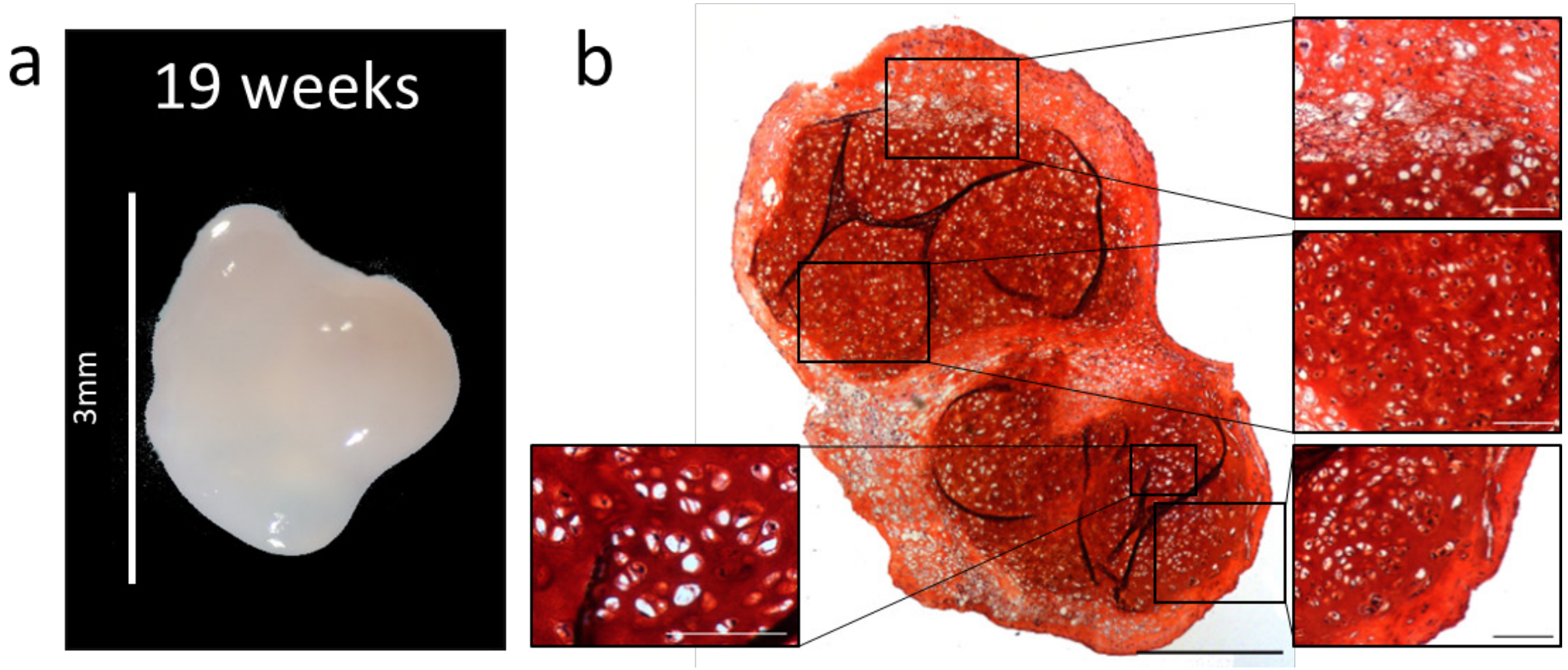

Figure 5.24 **Robust expression of proteoglycans in a hESC-derived cartilage pellet cultured for 16 weeks**

hESC-derived chondrocytes were cultured as a pellet for 16 weeks. The pellet measured 2.5mm in length (a). Proteoglycans were detected via Safranin O staining (b). Low magnification 500µm, high magnification 100µm.

Following 19 weeks culture the hESC-derived cartilage pellet exhibited only weak *SOX9* expression which was localised to peripheral regions where the tissue appeared less mature and was not hyaline-like in appearance (Figure 5.25a). Weak type II collagen staining was detected in regions lacking proteoglycans (Figure 5.25b). Type I collagen was also detected in regions lacking proteoglycans but was not present in the hyaline-like region of pellet (Figure 5.25c). In line with Safranin O staining, robust Aggrecan expression was detected in the majority of the pellet, particularly where the tissue had hyaline-like morphology (Figure 5.25d).

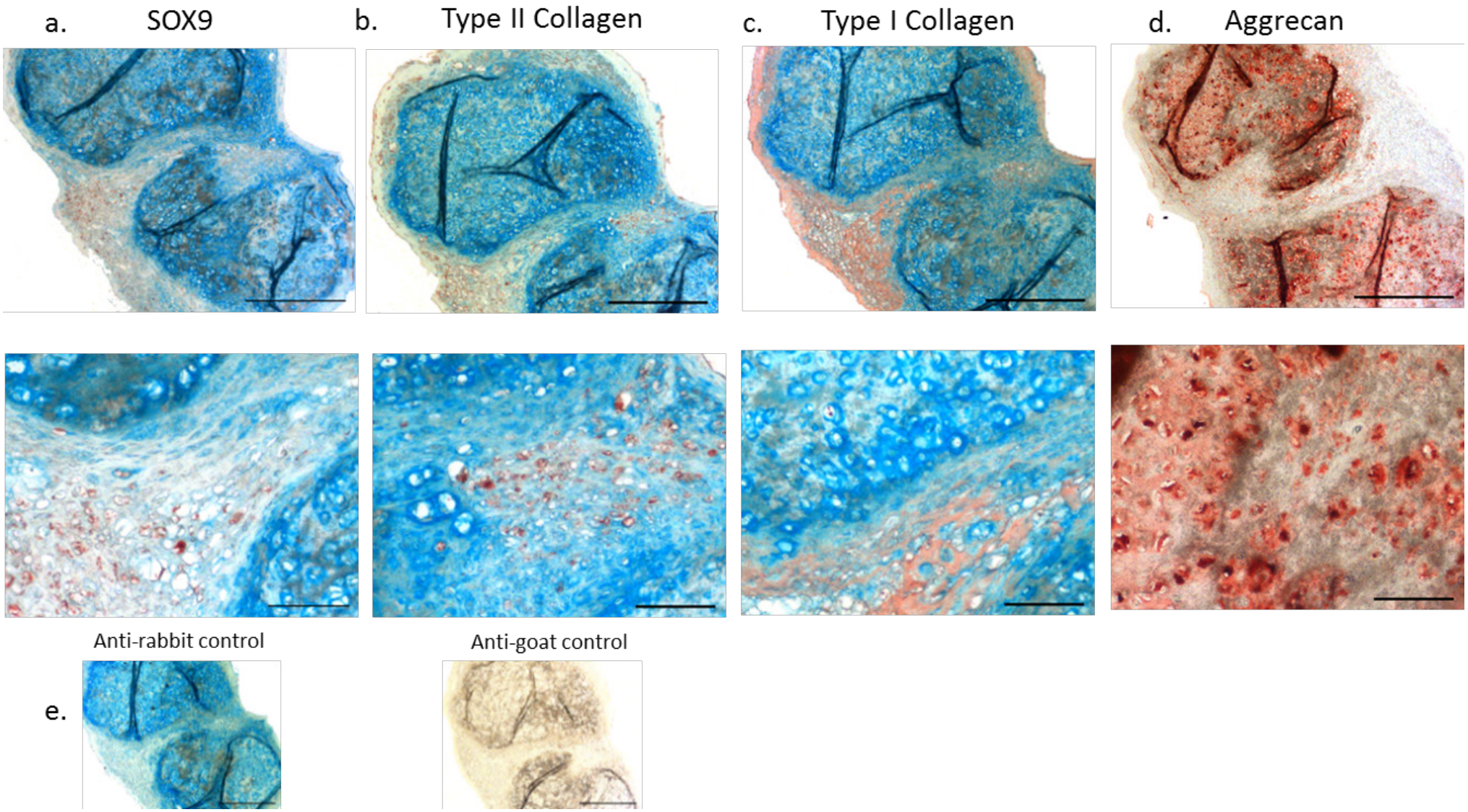
a. SOX9
b. Type II Collagen
c. Type I Collagen
d. Aggrecan
Anti-rabbit control
Anti-goat control
e.

Figure 5.25 **hESC-derived cartilage pellet cultured for 19 weeks expresses chondrogenic markers.**

hESC-derived chondrocytes were cultured as a pellet for 19 weeks. Chondrogenic markers were detected via immunostaining: SOX9 (a), type II collagen (b), type I collagen (c) and Aggrecan (d). Secondary antibody only negative controls are shown e. Anti-rabbit control corresponds to SOX9, type II collagen and type I collagen, anti-goat control corresponds to Aggrecan. Low magnification 500µm, high magnification 100µm.

MMP-13 expression was still detectable at 19 weeks. Positive staining was once again localised to the small peripheral regions lacking proteoglycans and was not detected in the hyaline-like cartilage of the pellet (Figure 5.26a). A similar pattern of staining was observed for both Ki67 and Connexin-43 (Figure 5.26b and c respectively) with positively stained cells concentrated in the immature tissue.

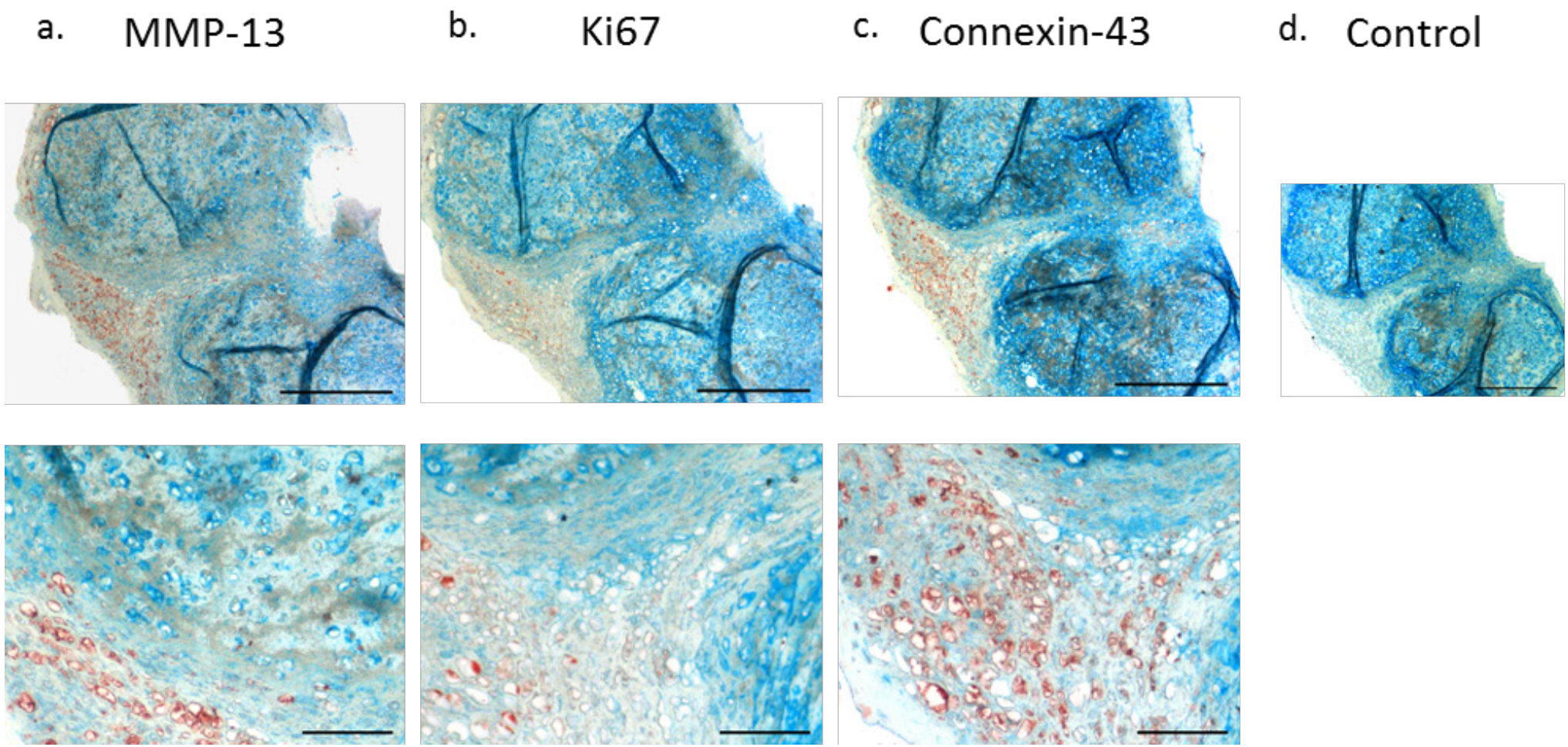
a. MMP-13
b. Ki67
c. Connexin-43
d. Control

Figure 5.26 **Remodelling of hESC-derived cartilage pellets cultured for 19 weeks.**

hESC-derived chondrocytes were cultured as a pellet for 19 weeks. Markers or matrix remodelling and proliferation were detected via immunostaining: MMP-13 (a), Ki67 (b) and Connexin-43 (c). Secondary antibody only negative controls are shown d. Low magnification 500µm, high magnification 100µm.

5.6.2.7 hESC-derived cartilage pellets are mechanically similar to native cartilage

In addition to investigating the expression of chondrogenic markers in hESC-derived cartilage pellets the mechanical characteristics of the cartilage generated was analysed by calculating the Young's Elastic modulus (E) for native cartilage, HAC pellets and hESC-derived cartilage pellets at 4 and 19 weeks of culture. Standard equations were used to determine E for native cartilage (5.4.5.1), however for pellets an equation based on Hertzian theory was used (0). No significant difference was found in E between any groups (Figure 5.27).

Individual values for pellets tested are shown in Table 5.3. An r^2 value was generated during analysis to indicate how well the data fitted the model used for analysis with an r^2 value of 1 representing a 'perfect fit'. For articular cartilage sections the average r^2 value was 0.98, and for pellets was 0.99.

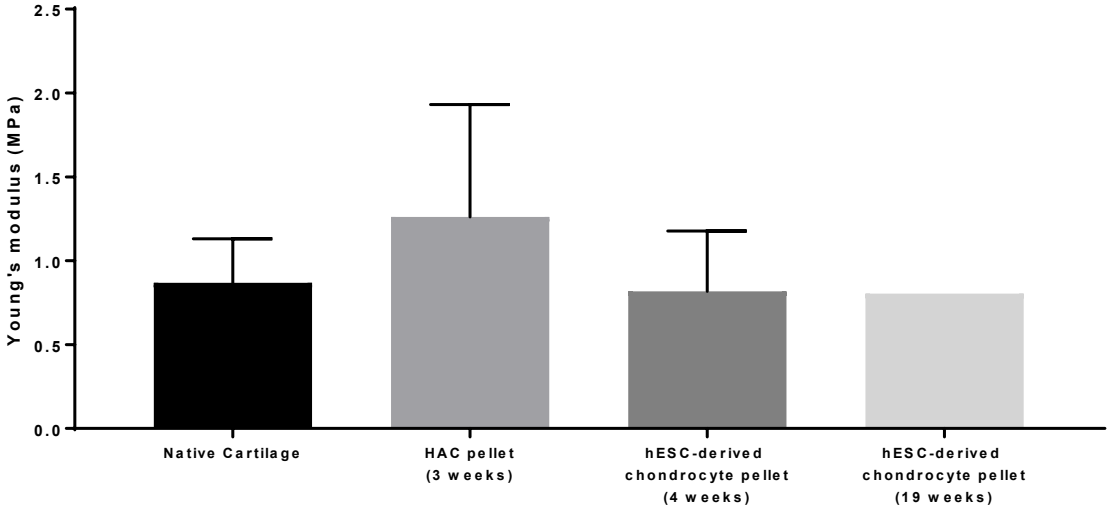

Figure 5.27 **Comparison of Young's elastic modulus between native cartilage and pellet cultures.**

A purpose built mechanical testing rig was used to compress samples between two flat metal plates. The Young's Elastic modulus (E) was assessed for native cartilage (n=9) and compared to that generated by HAC pellets cultured for 3 weeks (n=11) and hESC-derived cartilage pellets following 4 or 19 weeks culture (n=6, n=1). Bars represent mean ± SD.

Table 5.3 **Summary of mechanical testing data from articular cartilage and pellets.**

F refers to female and M to male. CI refers to 95% confidence intervals) for E value).

r^2 refers to how well the value for E fits the model tested by the Mathematica code.

	Sample ID	Young's Modulus (E)	Lower CI	Upper CI	r^2
Articular cartilage	F62 cartilage-1	0.990225	0.969113	1.01134	0.986047
	F62 cartilage-2	1.06197	1.01376	1.11019	0.967506
	F62 cartilage-3	1.29941	1.25153	1.3473	0.975653
	F78 cartilage-1	0.695964	0.677234	0.714695	0.972923
	F78 cartilage-2	0.625025	0.610794	0.639256	0.979822
	F78 cartilage-3	0.857526	0.847391	0.867661	0.994195
	F96 cartilage-1	1.11758	1.10631	1.12884	0.99682
	F96 cartilage-2	0.613276	0.601517	0.625035	0.990936
	F96 cartilage-3	0.552279	0.544662	0.559896	0.992745
Average		**0.868139444**			**0.984072**
HAC Pellets	F62-1	1.2311	1.21777	1.24443	0.990997
(3 Weeks)	F62-2	1.66094	1.64725	1.67463	0.995642
	F68	1.47395	1.43104	1.51687	0.96126
	F78-1	2.18614	2.13636	2.23591	0.974022
	F78-1	1.98356	1.96318	2.00393	0.994466
	F78-3	2.10364	2.07457	2.1327	0.99052
	M64-1	0.509725	0.505186	0.514264	0.992064
	M64-2	1.12423	1.11602	1.13244	0.996713
	M64-3	0.643317	0.632513	0.654121	0.984988
	M84-1	0.545417	0.538197	0.552637	0.987851
	M84-2	0.410814	0.404368	0.41726	0.983014
Average		**1.261166636**			**0.986503**
hESC-derived cartilage pellets	Pellet-1	0.665212	0.661642	0.668782	0.997028
(4 weeks)	Pellet-2	0.638217	0.635364	0.641069	0.997937
	Pellet-3	0.489947	0.482387	0.497508	0.98129
	Pellet-4	0.588134	0.58083	0.595438	0.989135
	Pellet-5	1.12423	1.11602	1.13244	0.996713
	Pellet-6	1.3978	1.38588	1.40972	0.995521
Average		**0.817256667**			**0.992937**
(19 weeks)	DDP-71	**0.803726**	0.796845	0.810607	**0.993035**

5.7 Discussion

Tissue engineering provides a platform that allows the generation of hyaline cartilage *in vitro* prior to implantation and enables a greater level of control over the generation of repair tissue compared to current restorative treatments for early stage OA such as mosaicplasty and ACI. Tissue engineering enables the 'like-for-like' replacement of damaged tissue that can be quality assessed prior to implantation. In 2.6 a robust population of hESC-derived chondrocytes was generated that has the potential to enhance current tissue engineering strategies.

The work described in this chapter includes two novel techniques developed as part of this project to help evaluate the quality of the tissue generated: histological image analysis using integrated density measurements, and mechanical testing. Image analysis in the form of histomorphometry is regularly used in the literature, but typically involves investigators visually assessing and point scoring samples. The technique used here minimised investigator bias by using the ImageJ/FIJI software to apply density measurements to the samples. This method allowed a widely used qualitative technique to provide a semi-quantitative output that aided tissue assessment. Safranin O is an ideal stain for such purposes as it is known to bind stoichiometrically to proteoglycans (Kiviranta et al., 1985), thus providing accurate quantitation of staining density. With regards to mechanical testing, it is crucial that the mechanical properties of engineered cartilage are assessed prior to implantation as the neocartilage would be subject to many physiological forces in vivo. The method of analysis used here was specifically designed for the mechanical testing of cartilage pellets and importantly accounts for continuous changes in contact area during the compression test by using Hertzian theory to provide an accurate measurement for E. The data generated was found to fit the model well as the average r^2 value for E was 0.99 (where 1 is equal to a perfect fit).

For this study a robust model for *in vitro* cartilage generation was established in the form of HAC pellet culture. 3D pellet culture is the current 'gold standard' for cartilage tissue engineering and has frequently been used to demonstrate the *in vitro* cartilage forming potential of chondrogenic cells (Li et al., 2015; Tare et al., 2005). Pellet culture is advantageous as it relies on the chondrocytes ability to generate ECM rather than incorporating scaffold materials, and it is relatively simple in comparison the bioreactor culture discussed in Chapter 4. Using pellet culture, it was demonstrated that HACs deposit a type II collagen rich matrix, with extensive proteoglycan deposition and SOX9 positive cells. The presence of proteoglycans in the cartilage is of particular importance as proteoglycans such as Aggrecan are able to trap water within the cartilage matrix, thus contributing to the compressibility of articular cartilage. Of the 8 patient donors used for this study, 7 were female and 1 male. It is therefore not possible to discern whether the patient's sex

influences cartilage forming potential *in vitro*. Differences in pellet morphology were observed, with more abundant type II collagen and proteoglycan deposition in some pellets relative to others. However this did not appear to be age-related. This highlights the donor-donor variability that is an inherent issue when using primary cells.

Based on the time frame known to generate hyaline-like HAC pellets, HACs and hESC-derived chondrocytes were cultured for 3, 4 or 5 weeks. Image analysis of HAC pellets identified 3 weeks as the optimum time for HAC pellet culture, which is in agreement with the literature (Li et al., 2015; Tare et al., 2005). However, the cartilage formed by hESC-derived chondrocytes was histologically different in comparison to HAC pellets. hESC-derived cartilage pellets did not accumulate proteoglycans, even after 5 weeks culture. Robust expression of the chondrogenic markers SOX9 and type II collagen was observed at all time points, and whilst there was no significant difference in type II collagen staining density at 3 weeks between HAC and hESC-derived cartilage pellets, following extended culture of hESC-derived cartilage pellets (4 and 5 weeks) type II collagen staining density was significantly more in hESC-derived cartilage pellets compared to the HAC pellet positive control. Interestingly, whilst these pellets were lacking proteoglycans they had an organised structure that was similar to HAC pellets with well-defined lacunae with resident chondrocytes by 4 weeks. It is unclear why hESC-derived chondrocytes do not respond to pellet culture in the same way as HACs; however, it is likely that due to the origin of hESC-derived chondrocytes they are in a more naïve chondrogenic state in comparison to HACs which, based on the deposition of proteoglycans, appear to have a relatively more mature phenotype. Native cartilage has a proteoglycan rich matrix, as well as type II collagen; the absence of proteoglycans in hESC-derived chondrocytes, despite the abundance of type II collagen, suggests that proteoglycans are a marker for mature hyaline cartilage.

For the purposes of clinical translation it is crucially important that a loss of pluripotency is achieved in tissues of hESC origin, as errant expression of pluripotency markers poses a risk of tumour formation. It is encouraging that the mRNA of the pluripotency markers *OCT4*, *SOX2* and *NANOG* was significantly decreased in hESC-derived cartilage compared to hESCs. Whilst there were detectable mRNA transcripts by RT-qPCR, the CT values for *OCT4*, *SOX2* and *NANOG* were relatively high (~30, ~30 and ~31 respectively), suggesting that very few transcripts were present prior to amplification. Unfortunately, due to a lack of positive control samples for OCT4, SOX2 and NANOG for immunohistochemistry it was not possible to examine the protein expression of these markers in hESC-derived cartilage pellets. However, in 2.6 a clear loss of OCT4, and significant decreases in SOX2 and NANOG protein was observed in hESC-derived chondrocytes.

Avoidance of chondrocyte hypertrophy is essential for cartilage tissue engineering. When chondrocytes become hypertrophic the process of endochondral ossification occurs and the cartilage template is eventually replaced by bone. It was therefore essential to investigate the expression of hypertrophic markers in the tissue engineered cartilage. Type X collagen is a marker of chondrocyte hypertrophy. Unfortunately, I was unable to obtain a suitable type X collagen antibody that did not produce non-specific staining in positive controls. Alkaline phosphatase (ALP) activity was therefore investigated as ALP is also a marker for hypertrophy. ALP was not detectable by histological staining of HAC or hESC-derived cartilage pellets. This suggests that hESC-derived chondrocytes generated via the DDP are not undergoing hypertrophy.

To induce proteoglycan expression in hESC-derived cartilage pellets, culture was extended to 13-, 16- or 19-weeks. As a result, discrete regions of proteoglycan accumulation were observed by 13- and 16-weeks culture that extended to a more homogenous distribution of proteoglycans and more hyaline-like pellet morphology by 19-weeks suggesting maturation of the neocartilage. Interestingly, alongside the accumulation of proteoglycans in the pellet matrix, there was a noticeable decrease in type II collagen expression, with the most intense staining localised to regions of low proteoglycan content. I hypothesise that cells create an initial cartilage template that is rich in type II collagen extracellular matrix that provides mechanical stability during early formation, this matrix is subsequently remodelled as proteoglycans are deposited. This is supported by the presence of the cartilage remodelling enzyme MMP-13 in regions with high type II collagen expression, but negligible proteoglycans. Whilst MMP-13 expression has become associated with the onset of osteoarthritis, it is also reported to be expressed during foetal femur development (de Andrés et al., 2013) and has even been reported to be constitutively expressed in human chondrocytes (Yamamoto et al., 2016). This suggests that MMP-13 is involved in the developmental and normal physiological remodelling of cartilage, which is likely the role it is playing in these hESC-derived chondrocyte pellets. There is little known regarding the order in which collagens and proteoglycans are expressed during cartilage development in humans, however one study did observe that in mice the expression of the basement membrane heperan sulfate proteoglycan, perlecan, was preceded by type II collagen expression (at the mRNA level) (French et al., 1999). It is therefore possible that the early expression of type II collagen in the 3-, 4- and 5-week hESC-derived chondrocyte pellets is a recapitulation of developmental chondrogenesis. This is likely because the differentiation method used here drives chondrogenesis through developmental pathways from pluripotent hESCs, through primitive streak/mesendoderm, mesoderm towards chondrocytes.

The expression of Connexin-43 in hESC-derived cartilage pellets at 13-, 16- and 19-weeks was investigated. Connexin-43 is a gap junction protein (GJP) and is the most highly expressed GJP in

chondrocytes (Gago-Fuentes et al., 2016). Gap junctions are intercellular channels that enable the diffusion of ions and small molecules. They consist of a pair of connected hemichannels that are themselves composed of connexin proteins. Mutations in the Connexin-43 gene are known to result in a number of developmental disorders and diseases which affect skeletal development (Laird, 2014). The distribution of Connexin-43 in the cartilage of rats and mice was examined by Schwab et al. (1998). Here they observed robust expression between growth-plate chondrocytes, fibrocartilage-like cells at the tendon and ligament insertions, and in the tendons and ligaments. Interestingly they found that in the hyaline cartilage Connexin-43 expression was diminished, leading them to conclude that Connexin-43 may play a role in cartilage development. This role has been demonstrated by Gago-Fuentes et al. (2016) who showed that deletion of the carboxyl terminal domain of Connexin-43 negatively impacted cartilage structure and chondrocyte phenotype. These findings support the data that demonstrated clear Connexin-43 positive staining in hESC-derived cartilage pellets cultured for 13-, 16- or 19-weeks that was localised to the regions of the pellets lacking hyaline-like morphology. Whilst positive staining was detected in regions of the pellets resembling hyaline cartilage, this was notably less than in the rest of the pellet. Here, Connexin-43 may be playing a critical role in the maturation of cartilage generated by hESC-derived chondrocytes by co-ordinating the cellular activities of the resident cell population.

For clinical applications the mechanical properties of engineered tissue are critical. Despite the importance of examining the mechanical properties of engineered cartilage, it is frequently overlooked. Here a custom-built mechanical testing rig was used to perform compression testing of tissue engineered cartilage and to determine the Young's Elastic modulus of the tissue. The elastic modulus of a substance is defined as the ratio of the force exerted upon a substance or body to the resultant deformation. Native cartilage is reported to have an elastic modulus in the range 0.45 to 0.80 MPa (Boschetti et al., 2004; Mansour, 2003). Here the elastic modulus for articular cartilage had a mean value of 0.87 MPa, with a range 0.55 to 1.12 MPa. Previously our group tested the Elastic modulus of bioreactor generated HAC derived cartilage and native cartilage using indentation type-atomic force microscopy and determined the Local Elastic Modulus for native cartilage to be approximately 1.3 MPa, and for the engineered cartilage approximately 1 MPa (Li et al., 2014b). Interestingly, other work from our group estimated the Elastic modulus of engineered and native cartilage to be in the region of 0.1-0.3MPa (Jonnalagadda et al., 2018). Here, a nanoindentation technique was used, but as with previous work from our group, and the data presented here, they found no significant difference in E between engineered and native cartilage.

It appears that different assessment methods may produce different values for E. To ensure accuracy or data interpretation it is imperative that studies test both native and engineered tissue

using the same device. Importantly, no significant difference in E was found between native cartilage, HAC pellets (3-weeks culture) and hESC-derived cartilage pellets (4-and 19-weeks culture). Furthermore, with values for E that are close to those reported in the literature I am confident of the analysis methods giving an accurate estimation of the elastic modulus of the tested samples. Despite being histologically different the 19 week pellet had an elastic modulus that was very similar to that of pellets cultured for 4 weeks (E=0.80 and 0.82 MPa respectively). The cause of this is unknown, however high type II collagen content was present in 4-week pellets which may have compensated for the lack of proteoglycans which contribute to the mechanical stability of native cartilage. Collagen is reported to have a relatively high elastic modulus, ranging from 2-200MPa depending on the solution it is tested in (Grant et al., 2009). Though the literature reports high variation, the values given are greater than the value here obtained for E, suggesting that collagen fibres have a high stiffness compared to the surrounding cartilage matrix, thus providing support for the theory presented here.

As previously discussed, conventional static tissue engineering techniques, such as pellet culture are associated with numerous caveats such as an inability to generate large constructs due to tissue necrosis and suboptimal tissue formation that occurs due to poor nutrient mass transfer rates and oxygen diffusion (Li et al., 2014c; Muschler et al., 2004). As a result, techniques such as pellet culture utilise relatively low cell numbers ($3x10^5$ cells per pellet) and produce small tissue constructs. Studies that have generated cartilage *in vitro* from PSCs have encountered this issue of scale up and typically generate constructs that are small in size, ~1mm diameter (Hwang et al., 2008; Yodmuang et al., 2015), ~2mm diameter (Ko et al., 2014). It is of note that when larger cartilage pellets are generated, these constructs often have a characteristic necrotic core (Li et al., 2014c). Diekman et al. (2012) describe the generation of chondrogenic cells from murine iPSCs by type II collagen (Col2)-driven green fluorescent protein (GFP) expression, and subsequent cartilage generation by pellet culture. The pellets generated exceeded 2mm in diameter, however it is of note that these pellets were not homogenous throughout but lacked the proteoglycan rich ECM at the core of the pellet. This is likely due to impaired nutrient diffusion as a result of diffusion distance to the core of the pellet. It is essential that the translational barriers of scale-up are overcome, particularly as tissue-engineered cartilage will be required to fill defects larger than the scaffold-free constructs generated in the studies discussed above (Diekman et al., 2012; Hwang et al., 2008; Ko et al., 2014; Yodmuang et al., 2015). Here, the ability to generate hyaline-like cartilage constructs that exceed the dimensions reported in the literature (~3mm diameter) has been demonstrated. Furthermore, the tissue generated showed no sign of necrosis, suggesting that nutrient diffusion has not been impeded by size. Using the hESC-derived

chondrocytes described here, it may be possible for further scale-up without central tissue necrosis.

In this chapter it has been demonstrated that hESC-derived chondrocytes can form large hyaline-like cartilage pellets with an elastic modulus analogous to native articular cartilage. After 4 weeks of culture, pellets are mechanically similar to native cartilage and with prolonged culture acquire hyaline-like morphology. I therefore hypothesise that pellets cultured for 4 weeks may be suitable for transplantation into a defect, thus reducing the pre-culture period required for clinical translation and providing a promising new avenue for treatment of cartilage defects.

Chapter 6 *Ex-vivo* organotypic culture

6.1 Introduction

Generating cartilage from hESC-derived chondrocytes *in vitro* is an achievement, however for clinical translation it is important to go beyond simply generating the tissue but towards functional testing. The question of whether this bioengineered tissue is capable of treating damaged cartilage must be addressed and before a treatment can progress to human studies, *in vivo* testing is required. However, *in vivo* work is expensive both in regard to the financial burden and animals required. Before approaching an *in vivo* study it is prudent to venture into the intermediary area of *ex vivo* organotypic culture. This involves 3D culture of cells to form tissues that recapitulate the *in vivo* setting by retaining the original structural and functional properties of the native tissue. This is in line with the principles of the 3Rs (Replacement, Reduction and Refinement), a framework developed over 50 years ago to encourage more humane animal research. Use of an *ex vivo* model prior to *in vivo* studies replaces animals at this stage of research, which allows refinement of the procedure, and therefore enabling a reduction in the number of animals needed for *in vivo* studies.

Work by Oldershaw et al. (2010b) provided a template for the chondrogenic differentiation upon which the modified DDP utilised here is based. This group did not use their differentiated cells to generate bioengineered constructs, however they did implant cells *in vivo* (Cheng et al., 2014). Here they created osteochondral defects in the trochlear groove of athymic RNU rats and implanted $3x10^6$ cells in 100µl fibrin gel (controls contained fibrin only). Whilst some repair tissue was observed at 12 weeks, due to the defect extending into the bone marrow cavity it is unclear as to whether the majority of the repair contribution was from the hESC-derived cells or cells from the bone marrow. It is likely to have been a combination of both as there were clearly cells present in the fibrin only control repair tissue that had presumably migrated from the bone marrow cavity, as no hESC-derived chondroprogenitors were used in the control. As such, this experiment did not sufficiently address the question of whether these cells can repair a cartilage defect.

Tissue engineering is superior to cell transplantation as engineering the tissue *in vitro* enables quality assessment of the cartilage prior to implantation and reduces the likelihood of cells being lost or accidental off-target transplantation. Whilst the approach here differs significantly to ours, particularly as this is essentially a cell-based rather than tissue engineering strategy, an *ex vivo* organotypic defect model would have been useful before progressing to the *in vivo* work.

The technique this study will employ is the generation of a partial thickness chondral defect in a full thickness section of human adult articular cartilage, and subsequent culture or a hESC-derived cartilage pellet in the defect, termed *ex vivo* partial thickness chondral defect organotypic culture. Similar techniques have been reported in the literature (Iwai et al., 2011; Li et al., 2014b; Min et al., 2016; Olee et al., 2013; Schwab et al., 2017), however *ex vivo* organ culture is rarely utilised in the field of cartilage tissue engineering. Typically studies have focussed on creating osteochondral defects (Iwai et al., 2011), or full thickness chondral defects in and osteochondral plug (Schwab et al., 2017). However, as discussed above, osteochondral defects allow for contribution of bone marrow derived cells to cartilage repair, which prevents a clear assessment of the potential for the applied treatment to repair the damage. Work has been done using partial thickness defects (Min et al., 2016; Olee et al., 2013) and also by our group in Li et al. (2014b). These studies utilised human cartilage, unlike Iwai et al. (2011) and Schwab et al. (2017) who used porcine cartilage. Whilst animal cartilage may be useful if human cartilage is unavailable, there are numerous benefits associated with using human tissue. Clearly if the treatment is ultimately intended for humans, then using human tissue will provide a more physiologically normal environment and also decreases the number of animals required, and thus adheres to the 3Rs principle.

Previous work from our group using this organotypic culture method showed promising results (Li et al., 2014b). Here an acoustofluidic perfusion bioreactor was used to generate neocartilage constructs from HACs. These constructs were then cultured in a partial thickness defect for 8 or 16 weeks before being used for mechanical testing and histological analysis. It was observed that following 16 weeks organotypic culture the original pellet had formed repair tissue that had integrated with the native cartilage. At 16 weeks the original implanted construct and the repair tissue were clearly defined, and the pellet did not appear to have increased in size other than in the repair tissue regions. Whilst the construct showed evidence of integration with native tissue there was still empty space in the defect surrounding the construct.

Using an alternative cell source, such as hESC-derived chondrocytes which are likely to be more proliferative than HACs due to their hESC origin, it is possible that these cells will be better equipped than HACs to fill the defect. Here, we will utilise two different models of the *ex-vivo* partial thickness organotypic culture. The first model will investigate how well the hESC-derived chondrocyte pellet integrates with native cartilage in a defect model, the second will investigate the effects of co-culturing a hESC-derived chondrocyte on top of a piece of native cartilage without the partial thickness defect.

6.2 Aims and objectives

- To assess the potential of hESC-derived cartilage to repair a partial thickness defect using an *ex vivo* organotypic partial thickness chondral defect model.
- To scale-up neocartilage generation using *ex vivo* organotypic co-culture of hESC-derived cartilage with native cartilage.
- To investigate the ultrastructure of hESC-derived chondrocytes in organotypic co-culture constructs.

6.3 Methods

6.3.1 *Ex-vivo* organotypic partial thickness chondral defect culture

Using a scalpel, full thickness sections of macroscopically normal cartilage were dissected from the non-load bearing region of femoral heads. The dissected cartilage was then trimmed to ~5 x 5 mm sections. A partial thickness defect extending to a depth of ~1.5 mm was created using a sterile drill bit and burr on the topside of the dissected cartilage into which a hESC-derived cartilage pellet, which had been cultured for 4 weeks, was placed (Figure 6.1).

The sample was then cultured on a transwell insert (Millipore) placed in the well of a 12-well plate. The sample was cultured at the air-liquid interface with 500 µl Chondrogenic medium per well. Samples were cultured for 16 weeks in a humidified incubator at 37°C, 5% CO_2 and 5% O_2; media changes were performed 2-3 times per week. Samples were then used for Histology.

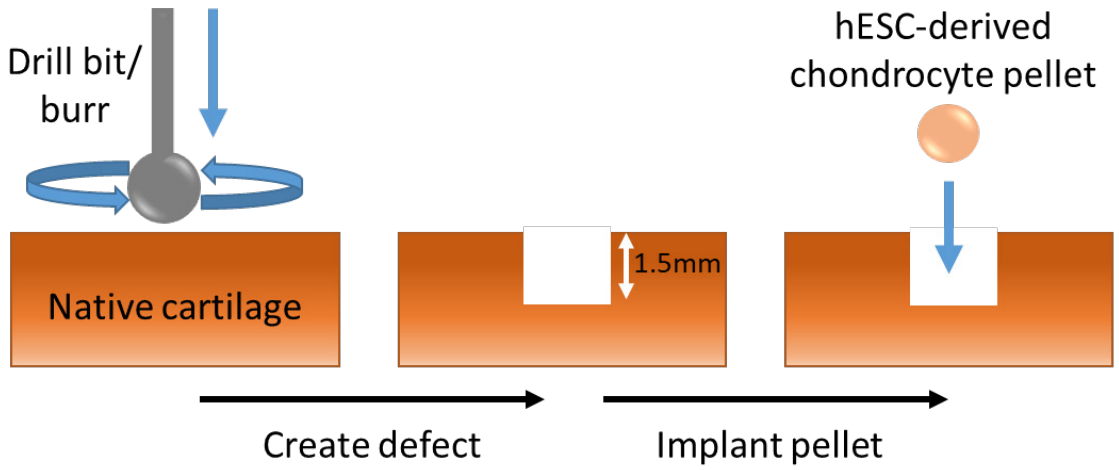

Figure 6.1 **Schematic depiction of *ex vivo* organotypic partial thickness chondral defect set up.** *A sterile drill bit/burr was used to create a defect approximately 1.5 mm deep in a full thickness native cartilage explant. A hESC-derived cartilage pellet was then inserted into the defect.*

6.3.2 *Ex-vivo* organotypic co-culture

Full thickness cartilage sections were dissected as in section 6.3.1. Using a sterile drill bit and burr (2.5 mm maximum diameter) a shallow indentation was made into the top-side of the dissected cartilage section upon which a hESC-derived cartilage pellet, which had been cultured for 4 weeks, was placed (Figure 6.2).

Culture occurred as in section 6.3.1.

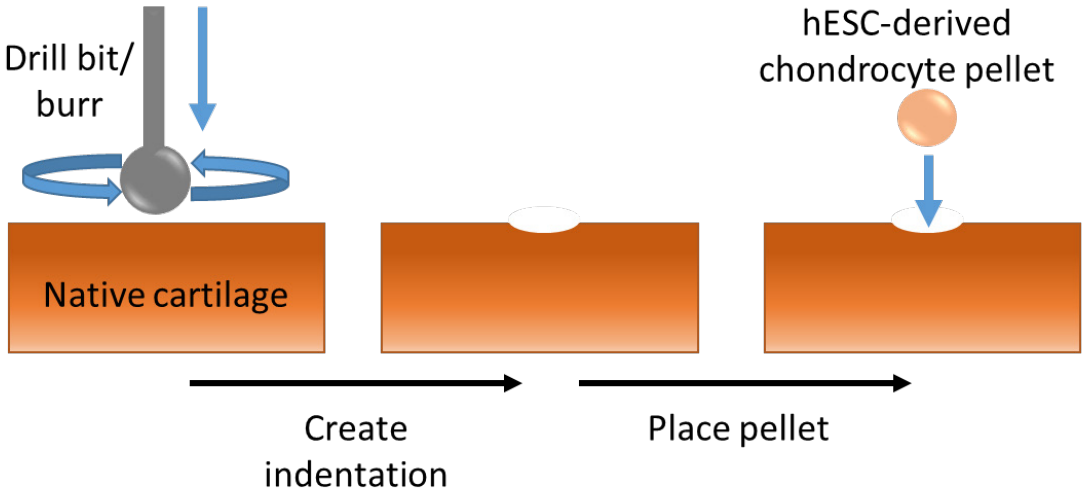

Figure 6.2 **Schematic depiction of *ex vivo* organotypic co-culture set up.**
A sterile drill bit/burr was used to create a shallow indentation in a full thickness native cartilage explant. A hESC-derived cartilage pellet was then placed atop the native cartilage.

6.3.3 Transmission Electron Microscopy (TEM)

A small portion of one *ex-vivo* organotypic co-culture sample was dissected and used for TEM imaging following 16 weeks culture.

6.3.3.1 Sample preparation

Following 16 weeks culture the sample was fixed in 4% PFA overnight at 4°C. The sample was washed in PBS and small (<1 mm^3) sections were dissected from the sample for TEM sample preparation.

Samples were washed in PBS twice with 10 minute incubations. Samples were then incubated in the post fixative solution (50:50, 2% Osmium tetroxide: 0.2 M phosphate buffer). Samples were washed in PBS as above. Samples were then washed in dH_2O twice with 10 minute incubations

before being incubated in Uranyl Acetate for 20 minutes. Samples were then incubated in graded Ethanol's of 30%, 50%, 70% and 95% for 10 minutes at each concentration. Samples were incubated in 100% EtOH twice with 20-minute incubations. Samples were then incubated in Acetonitrile for 10 minutes, followed by overnight incubation in a 50:50 mix of Acetonitrile: epoxy Resin. Each step was performed with agitation (orbital rotator).

Following the overnight incubation, samples were incubated in epoxy resin for 6 hours and then embedded in fresh epoxy resin which was polymerised at 60°C for 24 hours.

6.3.3.2 Sectioning

Sectioning was performed using an Ultracut E microtome. Blocks were trimmed and polished.

Ultra-thin sections were prepared by Regan Doherty in the Biomedical Imaging Unit at the University of Southampton.

6.3.3.3 Imaging

FEI Tecnai T12 Transmission Electron Microscope was used to image ultra-thin sections. The microscope was operated by Regan Doherty in the Biomedical Imaging Unit at the University of Southampton.

6.4 Results

6.4.1 hESC-derived cartilage pellet, organotypic defect culture

6.4.1.1 Culture of hESC-derived cartilage pellet in a partial thickness defect results in defect repair

To assess the ability of hESC-derived cartilage pellets to repair partial thickness defects a hESC-derived cartilage pellet (4-weeks culture) was inserted into a defect (~1mm^3) in a native cartilage explant. Following 16-weeks *ex vivo* organotypic culture the extent of defect repair was assessed.

Macroscopically, the defect appeared to have been filled with new tissue that had a glossy white appearance similar to the native cartilage (Figure 6.3a). There was a visible difference between the filled defect and the empty defect control, with the empty defect showing no sign of new tissue filling the defect site (Figure 6.3b). Interestingly, not only was there evidence of defect filling in Figure 6.3a, but there were also small nodules of neocartilage on the surface of the native cartilage. One of these areas is circled in Figure 6.3a and is discernibly separate from the original pellet.

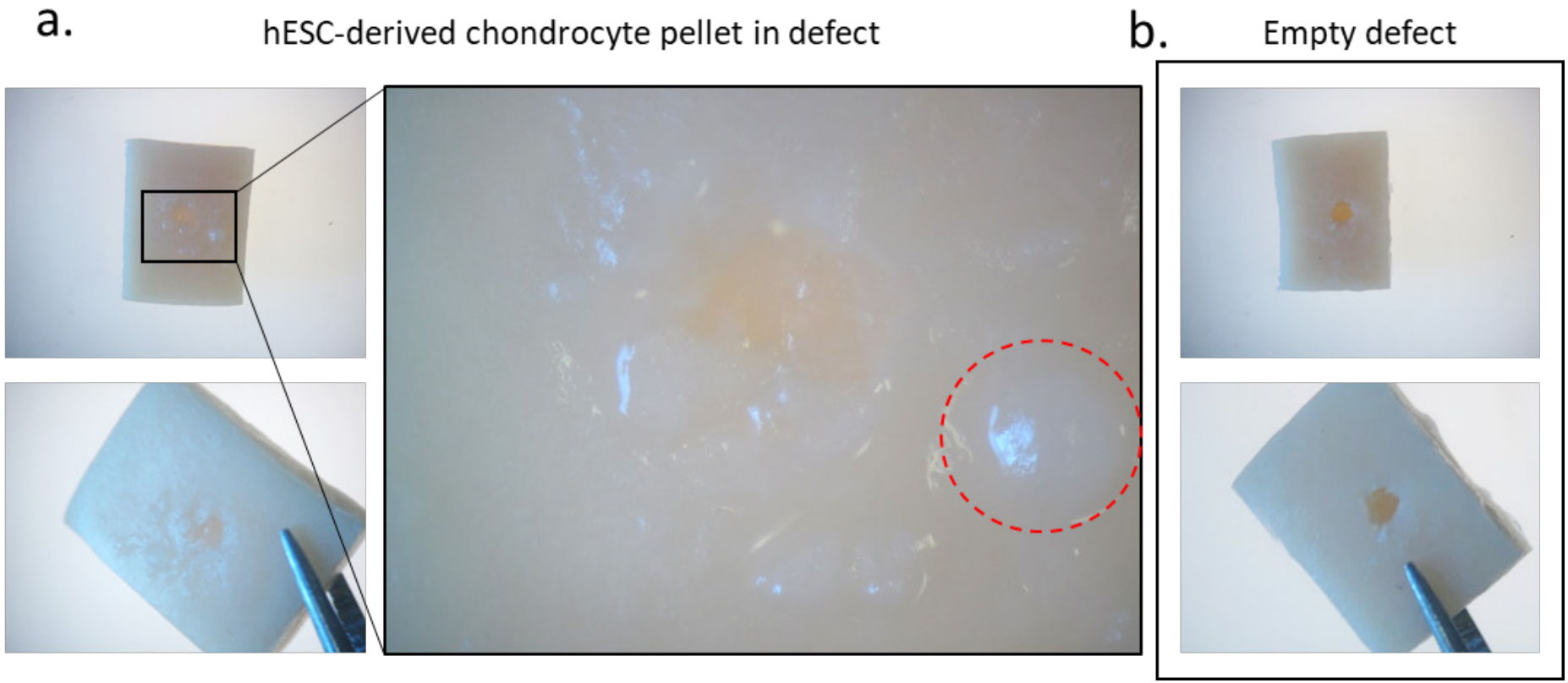

Figure 6.3 **Repair of a partial thickness defect in native cartilage by a hESC-derived cartilage pellet.**

A partial thickness defect was created in an approximately 1cm^2 native cartilage explant (F79) and a hESC-derived cartilage pellet was cultured in the defect for 16-weeks. a. shows repair of the defect with neocartilage, b. shows a noticeably unrepaired empty defect cultured for 16-weeks under identical conditions. The red dashed line indicates a mound of neocartilage distal to the original pellet.

Safranin O staining of the sample showed that the defect containing the hESC-derived cartilage pellet had been filled with a proteoglycan rich matrix resembling hyaline cartilage (Figure 6.4a), whereas the empty defect control showed no sign of repair (Figure 6.4b). The majority of the neocartilage had high Safranin O staining density (Figure 6.4a), was hypercellular compared to the native tissue (Figure 6.4a i), and contained clearly defined lacunae (Figure 6.4a iv). The neocartilage has integrated with the native tissue (Figure 6.4a iv) and a clear border between the native and neocartilage is difficult to determine, particularly on the left-hand side of the defect. To establish an approximate border between the two a white line was drawn based upon morphological differences (Figure 6.4a i). At the top of the defect site the tissue appears to be more fibrous and less mature, with a high cell density (Figure 6.4a ii). These cells appear to be migrating out of the original defect and producing neocartilage on the surface of the native tissue (See top right of Figure 6.4a i).

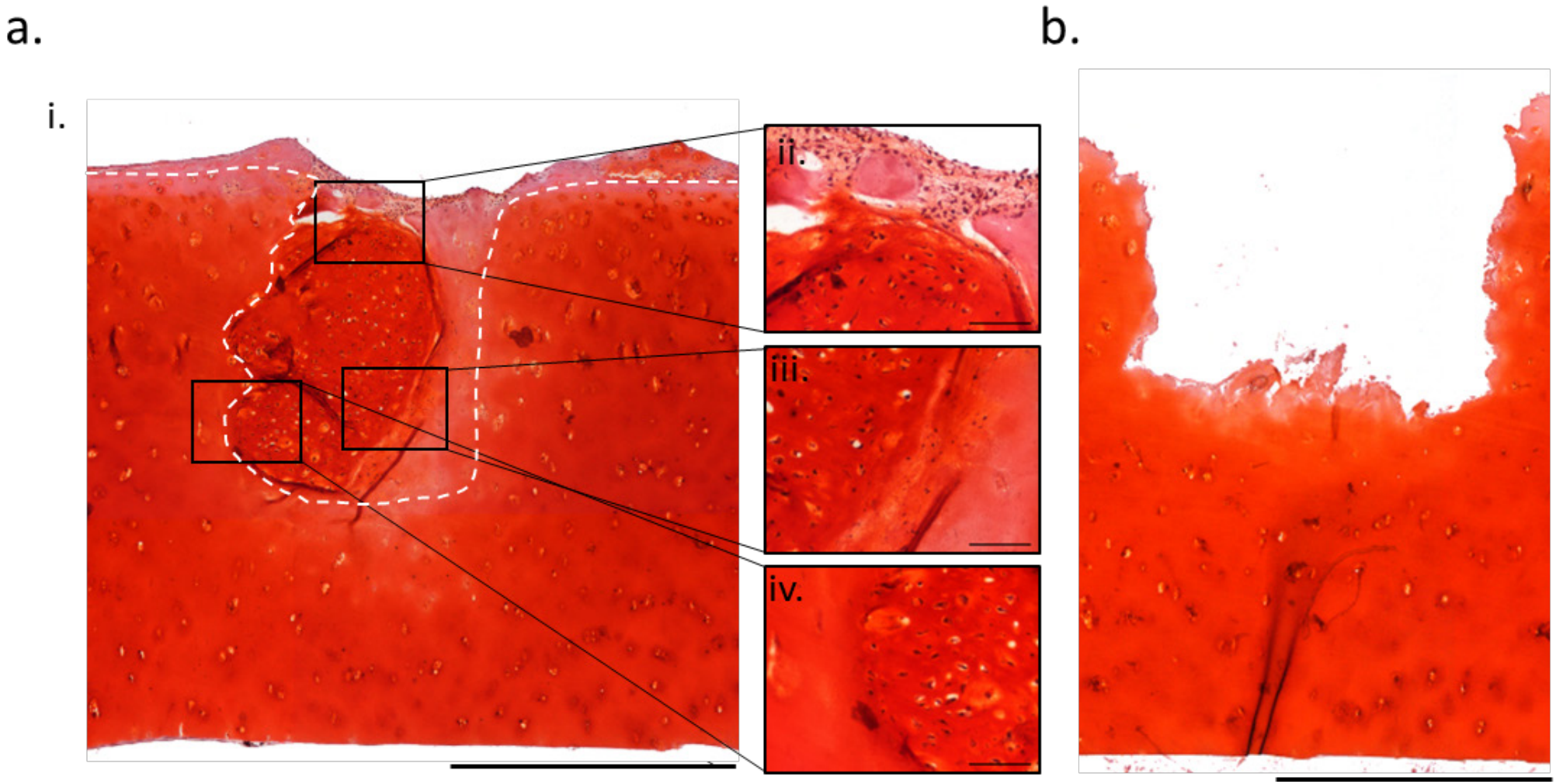
a.
i.
ii.
iii.
iv.
b.

Figure 6.4 **hESC-derived cartilage pellet generates hyaline-like repair tissue in partial thickness defect.**

Safranin O staining of a repaired cartilage defect was performed. a. shows a low magnification image of the repaired defect with a dashed white line approximately demarking the edge of the native tissue (ai) and high magnification images of the neocartilage (aii-iv). An unrepaired empty defect is shown in b. Low magnification 1 mm, high magnification 100 µm.

6.4.1.2 hESC-derived chondrocyte generated defect repair tissue expresses chondrogenic markers

Next the expression of chondrogenic markers was investigated using immunohistochemistry.

SOX9 expression in the central region was localised to the more fibrous repair tissue at the top of the defect (Figure 6.5a i). SOX9 expression was not detected in the mature hyaline repair tissue, or the native cartilage (Figure 6.5a i). In the outgrowth region on the right-hand side SOX9 was expressed in some of the cells, however not cells within the lacunae (Figure 6.5a ii).

Type II collagen staining was observed in both the mature hyaline-like cartilage region and the less mature fibrous region (Figure 6.5b). Staining density appeared to be higher in the fibrous region at the top of the defect and in other regions that had lower proteoglycan content (Figure 6.5b). There was a patch of type II collagen in the lower portion of the mature neocartilage that resembled the staining observed in the native tissue (Figure 6.5b i). Type I collagen expression was absent from the mature hyaline-like neocartilage both at the defect site and the neocartilage outgrowth on the top-right of the defect (Figure 6.5ci and c ii respectively), however staining was observed in the fibrous region at the top of the defect (Figure 6.5c ii).

Aggrecan expression in the mature neocartilage was similar to that observed in the native tissue (Figure 6.5d). Interestingly, the fibrous tissue exhibited more robust Aggrecan expression than the mature tissue despite appearing to be less hyaline (Figure 6.5d)

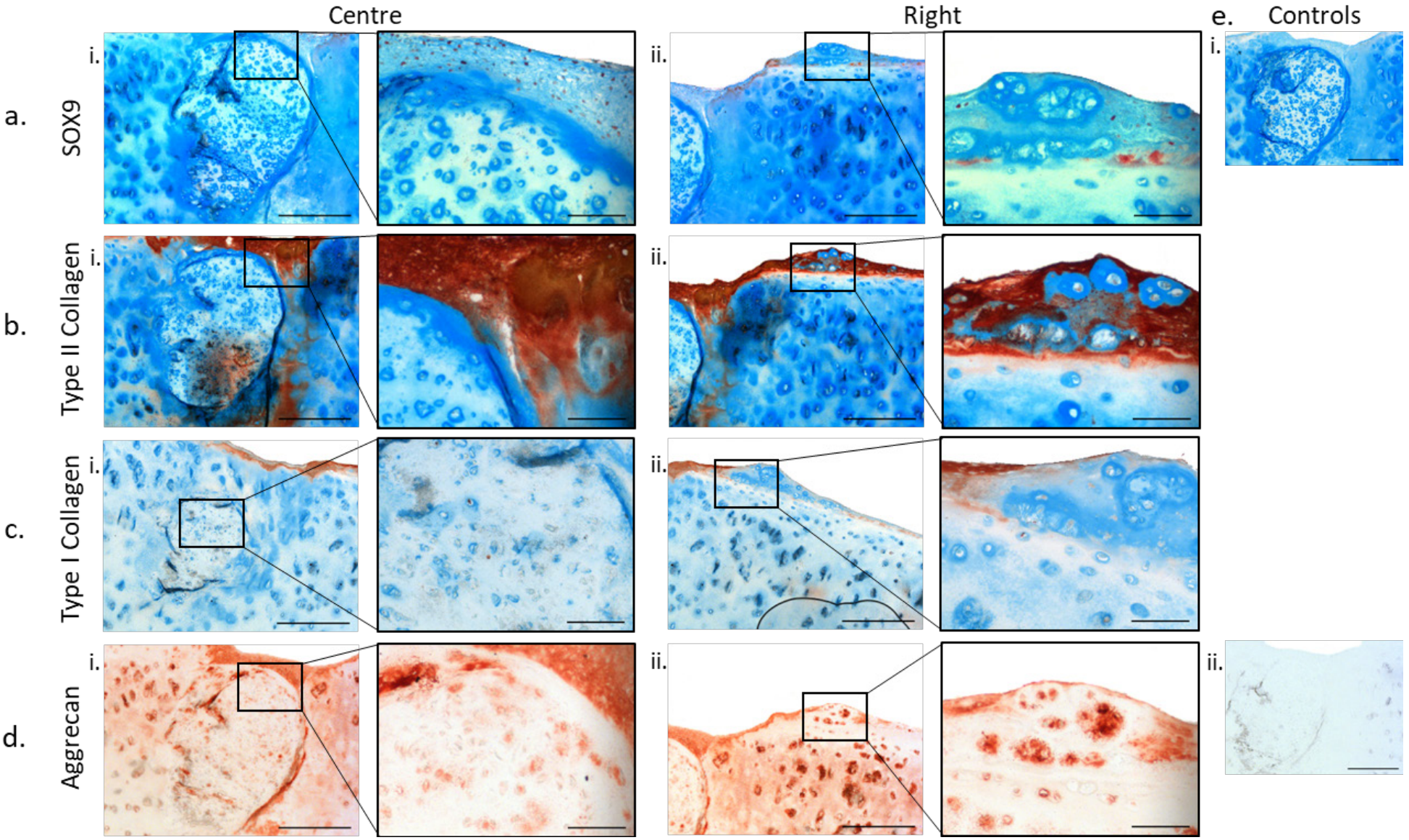
Centre
Right
e. Controls
a.
SOX9
i.
ii.
i.
b.
Type II Collagen
i.
ii.
c.
Type I Collagen
i.
ii.
d.
Aggrecan
i.
ii.
ii.

Figure 6.5 **hESC-derived cartilage pellet repair tissue expresses chondrogenic markers.**
hESC-derived chondrocyte neocartilage defect repair tissue was examined histologically for the expression of SOX9 (a), type II collagen (b), type I collagen (c) and Aggrecan (d). Secondary antibody only negative controls were included in immunohistochemistry protocols; anti-rabbit control shown in (ei), anti-goat control shown in (eii). Low magnification 500 µm, high magnification 100 µm.

6.4.1.3 Evidence of matrix remodelling in immature fibrous repair tissue but not mature neocartilage

To investigate the process of defect repair and matrix formation in hESC-derived chondrocyte generated neocartilage the expression of the matrix remodelling enzyme MMP-13, the gap-junction protein Connexin-43 and the proliferation marker Ki67 was investigated (Figure 6.6).

MMP-13 expression was found to be localised to the immature fibrous tissue at the top of the defect region and extending along the top of the native tissue (Figure 6.6a i). MMP-13 was not observed to be expressed in the mature neocartilage filling the defect (Figure 6.6a i). Connexin-43 and Ki67 expression was co-localised with MMP-13 expression in the immature fibrous tissue (Figure 6.6b and c respectively), and was not observed to be expressed in the mature hyaline tissue (Figure 6.6bi and ci respectively).

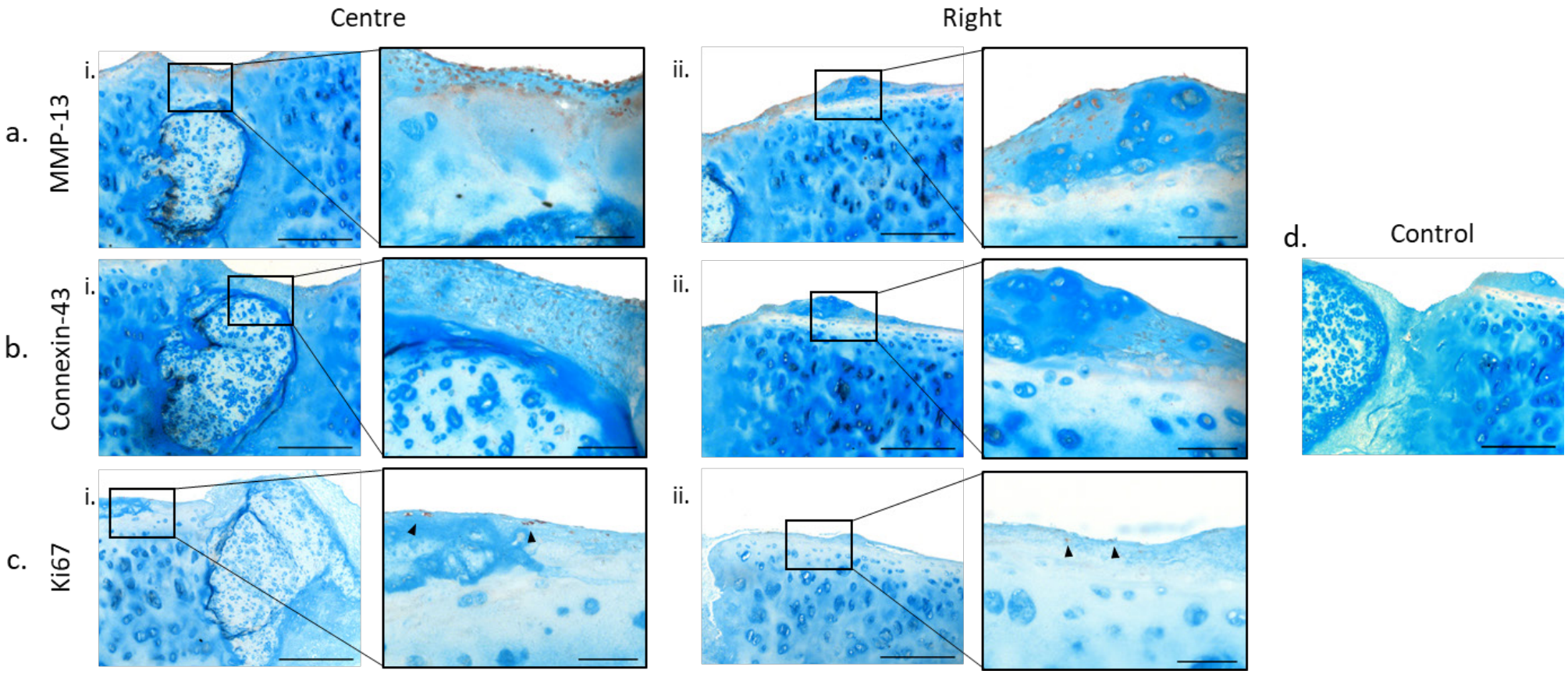

Figure 6.6 **Expression of remodelling markers in neocartilage generated from hESC-derived chondrocytes pellet defect repair tissue.**

hESC-derived chondrocyte neocartilage defect repair tissue was examined histologically for the expression of MMP13 (a), Connexin-43 (b) and Ki67 (c). Secondary antibody only negative control shown in d. Low magnification 500 µm, high magnification 100 µm.

6.4.2 hESC-derived cartilage pellet co-culture with native cartilage

6.4.2.1 hESC-derived chondrocyte co-culture with native cartilage results in large proteoglycan rich hyaline neocartilage constructs

hESC-derived chondrocytes were cultured as pellets for 4-weeks before being co-cultured with native cartilage for 16-weeks. The resulting organotypic co-cultures were then analysed histologically. The results from 2 separate cultures are described here and referred to as experiment 1 and experiment 2.

Following 16-weeks culture the hESC-derived cartilage pellet grew to cover a large majority of the native cartilage in experiment 1 (Figure 6.7a). The original pellet can be identified in the central region of Figure 6.7a i. The neocartilage grew to a height equal to, and even greater than in specific regions, that of the native tissue Figure 6.7a ii. The diameter of the tissue generated was 6.25mm in the section shown in Figure 6.7b i. The neocartilage tissue had a glossy appearance; however, the neocartilage appeared less opaque than the native tissue.

Safranin O staining revealed that the majority of the neocartilage is rich in proteoglycans (Figure 6.7bFigure 6.8), with Safranin O staining density appearing similar to the native tissue. The periphery of the neocartilage had lower proteoglycan content as indicated by less intense or absent proteoglycan staining (Figure 6.7bi and ii). Native cartilage had morphology typical of early stage osteoarthritis with proteoglycan depletion in the superficial zone (Figure 6.7b).

The neocartilage appeared hypercellular compared to the native cartilage (Figure 6.7b). The cells themselves had typical chondrocyte morphology with cells contained within defined lacunae (Figure 6.7b). Whilst chondrocytes in the native tissue typically had high proteoglycan density surrounding the lacunae periphery (Figure 6.7biii), hESC-derived chondrocytes in the neocartilage had high proteoglycan density even beyond this peripheral region (Figure 6.7b). Cell morphology varied between different regions of the neocartilage. Whist in the more central proteoglycan rich regions of the tissue the cells had typical chondrocyte morphology and clearly defined lacunae, in the extreme peripheral regions the tissue was more fibrous in appearance and cells appeared more elongated and fibroblastic (Figure 6.7b iv). These cells were not all confined within lacunae. These more fibrous protrusions extended from the neocartilage across then native cartilage, and can be seen to wrap around the edges and even the bottom of the native tissue forming, anchoring the neocartilage to the native cartilage (Figure 6.7b i).

In certain regions of the samples there is evidence of fusion between the neocartilage and native cartilage. In Figure 6.7b iii the two tissues are closely connected with no gaps, and a cell in a

lacunae can be seen at the border that appears to be part of both the native and neocartilage tissue (Figure 6.7biii). Interestingly, in Figure 6.7b iv a discrete region of tissue at the border of the native and neocartilage can be seen to mature and accumulate proteoglycans, despite being remote from the proteoglycan rich regions of the neocartilage. This area appears to be part of both the native and neocartilage and indicates integration of the tissues occurring.

The regions of high proteoglycan content and typical chondrocyte morphology will henceforth be referred to as mature neocartilage.

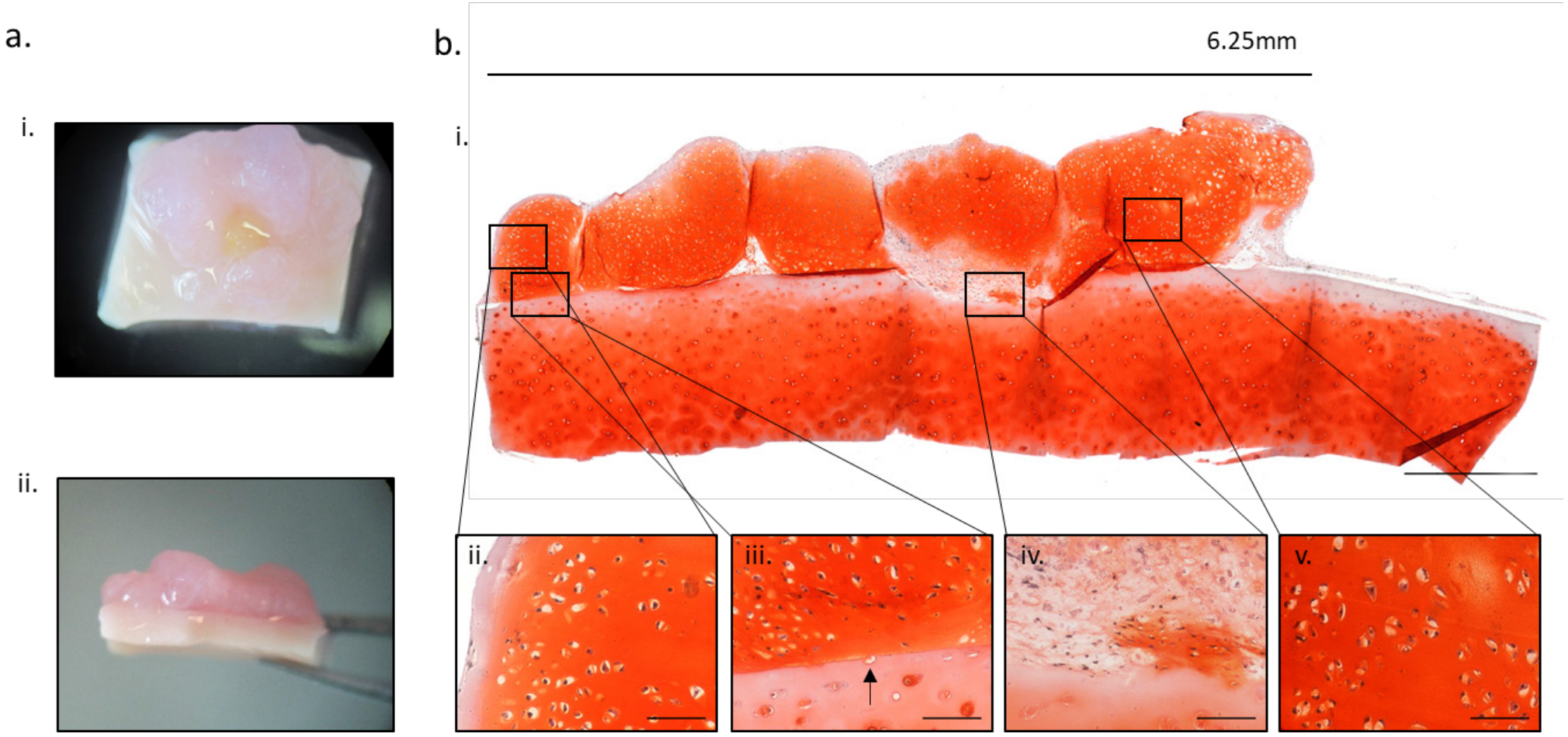
a.
i.
ii.
b.
6.25mm
i.
ii.
iii.
iv.
v.

Figure 6.7 **Neocartilage generation from hESC-derived chondrocytes following 16-weeks co-culture with native cartilage (experiment 1).**

One hESC-derived cartilage pellet was co-cultured with native cartilage for 16-weeks. During the culture period the pellet grew to cover much of the native cartilage (a) forming neocartilage. Safranin O staining of the neocartilage shows hyaline cartilage formation and fusion of the neocartilage with native tissue (b). Arrow in biii indicates a cell that appears to be part of both the native and neocartilage. Low magnification 1 mm, high magnification 100 µm.

In experiment 2 the hESC-derived chondrocyte grew over the course of the 16-week culture to form 2 mounds of hyaline-like neocartilage that were interconnected by a region of fibrous tissue (Figure 6.8a). As with experiment 1 the neocartilage grew to a height equal to, the native tissue Figure 6.7. Safranin O staining revealed that the majority of the neocartilage is rich in proteoglycans (Figure 6.8Figure 6.8), with Safranin O staining density appearing similar to the native tissue. The fibrous tissue connecting the mounds of neocartilage and the peripheral regions had low proteoglycan content as indicated by less intense or absent proteoglycan staining (Figure 6.8a and bi).

The neocartilage appeared hypercellular compared to the native cartilage (Figure 6.8). The cells themselves had typical chondrocyte morphology with cells contained within defined lacunae (Figure 6.8Figure 6.7bii and iii). Whilst chondrocytes in the native tissue typically had high proteoglycan density surrounding the lacunae periphery, hESC-derived chondrocytes in the neocartilage had high proteoglycan density even beyond this peripheral region (Figure 6.8bii). Cell morphology varied between different regions of the neocartilage. Whist in the more central proteoglycan rich regions of the tissue the cells had typical chondrocyte morphology and clearly defined lacunae (Figure 6.8b ii and iii), in the more fibrous regions cells appeared elongated and fibroblastic (Figure 6.8b iv). These cells were not all confined within lacunae, and the fibrous protrusions extended from the neocartilage across the native cartilage (Figure 6.8bi).

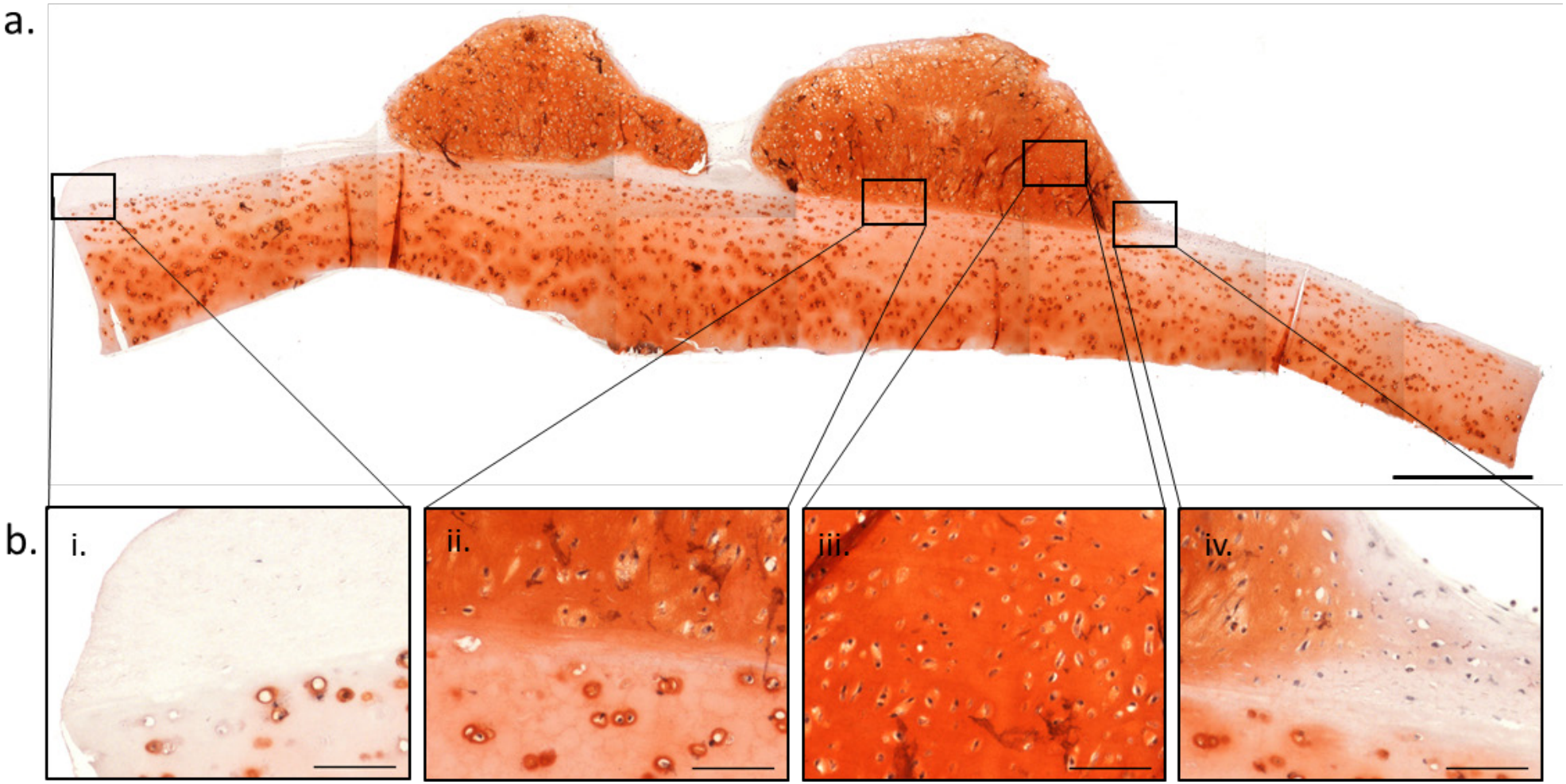
a.
b.
i.
ii.
iii.
iv.

Figure 6.8 **Neocartilage generation from hESC-derived chondrocytes following 16-weeks co-culture with native cartilage (experiment 2).**

One hESC-derived cartilage pellet was co-cultured with native cartilage for 16-weeks. During the culture period the pellet grew over the native cartilage (a) forming mounds of neocartilage. Safranin O staining of the neocartilage shows hyaline cartilage formation and fusion of the neocartilage with native tissue (b). Low magnification 1 mm, high magnification 100 µm.

6.4.2.2 hESC-derived chondrocyte neocartilage expresses key chondrogenic markers

Next the expression of chondrogenic markers was investigated using IHC.

In experiment 1, cells expressing the chondrogenic transcription factor SOX9 were mainly localised to the less mature, more fibrous tissue found at the periphery of the neocartilage and in connecting tissue (Figure 6.9a). SOX9 was not clearly expressed in cells of the mature neocartilage. However, it is also worth noting that SOX9 expression was not detected in most cells of the native cartilage.

Similar to the staining pattern observed for SOX9 expression, intense staining for type II collagen was found to be localised to regions at the periphery of the neocartilage, and also in the fibrous and less mature regions (Figure 6.9b). In certain regions type II collagen expression was observed in cells as well as the extracellular matrix (Figure 6.9b ii). Type II collagen staining appeared to be co-localised with weak staining for the typically bone specific type I collagen (Figure 6.9c). Type I collagen was not expressed in the mature neocartilage or native cartilage.

Robust expression of the proteoglycan Aggrecan was observed extracellular matrix of experiment 1 (Figure 6.9d), particularly surrounding the cell lacunae similar to the native cartilage.

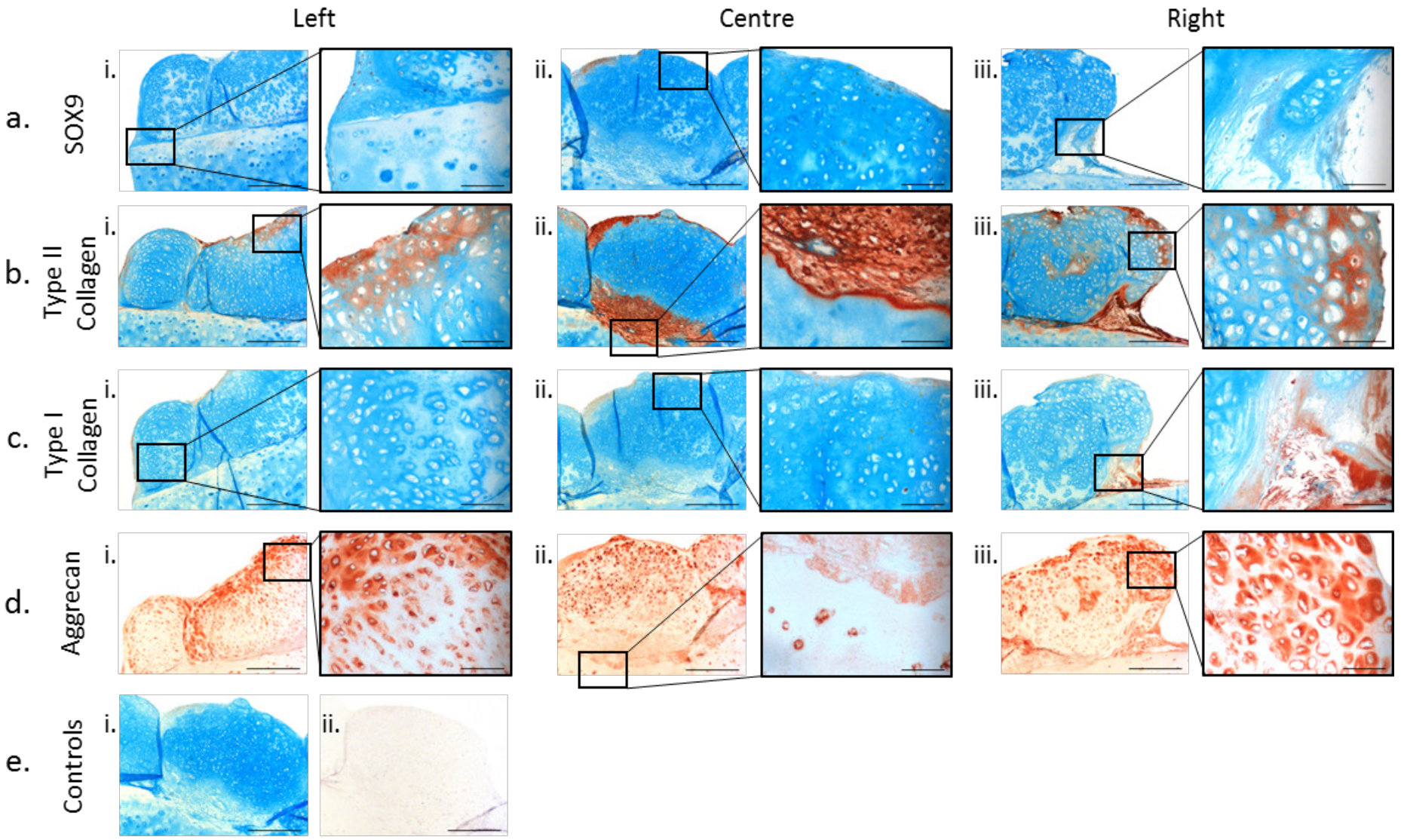
Left
Centre
Right
a.
SOX9
b.
Type II Collagen
c.
Type I Collagen
d.
Aggrecan
e.
Controls
i.
ii.
iii.

Figure 6.9 **Neocartilage generated via organotypic co-culture expresses chondrogenic markers (experiment 1).**

hESC-derived chondrocyte neocartilage was examined histologically for the expression of SOX9 (a), type II collagen (b), type I collagen (c) and Aggrecan (d). Secondary antibody only negative controls were included in immunohistochemistry protocols; anti-rabbit control shown in (ei), anti-goat control shown in (eii). Low magnification 500 µm, high magnification 100 µm.

In experiment 2, cells expressing the chondrogenic transcription factor SOX9 were mainly localised to the less mature, more fibrous tissue found at the periphery of the neocartilage and in connecting tissue (Figure 6.10aFigure 6.9). SOX9 expression appear to be more robust in experiment 2 compared to experiment 1 (Figure 6.9).

Similar to the staining pattern observed for SOX9 expression, intense staining for type II collagen was found to be localised to the fibrous region connecting the mounds of hyaline-like neocartilage (Figure 6.10bi) and in peripheral regions (Figure 6.10bii). Type II collagen staining appeared to be co-localised with weak staining for the typically bone specific type I collagen (Figure 6.10c). Type I collagen was not expressed in the mature neocartilage or native cartilage.

Robust expression of the proteoglycan Aggrecan was observed extracellular matrix of experiment 2 (Figure 6.10d), particularly surrounding the cell lacunae similar to the native cartilage.

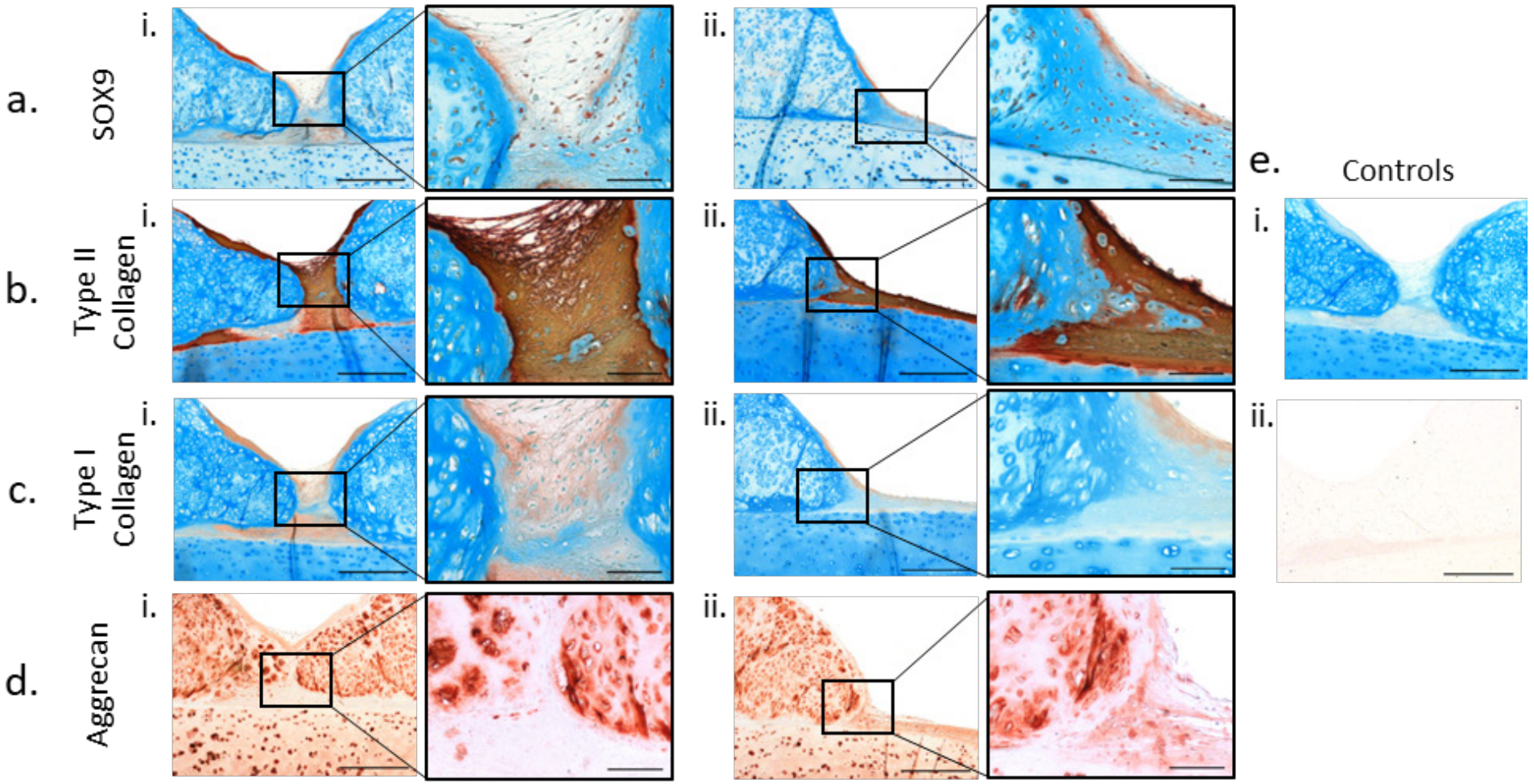
a.
SOX9
i.
ii.
b.
Type II Collagen
i.
ii.
c.
Type I Collagen
i.
ii.
d.
Aggrecan
i.
ii.
e.
Controls
i.
ii.

Figure 6.10 **Neocartilage generated via organotypic co-culture expresses chondrogenic markers (experiment 2).**

hESC-derived chondrocyte neocartilage was examined histologically for the expression of SOX9 (a), type II collagen (b), type I collagen (c) and Aggrecan (d). Secondary antibody only negative controls were included in immunohistochemistry protocols; anti-rabbit control shown in (ei), anti-goat control shown in (eii). Low magnification 500 µm, high magnification 100 µm.

6.4.2.3 Evidence of matrix remodelling in neocartilage co-cultures

To investigate the growth dynamic of the hESC-derived cartilage the expression of the matrix remodelling enzyme MMP-13, the gap-junction protein Connexin-43 and the proliferation marker Ki67 was expressed.

In experiment 1, MMP-13 was found to be expressed in the peripheral and more fibrous regions of the neocartilage (Figure 6.11a), rather than the mature proteoglycan rich regions. A similar expression pattern was observed for both Connexin-43 (Figure 6.11b) and Ki67 (Figure 6.11c). Interestingly, Connexin-43 was not clearly expressed in the regions where the neocartilage and the native cartilage connected, but instead expression was most evident in cells of the more fibrous tissue (Figure 6.11b). The most proliferative cells (Ki67 positive) were located peripherally and expression was particularly evident in the anchorage tissue that coated the sides of the native cartilage (Figure 6.11c).

MMP-13, Connexin-43 and Ki67 expression was not evident in the mature regions of the neocartilage or the native tissue (Figure 6.11).

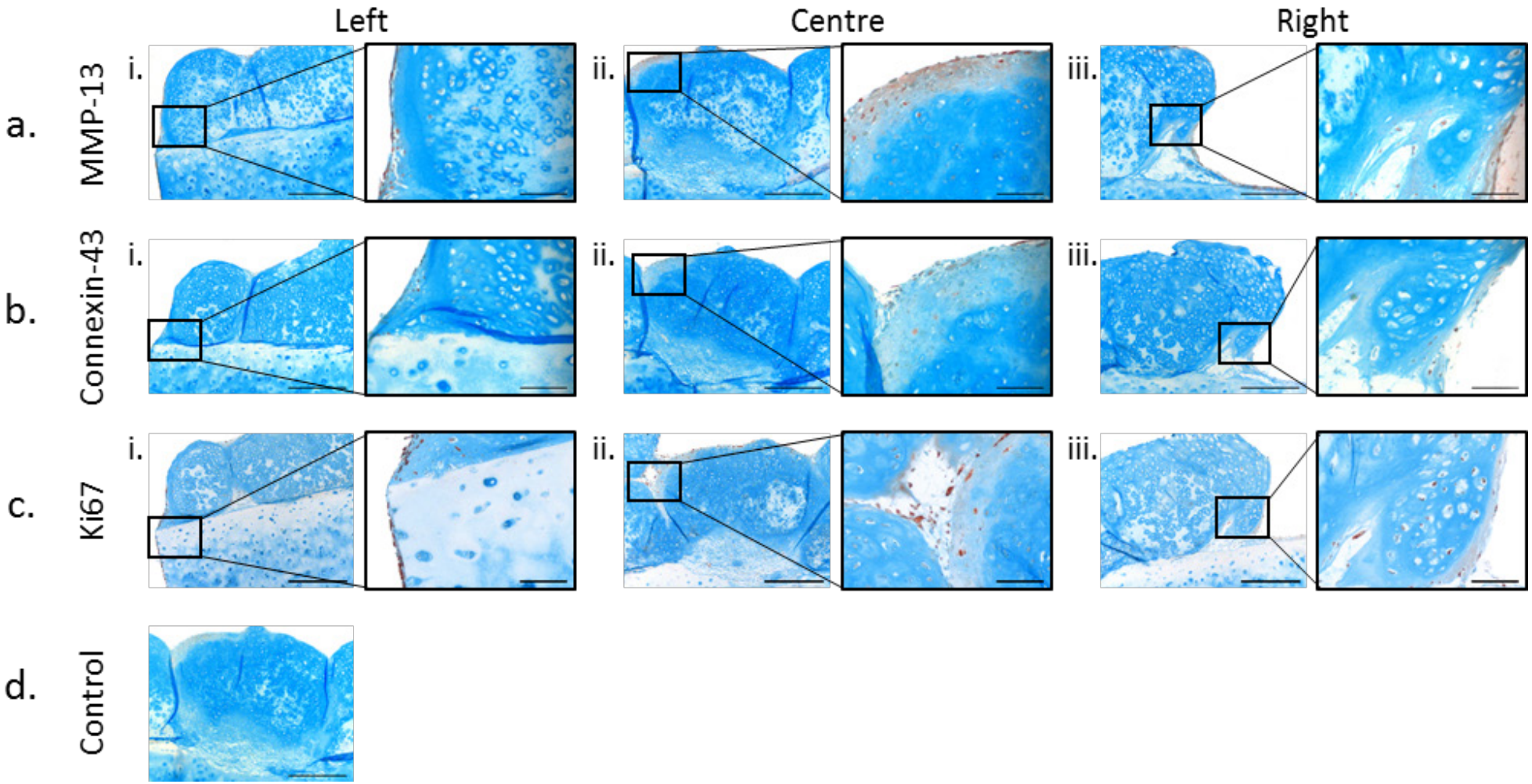
Left
Centre
Right
a.
MMP-13
i.
ii.
iii.
b.
Connexin-43
i.
ii.
iii.
c.
Ki67
i.
ii.
iii.
d.
Control

Figure 6.11 **Evidence of matrix remodelling in neocartilage generated via organotypic co-culture (experiment 1).**

HESC-derived chondrocyte neocartilage was examined histologically for the expression of MMP13 (a), Connexin-43 (b) and Ki67 (c). Secondary antibody only negative control shown in d. Low magnification 500 µm, high magnification 100 µm.

In experiment 2, MMP-13 was found to be expressed in the fibrous regions connecting the two mounds of neocartilage (Figure 6.12a) and peripheral regions (Figure 6.12) rather than the mature proteoglycan rich neocartilage. A similar expression pattern was observed for both Connexin-43 (Figure 6.12b) and Ki67 (Figure 6.12c). Connexin-43 was expressed in the fibrous regions where the neocartilage and the native cartilage connected (Figure 6.12b). The most proliferative cells (Ki67 positive) were located peripherally and expression was particularly evident in the anchorage tissue that spread distally from the neocartilage along the top of the native tissue (Figure 6.12cii).

MMP-13, Connexin-43 and Ki67 expression was not evident in the mature regions of the neocartilage or the native tissue (Figure 6.12).

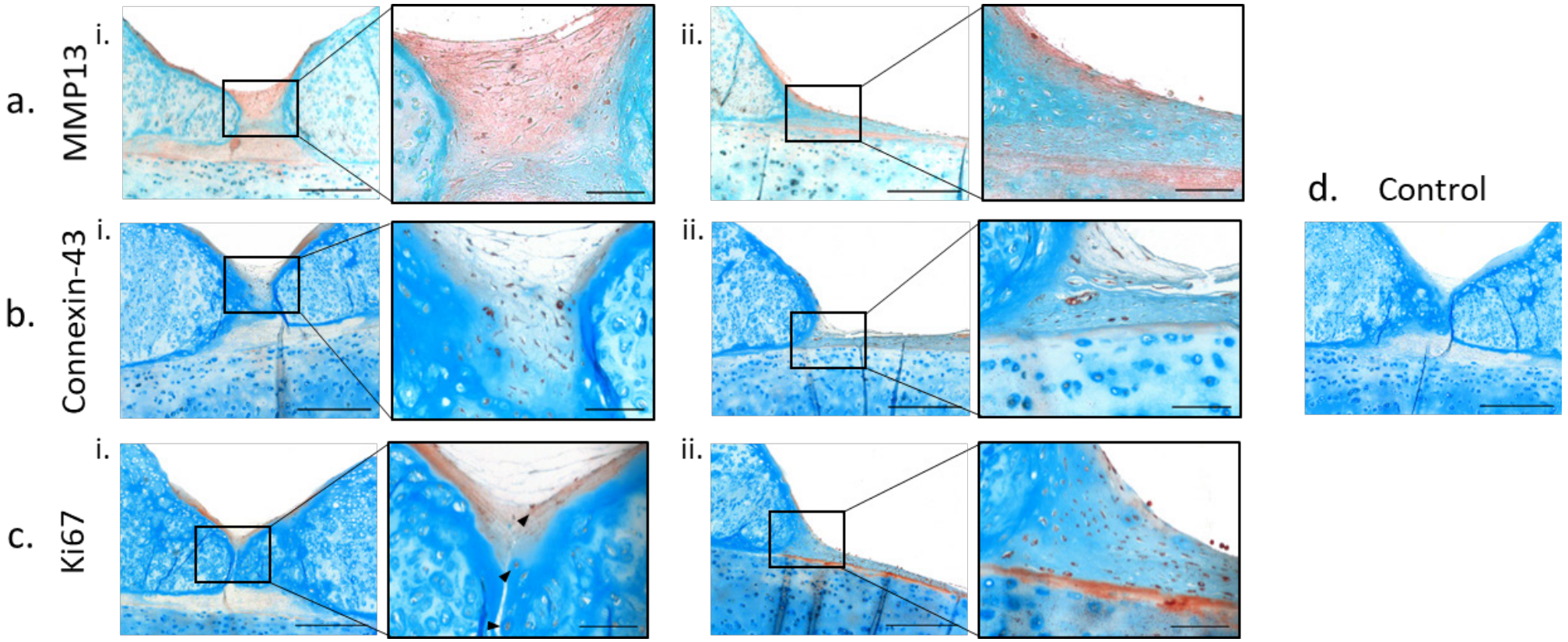
a.
MMP13
i.
ii.
b.
Connexin-43
i.
ii.
c.
Ki67
i.
ii.
d.
Control

Figure 6.12 **Evidence of matrix remodelling in neocartilage generated via organotypic co-culture (experiment 2).**

hESC-derived chondrocyte neocartilage was examined histologically for the expression of MMP13 (a), Connexin-43 (b) and Ki67 (c). Black arrows in ci. Indicate positively stained cells. Secondary antibody only negative control shown in d. Low magnification 500 µm, high magnification 100 µm.

6.4.3 Ultrastructure of bioengineered cartilage generated using co-culture

To investigate the ultrastructure of hESC-derived chondrocytes and the tissue they generate, one hESC-derived cartilage pellet/native cartilage co-culture sample was processed for transmission electron microscopy (TEM) imaging.

hESC-derived chondrocytes could be seen in the neocartilage section actively producing collagen and releasing fibrils into the extracellular environment (Figure 6.13a). The cells contained large quantities of the protein producing organelle the rough endoplasmic reticulum (RER) that contains many membrane-bound ribosomes. Deposited collagen fibrils can be seen in both the longitudinal and transverse orientation within the section (Figure 6.13b). At high magnification (87000x) the banding pattern of collagen is visible (Figure 6.13c). Unit fibrils of collagen show periodic cross striations every 67nm of their length.

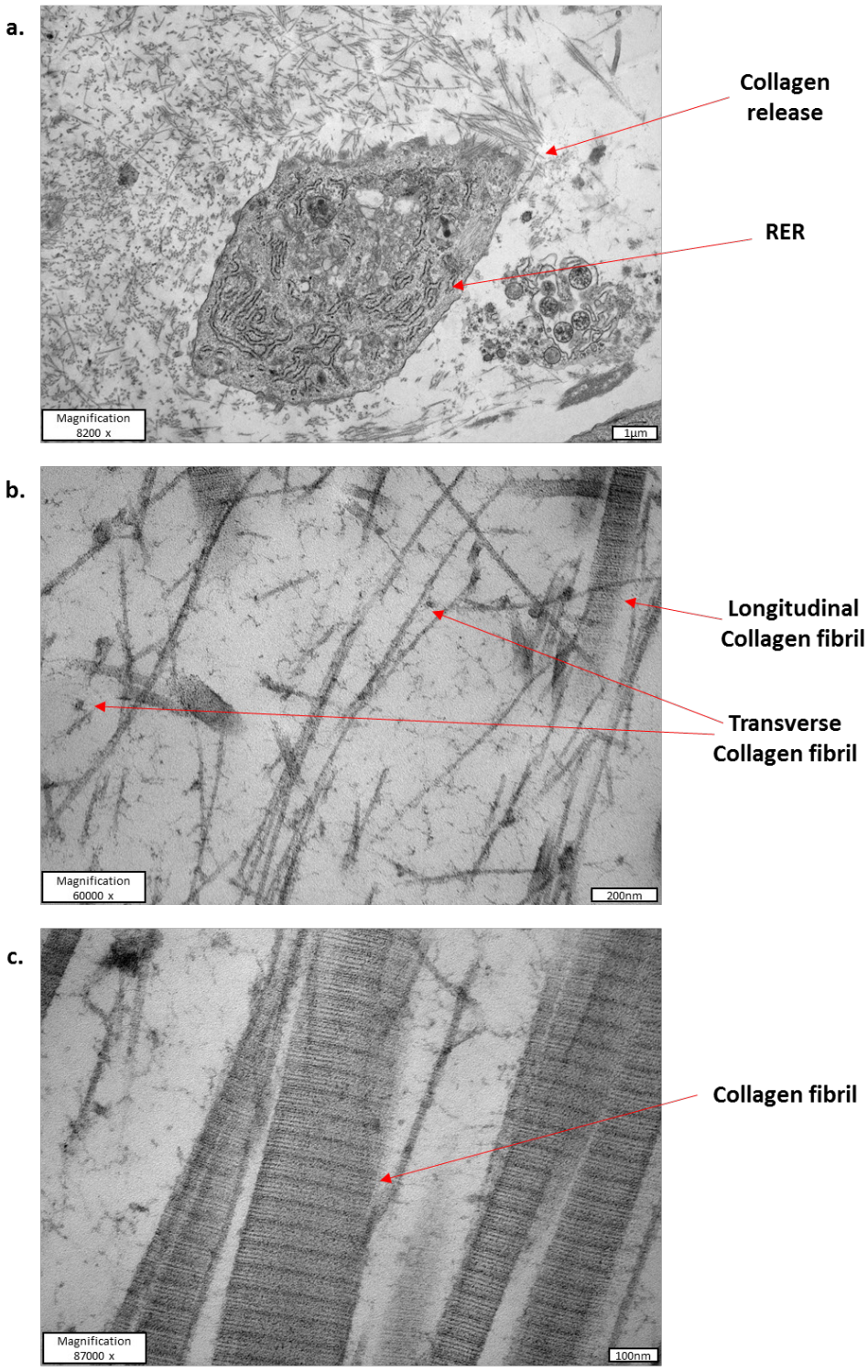

Figure 6.13 **Evidence of hESC-derived chondrocytes producing collagen in organotypic co-culture.**

Ultra-thin sections were cut from resin embedded co-culture tissue samples and imaged using TEM. a. shows a hESC-derived chondrocyte in the neocartilage region of the co-culture producing collagen. b. shows collagen fibrils in the extracellular matrix of the neocartilage, both in transverse and longitudinal orientation. c. shows high magnification of collagen fibrils, with clear banding.

hESC-derived chondrocytes were observed have an ultrastructure typical of native chondrocytes. Cells were visualised within the neocartilage lacunae (Figure 6.14), contained large nuclei surrounded by extensive RER, and contained lipid droplets (Figure 6.14). Interestingly, cells also appeared to release (Figure 6.14a) and contain (Figure 6.14b), multiple vesicles containing what appear to be concentric whorled structures. These vesicular structures were found in close proximity to the RER (Figure 6.14b).

hESC-derived chondrocytes were also found at the border between the native and neocartilage. Figure 6.14b shows a cell positioned against the edge of the native cartilage matrix. There is a visible gap between the cell and the native tissue at most points of the cell, however on the top and bottom of the cell there appears to be some components of ECM that are connected to both the hESC-derived chondrocyte and the native cartilage.

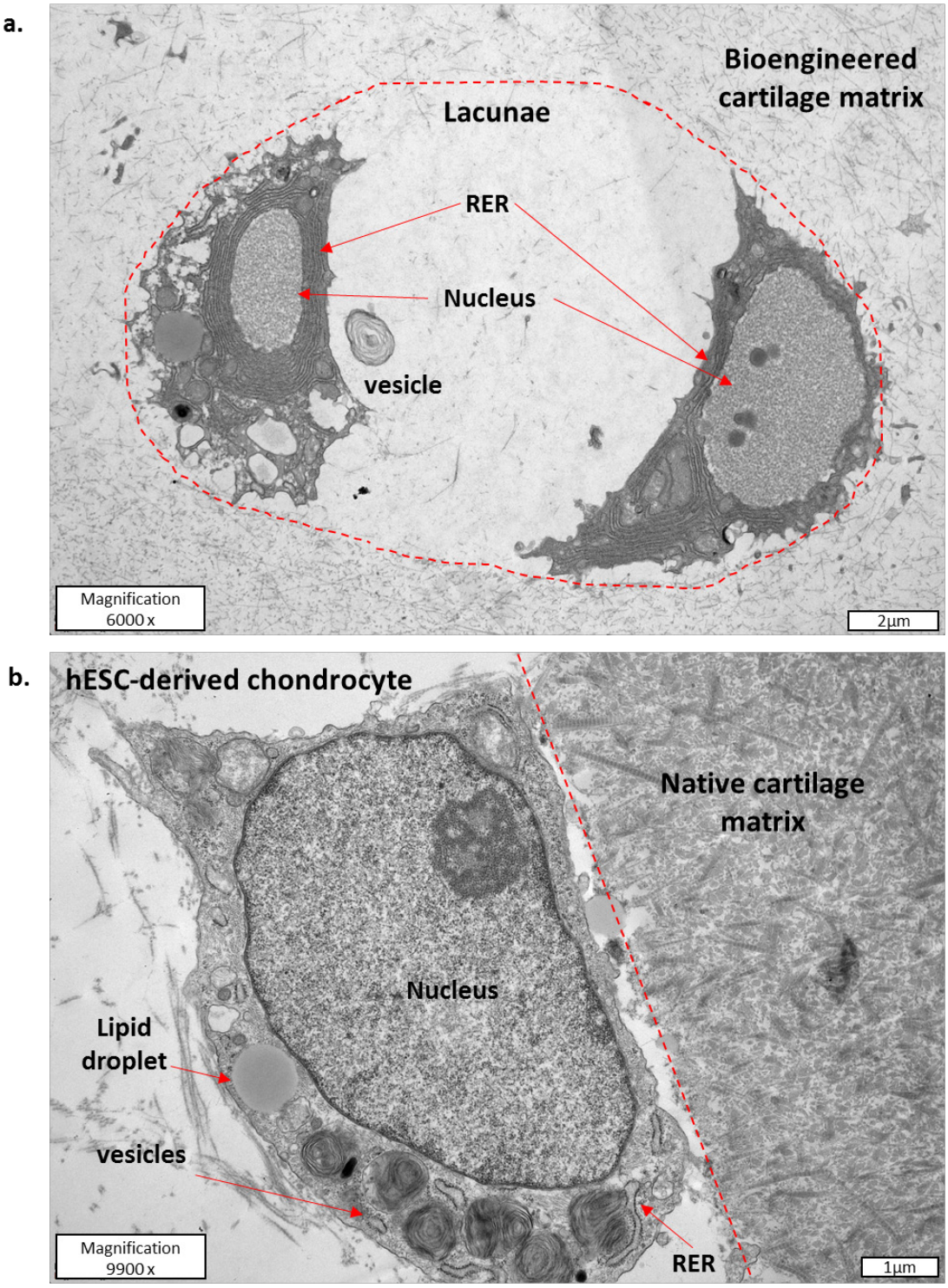

Figure 6.14 **TEM of chondrocytes in hESC-derived cartilage.**

Ultra-thin sections were cut from resin embedded co-culture tissue samples and imaged using TEM. a. shows two hESC-derived chondrocytes in a lacunae in the neocartilage region of the co-culture. b. shows a hESC-derived chondrocyte at the native cartilage border.

6.5 Discussion

NICE recently published guidelines that support the application of Autologous Chondrocyte Implantation (ACI) for patients with symptomatic articular cartilage defects in the knee (NICE, 2017). Those eligible for this treatment form only a small subpopulation of the total number of patients suffering from cartilage damage, however it is a step towards using tissue engineering strategies to treat damaged cartilage. Current ACI techniques involve using cells and scaffold materials to repair damaged tissue. Whilst ACI has been effective in certain cases, there are several potential issues related to cell-based therapies such as donor site morbidity, HAC dedifferentiation and generation of fibrocartilage to name a few. Cartilage tissue engineering using hESC-derived chondrocytes can overcome the issues associated with cell-based therapies for osteoarthritis and may provide a treatment solution for patients with more complex cartilage damage than those outlined in the NICE guidelines.

A recurring issue with cartilage tissue engineering is scale up. Typically, cartilage constructs generated *in vitro* are around 1mm in size. Diffusion distances greater than this are predicted to result in poor quality and tissue necrosis (Muschler et al., 2004). This limitation in size is a barrier to using 3D tissue engineering strategies to treat cartilage damage in the clinic as lesions are usually larger than 1mm when they become symptomatic, and the patient would therefore require the introduction of multiple tissue constructs into the defect in combination with a scaffold material to secure the implanted tissue. Here it has been demonstrated that large (>6mm) hyaline neocartilage constructs, with a thickness equivalent to that of native cartilage, can be generated from hESC-derived chondrocytes during 16-week co-culture with native cartilage. To my knowledge, this is the first time healthy hyaline cartilage construct of the proportions achieved here has been generated. Despite the large volume of neocartilage generated, the tissue did not show signs of poor nutrient diffusion as the tissue was not necrotic. Histologically the majority of the neocartilage generated was very similar to native cartilage, with high proteoglycan content and chondrocyte lacunae. Interestingly, the neocartilage was hypercellular relative to the native tissue. This is likely due the cell origin, as hESCs have an inherently high capacity for proliferation, unlike HACs.

A critical consideration for implantation of bioengineered cartilage is that it must integrate with the native tissue and be capable of repairing defects. During co-culture with native cartilage the hESC-derived chondrocyte neocartilage showed signs of integration with the native tissue in certain regions. However, in other regions, such as the immature fibrous tissue, there was a clear gap between the native and neocartilage. However, the fibrous outgrowths from the mature neocartilage did provide anchorage to the native tissue that could be seen to wrap around the

native cartilage. It is possible that with prolonged culture, these anchorage regions or immature tissue would eventually mature, becoming hyaline-like cartilage tissue. This hypothesis is based on the observation made in Chapter 5 that a pellet cultured for 13-weeks contained only a small region of mature proteoglycan rich tissue yet was rich in type II collagen, but by 19-weeks the pellet comprised almost entirely or mature proteoglycan rich neocartilage with a relative decrease in collagen content. Furthermore, French et al. (1999) demonstrated that type II collagen mRNA expression preceded expression of the proteoglycan perlecan during mouse embryogenesis. This is in line with the finding that suggest a collagen rich template is formed initially before proteoglycan accumulation and maturation. Whilst it is difficult to fully evaluate how well integrated the two tissues are, it is clear that the neocartilage is not simply resting atop the native tissue as the samples survived histological processing, a procedure with persistent sample agitation, without the two tissues disconnecting. Furthermore, in the defect repair model the neocartilage has shown clear signs of integration with the native cartilage within the defect. In this model there was no clear demarcation between the native and neocartilage like that observed in the co-culture model. It is possible that the hESC-derived chondrocytes were able to generate neocartilage that fused better with damaged tissue and resulted in the active repair of the defect.

Having generated such a large hyaline cartilage construct in a short space or time, I was interested in investigating the growth and remodelling dynamics of the tissue. Within the cartilage construct there were at least two distinct subpopulations of hESC-derived chondrocytes. The first are the mature chondrocyte cells that exist within lacunae and appear similar to the HACs of the native cartilage; expression of the early chondrogenic factor SOX9 could not always be detected by IHC in these cells, and they were surrounded by a proteoglycan rich matrix. The second population of cells were localised to the periphery of the neocartilage in the fibrous regions. These cells were more fibroblastic in appearance but exhibited robust SOX9 expression, along with MMP-13, Connexin-43 and Ki67. Articular cartilage is a zonal tissue (Chapter 1, see section 1.2.1) with distinct subpopulations of chondrocytes with varying morphology. The 2 subpopulations of cells observed in the hESC-derived chondrocyte neocartilage are similar to the rounded resting chondrocytes of the middles and deep zone cartilage, whilst the more fibroblastic cells are similar to the flattened chondrocytes of the superficial zone. This suggests that the neocartilage here has spatial patterning reminiscent of articular cartilage.

The neocartilage itself was comprised largely of what appeared to be mature hyaline-like cartilage, but also contained regions of immature fibrous tissue. I hypothesised that the hESC-derived chondrocytes initially, and rapidly, generated a collagen rich matrix lacking proteoglycans, which is later remodelled by collagen modifying enzymes and the production of proteoglycans

such as Aggrecan. This hypothesis was based on the observation that the fibrous tissue in the organotypic cultures had a similar appearance to the pellets generated after short culture periods in Chapter 5, and that this tissue appears to be localised to the periphery of the construct suggesting the observed immaturity is likely due to its naive state. This theory was strengthened by the observation that the expression of the enzyme MMP-13 was localised to the fibrous regions and not observed in the mature hyaline neocartilage. Regions containing MMP-13 expressing cells were found to be rich in type I and type II collagen; whilst type II collagen is a constituent of hyaline cartilage, type I collagen is associated with fibrous cartilage. This suggests that the hESC-derived chondrocytes initially produce an extracellular matrix that is not specifically hyaline but is remodelled to become more hyaline-like by matrix remodelling enzymes such as MMP-13. Whilst MMP-13 expression has become associated with the onset of osteoarthritis, it is also reported to be expressed during foetal femur development (de Andrés et al., 2013) and has even been reported to be constitutively expressed in human chondrocytes (Yamamoto et al., 2016). Expression of MMP-13 by hESC-derived chondrocytes may therefore be due to the chondrocytes developmental state, rather than an indicator of something pathological.

Cells in this fibrous region were also found to be highly proliferative as demonstrated by Ki67 expression, unlike the mature cells confined to their lacunae in the mature neocartilage. The laying down of a collagen rich fibrous ECM before subsequent maturation was likely enabled by this highly proliferative sub-population of hESC-derived chondrocytes. Their relatively high proliferation rate compared to the less active chondrocytes in the more mature regions probably enabled the rapid generation of ECM which provided a template for remodelling into a mature hyaline cartilage matrix.

As previously discussed in Chapter 5, Connexin-43 is a gap junction protein (GJP) that is thought to play an important role in cartilage development (Gago-Fuentes et al., 2016; Schwab et al., 1998). Here Connexin-43 was found to be expressed in the fibrous regions of the construct, indicating that these regions may be in the process of maturation.

Histological evaluation suggested that the mature hESC-derived chondrocytes were similar to the HACs in native cartilage, this was further investigated by examining the ultrastructure of the cells and the tissue they generated via TEM imaging. hESC-derived chondrocytes were observed to be actively producing collagen fibrils and releasing them into the extracellular environment. Collagen fibrils were found to be randomly orientated in the ECM. Interestingly the ECM of the bioengineered tissue appeared less dense than that of the native cartilage when examined via TEM. This difference in the ECM was not something that was observed at the histological level, and it is unclear as to which matrix components are responsible for this distinction. It may be due

to proportional differences in a single matrix component such as type II collagen, or a group of components such as multiple types of collagen, or differences across a range of ECM components. Whilst the banding of collagen makes it easily identifiable, other ECM components such as proteoglycans are less easy to distinguish.

With regard to the cell ultrastructure, hESC-derived chondrocytes generally appeared healthy, with large centrally located nuclei, lipid droplets characteristic of chondrocytes and large quantities of rough endoplasmic reticulum (RER). The cellular machinery of the hESC-derived chondrocytes is ideal for extracellular matrix synthesis due to the abundance of RER in the cytoplasm. Interestingly, there were a number of large vesicles containing concentric whorled structures that were found in close proximity to the RER. Few studies were found in the literature that reported observing these structures making it difficult to identify the vesicles. Similar looking vesicles have been observed in lung (Gil and Reiss, 1973) and synovial cells (Schwarz and Hills, 1996) and have been termed lamellar (or multilamellar) bodies. These studies suggested that the lamellar bodies contained surfactants. It is possible that the vesicles observed in the hESC-derived chondrocytes contain the surface-active mucinous glycoprotein lubricin, as this was proposed to be a component of the vesicular bodies in Schwarz and Hills (1996) and is a component of cartilage. Lubricin is known to bind cartilage proteins such as Cartilage Oligomeric Matrix Protein, fibronectin and type II collagen to the cartilage surface and lubricate the cartilage surface (Flowers et al., 2017). Similar structures have also been identified in chondrocytes. Palfrey and Davies (1966) report on the presence of “whorled bodies made up of irregular concentric lamellae of electron-dense material…” with regard to vesicles and dense bodies in chondrocytes as observed via TEM. Whilst the vesicle appearance was described, the content was not defined, and the TEM images did not clearly show these structures. Another report by Roy and Meachim (1968) observed presence of whorled vesicles in chondrocytes within human articular cartilage. Here they described the vesicles as “residual bodies”, a term relating to late-stage lysosomes, suggesting that the vesicles observed here may contain lysed cellular components in the process of exocytosis. The relatively high number of these vesicles observed within the hESc-derived chondrocytes may be indicative of impaired cellular transport, potentially caused by long-term culture, or may be a result of the cells being highly active in the generation of extracellular matrix.

It is unclear as to why the different organotypic models (co-culture vs defect) resulted in such contrasting results. The defect culture appeared to result in better integration compared to co-culture, and did not generate the volume of tissue observed in the co-culture model. It is possible that hESC-derived chondrocytes have the ability to detect damaged tissue and integrate more fully with it, whereas when tissue is undamaged (as in the co-culture model) cells are not constrained and produce large quantities of hyaline cartilage. However, to properly investigate

these differences and evaluate this hypothesis it would be necessary to increase n-numbers for the defect group as currently this is only one experiment.

As adult articular cartilage is a relatively quiescent tissue, with chondrocytes effectively trapped within the cartilage in lacunae, it is assumed that the cells responsible for generating the neocartilage are hESC-derived chondrocytes. With long term experiments, labelling cells can be difficult as temporary cell labelling dyes typically only last for a few cell generations. Here, pellets are cultured for 16-weeks, the equivalent of approximately 200 cell-divisions (assuming this occurs every 48h). A more practical solution would be to perform immunohistochemistry using a Y-chromosome specific antibody such as SRY to detect the hESC-derived chondrocytes as the HUES7 line from which they were generated is karyotypically XY. In experiments where the native cartilage is from a female donor, this would enable confirmation of the origin of the cells within the neocartilage. A time course experiment whereby samples are collected at 8-, 12- and 16-weeks would also help elucidate how the tissue matures, and whether maturation/proteoglycan accumulation occurs first at the site the original pellet was implanted, or if maturation is initiated elsewhere.

The results of this *ex-vivo* study provide compelling grounds for future *in vivo* experimentation in a lapine partial thickness defect model. Further *in vitro* work would involve culturing hESC-derived cartilage pellets for the same time period as the organotypic culture with and without co-culture native tissue and investigating the contribution of the native tissue to neocartilage generation. It would also be of interest to create a larger organotypic defect as osteoarthritic lesions often extend beyond $1mm^2$. As it was observed that the neocartilage extended out of the defect and created nodules of neocartilage in discrete regions, joined by fibrous tissue, it would be of interest to create a central defect in which a pellet is placed with multiple distal defects located away from the implantation site to investigate whether the hESC-derived chondrocytes are able to 'home' to damaged sites.

A critical, but currently unanswered, question from this study is whether the neocartilage growth would be controlled if the tissue was transplanted *in vivo*. Uncontrolled tissue growth is a concern with regards to stem cell-based treatments as the resulting and undesired tumour formation could have serious consequences. I hypothesise that if used in an *in vivo* partial thickness defect, signals from the external environment, both mechanical and chemical, may provide the appropriate cues for the cells to repair the damage without producing excess cartilage. In the *ex vivo* organotypic culture setting the tissue and cells was not subjected to any mechanical forces such as the compression and friction that occurs in a physiological setting. It is also likely that the cells were not receiving the same chemical cues they would usually receive from the native

cartilage as the health of the native tissue was not maintained during culture. Mechanical cues are known to be important for cartilage tissue homeostasis and matrix biosynthesis (Bader et al., 2011; Kim et al., 1994). Whilst it is possible that more physiological *ex vivo* set up including some form of mechanical compression could be devised, ultimately this needs to be tested *in vivo* before this theory can be fully elucidated.

With regards to scale up and clinical translation, the ability to generate the large quantities of neocartilage observed in the co-culture model could stimulate ideas about creating a "cartilage-farm" whereby large neocartilage constructs are generated via this method and harvested for clinical applications. Whilst this could be scaled up, the culture of pellets on donor cartilage is not likely to be considered appropriate for clinical application. Regardless, this would probably be an unnecessary step. Here the results show that a small hESC-derived chondrocyte pellet that has been cultured for just 4 weeks in pellet culture is capable of generating hyaline neocartilage exceeding 6 mm in diameter following 16-weeks culture with native cartilage. This volume of cartilage is sufficiently large for clinical applications, and requires only one small pellet. It is therefore possible that the implantation of a single 4-week hESC-derived chondrocyte pellet into a cartilage defect, would enable the replacement of damaged/lost cartilage. Scale up would therefore be at the differentiation stage to enable the generation of more pellets; something that could be enabled by use of bioreactors.

In summary, this chapter has demonstrated that hESC-derived chondrocytes are capable of producing healthy hyaline cartilage constructs larger than have previously been reported in the literature. Furthermore, these constructs did not show any signs of necrosis, and were able to repair partial thickness defects in an organotypic model. This research has provided evidence for the efficaciousness of hESC-derived chondrocytes as a potential cell source for regenerating and repairing damaged cartilage.

Chapter 7 Final discussion

The ability to generate large quantities of hyaline cartilage *in* vitro is of significant clinical relevance due to the high prevalence of osteoarthritis. This is the first report describing the generation of hyaline neocartilage from hESC-derived chondrocytes that is of clinically relevant proportions. Moreover, the cartilage was both mechanically and morphologically similar to native cartilage and able was to repair a partial thickness defect in an *ex vivo* organotypic culture model. Intriguingly, co-culture of hESC-derived cartilage pellets with native cartilage enabled the generation of large hyaline neocartilage explants exceeding 6mm in diameter without showing signs of tissue necrosis. Thus, this work holds great promise for the treatment of damaged cartilage.

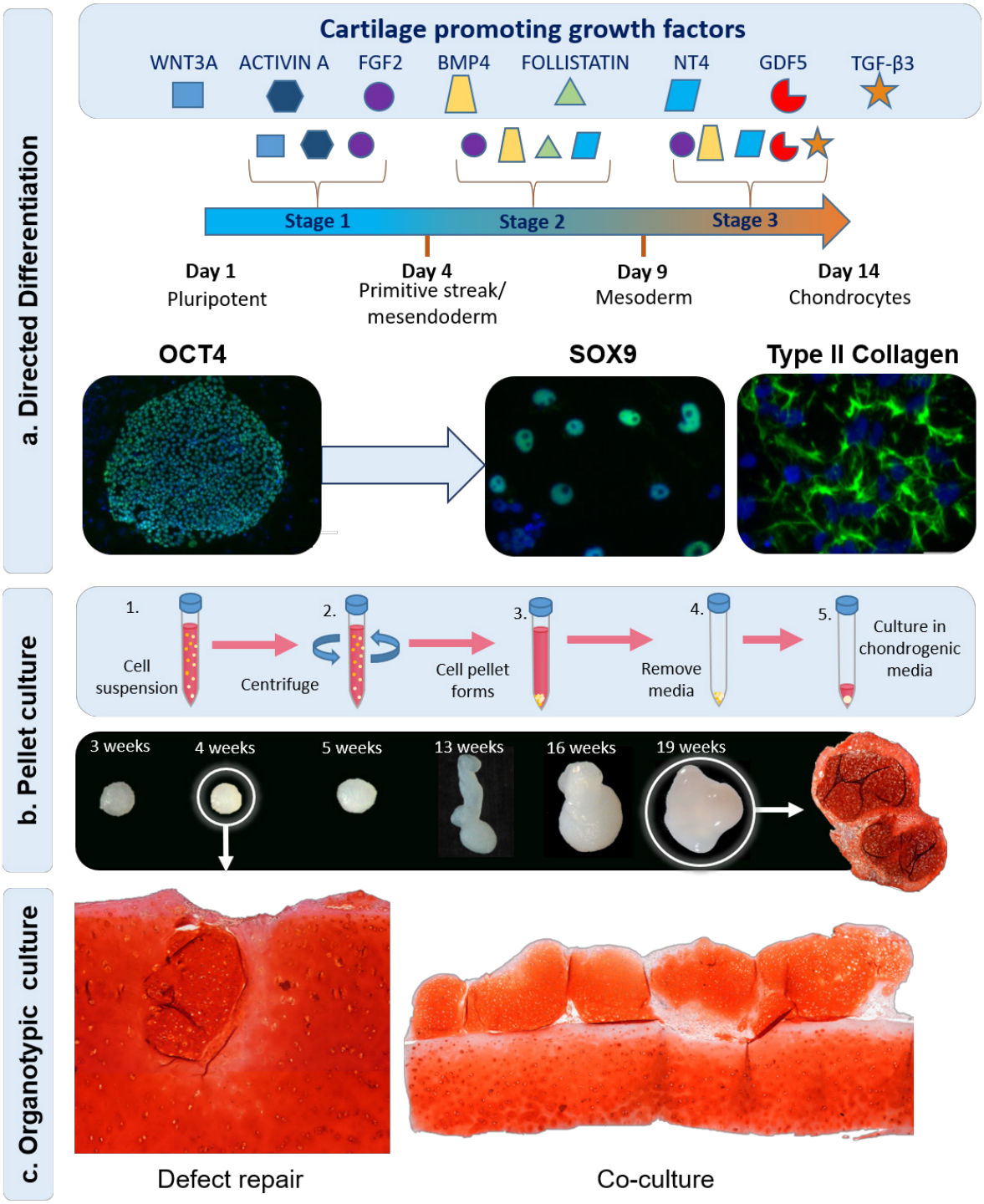
a. Directed Differentiation
Cartilage promoting growth factors
WNT3A
ACTIVIN A
FGF2
BMP4
FOLLISTATIN
NT4
GDF5
TGF-β3
Stage 1
Stage 2
Stage 3
Day 1
Pluripotent
Day 4
Primitive streak/
mesendoderm
Day 9
Mesoderm
Day 14
Chondrocytes
OCT4
SOX9
Type II Collagen
b. Pellet culture
1.
Cell
suspension
2.
Centrifuge
3.
Cell pellet
forms
4.
Remove
media
5.
Culture in
chondrogenic
media
3 weeks
4 weeks
5 weeks
13 weeks
16 weeks
19 weeks
c. Organotypic culture
Defect repair
Co-culture

Figure 7.1 **Schematic representation of cartilage generation from hESCs**

hESCs were cultured and differentiated at 5% O_2 via a directed differentiation protocol resulting in the generation of hESC-derived chondrocytes. These cells robustly expressed the chondrogenic markers SOX9 and Type II Collagen (a). hESC-derived chondrocytes formed hyaline-like cartilage in pellet culture following 19-weeks culture (b). hESC-derived cartilage pellets cultured for 4-weeks repaired a partial thickness defect in ex vivo organotypic culture during a 16-week culture period. In an ex vivo organotypic co-culture model, hESC-derived cartilage pellets generated large hyaline neocartilage exceeding 6mm in diameter.

To successfully treat cartilage damage, it is important to replace the tissue with high quality hyaline cartilage. It is therefore critical that tissue quality is assessed by first generating neocartilage *in vitro.* Pellet culture is generally considered the gold standard for *in vitro* cartilage generation. However, it is doubtful that this culture method would permit the generation of tissue constructs of a clinically relevant size as pellets typically measure ~1mm diameter. If larger pellets are allowed to form they typically contain necrotic cores (Li et al., 2014c; Muschler et al., 2004). Interestingly, using hESC-derived chondrocytes it was possible to generate large constructs (up to 4 mm diameter) without central tissue necrosis, suggesting that nutrient diffusion in these constructs is not as limited as the literature suggested (Li et al., 2014c; Muschler et al., 2004). This may be an innate characteristic of the hESC-derived chondrocytes themselves, or properties of the cartilage tissue generated.

Whilst hESC-derived chondrocyte pellets were relatively large, it was not until 19-weeks culture that the distribution of proteoglycans was homogenous, and the tissue appeared truly hyaline. It takes hESC-derived chondrocytes approximately 6-times longer than HACs to develop a homogenous distribution of proteoglycans in the ECM. Whilst the composition of the chondrogenic medium used in this study was sufficient for proteoglycan synthesis in HACs it was not able to stimulate proteoglycan synthesis by hESC-derived chondrocytes within the same timeframe; whilst the chondrogenic media contains numerous pro-chondrogenic factors, it is unlikely to fully replicate the signalling milieu cells are exposed to *in vivo*. With this is mind, further work to reduce this time frame may be beneficial; a potential method may be the introduction of growth factors such as BMP7 and IGF-1 to the chondrogenic medium to enhance proteoglycan synthesis (Asanbaeva et al., 2008; Loeser et al., 2003) thereby decreasing culture time.

The ability to withstand physiological forces is important as human articular cartilage can be subject to forces in the region of 18 MPa *in vivo* (Hodge et al., 1986). hESC-derived cartilage pellets cultured for 4-weeks have an elastic modulus (E) comparable to native cartilage. Thus, it is possible that a hESC-derived cartilage pellet cultured for 4-weeks could be implanted into a cartilage defect, and having a similar E to the surrounding tissue, could be expected to withstand the physiological forces cartilage is subjected to *in vivo*. With time the bioengineered tissue would presumably begin synthesising proteoglycans, as was observed *in vitro*. This process may be accelerated *in vivo* due to exposure to signals from the extracellular environment. This could be fully tested by preclinical *in vivo* animal studies.

Our *ex vivo* organotypic cultures provided two valuable and clinically relevant findings: hESC-derived cartilage pellets can repair cartilage defects, and hESC-derived chondrocytes can generate large hyaline cartilage constructs of clinically relevant size.

7.1 Clinical relevance

The ability to generate large neocartilage constructs of the proportions reported here is of clinical significance. One of the reported limitations of static scaffold free tissue engineering is the difficulty of scale up and maintaining healthy tissue. As diffusion distances increase, access to nutrients becomes limited (Muschler et al., 2004). Remarkably, such an issue was not observed with scaffold-free generated hESC-derived neocartilage as there was no apparent sign of tissue necrosis based upon histological evaluation.

In October 2017 NICE released new guidelines that supported the application of Autologous Chondrocyte Implantation (ACI) for patients with symptomatic articular cartilage defects in the knee (NICE, 2017). Currently, NICE recommends ACI only for patients who have not undergone previous knee surgeries, have defects over 2 cm^2 and have minimal evidence of OA. Whilst the patient cohort that this description identifies is relatively niche with regards to the population of patients suffering from cartilage disease and injury, it is conceivable that with certain modifications, such as the ability to generate larger neocartilage repair tissue *in vitro*, this type of treatment could be made suitable for a broader patient cohort and become more widely available in the future. Current ACI techniques involve using cells and collagen membranes to repair damaged tissue. Whilst ACI has been effective in certain cases, there are a number of potential issues related to cell-based therapies such as donor site morbidity, HAC dedifferentiation and generation of fibrocartilage to name a few.

The research described in this thesis offers the exciting potential to make a step-change improvement in current surgical techniques such as ACI used to treat early stage OA. Here, the ability for large hESC-derived cartilage constructs to be cultured *in vitro* and transplanted into a partial-thickness chondral defect, resulting in defect repair has been demonstrated. Whilst the ability to generate large neocartilage constructs via the co-culture method described would facilitate scale up of the *in vitro* tissue engineered cartilage, something that has remained a stumbling block within the field until now, the requirement for native cartilage explants is impractical. The exchange of unknown factors between the native and bioengineered tissue is a concern, as is the source of the tissue which is likely to be from patients with cartilage disease. Instead, I propose that the transplantation of small (4-week) cartilage pellets could result in repair of the damaged region even if the area is much larger than the original pellet. Pellets would be

generated and cultured *in vitro* for 4-weeks, at which point they would be ready to transplant into a patient. hESC-derived cartilage pellets cultured for 4-weeks have an elastic modulus (E) comparable to native cartilage. Thus, it is possible that a hESC-derived cartilage pellet cultured for 4-weeks could be implanted into a cartilage defect, and having a similar E to the surrounding tissue, could be expected to withstand the physiological forces cartilage is subjected to *in vivo*. As observed *in vitro*, the implanted pellet would most likely begin synthesising proteoglycans and would resemble native cartilage over time. This process may be accelerated *in vivo* due to exposure to signals from the extracellular environment. As the implanted pellet would be smaller than the defect area, a fibrin glue or matrix may be required to prevent the pellet from being dislodged.

For clinical translation, optimisation of pellet generation would be required. An automated approach and use of bioreactors to scale up pellet generation would be advantageous. Use of stirred-suspension bioreactors has been shown to induce aggregation of chondrocytes in culture and maintain their differentiated phenotype (Gigout et al., 2009; Lee et al., 2011b). This would enable increased throughput of pellet culture, however there would be less control over cell numbers in the aggregates.

The scaffold free nature of this approach is particularly appealing as it circumvents the potential issues associated with scaffold materials such as biofunctionality, biocompatibility, degradation rates and immunogenicity of the degradation products which can pose significant issues (Johnstone et al., 2013; Vacanti and Langer, 1999).

7.2 Future work

- hESCs

Further *ex-vivo* organotypic defect and co-cultures are required to increase n-numbers.

- hiPSCs.

The next phase of this work would involve testing the process of bioengineering cartilage from pluripotent stem cells *in vitro* using an alternative source of pluripotent stem cells. hiPSCs are of significant clinical interest as they offer the potential for personalised medicine which would negate any potential issues of immunogenicity. This work will involve generating hiPSC-derived chondrocytes and generating cartilage *in vitro*. Defect repair will be tested using a partial thickness *ex vivo* organotypic defect model.

- *In vivo*

For clinical applications of hESC-derived cartilage to become a possibility it is important that an *in vivo* study is conducted. This would involve creating a partial thickness defect in the lateral femoral condyle articular cartilage in rabbit knees and implanting a hESC-derived cartilage pellet. Samples of the joint would be collected after 6 months and examined histologically to determine how well the neocartilage integrated with the native tissue, and whether it could be contained to the defect region. If successful in the rabbit model, further testing in a large weight bearing animal model such as sheep or pig would be required.

- Phase I clinical trials

Following successful pre-clinical studies, research would progress to phase I clinical trials.

Appendix A

7.3 Mathematica code for generating E from full thickness native cartilage

```
In[]:= SetDirectory[NotebookDirectory[]];

In[]:= (*Import measured force data - ENTER FILE PATH & Sheet
  number if needed (first number in square bracket
  before All),
 e.g. case sheet number = sample number for F62*)CompleteForce=Import[
    "..."][[All,5]];

In[]:= (*Remove title from data*)CompleteForce = Delete[CompleteForce,1];

In[]:= (*Import measured distance from baseplate data - ENTER FILE PATH*)
  CompleteHeight=Import["..."][[All,7]];
In[]:= (*Remove title from data*)CompleteHeight=Delete[CompleteHeight,1];

In[]:= (*ENTER SAMPLE THICKNESS (mm) AND SURFACE AREA HERE
  (mm2)*) d=1.4; A = 25;

In[]:= (*Convert distance from baseplate into indentation -
   The adjusted force number shouldn't change (0.1
  default), unless graph obviously shows very flat
  region,
  then increase this by 0.05 until straight line is
  evident*)
  CompleteIndentation=d-CompleteHeight +1;
  AdjustedForce = CompleteForce-0.1;

In[]:= (*Remove values before plate touches pellet*)
  IndentationRange=Select[CompleteIndentation,#≥0&];

In[]:= ForceRange=Select[AdjustedForce,# ≥0&];

In[]:= (*Combine data*)
  ForceIndentationData={IndentationRange,ForceRange};

In[]:= (* Flatten data into 1 list*)
  FIData=ForceIndentationData~Flatten~{2};

In[]:= Map1=Map[Length,FIData,{1}];

In[]:= (*Count single points*)
  Num=Count[Map1,1];

In[]:= (*Compile useful data range*)
  FIDataUseful=Drop[FIData,-Num];
```



```
In[]:= (*Plot graph of full data*)FullDataPlot=ListPlot[FIDataUseful,
```

```
PlotRange->Full, AxesStyle→Directive[Black,16,FontFamily→"Arial"],
LabelStyle→Directive[Black,16,FontFamily→"Arial"],
Frame→True,
FrameStyle→Directive[Black,14,FontFamily→"Arial"],
FrameLabel→{"Indentation (mm)","Force (N)"],
GridLines→Automatic]
```

Out[]=

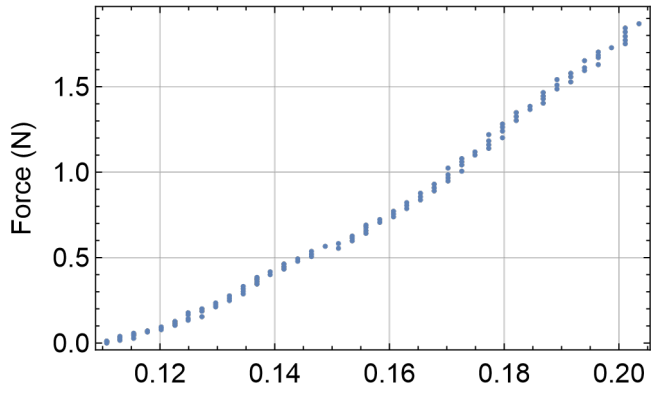

In[]:=
```
(*ADD INDENTATION OFFSET IF NEEDED -this is the lowest number on the x axis*)
offset=0.11;
FIDataOffset=Map[#+{-offset,0}&,FIDataUseful,{1}];
```

In[]:=
```
(*Limit data to initial region =
 NUMBER OF DATA POINTS -normally 200-400 is a good
range,  if 200 doesn't work just put All*)
LimitedData=Part[FIDataOffset,1;;All];
```

In[]:=
```
(*Plot inital region*)LimitedDataPlot=
 ListPlot[LimitedData,AxesStyle→Directive[Black,16,FontFamily→"Arial"],
  LabelStyle→Directive[Black,16,FontFamily→"Arial"],
  Frame→True,
  FrameStyle→Directive[Black,14,FontFamily→"Arial"],
  FrameLabel→{"Indentation (mm)","Force (N)"],
  GridLines→Automatic]
```

Out[]=

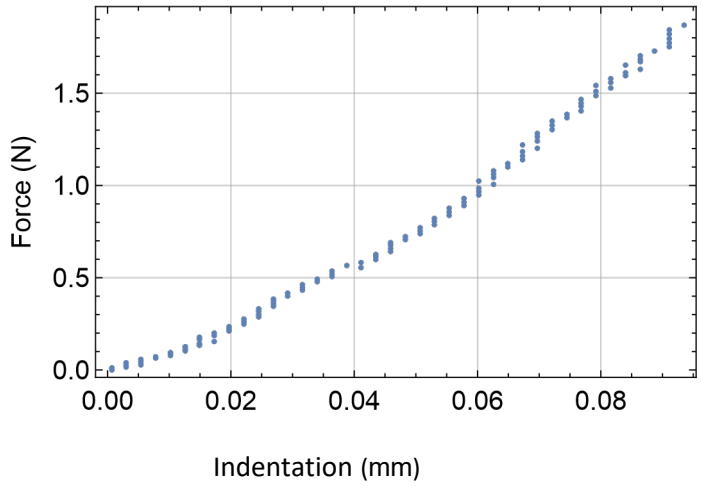

In[]:=
```
LimitedData[[All, 1]];
```


In[]:=
```
(* Create model based on simple equation *)
```

```
NLMO = NonlinearModelFit[LimitedData, a*25*x, a, x, ConfidenceLevel→0.95]
```

Out[]= FittedModel[17.6826 x]

```
(*Identify properties of model wanted*)
NLMO["Properties"];
```

```
{IdentifiedParameters, CalculatedConfidenceInterval, Residuals} =
  NLMO[{"BestFitParameters", "ParameterConfidenceIntervals", "FitResiduals"}];
```

```
(*Create line based on model*)
ModelCurve = Plot[(a*A*x) /. IdentifiedParameters, {x, 0, 0.9},
  PlotStyle→Red, AxesStyle→Directive[Black, 16, FontFamily→"Arial"],
  LabelStyle→Directive[Black, 16, FontFamily→"Arial"],
  Frame→True,
  FrameStyle→Directive[Black, 14, FontFamily→"Arial"],
  FrameLabel→{"Indentation (mm)", "Force (N)"},
  GridLines→Automatic]
```

Out[]=

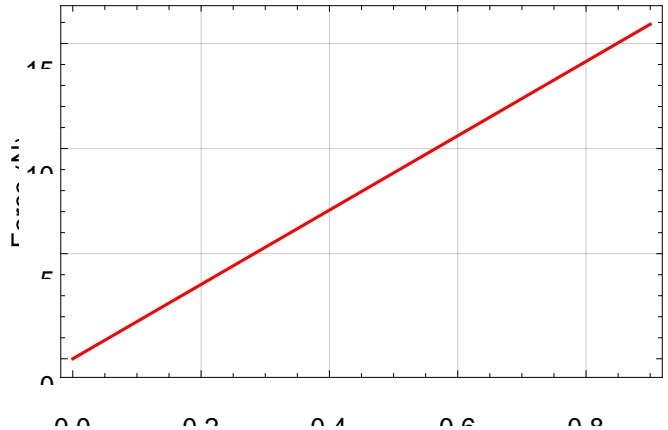


```
Show[LimitedDataPlot, ModelCurve]
```

Out[]=

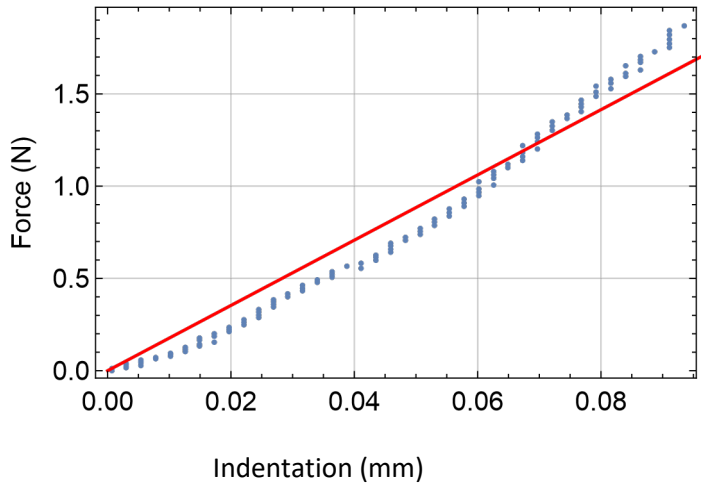


```
YoungsModulus = {a} /. IdentifiedParameters
```

Out[]= {0.990225]

```
In[]:= NLMO["ParameterConfidenceIntervals"]
Out[]= {{0.969113,1.01134]]

In[]:= NLMO["AdjustedRSquared"]
Out[]= 0.986047
```

7.4 Mathematica code for generating E from cartilage pellets

```
In[]:= SetDirectory[NotebookDirectory[]];

In[]:= (*Import measured force data - ENTER FILE PATH*)
       CompleteForce=Import["…"][[All,5]];

In[]:= (*Remove title from data*)CompleteForce = Delete[CompleteForce,1];

In[]:= (*Import measured distance from baseplate data - ENTER FILE PATH*)
       CompleteHeight=Import[
            "…"][[All,7]];

In[]:= (*Remove title from data*)CompleteHeight=Delete[CompleteHeight,1];

In[]:= (*ENTER PELLET DIAMETER HERE*)
       d=2.392065;

In[]:= (*Calculate pellet radius*)
       R=d⁄2;

In[]:= (*Adjust force data for any offset - ADD IN VALUE
       HERE, this gets rid of noise, normally 0.01 is
       about right*) AdjustedForce=CompleteForce-0.01;

In[]:= (*Convert distance from baseplate into indentation*)
       CompleteIndentation=d-CompleteHeight;

In[]:= (*Remove values before plate touches pellet*)
       IndentationRange=Select[CompleteIndentation,#≥0&];

In[]:= Length[IndentationRange]
Out[]= 2660

In[]:= (*Remove force values before plate touches*)

In[]:= ForceRange=Select[AdjustedForce,# ≥0&];

In[]:= Length[ForceRange]
Out[]= 563

In[]:= (*Combine data*)
       ForceIndentationData={IndentationRange,ForceRange];

In[]:= (* Flatten data into 1 list*)FIData=ForceIndentationData~Flatten~{2];

In[]:= (* Map number of points through list*)Map1=Map[Length,FIData,{1]];

In[]:= (*Count single points*)
       Num=Count[Map1,1]
```

Out[]= 2097

In[]:=
```
(* Compile useful data range*)FIDataUseful=Drop[FIData,-Num];
```


In[]:=
```
(*Plot graph of full data*)FullDataPlot=
 ListPlot[FIDataUseful,AxesStyle→Directive[Black,16,FontFamily→"Arial"],
  LabelStyle→Directive[Black,16,FontFamily→"Arial"],
  Frame→True,
  FrameStyle→Directive[Black,14,FontFamily→"Arial"],
  FrameLabel→{"Indentation (mm)","Force (N)"],
  GridLines→Automatic]
```

Out[]=

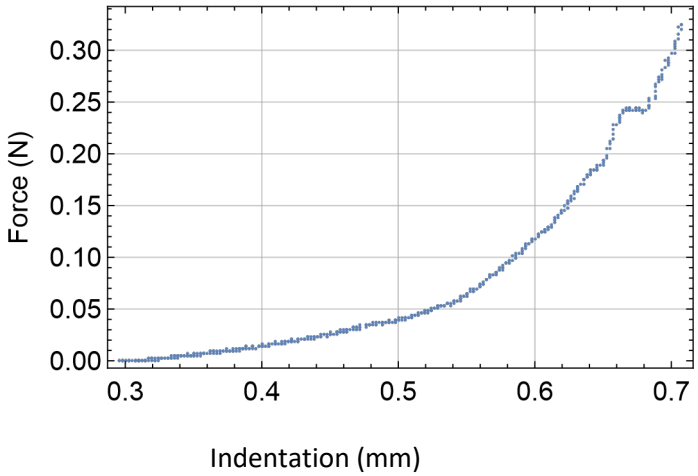

In[]:=
```
(*ADD INDENTATION OFFSET IF NEEDED - this is the lowest number on the x axis*)
offset=0.25;
FIDataOffset=Map[#+{-offset,0}&,FIDataUseful,{1}];
```

In[]:=
```
(*Limit data to initial region =
  NUMBER OF DATA POINTS - normally 200-400 is a good
range*) LimitedData=Part[FIDataOffset,1;;310];
```

In[]:=
```
(*Plot inital region*)LimitedDataPlot=
 ListPlot[LimitedData,AxesStyle→Directive[Black,16,FontFamily→"Arial"],
  LabelStyle→Directive[Black,16,FontFamily→"Arial"],
  Frame→True,
  FrameStyle→Directive[Black,14,FontFamily→"Arial"],
  FrameLabel→{"Indentation (mm)","Force (N)"],
  GridLines→Automatic]
```

Out[]=

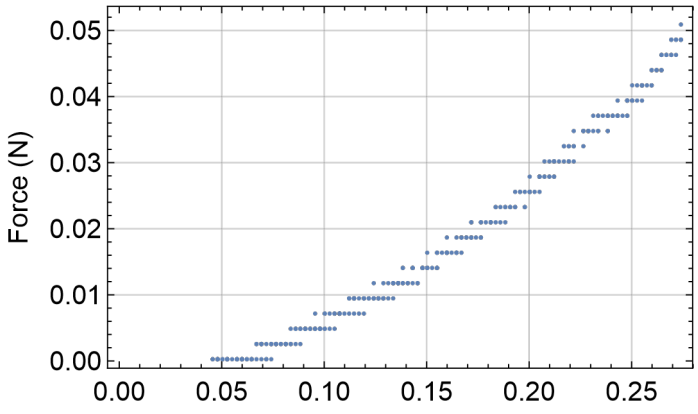

Indentation (mm)

In[]:=
```
(*Create model based on Hertzian theory eq. and data*)
NLMO=NonlinearModelFit[LimitedData,
  [(4*a)/(3*R*0.84)*(x*R)^2]^1.5,a,x,ConfidenceLevel→0.95]
```

Out[]= FittedModel[$0.300701\ x^{1.5}$]

In[]:=
```
(*Identify properties of model wanted*)
NLMO["Properties"];
```

In[]:=
```
(*Name properties of model wanted*)
{IdentifiedParameters,CalculatedConfidenceInterval,Residuals}=
  NLMO[{"BestFitParameters","ParameterConfidenceIntervals","FitResiduals"}];
```

In[]:=
```
(*Create curve based on model*)
ModelCurve=Plot[(4*a)/(3*R*0.84)*(x*R)^2]^1.5]/.IdentifiedParameters,
  {x,0,1.3},PlotStyle→Red,AxesStyle→Directive[Black,16,FontFamily→"Arial"],
  LabelStyle→Directive[Black,16,FontFamily→"Arial"],
  Frame→True,
  FrameStyle→Directive[Black,14,FontFamily→"Arial"],
  FrameLabel→{"Indentation (mm)","Force (N)"],
  GridLines→Automatic]
```

Out[]=

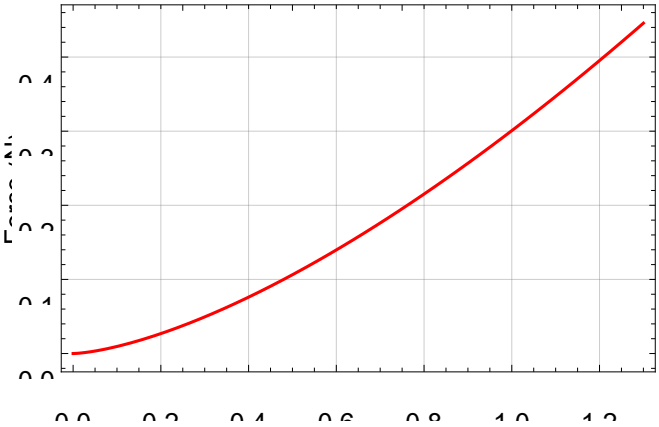

Indentation (mm)

In[]:=
```
Show[LimitedDataPlot,ModelCurve]
```

Out[]=

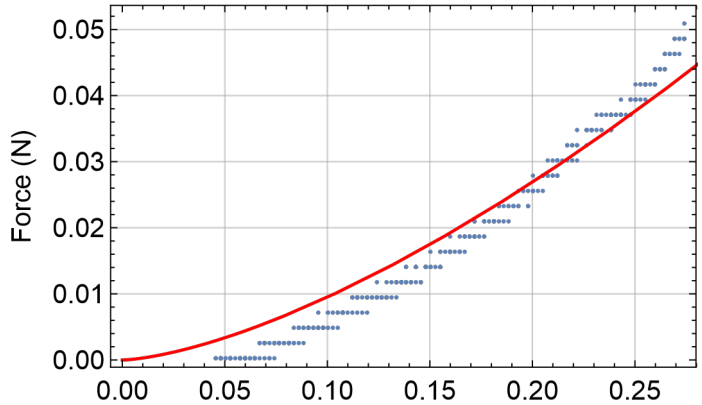

Indentation (mm)

In[]:= **YoungsModulus={a}/.IdentifiedParameters**

Out[]= {0.489947}

In[]:= NLMO["ParameterConfidenceIntervals"]

Out[]= {{0.482387,0.497508}}

In[]:= **NLMO["AdjustedRSquared"]**

Out[]= 0.98129

Appendix B Review article

Review

For reprint orders, please contact: reprints@futuremedicine.com

Regenerative Medicine

Augmentation of musculoskeletal regeneration: role for pluripotent stem cells

Lauren A Jevons[1], Franchesca D Houghton*,[1] & Rahul S Tare**,[1,2]

[1]Centre for Human Development, Stem Cells & Regeneration, Faculty of Medicine, University of Southampton, Southampton, SO16 6YD, UK

[2]Department of Mechanical Engineering, Faculty of Engineering & the Environment, University of Southampton, Southampton, SO17 1BJ, UK

* Author for correspondence: Tel.: +44 2381 208731; F.D.Houghton@soton.co.uk

** Author for correspondence: Tel.: +44 2381 205257; R.Tare@soton.ac.uk

The rise in the incidence of musculoskeletal diseases is attributed to an increasing ageing population. The debilitating effects of musculoskeletal diseases, coupled with a lack of effective therapies, contribute to huge financial strains on healthcare systems. The focus of regenerative medicine has shifted to pluripotent stem cells (PSCs), namely, human embryonic stem cells and human-induced PSCs, due to the limited success of adult stem cell-based interventions. PSCs constitute a valuable cell source for musculoskeletal regeneration due to their capacity for unlimited self-renewal, ability to differentiate into all cell lineages of the three germ layers and perceived immunoprivileged characteristics. This review summarizes methods for chondrogenic, osteogenic, myogenic and adipogenic differentiation of PSCs and their potential for therapeutic applications.

First draft submitted: 10 August 2017; Accepted for publication: 6 December 2017; Published online: 20 March 2018

Keywords: adipogenesis • chondrogenesis • human embryonic stem cells • human-induced pluripotent stem cells • musculoskeletal regeneration • myogenesis • osteogenesis • pluripotent stem cells • tissue engineering

Socioeconomic burden of musculoskeletal deterioration

Non-communicable disorders affecting the musculoskeletal system are a major cause of disability and morbidity. A decline in the function of bone, muscle and joint tissues is currently an inescapable consequence of ageing. Due to improved healthcare, longevity has increased; however, while lifespan has improved, a corresponding increase in healthy ageing has not been achieved. As a result, the incidence of musculoskeletal disorders has risen [1]. This has contributed to a huge financial strain on the healthcare systems, as well as on affected individuals [2]. The side effects of these disorders, such as intense and often chronic pain, coupled with decreased mobility, have a dramatic impact on the individual's quality of life. Current surgical and pharmacological treatments are limited in their efficacy [3–6]. Furthermore, the subsequent progressive deterioration of the musculoskeletal system results in an increased risk of falls and fractures [7,8]. The natural healing of fractures is often poor in the older population, and carries a higher risk of mortality [9]. Effective treatments for musculoskeletal disorders are therefore necessary to improve the quality of life of our ageing population, and decrease the burden placed on the healthcare system.

Current interventions for the treatment of major musculoskeletal diseases & their limitations

Osteoarthritis

Osteoarthritis (OA) is the most common joint disease among older adults [10], with a high global prevalence [11] (Table 1). While the percentage of global prevalence remained constant between 1990 and 2010, the years of life lived with disability increased dramatically. Thus, demonstrating the impact of increased lifespan without a corresponding improvement in health span. OA is caused by the degradation of hyaline articular cartilage and the abnormal remodeling of the joint tissues, which results in loss of joint function. Cartilage is avascular, has low cellularity and, therefore, a limited capacity for repair. Daily wear and tear or injury leads to the structural deterioration of articular cartilage at the joint surface. The early stages of OA are characterized by the formation of partial thickness chondral defects. If left untreated, the defects will extend into the marrow spaces of subchondral

Future Medicine

Table 1. Overview of epidemiology and treatment options for musculoskeletal diseases.

Disease	Incidence/risk	Treatments	Drawbacks
OA	• Worldwide incidence of knee OA estimated at 3.8%, and hip OA 0.85% [11]	*Total joint replacement*	Carries some degree of risk [13], late-stage intervention treatment
	• Lifetime risk of developing symptomatic knee OA ~40% in men and ~47% in women, with higher risk for obese individuals [30]	*Reparative techniques:* • Abrasion arthroplasty [14] • Debridement [15] • Microfracture [16]	Limited repair, and typically results in fibrocartilaginous tissue
		Restorative techniques: • Mosaicplasty • ACI [18] • MACI	Invasive procedure to procure chondrocytes, limited cell number, dedifferentiation during monolayer expansion, expensive, only recommended for patients with knee OA with no previous treatments, fibrocartilaginous tissue [31,32]
OP	• Estimated 22 million women, and 5.5 million men being affected within the EU [19] • Worldwide, OP results in over 8.9 million fractures each year	*Pharmacological agents:* *Antiresorptive:* • Oestrogen • Selective oestrogen receptor modulators • Bisphosphonates • Denosumab *Anabolic:* • Full-length parathyroid hormone (PTH1–8) • Teriparatide (PTH1–34) • Strontium ranelate *Other:* • Calcium • Vitamin D	Long-term administration is required, which can lead to poor compliancy Recommendation of taking bisphosphonate 'drug holidays' to reduce long-term adverse events can reduce benefits gained during treatment periods [33]
Myopathies	• 4.6% of men and 7.9% of women with a mean age of 67 in an English cohort study were diagnosed with sarcopenia [25] • Duchenne muscular dystrophy affects 1 in 3500 males worldwide [34]	Resistance exercise [35] Corticosteroids [36] Genetic interventions [37]	Poor adherence, difficulty to carry out without assistance due to inherent frailty of sufferers Delays symptoms only, multiple known severe side effects [36] Large organ to treat. Need to target skeletal and cardiac muscle. Limited success [37]

ACI: Autologous chondrocyte implantation; MACI: Matrix-assisted ACI; OA: Osteoarthritis; OP: Osteoporosis.

bone, giving access to bone marrow stem cells (BMSCs). The repair tissue formed by infiltrating BMSCs is typically fibrous rather than hyaline [12].

Effective treatments for OA are currently lacking (Table 1). Total joint-replacement surgery is widely used, however, the surgeries carry significant risks that increase with patient age [13] and are a late-stage treatment option. Early-stage interventions are available and focus on initiating cell-based repair. Reparative techniques such as abrasion arthroplasty [14], debridement [15] and microfracture [16] aim to encourage infiltration of stem cells from the marrow spaces of the underlying subchondral bone, to stimulate repair of the damaged tissue. Restorative techniques such as mosaicplasty [17] involve removing cartilage plugs from non-load-bearing regions of the joint and implanting them into the osteochondral defect zone. Another restorative surgical technique is autologous chondrocyte implantation (ACI) [18]; here, patient-derived autologous chondrocytes are harvested from the non-load-bearing region of the articular cartilage, expanded in monolayer culture and implanted at the site of the defect underneath a periosteal flap. This technique often utilizes a collagen scaffold to support the implanted cells and is referred to as matrix-assisted ACI (MACI). Following recently published NICE guidelines (4th October 2017), ACI is now a recommended treatment; however, patient selection criteria are restrictive. While ACI has been relatively successful compared with other techniques such as mosaicplasty [17], there are a number of drawbacks associated with the treatment (Table 1).

Osteoporosis

Osteoporosis (OP) is a prevalent osteodegenerative disease, with an estimated 22 million women, and 5.5 million men being affected within the EU [19]. Worldwide, it is estimated that OP results in over 8.9 million fractures annually (Table 1) [20].

OP is characterized by skeletal fragility, with the hallmark of low bone mass (T-score of -2.5 and below) or a prevalent radiographic vertebral fracture [21]. OP is caused by a disruption in bone turnover homeostasis, leading to accelerated trabecular bone loss that results in a more porous structure. OP is also associated with an increased fall risk and high incidence of fracture [7]. OP predominantly affects the older population, and with increased fracture risk there is a corresponding increase in the likelihood of morbidity. Unlike OA, there are a number of effective pharmacological treatments available for OP (Table 1). Treatment types can be divided into two categories: antiresorptive and anabolic agents. Antiresorptive treatments reduce bone turnover and preserve bone mineral density (BMD). Anabolic agents stimulate bone formation thereby increasing BMD. It has been shown that a combination of these had a synergistic effect on BMD [22]. While these treatments have been suggested to slow the progression of OP, they fail to offer long-term effective solutions [19] and are associated with multiple severe side effects [23,24], and patients are typically subjected to lifelong administration.

Myopathies

Myopathies (muscular diseases) are another key group of diseases that affect a large percentage of the population [1,2]. A common myopathy is sarcopenia [25] (age-related loss of muscle mass and strength); a disease associated with frailty and has a high incidence in the older population (Table 1). There are also numerous genetic diseases such as muscular dystrophies (MD) [26], for example, Duchene muscular dystrophy (DMD), and limb girdle MD. As with the aforementioned bone and joint diseases, there are limited effective treatments to combat the progression of muscular degeneration. Muscle itself has a resident population of stem cells, known as satellite cells [27]. These cells are responsible for the regeneration of muscle fibers following exercise or injury. However, the satellite cell-mediated repair mechanism can become compromised. For example, DMD is characterized by continuous rounds of degeneration and regeneration of muscle fibers that results in a depletion of the muscle stem cell pool [28], leading to a loss of skeletal muscle mass. Currently, there are no approved drugs that consistently result in an increase in both muscle mass and strength making treatment for myopathies extremely limited [29].

Challenges for musculoskeletal regeneration strategies harnessing adult stem cells

There is a clear paucity in the current available treatments for musculoskeletal diseases, and while for some diseases such as OP, pharmacological interventions have been shown to provide some patient benefit, there is an overall need for improved treatments. Stem cell therapy has emerged as a potential treatment option for a plethora of diseases. However, stem cell therapies are not yet offered as routine treatments for musculoskeletal diseases by health services. Stem cell treatment for musculoskeletal disorders typically utilizes adult stem cells (ASCs; Figure 1) such as bone marrow stromal tissue-derived mesenchymal stem cells (MSCs; synonymously referred to as skeletal stem cells) and satellite cells/myoblasts [38,39]. These SCs are multipotent and, therefore, have a broader treatment potential compared with somatic cells. One of the most widely researched cell types for stem cell therapy are MSCs; these can be obtained from a number of different sites (bone marrow, adipose tissue, muscle, dental pulp and umbilical cord blood) [40] with relative ease, making them a favorable candidate for cell therapy. They are also able to differentiate into many major cell types of the musculoskeletal system due to their mesodermal origin [41]. However, heterogeneity between MSCs from different donors is high [42] as demonstrated by variability between growth properties and osteogenic potential; furthermore, their capacity to proliferate and differentiate declines considerably with increasing patient age [43,44]. MSCs are also considered to have an immunomodulatory capacity, and there is evidence to suggest that *in vivo* their primary function is modulation of repair rather than differentiation into tissue-specific cells, which then contribute directly to tissue regeneration [45].

Injection of undifferentiated MSCs into patients suffering from OA has been shown to improve joint motion and decrease pain [46]. However, another study reported that benefits are transient and that long-term amelioration of the condition is not achieved [47]. Also, MSCs undergoing chondrogenic differentiation (*in vitro*) have a propensity to become hypertrophic, expressing markers such as type X collagen and alkaline phosphatase [48,49]. Stem cell-based therapies for diseases such as DMD have been prominent research areas for many years. The first stem cell transplant into a DMD patient was performed in 1990 using myoblasts and held great promise for this type of treatment due to the apparent safety of the procedure, and the production of dystrophin (the affected protein in DMD) following

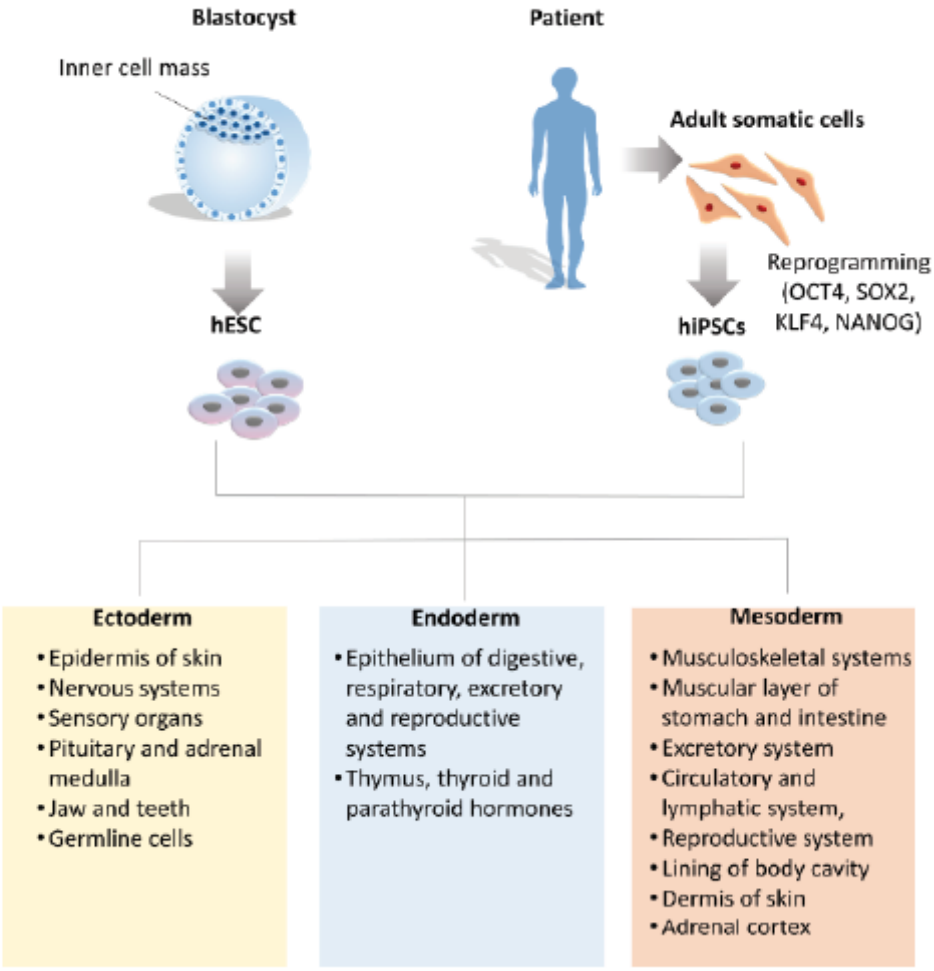

Figure 1. Benefits and drawbacks of using adult stem cells and pluripotent stem cells for clinical applications.
Comparison of the advantages and disadvantages of BM-MSCs, hESCs and hIPSCs for application in regenerative medicine.
BM-MSC: Bone marrow-derived mesenchymal stem cell; hESC: Human embryonic stem cell; hIPSC: Human-induced pluripotent stem cell.

transplantation [39]. However, in subsequent clinical trials, the results were inconsistent, with some, but not all, reporting dystrophin production and no significant clinical benefits [50,51].

While MSC/ASC therapy is an appealing prospect, it is clear that its application is problematic. One major drawback of using ASCs is that in order to prevent an immunological response, the cells must be autologous (patient derived), which can be challenging due to potentially low cell numbers, poor viability due to age and disease state. There is also the potential for donor site morbidity.

Pluripotent stem cells: a promising alternative for musculoskeletal regeneration

It is of significant clinical benefit to develop a method of restoring damaged tissue that maximizes quality of repair and minimizes the risk to the patient. To this end, there has been a surge of interest in the potential of pluripotent

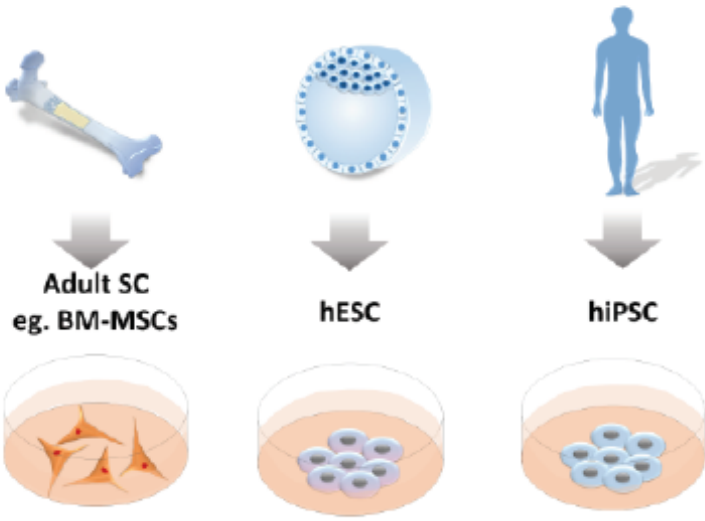

	Adult SC eg. BM-MSCs	hESC	hiPSC
Benefits	• Multipotent • Autologous • Comprehensive characterisation • Well established clinically	• Pluripotent • Allogenic • Extensive proliferation without senescence • High yield	• Pluripotent • Autologous • Extensive proliferation without senescence • High yield
Drawbacks	• Limited proliferation and differentiation capacity • Senescence • Heterogeneity • Low yields	• Possible immunogenicity • Ethical considerations • Risk of teratomas	• Low reprogramming efficiency • Epigenetic memory • Risk of teratomas

Figure 2. Derivation of pluripotent stem cells and subsequent tissue generation ability. hESCs can be derived from the inner cell mass of a blastocyst at the final stage of preimplantation development. hiPSCs can be reprogrammed from somatic cells using the forced expression of OCT4, SOX2, KLF4, NANOG. These cells can subsequently be differentiated into any derivative of the three germ layers (ectoderm, endoderm and mesoderm).
hESC: Human embryonic stem cell; hiPSC: Human-induced pluripotent stem cell.

stem cells (PSCs) for the treatment of skeletal disorders. PSCs have the ability to differentiate into all three germ layers (endoderm, mesoderm, ectoderm; Figure 2) and can, therefore, provide a source for any somatic cell in the body. PSCs can also proliferate indefinitely *in vitro*, without showing signs of cellular senescence. Therefore, PSCs have tremendous potential as a viable source of cells for musculoskeletal repair as they can be differentiated into cells of the mesodermal lineage, and therefore have the potential to generate tissues such as cartilage, bone, muscle and fat for clinical application (Figure 3).

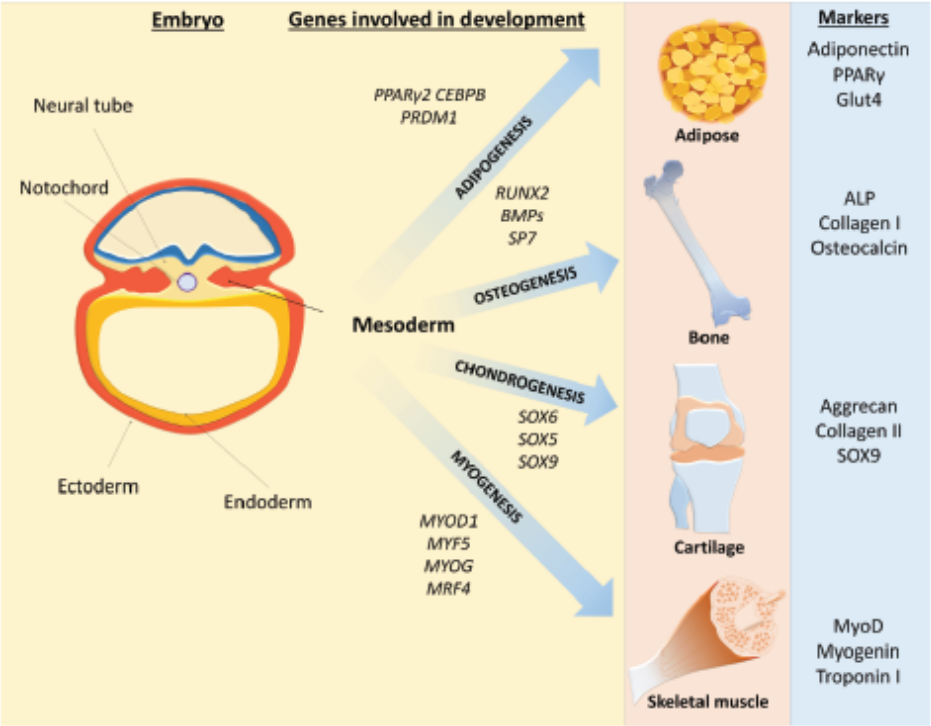

Figure 3. Differentiation of mesoderm into adipose, bone, cartilage and skeletal muscle during development.
During embryonic development, the embryo undergoes gastrulation and forms three germ layers: ectoderm, endoderm and mesoderm. The mesoderm gives rise to musculoskeletal tissues via the activation of key genes. In developed tissues, specific proteins can be used as markers.

There are two distinct types of PSCs, embryonic and induced PSCs (iPSCs; Figure 1). Embryonic stem cells (ESCs) are derived from the inner cell mass of the blastocyst [52], and were the only known source of PSC until 2006 when Takahashi and Yamanaka developed a technique of reprogramming somatic cells into iPSCs [53], for which Yamanaka was awarded the Nobel Prize. iPSCs offer the potential for personalized regenerative medicine therapy as they can be derived from the patient's own cells. More recently, multilineage differentiating stress enduring cells have been discovered as a potential source of PSCs within adult tissues [54]. Multilineage differentiating stress enduring cells are found within most adult connective tissues, are able to withstand extreme stress, express markers for pluripotency and can be isolated by SSEA-3 expression.

Human ESCs

Human ESCs (hESCs) were first derived in 1998 by Thomson *et al.* [52]. These cells derived from the preimplantation or peri-implantation embryo display prolonged undifferentiated proliferation, and stable developmental potential to form derivatives of all three embryonic germ layers even after prolonged culture [52]. This pluripotent potential can be tested *in vitro* via embryoid body (EB) formation, or *in vivo* via teratoma formation.

Since their discovery, hESCs have been heralded as a potential panacea for regenerative medicine. However, there has also been some debate over whether or not hESCs present an immunogenic risk. There is evidence to suggest that hESCs trigger an immune response [55], however, there is also contrasting evidence to suggest that they are immunoprivileged [56], or have negligible immunogenicity [57]. If hESCs do indeed elicit an immune response, this would hinder clinical application. Banks of clinical-grade hESC lines that can be human leukocyte antigen-matched to groups of individuals could ameliorate potential issues with immunogenicity and make hESCs a viable option

for regenerative medicine [58]. However, the additional challenge of aneuploidy arising from prolonged culture of hESCs is an issue that must be addressed before clinical application of hESCs [59].

Just 12 years after their discovery, hESCs were used in a clinical trial. Geron used hESCs for treatment of spinal cord injuries, however, this trial was prematurely halted [60]. Current trials are underway for the treatment of Stargardt's macular dystrophy, dry age-related macular dystrophy and diabetes [60,61].

Induced PSCs

Human iPSCs (hiPSCs) were first generated via the reprogramming of somatic cells to a pluripotent state by overexpressing a set of key transcription factors: OCT3/4, SOX2, KLF4, and C-MYC [62]. iPSCs have been found to be similar to hESCs in their morphological characteristics, self-renewal capacity, differentiation potential and gene expression profile (although there is some controversy regarding the latter [63]). The use of the patient's own cells place iPSCs at the forefront of personalized medicine by overcoming the possible immunogenicity of ESCs. The reprogramming of the cells was initially performed via retroviral or lentiviral transduction of the key factors. However, reprogramming efficiencies are low, and the process of creating patient-specific cell lines slow and costly. A further significant drawback is the potential for insertional mutagenesis, tumor formation and genetic dysfunction.

To overcome these limitations, non-integrating adenovirus, sendai virus, episomal vector or completely DNA-free techniques have been developed [64–67], with the first in-human iPSC clinical trial taking place in 2014 [68]. The successful implantation of iPSC-derived retinal pigment epithelium cells into a patient with age-related macular dystrophy was reported; however, the trial was prematurely suspended when it was found that the second patient's differentiated cells contained multiple mutations [60]. This raises important safety concerns. It has been suggested that an alternative trial using allogeneic hiPSCs may be a possibility [60].

While iPSCs display many of the characteristics of ESCs such as high proliferation under continuous culture without senescence, and the ability to form teratomas *in vivo*, there are also some fundamental differences. Once reprogrammed, iPSCs retained the epigenetic signature of the somatic parent cell [69], and exhibited altered methylation patterns in some of the key pluripotency genes such as *Oct-4* [63]. This 'epigenetic memory' can influence the behavior of the reprogrammed cells by directing them toward their lineage of origin, and thus affecting their potency. This could potentially hinder attempts to differentiate iPSCs toward a designated lineage for clinical applications.

A comparison of the benefits and drawbacks of different SC sources is shown in Figure 1. Over recent years, much research has concentrated on the development of potential treatments for musculoskeletal disorders using PSCs.

PSCs & chondrogenic differentiation

Chondrogenesis in EBs

There are numerous techniques that have been developed to induce the *in vitro* differentiation of PSCs into chondrocytes. One method is via the formation of embryoid bodies [70,71]. One study found that hypoxia and morphogenetic factors had synergistic effects on chondrogenesis in EBs [71]. It is established that ESCs are more pluripotent when cultured under hypoxic conditions [72], and *in vivo* cartilage is subjected to hypoxia, and thus may account for the enhanced chondrogenesis observed under hypoxic conditions. While the 3D environment of EBs partially recapitulates the *in vivo* developmental process, the resulting cell population is typically heterogeneous due to the emergence of endoderm and ectoderm lineage-derived cells as well as the desired mesoderm, making downstream processes such as cell sorting essential for achieving a purer cell population. Interestingly, the ability of the TGF-β family to induce chondrogenic differentiation in EBs has produced conflicting results, with inhibitory effects when added at some stages of EB differentiation [70,73,74]. This is despite the TGF-β family being potently prochondrogenic, something that remains true during MSC differentiation [75]. This highlights the distinct differences that exist between ASCs and ESCs in terms of chondrogenic differentiation, and gives an insight into the potential complexity of generating chondrocytes from PSCs. Chondrogenic differentiation of EBs has been achieved via various culture methods, such as pellet or micromass culture [71] methods, also used for cartilage generation using primary chondrocytes and MSCs [76].

As with ESCs, it has been shown that iPSCs can be used to generate EBs, which could subsequently be directed to differentiate into cartilaginous tissue [77]. Reprogrammed osteoarthritic-chondrocytes have also been used to generate hiPSCs, and subsequently differentiated to chondrocytes using TGF-β1 supplementation [78]. Cartilage markers, namely, type II collagen and aggrecan, were expressed by the differentiated hiPCs. This could indicate

that retaining an epigenetic memory may be beneficial for differentiation. However, it is beneficial to have an understanding of the iPSC methylation state as altered methylation patterns in certain genes, such as *COL10A1*, can be beneficial in promoting chondrogenesis and preventing hypertrophy [79].

Chondrogenesis in co-cultures

An alternative differentiation method is to co-culture PSCs with mature chondrocytes. This co-culture can be either direct or indirect [80,81]. In each case, secreted factors from the adult chondrocyte population created an extracellular milieu that enhanced chondrogenic differentiation. One of the factors secreted by mature chondrocytes is parathyroid-related hormone that plays an important role in chondrogenesis and the prevention of hypertrophy [82]. Fibrocartilaginous differentiation has also been shown using hESCs separated from a fibrocartilage-derived chondrocyte cell layer via nylon cell strainers: here indirect co-culture was combined with growth factor supplementation (BMP-4, TGF-β3), which improved differentiation significantly [83]. Direct co-culture in the form of high-density pellet culture of hESCs with mature chondrocytes was also shown to enhance differentiation along chondrogenic lines [84]. However, clinical applications of these methods would be difficult due to the need for an autologous chondrocyte population. Furthermore, these culture systems are difficult to scale up as larger cultures often result in poor nutrient diffusion leading to necrotic cores [85,86].

Chondrogenesis via MSC intermediates

Another technique involves differentiating hESCs, or hiPSCs, into chondrocytes via MSC intermediates. hESCs cultured on a monolayer of murine OP9 cells were differentiated toward MSCs [87]. The cells were analyzed following 40 days of culture, and $CD73^+$ cells were replated without a feeder layer. These cells were found to express adult MSC markers, and were subsequently successfully differentiated along chondrogenic, osteogenic, adipogenic and myogenic lineages [87]. However, due to the initial use of an animal feeder layer, this method of deriving ESC–MSCs is not clinically compliant and thus may introduce xenoantigens. Clinically compliant MSCs have been derived from hESCs [88]. Cells expressed MSC antigens and gene expression profiles similar to BM-MSCs and could be differentiated into chondrocytes. The hESC-derived MSCs were able to proliferate *in vitro* for at least 35 population doublings without developing any karyotypic abnormalities that would normally occur in *in vitro* cultures of BM-MSCs. This suggests that hESC-derived MSCs may have a much more robust karyotype than adult BM-MSCs.

Chemically defined methods for chondrogenesis

While the aforementioned methods have demonstrated success in the derivation of chondrocytes from PSCs, few systems were clinically compliant. For clinical applications, a fully defined feeder/serum-free culture method is required. To this end, Oldershaw *et al.* [89] have developed an effective, chemically defined protocol for deriving chondrocytes from hESCs [89,90]. This protocol is based on the sequential signaling pathways involved in the developmental process of chondrogenesis. Growth factors are used to direct differentiation of the hESCs toward chondrocytes over the course of 14 days. A substantial expansion of the cell population was reported during the differentiation protocol (8.5-fold), and between 75 and 97% SOX9-positive cells were obtained with four different hESC lines [91]. The protocol was also applied to two iPSC lines with similar success [91]. Following the 14 day protocol, there was no evidence of pluripotent cells remaining; this was particularly encouraging as residual pluripotent cells following transplantation could result in teratoma formation. This high efficiency and purity makes this a potentially useful protocol for both clinical and laboratory applications. To test the potential for clinical application of this technique, hESC-derived chondroprogenitors embedded in a fibrin gel were transplanted into an osteochondral defect in athymic RNU rats [91]. The transplanted cells formed hyaline cartilage, identifiable from 4 weeks, and fully developed by 13 weeks postimplantation. Defect repair was significantly improved by ESC-derived chondroprogenitors, compared with fibrin-only controls, and they reported significant cell survival of the transplanted population. However, as an osteochondral defect model was used here, it is unclear whether the repair was orchestrated by the implanted cells or the resident SCs from the bone marrow cavity.

PSCs & osteogenic differentiation

Osteogenesis in EBs

As with chondrogenesis, early methods of *in vitro* osteogenic differentiation from PSCs involved EB formation from ESCs and iPSCs [92,93]. However, enhanced osteogenic differentiation has been reported to occur without EB formation [94].

Early studies that utilized EB formation generally relied on *in vitro* assays to study the extent of osteogenic differentiation. However, the reliability of such assays is questionable as they frequently yield positive results despite only a small percentage of cells having been differentiated along the osteogenic lineage. One technique that is used to overcome this is use of flow cytometry to isolate osteoblast cells using lineage-specific markers; however, the markers used for isolation vary between groups. Incorporation of fluorescent reporters such as Col2.3GFP (2.3 kb fragment of the rat Col1a1 promoter) [95] has improved this technique and helped to reduce variation between research groups. Despite this improvement, *in vitro* assays are still not a reliable predictor of bone formation [96]. Techniques such as organotypic culture, and *in vivo* ectopic bone formation are more robust measures of osteogenic capacity.

Osteogenesis in co-culture

Osteogenic differentiation of hESCs has also been shown using direct and indirect co-culture with a variety of different cell types.

Direct co-culture of EBs with primary bone-derived cells was performed, after 14 days of co-culture mineralization and nodule formation was detected [97]. During direct co-culture with human periodontal ligaments fibroblasts *in vitro* mineralization occurred, suggesting that human periodontal ligaments fibroblasts have osteogenic-inducing potential [98].

Indirect co-culture of hESCs has also been performed using the transwell co-culture system [99]. Osteogenic differentiation of EBs was induced by the addition of osteogenic medium. Indirect co-culture with human bone marrow stromal cells (hBMSCs) for 28 days was then initiated 7, 14 or 24 days postdifferentiation. While there was a slight trend toward increased mineral deposition following co-culture compared with controls, the difference was not statistically significant. Furthermore, expression of the osteoblastic markers were more pronounced in hESCs exposed to osteogenic culture medium without co-culture, compared with hESCs co-cultured with differentiated hBMSCs. It is difficult to determine to what extent, if at all, co-culture with hBSCs was beneficial as there did not seem to be any significant improvement in osteogenic differentiation compared with supplementation with osteogenic media alone.

An interesting alternative to traditional co-culture techniques involves culturing hESCs with an autologous osteogenic-inducing culture supplement extracted from hESC-derived osteogenic cells [100]. This novel approach was devised in order to overcome the cost associated with large-scale bioreactor cultures for commercial applications, as the resultant cost of supplementing cultures with growth factors, cytokines and extracellular matrix (ECM) would prove to be prohibitively expensive. Here, a proof-of-principle investigation was performed to demonstrate a potential alternative to culture supplementation proposed to be useful for clinical application. They found that the whole-cell lysate from hESC-derived osteogenic cells promoted aggregation of the hESCs into nodules, and enhanced *in vitro* osteogenic differentiation compared with controls. However, due to the costs that would arise from serum-free culture, they used animal products in their cell culture media. This would have to be addressed for clinical translation.

PSCs & myogenic differentiation

Transplantation of myoblasts from satellite cells or other myogenic populations has been attempted in an effort to treat diseases such as MDs [101–103]; while this work has been promising, the drawbacks of using ASCs prevail. Transplantation of PSC-derived satellite cells into muscle is appealing as this could help simultaneously replenish a depleted resident satellite cell pool, as well as regenerate the muscle tissue itself.

Unlike chondrogenesis and osteogenesis, it has proved very difficult to induce *in vitro* myogenesis via EB formation. While it has been shown that the early stages of myogenesis occur in EBs [104,105], generating cells with the desired regenerative capacity for tissue engineering purposes have proved elusive. It has been postulated that this is because *in vitro* cultures do not form the notochord or neural tube, and so the key signaling events that are orchestrated by these structures *in vivo* cannot occur [106].

Myogenesis in co-culture

Techniques such as co-culture [87,107], and the addition of myogenic medium [108] have demonstrated some success in deriving myogenic cells from ESCs, and have shown some evidence of engraftment when the cells were transplanted into mice [108]. However, assessments were limited to qualitative detection and did not assess the functional capabilities of the engrafted tissue.

Myogenesis via genetic manipulation

An effective myogenic differentiation method includes the application of genetic manipulation techniques to induce expression of myogenic master regulators Pax3 or Pax7 [106] during development of early mesoderm. This bypasses the requirement for early inductive signals from the notochord and neural tube, and provides a method for generating larger quantities of myogenic progenitors, compared with non-genetic techniques. Cells derived from both ESCs and iPSCs have been transplanted into models of MD with some success, demonstrating an overall improvement in functional capacity in terms of muscle force generation [106,109–111]. Myogenic induction of ESCs and iPSCs has also been shown by inducing expression of Met Activating Genetically Improved Chimeric Factor-1 [112]. The myogenic regulatory factor Myo-D has also proved to be useful for the induction of myogenesis in iPSCs [113]. Here, transplantation of the differentiated cells ameliorated the dystrophic phenotype, restored depleted progenitors and improved functional capacity of the muscle. This method could potentially be used to treat various different forms of MD in humans, with the aspect of gene correction offering a personalized approach for patients with inheritable diseases.

While PSCs are particularly amenable to genome editing as they are able to undergo multiple culture manipulations without losing their pluripotency, this method of derivation can be extremely time consuming, and the use of certain vectors carry risks such as mutagenesis, and therefore limit their clinical use. Excisable, non-integrating vectors overcome these issues but are typically less efficient. However, use of animal sera remains an issue, as serum is frequently used as a stimulus for terminal myogenic differentiation [106,110,111], and is therefore a limiting factor in clinical application.

Myogenesis via MSC intermediates

As with chondrogenesis and osteogenesis, MSCs have also been derived from PSCs to facilitate myogenesis. Multipotent iPSC-derived MSCs have been demonstrated to attenuate limb ischemia in mice [114]. Transplantation of iPSC-derived MSCs via intramuscular injection was found to increase myogenesis and neovascularization, and improve limb function compared with injection of BM-MSCs or vehicle only.

Epigenetic memory of iPSCs is often considered to be disadvantageous when comparing iPSCs and ESCs. However, as previously mentioned with regard to *in vitro* chondrogenesis, epigenetic memory of the parent cell may improve differentiation of the iPSC; this phenomenon has also been reported for iPSCs derived from mesangioblasts [115], suggesting a more robust myogenic lineage commitment when iPSCs are derived from the same lineage.

PSCs & adipogenic differentiation

Adipose tissue is generally thought to develop from the mesoderm. The ability to derive white adipocytes (the most abundant fat cell type in the body) *in vitro* from stem cells would be of particular benefit to patients requiring surgical reconstruction of soft tissues, something that is often required following trauma caused by disease or injury. Application of PSC-derived adipose tissue would be of significant benefit to patients as current reconstructive methods such as autologous grafting can result in donor site morbidity [116].

Adipogenesis in EBs

In vitro adipogenesis from PSCs has so far relied on the generation of EBs from ESCs and iPSCs, and subsequent differentiation into adipocytes [117–119]. Retinoic acid (RA) is well documented as being an inducer of adipogenesis. Using RA as the differentiation stimulus, a comparison of the adipogenic potential of ESCs and iPSCs has been performed [119]. The authors reported no significant variation between the adipogenic potential of hESCs and hiPSCs overall, however, there was heterogeneity between different iPSC cell lines, despite having the same genetic origin. While RA has been shown to have potent effects on adipogenic differentiation, it is not a standard component of adipogenic medium. Other growth factor combinations such as BMP-2, TGF-ß1, insulin and ascorbic acid are more commonly used [120].

Adipogenesis via genetic manipulation

Another method for inducing adipogenic differentiation in PSCs is to use genetic reprogramming techniques to induce expression of genes involved in adipogenesis. Brown adipose tissue is far less abundant within the body and functions to produce heat through non-shivering thermogenesis. It has been discovered that adults have depots of brown adipose tissue that are inversely correlated in size with BMI [121–123]. This finding has led to considerable interest in the potential therapeutic benefits of brown adipocytes. Retroviral transduction of the *PPARγ2*, *CEBPB* and *PRDM1* genes into hESCs and hiPSCs has been shown to induce adipocyte differentiation into brown adipocytes [117]. Here, the authors found variable adipocyte differentiation potential between cell lines and also reported that efficiency was less in PSCs compared with adipose-derived stromal vascular cells. However, following derivation of both white and brown adipocytes, it was found that *in vivo* transplantation resulted in the formation of tissues with functional and morphological similarities to primary cells, and importantly they reported no teratoma formation after 4–6 weeks.

Adipogenesis via addition of growth factors

Differentiation into functional brown adipocytes has also been achieved without exogenous gene transfer [118]. Supplementation with the cocktail comprising of KITLG, IL6, FLT3LG and VEGF was found to be essential for brown adipose differentiation of hPSCs, both hESCs and hiPSCs. One of their most interesting findings was that inhibitor analyses revealed that p38 MAPK signaling played a role in brown adipose differentiation in hESCs, but MEK signaling did not; however, in hiPSCs MEK signaling was involved in differentiation. This highlighted a distinct difference between hiPSC and hESC-derived brown adipocytes.

From cell-based strategies to tissue engineering 3D constructs

Cell-based therapies for regenerative medicine have not yet demonstrated a full restoration of the damaged tissue to its original state. A tissue engineering approach provides an alternative method to introducing differentiated cells directly into damaged tissue, which incorporates cells, appropriate growth factors, biomaterial scaffold-based/scaffold-free approaches in combination with bioreactor technology to generate a 3D issue construct *in vitro*, before implantation. Thus, mitigating the risk of transferring undifferentiated cells to the patient. 3D culture also aims to recapitulate the *in vivo* environment and facilitates the successful generation of tissues such as cartilage, bone and muscle *in vitro*. Furthermore, this approach ensures that suitable tissue constructs with the appropriate physiological and biomechanical properties are formed, thus providing a level of control that is not possible with cell transplantation.

The use of biomaterial scaffolds in the generation of cartilage tissue is well documented [78–81,84,91], and shares similarities with current clinical interventions for OA (MACI). However, since the native tissue has a low capacity for self-repair, it is desirable to create *in vitro* constructs that are functionally and morphologically identical to native cartilage to improve the ease of integration. Scaffold-free techniques for cartilage tissue engineering have been successful in producing *in vitro* cartilage constructs via chondrogenic differentiation of hPSCs in 3D pellet culture [71,79,81,84,87]. However, limited testing of these cartilage constructs has been performed in a physiologically relevant environment, for example, load-bearing animal model. In one study, hiPSC-derived cartilage pellets were shown to promote healing when introduced into osteochondral defects in the palate groove of immunosuppressed rats [79].

Unlike cartilage which has a very limited capacity for self-repair, bone is a dynamic tissue that is constantly undergoing remodeling and has a much higher repair capacity. Here, scaffolds and various biomaterials have provided an invaluable tool for bone tissue engineering as they can enable a greater level of control over form and structure, and can also be supplemented with osteoinductive agents. Mineralized tissue formed by differentiated PSCs has been shown using various different scaffold materials [93,124–127]. In these studies, the engineered tissue was subcutaneously implanted in animal models and *in vivo* mineralization capacity was evaluated; however, there is a lack of studies that have investigated the *in vivo* reparative effects of the PSC-derived engineered tissue. A stumbling block for bone tissue engineering is the inability to generate/bioengineer a functional blood supply.

For skeletal muscle and adipose tissue trauma such as volumetric muscle loss, or damage that occurs as a result of surgical procedures, tissue engineering using scaffolds has been shown to be of significant clinical benefit [128]. Tissue engineering for such purposes may be either *in vitro* or *in vivo*. There are numerous difficulties associated with *in vitro* construct formation, for example, producing large enough constructs for the affected area takes a long time. It is also difficult to attain good vascularization of muscle constructs and physiologically relevant contraction

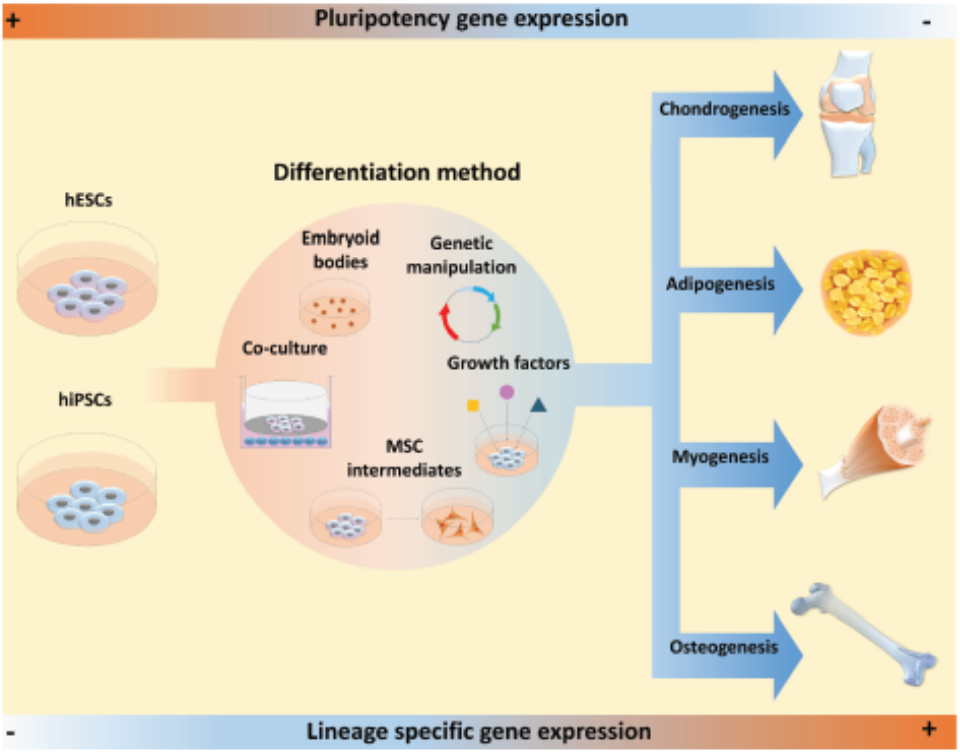

Figure 4. Schematic summarizing methods used to generate cells of mesodermal lineages, namely, chondrogenic, adipogenic, myogenic and osteogenic, from human embryonic stem cells and human-induced pluripotent stem cells.
A wide range of methods, including embryoid body generation, genetic manipulation, application of appropriate growth factors, co-culture and differentiation via MSC intermediates, have been applied to generate chondrogenic, adipogenic, myogenic and osteogenic lineages from hPSCs for musculoskeletal regeneration.
hESC: Human embryonics stem cell; hPSC: Human pluripotent stem cell; MSC: Mesenchymal stem cell.

forces. The *in vivo* approach to muscle and adipose generation is, therefore, generally more favorable. Here, cells are transplanted with, or into, a biomaterial scaffold that can integrate with the host tissue and form a niche where tissue regeneration may occur [128].

Conclusion & Future perspectives

Musculoskeletal regeneration has become a prominent research area, no doubt due to the sociological and economic pressures imposed by the current ageing population. The ability of PSCs to self-renew and differentiate into any somatic cell type may well prove to be a highly effective tool in the treatment of such diseases. With regard to iPSCs, their potential is irrefutable, and the opportunity to derive allogenic cells from patients is extremely enticing. However, several issues remain to be addressed, such as the efficiency of reprogramming using non-viral vectors and the impact of 'epigenetic memory' on therapeutic treatments. In contrast, hESCs are not associated with these problems.

Regarding differentiation protocols, cells of mesodermal origin have been derived via a variety of methods (Figure 4); however, it is clear that there is a requirement for clinically compliant, chemically defined methods of deriving specific cell types while keeping costs as low as possible. This review has gone some way toward showing that such protocols are a possibility, for instance, Oldershaw *et al.* developed a protocol for the directed differentiation of hESCs/hiPSCs to chondrocytes that resulted in a high cell yield, and was fully chemically defined which would ease generation of a clinically compliant protocol [89]; however, to make such treatments accessible, cost would

likely remain an issue. It is also prudent to acknowledge that protocols using PSCs to derive cells for application in drug testing, for example, myogenic progenitors and myotubes [129], are also of value for tissue engineering and knowledge gained from such studies is of significant value to the field.

Treatment approaches in the future are likely to focus on tissue engineering as this would enable the existence of a quality control system, whereby 3D explants that are generated can be assessed in terms of their morphological, mechanical and physiological properties prior to implantation. Use of bioreactors is likely to increase in popularity as they allow for precise and accurate manipulation of environmental factors that allows for a more physiological culture setting. However, for clinical purposes, more high-throughput systems will ultimately be required. Importantly, to fully elucidate the functional capacity of tissue-engineered musculoskeletal constructs, it is vitally important that these are tested in appropriate *in vivo* models, and the parameters relating to their function are fully assessed.

Executive summary

Socioeconomic burden of musculoskeletal deterioration

- Diseases affecting the musculoskeletal system are a major cause of disability and morbidity.
- Effective long-term treatment options are lacking, resulting in increased strain on healthcare systems and individuals.

Current interventions for the treatment of major musculoskeletal diseases & their limitations

- Osteoarthritis: Current surgical interventions such as mosaicplasty and autologous chondrocyte implantation produce fibrous repair cartilage, and do not offer long-term treatment solutions. Joint replacement surgery is a late-stage treatment option.
- Osteoporosis: Current pharmacological interventions may be effective but typically require life-long administration and can have side effects.
- Myopathies: Currently, there are no approved drugs or exercise interventions that consistently result in an increase in both muscle mass and strength.

Pluripotent stem cells: a promising alternative for musculoskeletal regeneration

- There are two known types of pluripotent stem cells (PSCs): embryonic stem cells and induced PSCs.
- Due to their capacity to differentiate into any somatic cell type, and ability to proliferate indefinitely *in vitro* without undergoing cellular senescence, PSCs are an idea candidate cell type for regenerative medicine.

PSCs & chondrogenic, osteogenic, myogenic & adipogenic differentiation

- The most commonly used methods for differentiation into mesodermal lineages are:
  - via embryoid body formation
  - via mesenchymal stem cell intermediates
  - co-culture
  - genetic manipulation
  - growth factor addition.
- There is a requirement for clinically compliant differentiation protocols for clinical translation.

From cell-based strategies to tissue engineering 3D constructs

- A tissue engineering approach mitigates the risk of transferring undifferentiated cells to the patient, and enables the assessment of tissue quality prior to implantation.

Future perspective

- Future work will most likely involve tissue engineering rather than cell transplantation, and will require clinically compliant methods of cell derivation.

Financial & competing interests disclosure

The authors acknowledge funding to RS Tare and FD Houghton from the Rosetrees Trust, the Faculty of Medicine and the Institute for Life Sciences, University of Southampton for PhD Studentship support to LA Jevons. FD Houghton also acknowledges funding from the Medical Research Council (G0701153). The authors have no other relevant affiliations or financial involvement with any organization or entity with a financial interest in or financial conflict with the subject matter or materials discussed in the manuscript apart from those disclosed.

No writing assistance was utilized in the production of this manuscript.

Open access

This work is licensed under the Creative Commons Attribution 4.0 License. To view a copy of this license, visit http://creativecommons.org/licenses/by/4.0/

References

Papers of special note have been highlighted as: • of interest; •• of considerable interest

1. Nedergaard A, Henriksen K, Karsdal MA, Christiansen C. Musculoskeletal ageing and primary prevention. *Best Practice Res. Clin. Obstetr. Gynaecol.* 27(5), 673–688 (2013).
2. Woolf AD, Pfleger B. Burden of major musculoskeletal conditions. *Bull. WHO* 81(9), 646–656 (2003).
3. Malafarina V, Úriz-Otano F, Iniesta R, Gil-Guerrero L. Sarcopenia in the elderly: diagnosis, physiopathology and treatment. *Maturitas* 71(2), 109–114 (2012).
4. Rodino-Klapac LR, Mendell JR, Sahenk Z. Update on the treatment of Duchenne muscular dystrophy. *Curr. Neurol. Neurosci. Rep.* 13(3), 1–7 (2013).
5. Hunter DJ, Neogi T, Hochberg MC. Quality of osteoarthritis management and the need for reform in the US. *Arthritis Care Res. (Hoboken)* 63(1), 31–38 (2011).
6. Antebi B, Pelled G, Gazit D. Stem cell therapy for osteoporosis. *Curr. Osteoporos. Rep.* 12(1), 41–47 (2014).
7. Dargent-Molina P, Favier F, Grandjean H *et al.* Fall-related factors and risk of hip fracture: the EPIDOS prospective study. *Lancet* 348(9021), 145–149 (1996).
8. Landi F, Liperoti R, Russo A *et al.* Sarcopenia as a risk factor for falls in elderly individuals: results from the ilSIRENTE study. *Clin. Nutr.* 31(5), 652–658 (2012).
9. Johnell O, Kanis J. An estimate of the worldwide prevalence, mortality and disability associated with hip fracture. *Osteoporosis Int.* 15(11), 897–902 (2004).
10. Control CFD, Prevention. Prevalence of doctor-diagnosed arthritis and arthritis-attributable activity limitation – United States, 2007–2009. *Morb. Mortal. Week. Rep.* 59(39), 1261 (2010).
11. Cross M, Smith E, Hoy D *et al.* The global burden of hip and knee osteoarthritis: estimates from the global burden of disease 2010 study. *Ann. Rheum. Dis.* 73(7), 1323–1330 (2014).
12. Pritzker K, Gay S, Jimenez S *et al.* Osteoarthritis cartilage histopathology: grading and staging. *Osteoarthritis Cartilage* 14(1), 13–29 (2006).
13. D'apuzzo MR, Pao AW, Novicoff WM, Browne JA. Age as an independent risk factor for postoperative morbidity and mortality after total joint arthroplasty in patients 90 years of age or older. *J. Arthroplasty* 29(3), 477–480 (2014).
14. Johnson LL. Arthroscopic abrasion arthroplasty: a review. *Clin. Orthop. Relat. Res.* 391, S306–S317 (2001).
15. Insall J. The Pridie debridement operation for osteoarthritis of the knee. *Clin. Orthop. Relat. Res.* 101, 61–67 (1974).
16. Mithoefer K, Williams RJ, Warren RF *et al.* Chondral resurfacing of articular cartilage defects in the knee with the microfracture technique. *J. Bone Joint Surg. Am.* 88(1 Suppl. 2), 294–304 (2006).
17. Bentley G, Biant L, Vijayan S, Macmull S, Skinner J, Carrington R. Minimum ten-year results of a prospective randomised study of autologous chondrocyte implantation versus mosaicplasty for symptomatic articular cartilage lesions of the knee. *J. Bone Joint Surg. Br.* 94(4), 504–509 (2012).
18. Brittberg M, Lindahl A, Nilsson A, Ohlsson C, Isaksson O, Peterson L. Treatment of deep cartilage defects in the knee with autologous chondrocyte transplantation. *N. Engl. J. Med.* 331(14), 889–895 (1994).
19. Hernlund E, Svedbom A, Ivergård M *et al.* Osteoporosis in the European Union: medical management, epidemiology and economic burden. *Arch. Osteoporos.* 8(1–2), 1–115 (2013).
20. Johnell O, Kanis J. An estimate of the worldwide prevalence and disability associated with osteoporotic fractures. *Osteoporosis Int.* 17(12), 1726–1733 (2006).
21. Kanis JA. Assessment of fracture risk and its application to screening for postmenopausal osteoporosis: synopsis of a WHO report. *Osteoporosis Int.* 4(6), 368–381 (1994).
22. Tsai JN, Uihlein AV, Lee H *et al.* Teriparatide and denosumab, alone or combined, in women with postmenopausal osteoporosis: the DATA study randomised trial. *Lancet* 382(9886), 50–56 (2013).
23. Khan AA, Sandor GK, Dore E *et al.* Bisphosphonate associated osteonecrosis of the jaw. *J. Rheumatol.* 36(3), 478–490 (2009).
24. Nieves JW, Cosman F. Atypical subtrochanteric and femoral shaft fractures and possible association with bisphosphonates. *Curr. Osteoporos. Rep.* 8(1), 34–39 (2010).
25. Patel HP, Syddall HE, Jameson K *et al.* Prevalence of sarcopenia in community-dwelling older people in the UK using the European Working Group on Sarcopenia in Older People (EWGSOP) definition: findings from the Hertfordshire Cohort Study (HCS). *Age Ageing* 42(3), 378–384 (2013).
26. Emery AE. The muscular dystrophies. *Lancet* 359(9307), 687–695 (2002).
27. Mauro A. Satellite cell of skeletal muscle fibers. *J. Biophys. Biochem. Cytol.* 9(2), 493–495 (1961).
28. Webster C, Blau HM. Accelerated age-related decline in replicative life-span of Duchenne muscular dystrophy myoblasts: implications for cell and gene therapy. *Somatic Cell Mol. Genet.* 16(6), 557–565 (1990).

29. Meriggioli MN, Roubenoff R. Prospect for pharmacological therapies to treat skeletal muscle dysfunction. *Calcif. Tissue Int.* 96(3), 234–242 (2015).

30. Murphy L, Schwartz TA, Helmick CG *et al.* Lifetime risk of symptomatic knee osteoarthritis. *Arthritis Care Res. (Hoboken)* 59(9), 1207–1213 (2008).

31. Redman S, Oldfield S, Archer C. Current strategies for articular cartilage repair. *Eur. Cells Mater.* 9(23–32), 23–32 (2005).

32. Horas U, Pelinkovic D, Herr G, Aigner T, Schnettler R. Autologous chondrocyte implantation and osteochondral cylinder transplantation in cartilage repair of the knee joint. *J. Bone Joint Surg.* 85(2), 185–192 (2003).

33. Roberts J, Castro C, Moore A, Fogelman I, Hampson G. Changes in bone mineral density and bone turnover in patients on 'drug holiday'following bisphosphonate therapy: real-life clinic setting. *Clin. Endocrinol. (Oxf.)* 84(4), 509–515 (2016).

34. Dooley J, Gordon KE, Dodds L, Macsween J. Duchenne muscular dystrophy: a 30-year population-based incidence study. *Clin. Pediatr. (Phila.)* 49(2), 177–179 (2010).

35. Hasten DL, Pak-Loduca J, Obert KA, Yarasheski KE. Resistance exercise acutely increases MHC and mixed muscle protein synthesis rates in 78–84 and 23–32 yr olds. *Am. J. Physiol. Endocrinol. Metabol.* 278(4), E620–E626 (2000).

36. Gloss D, Moxley RT, Ashwal S, Oskoui M. Practice guideline update summary: corticosteroid treatment of Duchenne muscular dystrophy report of the Guideline Development Subcommittee of the American Academy of Neurology. *Neurology* 86(5), 465–472 (2016).

37. Fairclough RJ, Wood MJ, Davies KE. Therapy for Duchenne muscular dystrophy: renewed optimism from genetic approaches. *Nat. Rev. Genet.* 14(6), 373–378 (2013).

38. Vangsness CTJ, Farr JI, Boyd J, Dellaero DT, Mills CR, Leroux-Williams M. Adult human mesenchymal stem cells delivered via intra-articular injection to the knee following partial medial meniscectomy: a randomized, double-blind, controlled study. *J. Bone Joint Surg. Am.* 96(2), 90–98 (2014).

39. Law P, Bertorini T, Goodwin T *et al.* Dystrophin production induced by myoblast transfer therapy in Duchenne muscular dystrophy. *Lancet* 336(8707), 114–115 (1990).

40. Huang G-J, Gronthos S, Shi S. Mesenchymal stem cells derived from dental tissues vs. those from other sources: their biology and role in regenerative medicine. *J. Dent. Res.* 88(9), 792–806 (2009).

41. Pittenger MF, Mackay AM, Beck SC *et al.* Multilineage potential of adult human mesenchymal stem cells. *Science* 284(5411), 143–147 (1999).

42. Phinney DG, Kopen G, Righter W, Webster S, Tremain N, Prockop DJ. Donor variation in the growth properties and osteogenic potential of human marrow stromal cells. *J. Cell. Biochem.* 75(3), 424–436 (1999).

43. Stenderup K, Justesen J, Clausen C, Kassem M. Aging is associated with decreased maximal life span and accelerated senescence of bone marrow stromal cells. *Bone* 33(6), 919–926 (2003).

44. Sethe S, Scutt A, Stolzing A. Aging of mesenchymal stem cells. *Ageing Res. Rev.* 5(1), 91–116 (2006).

45. Caplan AI, Sorrell JM. The MSC curtain that stops the immune system. *Immunol. Lett.* 168(2), 136–139 (2015).

46. Davatchi F, Abdollahi BS, Mohyeddin M, Shahram F, Nikbin B. Mesenchymal stem cell therapy for knee osteoarthritis. Preliminary report of four patients. *Int. J. Rheum. Dis.* 14(2), 211–215 (2011).

47. Mohsen Emadedin M, Roghayeh Fazeli M, Reza Farjad M. Intra-articular injection of autologous mesenchymal stem cells in six patients with knee osteoarthritis. *Arch. Iran. Med.* 15(7), 422 (2012).

48. Johnstone B, Hering T, Caplan A, Goldberg V, Yoo J. *In vitro* chondrogenesis of bone marrow-derived mesenchymal progenitor cells. *Exp. Cell Res.* 238(1), 265–272 (1998).

49. Yoo JU, Barthel TS, Nishimura K *et al.* The chondrogenic potential of human bone-marrow-derived mesenchymal progenitor cells. *J. Bone Joint Surg.* 80(12), 1745–1757 (1998).

50. Morandi L, Bernasconi P, Gebbia M *et al.* Lack of mRNA and dystrophin expression in DMD patients three months after myoblast transfer. *Neuromuscul. Disord.* 5(4), 291–295 (1995).

51. Gussoni E, Pavlath GK, Lanctoti AM, Sharmaii KR. Normal dystrophin transcripts detected in Duchenne muscular dystrophy patients after myoblast transplantation. *Nature* 356, 2 (1992).

52. Thomson JA, Itskovitz-Eldor J, Shapiro SS *et al.* Embryonic stem cell lines derived from human blastocysts. *Science* 282(5391), 1145–1147 (1998).

- **First demonstrated the generation of human embryonic stem cell (hESC) lines from human blastocyts.**

53. Takahashi K, Yamanaka S. Induction of pluripotent stem cells from mouse embryonic and adult fibroblast cultures by defined factors. *Cell* 126(4), 663–676 (2006).

54. Kuroda Y, Kitada M, Wakao S *et al.* Unique multipotent cells in adult human mesenchymal cell populations. *Proc. Natl Acad. Sci. USA* 107(19), 8639–8643 (2010).

55. Grinnemo K-H, Kumagai-Braesch M, Månsson-Broberg A *et al.* Human embryonic stem cells are immunogenic in allogeneic and xenogeneic settings. *Reprod. Biomed. Online* 13(5), 712–724 (2006).

56. Li L, Baroja ML, Majumdar A *et al.* Human embryonic stem cells possess immune-privileged properties. *Stem Cells* 22(4), 448–456 (2004).

57. Araki R, Uda M, Hoki Y *et al.* Negligible immunogenicity of terminally differentiated cells derived from induced pluripotent or embryonic stem cells. *Nature* 494(7435), 100–104 (2013).

58. Nakajima F, Tokunaga K, Nakatsuji N. Human leukocyte antigen matching estimations in a hypothetical bank of human embryonic stem cell lines in the Japanese population for use in cell transplantation therapy. *Stem Cells* 25(4), 983–985 (2007).

59. Draper JS, Smith K, Gokhale P *et al.* Recurrent gain of chromosomes 17q and 12 in cultured human embryonic stem cells. *Nat. Biotechnol.* 22(1), 53 (2004).

60. Ilic D, Devito L, Miere C, Codognotto S. Human embryonic and induced pluripotent stem cells in clinical trials. *Br. Med. Bull.* ldv045 (2015).

61. Schwartz SD, Hubschman J-P, Heilwell G *et al.* Embryonic stem cell trials for macular degeneration: a preliminary report. *Lancet* 379(9817), 713–720 (2012).

62. Takahashi K, Tanabe K, Ohnuki M *et al.* Induction of pluripotent stem cells from adult human fibroblasts by defined factors. *Cell* 131(5), 861–872 (2007).

- **The revolutionary paper that first demonstrated the reprogramming of somatic cells to a pluripotent state.**

63. Doi A, Park I-H, Wen B *et al.* Differential methylation of tissue-and cancer-specific CpG island shores distinguishes human induced pluripotent stem cells, embryonic stem cells and fibroblasts. *Nat. Genet.* 41(12), 1350–1353 (2009).

64. Yu J, Hu K, Smuga-Otto K *et al.* Human induced pluripotent stem cells free of vector and transgene sequences. *Science* 324(5928), 797–801 (2009).

65. Kim D, Kim C-H, Moon J-I *et al.* Generation of human induced pluripotent stem cells by direct delivery of reprogramming proteins. *Cell Stem Cell* 4(6), 472 (2009).

66. Okita K, Matsumura Y, Sato Y *et al.* A more efficient method to generate integration-free human iPS cells. *Nat. Methods* 8(5), 409–412 (2011).

67. Fusaki N, Ban H, Nishiyama A, Saeki K, Hasegawa M. Efficient induction of transgene-free human pluripotent stem cells using a vector based on Sendai virus, an RNA virus that does not integrate into the host genome. *Proc. Jpn. Acad. Ser. B Phys. Biol. Sci.* 85(8), 348–362 (2009).

68. Li MD, Atkins H, Bubela T. The global landscape of stem cell clinical trials. *Regen. Med.* 9(1), 27–39 (2014).

69. Kim K, Doi A, Wen B *et al.* Epigenetic memory in induced pluripotent stem cells. *Nature* 467(7313), 285–290 (2010).

70. Toh WS, Yang Z, Liu H, Heng BC, Lee EH, Cao T. Effects of culture conditions and bone morphogenetic protein 2 on extent of chondrogenesis from human embryonic stem cells. *Stem Cells* 25(4), 950–960 (2007).

71. Yodmuang S, Marolt D, Marcos-Campos I, Gadjanski I, Vunjak-Novakovic G. Synergistic effects of hypoxia and morphogenetic factors on early chondrogenic commitment of human embryonic stem cells in embryoid body culture. *Stem Cell Rev. Rep.* 11(2), 228–241 (2015).

72. Forristal CE, Wright KL, Hanley NA, Oreffo RO, Houghton FD. Hypoxia inducible factors regulate pluripotency and proliferation in human embryonic stem cells cultured at reduced oxygen tensions. *Reproduction* 139(1), 85–97 (2010).

73. Yang Z, Sui L, Toh WS, Lee EH, Cao T. Stage-dependent effect of TGF-β1 on chondrogenic differentiation of human embryonic stem cells. *Stem Cells Dev.* 18(6), 929–940 (2009).

74. Kramer J, Hegert C, Guan K, Wobus AM, Müller PK, Rohwedel J. Embryonic stem cell-derived chondrogenic differentiation *in vitro*: activation by BMP-2 and BMP-4. *Mech. Dev.* 92(2), 193–205 (2000).

75. Mackay AM, Beck SC, Murphy JM, Barry FP, Chichester CO, Pittenger MF. Chondrogenic differentiation of cultured human mesenchymal stem cells from marrow. *Tissue Eng.* 4(4), 415–428 (1998).

76. Zhang L, Su P, Xu C, Yang J, Yu W, Huang D. Chondrogenic differentiation of human mesenchymal stem cells: a comparison between micromass and pellet culture systems. *Biotechnol. Lett.* 32(9), 1339–1346 (2010).

77. Kim MJ, Son MJ, Son MY *et al.* Generation of human induced pluripotent stem cells from osteoarthritis patient–derived synovial cells. *Arthritis Rheum.* 63(10), 3010–3021 (2011).

78. Wei Y, Zeng W, Wan R *et al.* Chondrogenic differentiation of induced pluripotent stem cells from osteoarthritic chondrocytes in alginate matrix. *Eur. Cells Mater.* 23, 1–12 (2012).

79. Ko J-Y, Kim K-I, Park S, Im G-I. *In vitro* chondrogenesis and *in vivo* repair of osteochondral defect with human induced pluripotent stem cells. *Biomaterials* 35(11), 3571–3581 (2014).

80. Vats A, Bielby RC, Tolley N *et al.* Chondrogenic differentiation of human embryonic stem cells: the effect of the micro-environment. *Tissue Eng.* 12(6), 1687–1697 (2006).

81. Hwang NS, Varghese S, Elisseeff J. Derivation of chondrogenically-committed cells from human embryonic cells for cartilage tissue regeneration. *PLoS ONE* 3(6), e2498 (2008).

82. Fischer J, Dickhut A, Rickert M, Richter W. Human articular chondrocytes secrete parathyroid hormone–related protein and inhibit hypertrophy of mesenchymal stem cells in coculture during chondrogenesis. *Arthritis Rheum.* 62(9), 2696–2706 (2010).

83. Hoben GM, Willard VP, Athanasiou KA. Fibrochondrogenesis of hESCs: growth factor combinations and cocultures. *Stem Cells Dev.* 18(2), 283–292 (2009).

84. Bigdeli N, Karlsson C, Strehl R, Concaro S, Hyllner J, Lindahl A. Coculture of human embryonic stem cells and human articular chondrocytes results in significantly altered phenotype and improved chondrogenic differentiation. *Stem Cells* 27(8), 1812–1821 (2009).

85. Tare RS, Howard D, Pound JC, Roach HI, Oreffo RO. Tissue engineering strategies for cartilage generation—micromass and three dimensional cultures using human chondrocytes and a continuous cell line. *Biochem. Biophys. Res. Commun.* 333(2), 609–621 (2005).

86. Kafienah W, Mistry S, Dickinson SC, Sims TJ, Learmonth I, Hollander AP. Three-dimensional cartilage tissue engineering using adult stem cells from osteoarthritis patients. *Arthritis Rheum.* 56(1), 177–187 (2007).

87. Barberi T, Willis LM, Socci ND, Studer L. Derivation of multipotent mesenchymal precursors from human embryonic stem cells. *PLoS Med.* 2(6), 554 (2005).

88. Lian Q, Lye E, Suan Yeo K *et al.* Derivation of clinically compliant MSCs from CD105+, CD24− differentiated human ESCs. *Stem Cells* 25(2), 425–436 (2007).

• **Isolation of a pure osteoblast population from differentiated hESCs using a Col2.3GFP reporter.**

89. Oldershaw RA, Baxter MA, Lowe ET *et al.* Directed differentiation of human embryonic stem cells toward chondrocytes. *Nat. Biotechnol.* 28(11), 1187–1194 (2010).

•• **Reports a chemically defined and scalable protocol for the directed differentiation of hESCs toward chondrocytes that mimics developmental chondrogenesis.**

90. Oldershaw RA, Baxter MA, Lowe ET *et al.* Chondrocyte protocol. In: *StemBook.* Harvard Stem Cell Institute, Cambridge, MA (2010).

91. Cheng A, Kapacee Z, Peng J *et al.* Cartilage repair using human embryonic stem cell-derived chondroprogenitors. *Stem Cells Transl. Med.* 3(11), 1287–1294 (2014).

92. Sottile V, Thomson A, Mcwhir J. *In vitro* osteogenic differentiation of human ES cells. *Cloning Stem Cells* 5(2), 149–155 (2003).

93. Bielby RC, Boccaccini AR, Polak JM, Buttery LD. *In vitro* differentiation and *in vivo* mineralization of osteogenic cells derived from human embryonic stem cells. *Tissue Eng.* 10(9–10), 1518–1525 (2004).

94. Karp JM, Ferreira LS, Khademhosseini A, Kwon AH, Yeh J, Langer RS. Cultivation of human embryonic stem cells without the embryoid body step enhances osteogenesis *in vitro*. *Stem Cells* 24(4), 835–843 (2006).

95. Xin X, Jiang X, Wang L *et al.* A site-specific integrated Col2. 3GFP reporter identifies osteoblasts within mineralized tissue formed *in vivo* by human embryonic stem cells. *Stem Cells Transl. Med.* 3(10), 1125 (2014).

• **Isolation of a pure osteoblast population from differentiated hESCs using a Col2.3GFP reporter.**

96. Robey PG, Kuznetsov SA, Riminucci M, Bianco P. Bone marrow stromal cell assays: *in vitro* and *in vivo*. In: *Skeletal Development and Repair: Methods and Protocols.* Springer, NY, USA, 279–293 (2014).

97. Ahn SE, Kim S, Park KH *et al.* Primary bone-derived cells induce osteogenic differentiation without exogenous factors in human embryonic stem cells. *Biochem. Biophys. Res. Commun.* 340(2), 403–408 (2006).

98. Inanç B, Elçin AE, Elçin YM. Effect of osteogenic induction on the *in vitro* differentiation of human embryonic stem cells cocultured with periodontal ligament fibroblasts. *Artif. Organs* 31(11), 792–800 (2007).

99. Tong W, Brown SE, Krebsbach PH. Human embryonic stem cells undergo osteogenic differentiation in human bone marrow stromal cell microenvironments. *J. Stem Cells* 2(3), 139 (2007).

100. Heng BC, Toh WS, Pereira BP *et al.* An autologous cell lysate extract from human embryonic stem cell (hESC) derived osteoblasts can enhance osteogenesis of hESC. *Tissue Cell* 40(3), 219–228 (2008).

101. Neumeyer A, Cross D, Mckenna-Yasek D *et al.* Pilot study of myoblast transfer in the treatment of Becker muscular dystrophy. *Neurology* 51(2), 589–592 (1998).

102. Karpati G, Ajdukovic D, Arnold D *et al.* Myoblast transfer in Duchenne muscular dystrophy. *Ann. Neurol.* 34(1), 8–17 (1993).

103. Law PK, Goodwin TG, Fang Q *et al.* Myoblast transfer therapy for Duchenne muscular dystrophy. *Pediatr. Int.* 33(2), 206–215 (1991).

104. Rohwedel J, Maltsev V, Bober E, Arnold H-H, Hescheler J, Wobus A. Muscle cell differentiation of embryonic stem cells reflects myogenesis *in vivo*: developmentally regulated expression of myogenic determination genes and functional expression of ionic currents. *Dev. Biol.* 164(1), 87–101 (1994).

105. Zheng JK, Wang Y, Karandikar A *et al.* Skeletal myogenesis by human embryonic stem cells. *Cell Res.* 16(8), 713–722 (2006).

106. Darabi R, Gehlbach K, Bachoo RM *et al.* Functional skeletal muscle regeneration from differentiating embryonic stem cells. *Nat. Med.* 14(2), 134–143 (2008).

107. Bhagavati S, Xu W. Generation of skeletal muscle from transplanted embryonic stem cells in dystrophic mice. *Biochem. Biophys. Res. Commun.* 333(2), 644–649 (2005).

108. Barberi T, Bradbury M, Dincer Z, Panagiotakos G, Socci ND, Studer L. Derivation of engraftable skeletal myoblasts from human embryonic stem cells. *Nat. Med.* 13(5), 642–648 (2007).

109. Darabi R, Baik J, Clee M, Kyba M, Tupler R, Perlingeiro RC. Engraftment of embryonic stem cell-derived myogenic progenitors in a dominant model of muscular dystrophy. *Exp. Neurol.* 220(1), 212–216 (2009).

110. Darabi R, Santos FN, Filareto A *et al.* Assessment of the myogenic stem cell compartment following transplantation of Pax3/Pax7-induced embryonic stem cell-derived progenitors. *Stem Cells* 29(5), 777–790 (2011).

111. Darabi R, Arpke RW, Irion S *et al.* Human ES- and iPS-derived myogenic progenitors restore DYSTROPHIN and improve contractility upon transplantation in dystrophic mice. *Cell Stem Cell* 10(5), 610–619 (2012).

- **Here, it was demonstrated that conditional expression of PAX7 in hESCs/inducedpluripotent stem cells can be used to derive large quantities of myogenicprecursors capable of engraftment and long-term survival in a dystrophic mousemodel. Notably, they achieved an improvement in muscle function.**

112. Perini I, Elia I, Nigro AL *et al.* Myogenic induction of adult and pluripotent stem cells using recombinant proteins. *Biochem. Biophys. Res. Commun.* 464(3), 755–761 (2015).

113. Shoji E, Woltjen K, Sakurai H. Directed myogenic differentiation of human induced pluripotent stem cells. *Methods Mol. Biol.* 1353, 89–99 (2016).

114. Lian Q, Zhang Y, Zhang J *et al.* Functional mesenchymal stem cells derived from human induced pluripotent stem cells attenuate limb ischemia in mice. *Circulation* 121(9), 1113–1123 (2010).

115. Quattrocelli M, Palazzolo G, Floris G *et al.* Intrinsic cell memory reinforces myogenic commitment of pericyte-derived iPSCs. *J. Pathol.* 223(5), 593–603 (2011).

116. Choi JH, Gimble JM, Lee K *et al.* Adipose tissue engineering for soft tissue regeneration. *Tissue Eng. B. Rev.* 16(4), 413–426 (2010).

117. Ahfeldt T, Schinzel RT, Lee Y-K *et al.* Programming human pluripotent stem cells into white and brown adipocytes. *Nat. Cell Biol.* 14(2), 209–219 (2012).

118. Nishio M, Yoneshiro T, Nakahara M *et al.* Production of functional classical brown adipocytes from human pluripotent stem cells using specific hemopoietin cocktail without gene transfer. *Cell Metab.* 16(3), 394–406 (2012).

- **Describes an efficient method for the generation of functional brown adipocytesfrom pluripotent stem cells without using exogenous gene transfer. Here, theydemonstrated that key differences in signaling pathways exist between hESC andinduced pluripotent stem cell-derived brown adipocytes.**

119. Taura D, Noguchi M, Sone M *et al.* Adipogenic differentiation of human induced pluripotent stem cells: comparison with that of human embryonic stem cells. *FEBS Lett.* 583(6), 1029–1033 (2009).

120. Zur Nieden NI, Kempka G, Rancourt DE, Ahr H-J. Induction of chondro-, osteo-and adipogenesis in embryonic stem cells by bone morphogenetic protein-2: effect of cofactors on differentiating lineages. *BMC Dev. Biol.* 5(1), 1 (2005).

121. Cypess AM, Lehman S, Williams G *et al.* Identification and importance of brown adipose tissue in adult humans. *N. Engl. J. Med.* 360(15), 1509–1517 (2009).

122. Saito M, Okamatsu-Ogura Y, Matsushita M *et al.* High incidence of metabolically active brown adipose tissue in healthy adult humans effects of cold exposure and adiposity. *Diabetes* 58(7), 1526–1531 (2009).

123. Virtanen KA, Lidell ME, Orava J *et al.* Functional brown adipose tissue in healthy adults. *N. Engl. J. Med.* 360(15), 1518–1525 (2009).

124. De Peppo GM, Marcos-Campos I, Kahler DJ *et al.* Engineering bone tissue substitutes from human induced pluripotent stem cells. *Proc. Natl Acad. Sci. USA* 110(21), 8680–8685 (2013).

125. Marolt D, Campos IM, Bhumiratana S *et al.* Engineering bone tissue from human embryonic stem cells. *Proc. Natl Acad. Sci. USA* 109(22), 8705–8709 (2012).

126. Jin GZ, Kim TH, Kim JH *et al.* Bone tissue engineering of induced pluripotent stem cells cultured with macrochanneled polymer scaffold. *J. Biomed. Mater. Res. A* 101(5), 1283–1291 (2013).

127. Wen C, Kang H, Shih Y-RV, Hwang Y, Varghese S. *In vivo* comparison of biomineralized scaffold-directed osteogenic differentiation of human embryonic and mesenchymal stem cells. *Drug Deliv. Transl. Res.* 6(2), 121–131 (2015).

128. Qazi TH, Mooney DJ, Pumberger M, Geißler S, Duda GN. Biomaterials based strategies for skeletal muscle tissue engineering: existing technologies and future trends. *Biomaterials* 53, 502–521 (2015).

129. Chal J, Al Tanoury Z, Hestin M *et al.* Generation of human muscle fibers and satellite-like cells from human pluripotent stem cells *in vitro*. *Nat. Protoc.* 11(10), 1833–1850 (2016).

List of References

Alvarez-Tejado, M., Naranjo-Suárez, S., Jiménez, C., Carrera, A.C., Landázuri, M.O., and del Peso, L. (2001). Hypoxia induces the activation of the phosphatidylinositol 3-Kinase/Akt cell survival pathway in PC12 cells protective role in apoptosis. Journal of Biological Chemistry *276*, 22368-22374.

Amarilio, R., Viukov, S.V., Sharir, A., Eshkar-Oren, I., Johnson, R.S., and Zelzer, E. (2007). HIF1α regulation of Sox9 is necessary to maintain differentiation of hypoxic prechondrogenic cells during early skeletogenesis. Development *134*, 3917-3928.

Antebi, B., Pelled, G., and Gazit, D. (2014). Stem cell therapy for osteoporosis. Current osteoporosis reports *12*, 41-47.

Araki, R., Uda, M., Hoki, Y., Sunayama, M., Nakamura, M., Ando, S., Sugiura, M., Ideno, H., Shimada, A., and Nifuji, A. (2013). Negligible immunogenicity of terminally differentiated cells derived from induced pluripotent or embryonic stem cells. Nature *494*, 100-104.

Arthur, S.A., Blaydes, J.P., and Houghton, F.D. (2019). Glycolysis Regulates Human Embryonic Stem Cell Self-Renewal under Hypoxia through HIF-2α and the Glycolytic Sensors CTBPs. Stem cell reports.

Arzi, B., DuRaine, G., Lee, C.A., Huey, D., Borjesson, D.L., Murphy, B.G., Hu, J., Baumgarth, N., and Athanasiou, K. (2015). Cartilage immunoprivilege depends on donor source and lesion location. Acta biomaterialia *23*, 72-81.

Asanbaeva, A., Masuda, K., Thonar, E.J.A., Klisch, S.M., Sah, R.L.J.B., and mechanobiology, m.i. (2008). Regulation of immature cartilage growth by IGF-I, TGF-β1, BMP-7, and PDGF-AB: role of metabolic balance between fixed charge and collagen network. *7*, 263.

Athanasiou, K.A., Eswaramoorthy, R., Hadidi, P., and Hu, J.C. (2013). Self-organization and the self-assembling process in tissue engineering. Annual review of biomedical engineering *15*, 115-136.

Aung, A., Gupta, G., Majid, G., and Varghese, S. (2011). Osteoarthritic chondrocyte–secreted morphogens induce chondrogenic differentiation of human mesenchymal stem cells. Arthritis & Rheumatism *63*, 148-158.

Avilion, A.A., Nicolis, S.K., Pevny, L.H., Perez, L., Vivian, N., and Lovell-Badge, R. (2003). Multipotent cell lineages in early mouse development depend on SOX2 function. Genes & development *17*, 126-140.

Bader, D.L., Salter, D., and Chowdhury, T.J.A. (2011). Biomechanical influence of cartilage homeostasis in health and disease. *2011*.

Barberi, T., Willis, L.M., Socci, N.D., and Studer, L. (2005). Derivation of multipotent mesenchymal precursors from human embryonic stem cells. PLoS medicine *2*, 554.

Barbero, A., Grogan, S., Schäfer, D., Heberer, M., Mainil-Varlet, P., and Martin, I. (2004). Age related changes in human articular chondrocyte yield, proliferation and post-expansion chondrogenic capacity. Osteoarthritis and cartilage *12*, 476-484.

Barter, M., Bui, C., and Young, D. (2012). Epigenetic mechanisms in cartilage and osteoarthritis: DNA methylation, histone modifications and microRNAs. Osteoarthritis and cartilage *20*, 339-349.

Baxter, M.A., Camarasa, M.V., Bates, N., Small, F., Murray, P., Edgar, D., and Kimber, S.J. (2009). Analysis of the distinct functions of growth factors and tissue culture substrates necessary for the long-term self-renewal of human embryonic stem cell lines. Stem cell research *3*, 28-38.

Bazou, D., Kearney, R., Mansergh, F., Bourdon, C., Farrar, J., and Wride, M. (2011). Gene expression analysis of mouse embryonic stem cells following levitation in an ultrasound standing wave trap. Ultrasound in medicine & biology *37*, 321-330.

Bell, D.M., Leung, K., Wheatley, S.C., Ng, L.J., Zhou, S., Ling, K.W., Sham, M., Koopman, P., Tam, P., and Cheah, K. (1997). SOX9 directly regulates the Type 2 collagen gene. Nat Genet *16*, 174-178.

Bellgrau, D., Gold, D., Selawry, H., Moore, J., Franzusoff, A., and Duke, R.C. (1995). A role for CD95 ligand in preventing graft rejection. Nature *377*, 630.

Bentley, G., Biant, L., Vijayan, S., Macmull, S., Skinner, J., and Carrington, R. (2012). Minimum ten-year results of a prospective randomised study of autologous chondrocyte implantation versus mosaicplasty for symptomatic articular cartilage lesions of the knee. Journal of Bone & Joint Surgery, British Volume *94*, 504-509.

Benya, P.D., Padilla, S.R., and Nimni, M.E. (1978). Independent regulation of collagen types by chondrocytes during the loss of differentiated function in culture. Cell *15*, 1313-1321.

Benya, P.D., and Shaffer, J.D. (1982). Dedifferentiated chondrocytes reexpress the differentiated collagen phenotype when cultured in agarose gels. Cell *30*, 215-224.

Bernstein, P., Dong, M., Corbeil, D., Gelinsky, M., Günther, K.P., and Fickert, S. (2009). Pellet culture elicits superior chondrogenic redifferentiation than alginate-based systems. Biotechnology progress *25*, 1146-1152.

Bi, W., Deng, J.M., Zhang, Z., Behringer, R.R., and de Crombrugghe, B. (1999). Sox9 is required for cartilage formation. Nature genetics *22*, 85.

Bianco, P., and Robey, P.G. (2015). Skeletal stem cells. Development *142*, 1023-1027.

Bigdeli, N., Karlsson, C., Strehl, R., Concaro, S., Hyllner, J., and Lindahl, A. (2009). Coculture of human embryonic stem cells and human articular chondrocytes results in significantly altered phenotype and improved chondrogenic differentiation. Stem Cells *27*, 1812-1821.

Blandizzi, C., Tuccori, M., Colucci, R., Fornai, M., Antonioli, L., Ghisu, N., and Del Tacca, M. (2009). Role of coxibs in the strategies for gastrointestinal protection in patients requiring chronic non-steroidal anti-inflammatory therapy. Pharmacological research *59*, 90-100.

Boreström, C., Simonsson, S., Enochson, L., Bigdeli, N., Brantsing, C., Ellerström, C., Hyllner, J., and Lindahl, A. (2014). Footprint-Free Human Induced Pluripotent Stem Cells From Articular Cartilage With Redifferentiation Capacity: A First Step Toward a Clinical-Grade Cell Source. Stem cells translational medicine *3*, 433-447.

Boschetti, F., Pennati, G., Gervaso, F., Peretti, G.M., and Dubini, G. (2004). Biomechanical properties of human articular cartilage under compressive loads. Biorheology *41*, 159-166.

Bouyer, C., Chen, P., Güven, S., Demirtaş, T.T., Nieland, T.J., Padilla, F., and Demirci, U. (2016). A Bio-Acoustic Levitational (BAL) Assembly Method for Engineering of Multilayered, 3D Brain-Like Constructs, Using Human Embryonic Stem Cell Derived Neuro-Progenitors. Advanced Materials *28*, 161-167.

Brittberg, M., Lindahl, A., Nilsson, A., Ohlsson, C., Isaksson, O., and Peterson, L. (1994). Treatment of deep cartilage defects in the knee with autologous chondrocyte transplantation. New england journal of medicine *331*, 889-895.

Browning, M.B., and Cosgriff-Hernandez, E. (2012). Development of a biostable replacement for PEGDA hydrogels. Biomacromolecules *13*, 779-786.

Chen, G., Gulbranson, D.R., Hou, Z., Bolin, J.M., Ruotti, V., Probasco, M.D., Smuga-Otto, K., Howden, S.E., Diol, N.R., and Propson, N.E. (2011). Chemically defined conditions for human iPSC derivation and culture. Nature methods *8*, 424-429.

Chen, J.-L., Zou, C., Chen, Y., Zhu, W., Liu, W., Huang, J., Liu, Q., Wang, D., Duan, L., and Xiong, J. (2017). TGFβ1 induces hypertrophic change and expression of angiogenic factors in human chondrocytes. Oncotarget *8*, 91316.

Cheng, A., Cain, S.A., Tian, P., Baldwin, A.K., Uppanan, P., Kielty, C.M., and Kimber, S.J. (2018). Recombinant extracellular matrix protein fragments support human embryonic stem cell chondrogenesis. Tissue Engineering Part A *24*, 968-978.

Cheng, A., Kapacee, Z., Peng, J., Lu, S., Lucas, R.J., Hardingham, T.E., and Kimber, S.J. (2014). Cartilage repair using human embryonic stem cell-derived chondroprogenitors. Stem cells translational medicine *3*, 1287-1294.

Cherubino, P., Grassi, F., Bulgheroni, P., and Ronga, M. (2003). Autologous chondrocyte implantation using a bilayer collagen membrane: a preliminary report. Journal of Orthopaedic Surgery *11*, 10-15.

Christensen, D.R., Calder, P.C., and Houghton, F.D. (2015). GLUT3 and PKM2 regulate OCT4 expression and support the hypoxic culture of human embryonic stem cells. Scientific reports *5*, 17500.

Control, C.f.D., and Prevention (2010). Prevalence of doctor-diagnosed arthritis and arthritis-attributable activity limitation---United States, 2007-2009. MMWR Morbidity and mortality weekly report *59*, 1261.

Cook, S.D., Salkeld, S.L., Patron, L.P., Doughty, E.S., and Jones, D.G. (2008). The effect of low-intensity pulsed ultrasound on autologous osteochondral plugs in a canine model. The American journal of sports medicine *36*, 1733-1741.

Cook, S.D., Salkeld, S.L., Popich-Patron, L.S., Ryaby, J.P., Jones, D.G., and Barrack, R.L. (2001). Improved cartilage repair after treatment with low-intensity pulsed ultrasound. Clinical orthopaedics and related research *391*, S231-S243.

Coricor, G., and Serra, R. (2016). TGF-β regulates phosphorylation and stabilization of Sox9 protein in chondrocytes through p38 and Smad dependent mechanisms. Scientific Reports *6*.

Cortés, F., Debacker, C., Péault, B., and Labastie, M.-C. (1999). Differential expression of KDR/VEGFR-2 and CD34 during mesoderm development of the early human embryo. Mechanisms of development *83*, 161-164.

Cross, M., Smith, E., Hoy, D., Nolte, S., Ackerman, I., Fransen, M., Bridgett, L., Williams, S., Guillemin, F., and Hill, C.L. (2014). The global burden of hip and knee osteoarthritis: estimates from the global burden of disease 2010 study. Annals of the rheumatic diseases, annrheumdis-2013-204763.

D'Apuzzo, M.R., Pao, A.W., Novicoff, W.M., and Browne, J.A. (2014). Age as an independent risk factor for postoperative morbidity and mortality after total joint arthroplasty in patients 90 years of age or older. The Journal of arthroplasty *29*, 477-480.

da Cruz, L., Fynes, K., Georgiadis, O., Kerby, J., Luo, Y.H., Ahmado, A., Vernon, A., Daniels, J.T., Nommiste, B., and Hasan, S.M. (2018). Phase 1 clinical study of an embryonic stem cell–derived retinal pigment epithelium patch in age-related macular degeneration. Nature biotechnology *36*, 328.

Dargent-Molina, P., Favier, F., Grandjean, H., Baudoin, C., Schott, A., Hausherr, E., Meunier, P., Breart, G., and Group, E. (1996). Fall-related factors and risk of hip fracture: the EPIDOS prospective study. The Lancet *348*, 145-149.

Davisson, T., Sah, R.L., and Ratcliffe, A. (2002). Perfusion increases cell content and matrix synthesis in chondrocyte three-dimensional cultures. Tissue engineering *8*, 807-816.

de Andrés, M.C., Kingham, E., Imagawa, K., Gonzalez, A., Roach, H.I., Wilson, D.I., and Oreffo, R.O. (2013). Epigenetic regulation during fetal femur development: DNA methylation matters. PloS one *8*, e54957.

Diekman, B.O., Christoforou, N., Willard, V.P., Sun, H., Sanchez-Adams, J., Leong, K.W., and Guilak, F. (2012). Cartilage tissue engineering using differentiated and purified induced pluripotent stem cells. Proceedings of the National Academy of Sciences *109*, 19172-19177.

Doi, A., Park, I.-H., Wen, B., Murakami, P., Aryee, M.J., Irizarry, R., Herb, B., Ladd-Acosta, C., Rho, J., and Loewer, S. (2009). Differential methylation of tissue-and cancer-specific CpG island shores distinguishes human induced pluripotent stem cells, embryonic stem cells and fibroblasts. Nature genetics *41*, 1350-1353.

Dy, P., Wang, W., Bhattaram, P., Wang, Q., Wang, L., Ballock, R.T., and Lefebvre, V. (2012). Sox9 directs hypertrophic maturation and blocks osteoblast differentiation of growth plate chondrocytes. Developmental cell *22*, 597-609.

Elayyan, J., Lee, E.-J., Gabay, O., Smith, C.A., Qiq, O., Reich, E., Mobasheri, A., Henrotin, Y., Kimber, S.J., and Dvir-Ginzberg, M. (2017). LEF1-mediated MMP13 gene expression is repressed by SIRT1 in human chondrocytes. The FASEB Journal, fj. 201601253R.

Engler, A.J., Sen, S., Sweeney, H.L., and Discher, D.E. (2006). Matrix elasticity directs stem cell lineage specification. Cell *126*, 677-689.

Evans, M.J., and Kaufman, M.H. (1981). Establishment in culture of pluripotential cells from mouse embryos. Nature *292*, 154-156.

Evans, N.D., Minelli, C., Gentleman, E., LaPointe, V., Patankar, S.N., Kallivretaki, M., Chen, X., Roberts, C.J., and Stevens, M.M. (2009). Substrate stiffness affects early differentiation events in embryonic stem cells. Eur cell mater *18*, e13.

Ezashi, T., Das, P., and Roberts, R.M. (2005). Low O2 tensions and the prevention of differentiation of hES cells. Proceedings of the National Academy of Sciences of the United States of America *102*, 4783-4788.

Fischer, B., and Bavister, B. (1993). Oxygen tension in the oviduct and uterus of rhesus monkeys, hamsters and rabbits. Reproduction *99*, 673-679.

Fischer, J., Dickhut, A., Rickert, M., and Richter, W. (2010). Human articular chondrocytes secrete parathyroid hormone–related protein and inhibit hypertrophy of mesenchymal stem cells in coculture during chondrogenesis. Arthritis & Rheumatism *62*, 2696-2706.

Flowers, S.A., Zieba, A., Örnros, J., Jin, C., Rolfson, O., Björkman, L.I., Eisler, T., Kalamajski, S., Kamali-Moghaddam, M., and Karlsson, N.G. (2017). Lubricin binds cartilage proteins, cartilage oligomeric matrix protein, fibronectin and collagen II at the cartilage surface. Scientific reports *7*, 13149.

Forristal, C.E., Christensen, D.R., Chinnery, F.E., Petruzzelli, R., Parry, K.L., Sanchez-Elsner, T., and Houghton, F.D. (2013). Environmental oxygen tension regulates the energy metabolism and self-renewal of human embryonic stem cells.

Forristal, C.E., Wright, K.L., Hanley, N.A., Oreffo, R.O., and Houghton, F.D. (2010). Hypoxia inducible factors regulate pluripotency and proliferation in human embryonic stem cells cultured at reduced oxygen tensions. Reproduction *139*, 85-97.

Fortier, L.A., Barker, J.U., Strauss, E.J., McCarrel, T.M., and Cole, B.J. (2011). The role of growth factors in cartilage repair. Clinical Orthopaedics and Related Research® *469*, 2706-2715.

French, M., Smith, S., Akanbi, K., Sanford, T., Hecht, J., Farach-Carson, M., and Carson, D. (1999). Expression of the heparan sulfate proteoglycan, perlecan, during mouse embryogenesis and perlecan chondrogenic activity in vitro. The Journal of cell biology *145*, 1103-1115.

Fujihara, Y., Takato, T., and Hoshi, K. (2010). Immunological response to tissue-engineered cartilage derived from auricular chondrocytes and a PLLA scaffold in transgenic mice. Biomaterials *31*, 1227-1234.

Fujihara, Y., Takato, T., and Hoshi, K. (2014). Macrophage-inducing FasL on chondrocytes forms immune privilege in cartilage tissue engineering, enhancing in vivo regeneration. Stem Cells *32*, 1208-1219.

Gago-Fuentes, R., Bechberger, J.F., Varela-Eirin, M., Varela-Vazquez, A., Acea, B., Fonseca, E., Naus, C.C., and Mayan, M.D. (2016). The C-terminal domain of connexin43 modulates cartilage structure via chondrocyte phenotypic changes. Oncotarget *7*, 73055.

Garvin, K.A., Dalecki, D., and Hocking, D.C. (2011). Vascularization of three-dimensional collagen hydrogels using ultrasound standing wave fields. Ultrasound in medicine & biology *37*, 1853-1864.

Gegg, C., and Yang, F. (2020). Spatially patterned microribbon-based hydrogels induce zonally-organized cartilage regeneration by stem cells in 3D. Acta biomaterialia *101*, 196-205.

Gigout, A., Buschmann, M.D., and Jolicoeur, M. (2009). Chondrocytes cultured in stirred suspension with serum-free medium containing pluronic-68 aggregate and proliferate while maintaining their differentiated phenotype. Tissue Engineering Part A *15*, 2237-2248.

Gil, J., and Reiss, O.K. (1973). Isolation and characterization of lamellar bodies and tubular myelin from rat lung homogenates. The Journal of cell biology *58*, 152-171.

Gobbi, A., Karnatzikos, G., and Kumar, A. (2014). Long-term results after microfracture treatment for full-thickness knee chondral lesions in athletes. Knee Surgery, Sports Traumatology, Arthroscopy *22*, 1986-1996.

Grant, C.A., Brockwell, D.J., Radford, S.E., and Thomson, N.H. (2009). Tuning the elastic modulus of hydrated collagen fibrils. Biophysical journal *97*, 2985-2992.

Grinnemo, K.-H., Kumagai-Braesch, M., Mânsson-Broberg, A., Skottman, H., Hao, X., Siddiqui, A., Andersson, A., Strömberg, A.-M., Lahesmaa, R., and Hovatta, O. (2006). Human embryonic stem cells are immunogenic in allogeneic and xenogeneic settings. Reproductive biomedicine online *13*, 712-724.

Guilak, F., Butler, D.L., Goldstein, S.A., and Baaijens, F.P. (2014). Biomechanics and mechanobiology in functional tissue engineering. Journal of biomechanics *47*, 1933-1940.

Gupta, M.S., Cooper, E.S., and Nicoll, S.B. (2011). Transforming growth factor-beta 3 stimulates cartilage matrix elaboration by human marrow-derived stromal cells encapsulated in photocrosslinked carboxymethylcellulose hydrogels: potential for nucleus pulposus replacement. Tissue Engineering Part A *17*, 2903-2910.

Gutierrez-Aranda, I., Ramos-Mejia, V., Bueno, C., Munoz-Lopez, M., Real, P.J., Mácia, A., Sanchez, L., Ligero, G., Garcia-Parez, J.L., and Menendez, P. (2010). Human induced pluripotent stem cells develop teratoma more efficiently and faster than human embryonic stem cells regardless the site of injection. Stem cells *28*, 1568-1570.

Gygi, S.P., Rochon, Y., Franza, B.R., and Aebersold, R. (1999). Correlation between protein and mRNA abundance in yeast. Molecular and cellular biology *19*, 1720-1730.

Harris, J.D., Siston, R.A., Pan, X., and Flanigan, D.C. (2010). Autologous Chondrocyte Implantation. The Journal of Bone & Joint Surgery *92*, 2220-2233.

Hata, R.I., and Senoo, H. (1989). L-ascorbic acid 2-phosphate stimulates collagen accumulation, cell proliferation, and formation of a three-dimensional tissuelike substance by skin fibroblasts. Journal of cellular physiology *138*, 8-16.

Hattori, T., Müller, C., Gebhard, S., Bauer, E., Pausch, F., Schlund, B., Bösl, M.R., Hess, A., Surmann-Schmitt, C., and von der Mark, H. (2010). SOX9 is a major negative regulator of cartilage vascularization, bone marrow formation and endochondral ossification. Development *137*, 901-911.

Heinemeier, K.M., Schjerling, P., Heinemeier, J., Møller, M.B., Krogsgaard, M.R., Grum-Schwensen, T., Petersen, M.M., and Kjaer, M. (2016). Radiocarbon dating reveals minimal collagen turnover in both healthy and osteoarthritic human cartilage. Science translational medicine *8*, 346ra390-346ra390.

Henry, S.P., Liang, S., Akdemir, K.C., and de Crombrugghe, B. (2012). The postnatal role of Sox9 in cartilage. Journal of Bone and Mineral Research *27*, 2511-2525.

Hoben, G.M., Willard, V.P., and Athanasiou, K.A. (2009). Fibrochondrogenesis of hESCs: growth factor combinations and cocultures. Stem cells and development *18*, 283-292.

Hodge, W., Fijan, R., Carlson, K., Burgess, R., Harris, W., and Mann, R.J.P.o.t.N.A.o.S. (1986). Contact pressures in the human hip joint measured in vivo. *83*, 2879-2883.

Horas, U., Pelinkovic, D., Herr, G., Aigner, T., and Schnettler, R. (2003). Autologous chondrocyte implantation and osteochondral cylinder transplantation in cartilage repair of the knee joint. The Journal of Bone & Joint Surgery *85*, 185-192.

Horlings, C.G., van Engelen, B.G., Allum, J.H., and Bloem, B.R. (2008). A weak balance: the contribution of muscle weakness to postural instability and falls. Nature Clinical Practice Neurology *4*, 504-515.

hPSCreg (2019). hESC lines (https://hpscreg.eu/search?cell-type=hesc).

Hunter, D.J., Neogi, T., and Hochberg, M.C. (2011). Quality of osteoarthritis management and the need for reform in the US. Arthritis care & research *63*, 31-38.

Hwang, N.S., Varghese, S., and Elisseeff, J. (2008). Derivation of chondrogenically-committed cells from human embryonic cells for cartilage tissue regeneration. PLoS One *3*, e2498.

Ikegami, D., Akiyama, H., Suzuki, A., Nakamura, T., Nakano, T., Yoshikawa, H., and Tsumaki, N. (2011). Sox9 sustains chondrocyte survival and hypertrophy in part through Pik3ca-Akt pathways. Development *138*, 1507-1519.

Ilic, D., Devito, L., Miere, C., and Codognotto, S. (2015). Human embryonic and induced pluripotent stem cells in clinical trials. British Medical Bulletin, ldv045.

Insall, J. (1974). The Pridie debridement operation for osteoarthritis of the knee. Clinical orthopaedics and related research *101*, 61-67.

Iwai, R., Fujiwara, M., Wakitani, S., and Takagi, M. (2011). Ex vivo cartilage defect model for the evaluation of cartilage regeneration using mesenchymal stem cells. Journal of bioscience and bioengineering *111*, 357-364.

Jevons, L.A., Houghton, F.D., and Tare, R.S. (2018). Augmentation of musculoskeletal regeneration: role for pluripotent stem cells. Regenerative medicine *13*, 189-206.

Jin, H., and Lewis, J.L. (2004). Determination of Poisson's ratio of articular cartilage by indentation using different-sized indenters. Journal of biomechanical engineering *126*, 138-145.

Johnell, O., and Kanis, J. (2004). An estimate of the worldwide prevalence, mortality and disability associated with hip fracture. Osteoporosis International *15*, 897-902.

Johnson, L.L. (2001). Arthroscopic abrasion arthroplasty: a review. Clinical orthopaedics and related research *391*, S306-S317.

Johnstone, B., Alini, M., Cucchiarini, M., Dodge, G.R., Eglin, D., Guilak, F., Madry, H., Mata, A., Mauck, R.L., and Semino, C.E. (2013). Tissue engineering for articular cartilage repair–the state of the art. Eur Cell Mater *25*, e67.

Johnstone, B., Hering, T., Caplan, A., Goldberg, V., and Yoo, J. (1998). In vitro chondrogenesis of bone marrow-derived mesenchymal progenitor cells. Experimental cell research *238*, 265-272.

Jonnalagadda, U.S., Hill, M., Messaoudi, W., Cook, R.B., Oreffo, R.O., Glynne-Jones, P., and Tare, R.S. (2018). Acoustically modulated biomechanical stimulation for human cartilage tissue engineering. Lab on a chip *18*, 473-485.

Kafienah, W., Mistry, S., Dickinson, S.C., Sims, T.J., Learmonth, I., and Hollander, A.P. (2007). Three-dimensional cartilage tissue engineering using adult stem cells from osteoarthritis patients. Arthritis & Rheumatism *56*, 177-187.

Kawaguchi, J., Mee, P.J., and Smith, A.G. (2005). Osteogenic and chondrogenic differentiation of embryonic stem cells in response to specific growth factors. Bone *36*, 758-769.

Kim, D., Kim, C.-H., Moon, J.-I., Chung, Y.-G., Chang, M.-Y., Han, B.-S., Ko, S., Yang, E., Cha, K.Y., and Lanza, R. (2009). Generation of human induced pluripotent stem cells by direct delivery of reprogramming proteins. Cell stem cell *4*, 472.

Kim, K., Doi, A., Wen, B., Ng, K., Zhao, R., Cahan, P., Kim, J., Aryee, M., Ji, H., and Ehrlich, L. (2010). Epigenetic memory in induced pluripotent stem cells. Nature *467*, 285-290.

Kim, K., Zhao, R., Doi, A., Ng, K., Unternaehrer, J., Cahan, P., Hongguang, H., Loh, Y.-H., Aryee, M.J., and Lensch, M.W. (2011). Donor cell type can influence the epigenome and differentiation potential of human induced pluripotent stem cells. Nature biotechnology *29*, 1117.

Kim, T.-K., Sharma, B., Williams, C., Ruffner, M., Malik, A., McFarland, E.G., and Elisseeff, J.H. (2003). Experimental model for cartilage tissue engineering to regenerate the zonal organization of articular cartilage. Osteoarthritis and cartilage *11*, 653-664.

Kim, Y.-J., Sah, R.L., Grodzinsky, A.J., Plaas, A.H., Sandy, J.D.J.A.o.B., and Biophysics (1994). Mechanical regulation of cartilage biosynthetic behavior: physical stimuli. *311*, 1-12.

Kiviranta, I., Jurvelin, J., Säämänen, A.-M., and Helminen, H. (1985). Microspectrophotometric quantitation of glycosaminoglycans in articular cartilage sections stained with Safranin O. Histochemistry *82*, 249-255.

Ko, J.-Y., Kim, K.-I., Park, S., and Im, G.-I. (2014). In vitro chondrogenesis and in vivo repair of osteochondral defect with human induced pluripotent stem cells. Biomaterials *35*, 3571-3581.

Kongtharvonskul, J., Anothaisintawee, T., McEvoy, M., Attia, J., Woratanarat, P., and Thakkinstian, A. (2015). Efficacy and safety of glucosamine, diacerein, and NSAIDs in osteoarthritis knee: a systematic review and network meta-analysis. European journal of medical research *20*, 24.

Kraeutler, M.J., Belk, J.W., Purcell, J.M., and McCarty, E.C. (2018). Microfracture versus autologous chondrocyte implantation for articular cartilage lesions in the knee: a systematic review of 5-year outcomes. The American journal of sports medicine *46*, 995-999.

Kramer, J., Hegert, C., Guan, K., Wobus, A.M., Müller, P.K., and Rohwedel, J. (2000). Embryonic stem cell-derived chondrogenic differentiation in vitro: activation by BMP-2 and BMP-4. Mechanisms of development *92*, 193-205.

Laird, D.W. (2014). Syndromic and non-syndromic disease-linked Cx43 mutations. FEBS letters *588*, 1339-1348.

Landi, F., Liperoti, R., Russo, A., Giovannini, S., Tosato, M., Capoluongo, E., Bernabei, R., and Onder, G. (2012). Sarcopenia as a risk factor for falls in elderly individuals: results from the ilSIRENTE study. Clinical nutrition *31*, 652-658.

Lee, D.A., Knight, M.M., Campbell, J.J., and Bader, D.L. (2011a). Stem cell mechanobiology. Journal of cellular biochemistry *112*, 1-9.

Lee, H.-H., Chang, C.-C., Shieh, M.-J., Wang, J.-P., Chen, Y.-T., Young, T.-H., and Hung, S.-C. (2013). Hypoxia enhances chondrogenesis and prevents terminal differentiation through PI3K/Akt/FoxO dependent anti-apoptotic effect. Scientific reports *3*, 2683.

Lee, J., Taylor, S.E., Smeriglio, P., Lai, J., Maloney, W.J., Yang, F., and Bhutani, N. (2015). Early induction of a prechondrogenic population allows efficient generation of stable chondrocytes from human induced pluripotent stem cells. The FASEB Journal *29*, 3399-3410.

Lee, S.-H., and Shin, H. (2007). Matrices and scaffolds for delivery of bioactive molecules in bone and cartilage tissue engineering. Advanced drug delivery reviews *59*, 339-359.

Lee, T.-J., Bhang, S.H., La, W.-G., Yang, H.S., Seong, J.Y., Lee, H., Im, G.-I., Lee, S.-H., and Kim, B.-S. (2011b). Spinner-flask culture induces redifferentiation of de-differentiated chondrocytes. Biotechnology letters *33*, 829-836.

Lefebvre, V., Huang, W., Harley, V.R., Goodfellow, P.N., and De Crombrugghe, B. (1997). SOX9 is a potent activator of the chondrocyte-specific enhancer of the pro alpha1 (II) collagen gene. Molecular and cellular biology *17*, 2336-2346.

Li, L., Baroja, M.L., Majumdar, A., Chadwick, K., Rouleau, A., Gallacher, L., Ferber, I., Lebkowski, J., Martin, T., and Madrenas, J. (2004). Human embryonic stem cells possess immune-privileged properties. Stem Cells *22*, 448-456.

Li, M., and Belmonte, J.C.I. (2017). Ground rules of the pluripotency gene regulatory network. Nature Reviews Genetics *18*, 180.

Li, M.D., Atkins, H., and Bubela, T. (2014a). The global landscape of stem cell clinical trials. Regenerative medicine *9*, 27-39.

Li, S., Glynne-Jones, P., Andriotis, O.G., Ching, K.Y., Jonnalagadda, U.S., Oreffo, R.O., Hill, M., and Tare, R.S. (2014b). Application of an acoustofluidic perfusion bioreactor for cartilage tissue engineering. Lab on a chip *14*, 4475-4485.

Li, S., Oreffo, R.O., Sengers, B.G., and Tare, R.S. (2014c). The effect of oxygen tension on human articular chondrocyte matrix synthesis: Integration of experimental and computational approaches. Biotechnology and bioengineering *111*, 1876-1885.

Li, S., Sengers, B.G., Oreffo, R.O., and Tare, R.S. (2015). Chondrogenic potential of human articular chondrocytes and skeletal stem cells: A comparative study. Journal of biomaterials applications *29*, 824-836.

Li, Z., Kupcsik, L., Yao, S.J., Alini, M., and Stoddart, M.J. (2010). Mechanical load modulates chondrogenesis of human mesenchymal stem cells through the TGF-β pathway. Journal of cellular and molecular medicine *14*, 1338-1346.

Lian, Q., Lye, E., Suan Yeo, K., Khia Way Tan, E., Salto-Tellez, M., Liu, T.M., Palanisamy, N., El Oakley, R.M., Lee, E.H., and Lim, B. (2007). Derivation of clinically compliant MSCs from CD105+, CD24− differentiated human ESCs. Stem cells *25*, 425-436.

Lian, Q., Zhang, Y., Zhang, J., Zhang, H.K., Wu, X., Zhang, Y., Lam, F.F.-Y., Kang, S., Xia, J.C., and Lai, W.-H. (2010). Functional mesenchymal stem cells derived from human induced pluripotent stem cells attenuate limb ischemia in mice. Circulation *121*, 1113-1123.

Liu, Y., Song, Z., Zhao, Y., Qin, H., Cai, J., Zhang, H., Yu, T., Jiang, S., Wang, G., and Ding, M. (2006). A novel chemical-defined medium with bFGF and N2B27 supplements supports undifferentiated growth in human embryonic stem cells. Biochemical and biophysical research communications *346*, 131-139.

Loeser, R.F., Pacione, C.A., and Chubinskaya, S. (2003). The combination of insulin-like growth factor 1 and osteogenic protein 1 promotes increased survival of and matrix synthesis by normal and osteoarthritic human articular chondrocytes. Arthritis & Rheumatology *48*, 2188-2196.

Ludwig, T.E., Bergendahl, V., Levenstein, M.E., Yu, J., Probasco, M.D., and Thomson, J.A. (2006a). Feeder-independent culture of human embryonic stem cells. Nature methods *3*, 637-646.

Ludwig, T.E., Levenstein, M.E., Jones, J.M., Berggren, W.T., Mitchen, E.R., Frane, J.L., Crandall, L.J., Daigh, C.A., Conard, K.R., and Piekarczyk, M.S. (2006b). Derivation of human embryonic stem cells in defined conditions. Nature biotechnology *24*, 185-187.

Mackay, A.M., Beck, S.C., Murphy, J.M., Barry, F.P., Chichester, C.O., and Pittenger, M.F. (1998). Chondrogenic differentiation of cultured human mesenchymal stem cells from marrow. Tissue engineering *4*, 415-428.

Maier, T., Güell, M., and Serrano, L. (2009). Correlation of mRNA and protein in complex biological samples. FEBS letters *583*, 3966-3973.

Malafarina, V., Úriz-Otano, F., Iniesta, R., and Gil-Guerrero, L. (2012). Sarcopenia in the elderly: diagnosis, physiopathology and treatment. Maturitas *71*, 109-114.

Manning, W.K., and Bonner Jr, W.M. (1967). Isolation and culture of chondrocytes from human adult articular cartilage. Arthritis & Rheumatism: Official Journal of the American College of Rheumatology *10*, 235-239.

Mansour, J.M. (2003). Biomechanics of cartilage. Kinesiology: the mechanics and pathomechanics of human movement, 66-79.

Marcacci, M., Kon, E., Zaffagnini, S., Filardo, G., Delcogliano, M., Neri, M.P., Iacono, F., and Hollander, A.P. (2007). Arthroscopic second generation autologous chondrocyte implantation. Knee Surgery, Sports Traumatology, Arthroscopy *15*, 610-619.

Markway, B.D., Cho, H., and Johnstone, B. (2013). Hypoxia promotes redifferentiation and suppresses markers of hypertrophy and degeneration in both healthy and osteoarthritic chondrocytes. Arthritis research & therapy *15*, R92.

Martin, M.J., Muotri, A., Gage, F., and Varki, A. (2005). Human embryonic stem cells express an immunogenic nonhuman sialic acid. Nature medicine *11*, 228-232.

Masui, S., Nakatake, Y., Toyooka, Y., Shimosato, D., Yagi, R., Takahashi, K., Okochi, H., Okuda, A., Matoba, R., and Sharov, A.A. (2007). Pluripotency governed by Sox2 via regulation of Oct3/4 expression in mouse embryonic stem cells. Nature cell biology *9*, 625.

McGrath, K.E., Koniski, A.D., Maltby, K.M., McGann, J.K., and Palis, J. (1999). Embryonic expression and function of the chemokine SDF-1 and its receptor, CXCR4. Developmental biology *213*, 442-456.

Min, B.-H., Lee, H.J., Kim, Y.J., and Choi, B.H. (2016). Repair of partial thickness cartilage defects using cartilage extracellular matrix membrane-based chondrocyte delivery system in human Ex Vivo model. Tissue Engineering and Regenerative Medicine *13*, 182-190.

Mithoefer, K., McAdams, T., Williams, R.J., Kreuz, P.C., and Mandelbaum, B.R. (2009). Clinical efficacy of the microfracture technique for articular cartilage repair in the knee: an evidence-based systematic analysis. The American journal of sports medicine *37*, 2053-2063.

Mithoefer, K., Williams, R.J., Warren, R.F., Potter, H.G., Spock, C.R., Jones, E.C., Wickiewicz, T.L., and Marx, R.G. (2006). Chondral resurfacing of articular cartilage defects in the knee with the microfracture technique. JBJS Essential Surgical Techniques, 294-304.

Mukherjee, D., Nissen, S.E., and Topol, E.J. (2001). Risk of cardiovascular events associated with selective COX-2 inhibitors. Jama *286*, 954-959.

Murad, S., Grove, D., Lindberg, K., Reynolds, G., Sivarajah, A., and Pinnell, S. (1981). Regulation of collagen synthesis by ascorbic acid. Proceedings of the National Academy of Sciences *78*, 2879-2882.

Murphy, L., Schwartz, T.A., Helmick, C.G., Renner, J.B., Tudor, G., Koch, G., Dragomir, A., Kalsbeek, W.D., Luta, G., and Jordan, J.M. (2008). Lifetime risk of symptomatic knee osteoarthritis. Arthritis Care & Research *59*, 1207-1213.

Murray, C.J., Barber, R.M., Foreman, K.J., Ozgoren, A.A., Abd-Allah, F., Abera, S.F., Aboyans, V., Abraham, J.P., Abubakar, I., and Abu-Raddad, L.J. (2015). Global, regional, and national disability-adjusted life years (DALYs) for 306 diseases and injuries and healthy life expectancy (HALE) for 188 countries, 1990–2013: quantifying the epidemiological transition. The Lancet *386*, 2145-2191.

Muschler, G.F., Nakamoto, C., and Griffith, L.G. (2004). Engineering principles of clinical cell-based tissue engineering. JBJS *86*, 1541-1558.

Nakajima, F., Tokunaga, K., and Nakatsuji, N. (2007). Human leukocyte antigen matching estimations in a hypothetical bank of human embryonic stem cell lines in the Japanese population for use in cell transplantation therapy. Stem Cells *25*, 983-985.

Nava, M.M., Raimondi, M.T., and Pietrabissa, R. (2012). Controlling self-renewal and differentiation of stem cells via mechanical cues. BioMed Research International *2012*.

Nedergaard, A., Henriksen, K., Karsdal, M.A., and Christiansen, C. (2013). Musculoskeletal ageing and primary prevention. Best Practice & Research Clinical Obstetrics & Gynaecology *27*, 673-688.

Nehrer, S., Domayer, S., Dorotka, R., Schatz, K., Bindreiter, U., and Kotz, R. (2006). Three-year clinical outcome after chondrocyte transplantation using a hyaluronan matrix for cartilage repair. European journal of radiology *57*, 3-8.

NICE, N.I.f.H.a.C.E. (2017). Autologous chondrocyte implantation for treating symptomatic articular cartilage defects of the knee. Technology appraisal guidance [TA477] (https://www.nice.org.uk/guidance/ta477).

NICE, N.I.f.H.C.E. (2018). Autologous chondrocyte implantation using chondrosphere for treating symptomatic articular cartilage defects of the knee. Technology appraisal guidance [TA508] (https://www.nice.org.uk/guidance/ta508).

Nichols, J., Zevnik, B., Anastassiadis, K., Niwa, H., Klewe-Nebenius, D., Chambers, I., Schöler, H., and Smith, A. (1998). Formation of pluripotent stem cells in the mammalian embryo depends on the POU transcription factor Oct4. Cell *95*, 379-391.

NIH (2019). NIH human Embryonic Stem Cell Registry.

Niwa, H., Miyazaki, J.-i., and Smith, A.G. (2000). Quantitative expression of Oct-3/4 defines differentiation, dedifferentiation or self-renewal of ES cells. Nature genetics *24*, 372.

Okada, M., Ikegawa, S., Morioka, M., Yamashita, A., Saito, A., Sawai, H., Murotsuki, J., Ohashi, H., Okamoto, T., and Nishimura, G. (2014). Modeling type II collagenopathy skeletal dysplasia by directed conversion and induced pluripotent stem cells. Human molecular genetics, ddu444.

Oldershaw, R.A., Baxter, M.A., Lowe, E.T., Bates, N., Grady, L.M., Soncin, F., Brison, D.R., Hardingham, T.E., and Kimber, S.J. (2010a). Chondrocyte protocol. StemBook [Internet].

Oldershaw, R.A., Baxter, M.A., Lowe, E.T., Bates, N., Grady, L.M., Soncin, F., Brison, D.R., Hardingham, T.E., and Kimber, S.J. (2010b). Directed differentiation of human embryonic stem cells toward chondrocytes. Nature biotechnology *28*, 1187-1194.

Olee, T., Grogan, S.P., Lotz, M.K., Colwell Jr, C.W., D'Lima, D.D., and Snyder, E.Y. (2013). Repair of cartilage defects in arthritic tissue with differentiated human embryonic stem cells. Tissue Engineering Part A *20*, 683-692.

Palfrey, A., and Davies, D. (1966). The fine structure of chondrocytes. Journal of anatomy *100*, 213.

Park, I.S., Jin, R.L., Oh, H.J., Truong, M.D., Choi, B.H., Park, S.H., Park, D.Y., and Min, B.H. (2019). Sizable Scaffold-Free Tissue-Engineered Articular Cartilage Construct for Cartilage Defect Repair. Artificial organs *43*, 278-287.

Peterson, L., Vasiliadis, H.S., Brittberg, M., and Lindahl, A. (2010). Autologous chondrocyte implantation: a long-term follow-up. The American journal of sports medicine *38*, 1117-1124.

Petruzzelli, R., Christensen, D.R., Parry, K.L., Sanchez-Elsner, T., and Houghton, F.D. (2014). HIF-2α regulates NANOG expression in human embryonic stem cells following hypoxia and reoxygenation through the interaction with an Oct-Sox cis regulatory element. PloS one *9*, e108309.

Pfander, D., Cramer, T., Schipani, E., and Johnson, R.S. (2003). HIF-1α controls extracellular matrix synthesis by epiphyseal chondrocytes. Journal of cell science *116*, 1819-1826.

Pritzker, K., Gay, S., Jimenez, S., Ostergaard, K., Pelletier, J.-P., Revell, P., Salter, D., and Van den Berg, W. (2006). Osteoarthritis cartilage histopathology: grading and staging. Osteoarthritis and cartilage *14*, 13-29.

Redman, S., Oldfield, S., and Archer, C. (2005). Current strategies for articular cartilage repair. Eur Cell Mater *9*, 23-32.

Revell, C.M., and Athanasiou, K.A. (2008). Success rates and immunologic responses of autogenic, allogenic, and xenogenic treatments to repair articular cartilage defects. Tissue Engineering Part B: Reviews *15*, 1-15.

Robins, J.C., Akeno, N., Mukherjee, A., Dalal, R.R., Aronow, B.J., Koopman, P., and Clemens, T.L. (2005). Hypoxia induces chondrocyte-specific gene expression in mesenchymal cells in association with transcriptional activation of Sox9. Bone *37*, 313-322.

Rodda, D.J., Chew, J.-L., Lim, L.-H., Loh, Y.-H., Wang, B., Ng, H.-H., and Robson, P. (2005). Transcriptional regulation of nanog by OCT4 and SOX2. Journal of Biological Chemistry *280*, 24731-24737.

Rodino-Klapac, L.R., Mendell, J.R., and Sahenk, Z. (2013). Update on the treatment of Duchenne muscular dystrophy. Current neurology and neuroscience reports *13*, 1-7.

Roy, S., and Meachim, G. (1968). Chondrocyte ultrastructure in adult human articular cartilage. Annals of the rheumatic diseases *27*, 544.

Schandelmaier, S., Kaushal, A., Lytvyn, L., Heels-Ansdell, D., Siemieniuk, R.A., Agoritsas, T., Guyatt, G.H., Vandvik, P.O., Couban, R., and Mollon, B. (2017). Low intensity pulsed ultrasound for bone healing: systematic review of randomized controlled trials. BMJ *356*, j656.

Schlaeger, T.M., Daheron, L., Brickler, T.R., Entwisle, S., Chan, K., Cianci, A., DeVine, A., Ettenger, A., Fitzgerald, K., and Godfrey, M. (2015). A comparison of non-integrating reprogramming methods. Nature biotechnology *33*, 58.

Schnabel, M., Marlovits, S., Eckhoff, G., Fichtel, I., Gotzen, L., Vecsei, V., and Schlegel, J. (2002). Dedifferentiation-associated changes in morphology and gene expression in primary human articular chondrocytes in cell culture. Osteoarthritis and Cartilage *10*, 62-70.

Schöler, H., Hatzopoulos, A.K., Balling, R., Suzuki, N., and Gruss, P. (1989). A family of octamer-specific proteins present during mouse embryogenesis: evidence for germline-specific expression of an Oct factor. The EMBO journal *8*, 2543-2550.

Schulz, R.M., and Bader, A. (2007). Cartilage tissue engineering and bioreactor systems for the cultivation and stimulation of chondrocytes. European Biophysics Journal *36*, 539-568.

Schwab, A., Meeuwsen, A., Ehlicke, F., Hansmann, J., Mulder, L., Smits, A., Walles, H., and Kock, L. (2017). Ex vivo culture platform for assessment of cartilage repair treatment strategies. ALTEX-Alternatives to animal experimentation *34*, 267-277.

Schwab, W., Hofer, A., and Kasper, M. (1998). Immunohistochemical distribution of connexin 43 in the cartilage of rats and mice. The Histochemical journal *30*, 413-419.

Schwartz, S.D., Hubschman, J.-P., Heilwell, G., Franco-Cardenas, V., Pan, C.K., Ostrick, R.M., Mickunas, E., Gay, R., Klimanskaya, I., and Lanza, R. (2012). Embryonic stem cell trials for macular degeneration: a preliminary report. The Lancet *379*, 713-720.

Schwarz, B.A., Bar-Nur, O., Silva, J.C., and Hochedlinger, K. (2014). Nanog is dispensable for the generation of induced pluripotent stem cells. Current Biology *24*, 347-350.

Schwarz, I., and Hills, B. (1996). Synovial surfactant: lamellar bodies in type B synoviocytes and proteolipid in synovial fluid and the articular lining. Rheumatology *35*, 821-827.

Science (2018). First-of-its-kind clinical trial will use reprogrammed adult stem cells to treat Parkinson's (www.sciencemag.org).

Scott, C.T., and Magnus, D. (2014). Wrongful termination: lessons from the Geron clinical trial. Stem cells translational medicine *3*, 1398-1401.

Selmi, T.A.S., Verdonk, P., Chambat, P., Dubrana, F., Potel, J.-F., Barnouin, L., and Neyret, P. (2008). Autologous chondrocyte implantation in a novel alginate-agarose hydrogel: outcome at two years. The Journal of bone and joint surgery British volume *90*, 597-604.

Sharma, B., Williams, C.G., Kim, T.K., Sun, D., Malik, A., Khan, M., Leong, K., and Elisseeff, J.H. (2007). Designing zonal organization into tissue-engineered cartilage. Tissue engineering *13*, 405-414.

Silva, J., Nichols, J., Theunissen, T.W., Guo, G., van Oosten, A.L., Barrandon, O., Wray, J., Yamanaka, S., Chambers, I., and Smith, A. (2009). Nanog is the gateway to the pluripotent ground state. Cell *138*, 722-737.

Sophia Fox, A.J., Bedi, A., and Rodeo, S.A. (2009). The basic science of articular cartilage: structure, composition, and function. Sports health *1*, 461-468.

Stegen, S., Laperre, K., Eelen, G., Rinaldi, G., Fraisl, P., Torrekens, S., Van Looveren, R., Loopmans, S., Bultynck, G., and Vinckier, S. (2019). HIF-1α metabolically controls collagen synthesis and modification in chondrocytes. Nature, 1.

Streilein, J.W. (1995). Unraveling immune privilege. Science *270*, 1158-1158.

Suchorska, W.M., Lach, M.S., Richter, M., Kaczmarczyk, J., and Trzeciak, T. (2016). Bioimaging: an useful tool to monitor differentiation of human embryonic stem cells into chondrocytes. Annals of biomedical engineering *44*, 1845-1859.

Takahashi, K., Tanabe, K., Ohnuki, M., Narita, M., Ichisaka, T., Tomoda, K., and Yamanaka, S. (2007). Induction of pluripotent stem cells from adult human fibroblasts by defined factors. cell *131*, 861-872.

Takahashi, K., and Yamanaka, S. (2006). Induction of pluripotent stem cells from mouse embryonic and adult fibroblast cultures by defined factors. cell *126*, 663-676.

Tanaka, H., Murphy, C.L., Murphy, C., Kimura, M., Kawai, S., and Polak, J.M. (2004). Chondrogenic differentiation of murine embryonic stem cells: effects of culture conditions and dexamethasone. Journal of cellular biochemistry *93*, 454-462.

Tang, Q.O., Shakib, K., Heliotis, M., Tsiridis, E., Mantalaris, A., Ripamonti, U., and Tsiridis, E. (2009). TGF-β3: A potential biological therapy for enhancing chondrogenesis. Expert opinion on biological therapy *9*, 689-701.

Tare, R.S., Howard, D., Pound, J.C., Roach, H.I., and Oreffo, R.O. (2005). Tissue engineering strategies for cartilage generation—micromass and three dimensional cultures using human chondrocytes and a continuous cell line. Biochemical and biophysical research communications *333*, 609-621.

Taylor, C.J., Bolton, E.M., Pocock, S., Sharples, L.D., Pedersen, R.A., and Bradley, J.A. (2005). Banking on human embryonic stem cells: estimating the number of donor cell lines needed for HLA matching. The Lancet *366*, 2019-2025.

Temu, T.M., Wu, K.-Y., Gruppuso, P.A., and Phornphutkul, C. (2010). The mechanism of ascorbic acid-induced differentiation of ATDC5 chondrogenic cells. American Journal of Physiology-Endocrinology and Metabolism *299*, E325-E334.

Thoms, B.L., Dudek, K.A., Lafont, J.E., and Murphy, C.L. (2013). Hypoxia promotes the production and inhibits the destruction of human articular cartilage. Arthritis & Rheumatism *65*, 1302-1312.

Thomson, J.A., Itskovitz-Eldor, J., Shapiro, S.S., Waknitz, M.A., Swiergiel, J.J., Marshall, V.S., and Jones, J.M. (1998). Embryonic stem cell lines derived from human blastocysts. science *282*, 1145-1147.

Thomson, M., Liu, S.J., Zou, L.-N., Smith, Z., Meissner, A., and Ramanathan, S. (2011). Pluripotency factors in embryonic stem cells regulate differentiation into germ layers. Cell *145*, 875-889.

Tığlı, R.S., Cannizaro, C., Gümüşderelioğlu, M., and Kaplan, D.L. (2011). Chondrogenesis in perfusion bioreactors using porous silk scaffolds and hESC-derived MSCs. Journal of Biomedical Materials Research Part A *96*, 21-28.

Toh, W.S., Yang, Z., Liu, H., Heng, B.C., Lee, E.H., and Cao, T. (2007). Effects of culture conditions and bone morphogenetic protein 2 on extent of chondrogenesis from human embryonic stem cells. Stem Cells *25*, 950-960.

Vacanti, J.P., and Langer, R. (1999). Tissue engineering: the design and fabrication of living replacement devices for surgical reconstruction and transplantation. The lancet *354*, S32-S34.

Vats, A., Bielby, R.C., Tolley, N., Dickinson, S.C., Boccaccini, A.R., Hollander, A.P., Bishop, A.E., and Polak, J.M. (2006). Chondrogenic differentiation of human embryonic stem cells: the effect of the micro-environment. Tissue engineering *12*, 1687-1697.

Vinatier, C., and Guicheux, J. (2016). Cartilage tissue engineering: From biomaterials and stem cells to osteoarthritis treatments. Annals of physical and rehabilitation medicine *59*, 139-144.

Waddell, S.J., de Andrés, M.C., Tsimbouri, P.M., Alakpa, E.V., Cusack, M., Dalby, M.J., and Oreffo, R.O. (2018). Biomimetic oyster shell–replicated topography alters the behaviour of human skeletal stem cells. Journal of tissue engineering *9*, 2041731418794007.

Wei, Y., Zeng, W., Wan, R., Wang, J., Zhou, Q., Qiu, S., and Singh, S.R. (2012). Chondrogenic differentiation of induced pluripotent stem cells from osteoarthritic chondrocytes in alginate matrix. Eur Cell Mater *23*.

Welch, T., Mandelbaum, B., and Tom, M. (2016). Autologous chondrocyte implantation: past, present, and future. Sports medicine and arthroscopy review *24*, 85-91.

Westfall, S.D., Sachdev, S., Das, P., Hearne, L.B., Hannink, M., Roberts, R.M., and Ezashi, T. (2008). Identification of oxygen-sensitive transcriptional programs in human embryonic stem cells. Stem cells and development *17*, 869-882.

Wild, D., Nayak, U., and Isaacs, B. (1980). Characteristics of old people who fell at home. J Clin Exp Gerontol *2*, 271-287.

Xu, C., Inokuma, M.S., Denham, J., Golds, K., Kundu, P., Gold, J.D., and Carpenter, M.K. (2001). Feeder-free growth of undifferentiated human embryonic stem cells. Nature biotechnology *19*, 971-974.

Yamamoto, K., Okano, H., Miyagawa, W., Visse, R., Shitomi, Y., Santamaria, S., Dudhia, J., Troeberg, L., Strickland, D.K., and Hirohata, S. (2016). MMP-13 is constitutively produced in

human chondrocytes and co-endocytosed with ADAMTS-5 and TIMP-3 by the endocytic receptor LRP1. Matrix Biology *56*, 57-73.

Yamashita, A., Morioka, M., Yahara, Y., Okada, M., Kobayashi, T., Kuriyama, S., Matsuda, S., and Tsumaki, N. (2015). Generation of scaffoldless hyaline cartilaginous tissue from human iPSCs. Stem cell reports *4*, 404-418.

Yang, Z., Sui, L., Toh, W.S., Lee, E.H., and Cao, T. (2009). Stage-dependent effect of TGF-β1 on chondrogenic differentiation of human embryonic stem cells. Stem cells and development *18*, 929-940.

Yao, S., Chen, S., Clark, J., Hao, E., Beattie, G.M., Hayek, A., and Ding, S. (2006). Long-term self-renewal and directed differentiation of human embryonic stem cells in chemically defined conditions. Proceedings of the National Academy of Sciences *103*, 6907-6912.

Yodmuang, S., Marolt, D., Marcos-Campos, I., Gadjanski, I., and Vunjak-Novakovic, G. (2015). Synergistic effects of hypoxia and morphogenetic factors on early chondrogenic commitment of human embryonic stem cells in embryoid body culture. Stem Cell Reviews and Reports *11*, 228-241.

Yoo, J.U., Barthel, T.S., Nishimura, K., Solchaga, L., Caplan, A.I., Goldberg, V.M., and Johnstone, B. (1998). The Chondrogenic Potential of Human Bone-Marrow-Derived Mesenchymal Progenitor Cells*. The Journal of Bone & Joint Surgery *80*, 1745-1757.

Young, R.A. (2011). Control of the embryonic stem cell state. Cell *144*, 940-954.

Yu, J., Hu, K., Smuga-Otto, K., Tian, S., Stewart, R., Slukvin, I.I., and Thomson, J.A. (2009). Human induced pluripotent stem cells free of vector and transgene sequences. Science *324*, 797-801.

Yu, J., Vodyanik, M.A., Smuga-Otto, K., Antosiewicz-Bourget, J., Frane, J.L., Tian, S., Nie, J., Jonsdottir, G.A., Ruotti, V., and Stewart, R. (2007). Induced pluripotent stem cell lines derived from human somatic cells. Science *318*, 1917-1920.

Zhang, L., Su, P., Xu, C., Yang, J., Yu, W., and Huang, D. (2010). Chondrogenic differentiation of human mesenchymal stem cells: a comparison between micromass and pellet culture systems. Biotechnology letters *32*, 1339-1346.

Zhang, W., Moskowitz, R., Nuki, G., Abramson, S., Altman, R., Arden, N., Bierma-Zeinstra, S., Brandt, K., Croft, P., and Doherty, M. (2008). OARSI recommendations for the management of hip and knee osteoarthritis, Part II: OARSI evidence-based, expert consensus guidelines. Osteoarthritis and cartilage *16*, 137-162.

Zhu, D., Tong, X., Trinh, P., and Yang, F. (2018). Mimicking cartilage tissue zonal organization by engineering tissue-scale gradient hydrogels as 3D cell niche. Tissue Engineering Part A *24*, 1-10.